BIOLOGICAL DENITRIFICATION USING COCONUT SHELLS IN A FLUIDISED BED REACTOR

A thesis

submitted in accordance with

the requirements for the Degree

of

Doctor of Philosophy

in the

University of Canterbury

School of Engineering

by

Mark J. Ellis

University of Canterbury

2005

ACKNOWLEDGEMENTS

In undertaking this research, I have received a great deal of assistance, encouragement and inspiration from various sources that I would like to acknowledge.

Thanks are due to Dr David Wareham, by academic supervisor, whose time, patience, guidance and assistance has made this study most enriching and stimulating, and to whom I am deeply indebted.

I would wish to thank the technical staff who assisted in the construction of the test equipment, and provided guidance in the laboratory especially Mr D. MacPherson.

Finally I would like to acknowledge the support and assistance provided by my family, in particular my wife Kyla.

CONTENTS

List of Tables

List of Figures

List of Equations

1 Abstract

Biological denitrification is the process of utilising bacteria to denitrify nitrate in the absence of oxygen. The denitrifying bacteria anaerobically respire the nitrate to gaseous nitrogen products.

Most experience with biological denitrification is in the field of drinking water treatment, predominantly in Europe. As most potable water sources are low in organic carbon, a supplementary carbon feed source is required. Methanol, ethanol and acetic acid has been demonstrated to be effective in biological granular media filters and fluidised bed reactors (Bosman and Hendricks, 1981)

This research builds upon these concepts and investigates the application of coconut shell fragments within a fluidised bed to sustain biological denitrification where the coconut shell fragments not only provide the only source of organic carbon for the biological process, but provide the media on which the bacteria will attach within a fluidised bed.

Three sets of parallel laboratory scale investigations were undertaken. The first considered several combinations of the physical and chemical pretreatments on the coconut shell fragments (substrate) to increase the medium to long term sustainable release of organic carbon. The second set, takes the pretreated substrate and assesses the rate of biological denitrification the substrate will support. This study was conducted in 6L biological denitrification batch reactors.

In the first two set of laboratory investigations, a total of thirty six unique combinations of four physical and fifteen chemical pretreatments were evaluated. The pretreatment of the substrate with sodium hydroxide (NaOH) and lime showed the most promise. The NaOH pretreated (pH=14) substrate was able to denitrify at an average rate of 1.3 mg/L/day (3.1 mg/L/day peak), whilst the lime pretreated substrate ($Ca(OH)_2$ pretreatment dosage of 500mg/L) was observed to remove nitrate at an average rate of 0.83 mg/L/day.

During the pretreatment batch trials, it was observed that hydroxide pretreatments (NaOH and lime) would become more acidic with time. This was most likely as the result of the formation of alkali cellulose, in which the hydroxyl hydrogen from cellulose (with the

substrate) is substitutes with either a sodium ion in the case of NaOH pretreatment or with a $CaOH^+$ ion in the case of Lime pretreatment.

Whilst NaOH pretreatment provided the greatest improvement in denitrification capacity, the preferred substrate pretreatment was to chemically pretreat the coconut fragments with 500 mg/L of Lime ($Ca(OH)_2$) solution. Sodium hydroxide was discounted due to issues associated with the full scale application of this technique, in that sodium hydroxide is expensive, extremely caustic and requires specific handling and storage facilities.

The third set of laboratory trails involved a parallel study of two laboratory scale (2.2m high, volume 11.26L) fluidised bed reactors. One reactor contained lime pretreated coconut fragments, while the other baseline reactor utilised similar crushed but untreated coconut fragments during the denitrification trials. In total six series of trials were undertaken, with each series comprising several unique flow/loading conditions (thirty eight unique trials were evaluated).

The fluidised bed reactor trials demonstrated that under ideal conditions a COD:TNO_x ratio of 4:1 is required for denitrification.

Whilst the lime pretreatment technique and utilisation of a fluidised bed provided improved denitrification rates, the ability of the coconut substrate to release organic carbon still continued to restrict the biological processes. The pretreatment of the substrate with lime increased the rate of denitrification from 7.1 mg/L/day (for the untreated substrate) to 11.6 mg/L/day for the lime treated substrate.

A numerical evaluation of the biological processes developed in this study (Eqn. 1-1) estimates that the denitrification rate parameter (r_b) of the lime pretreated substrate fluidised bed was approximately 198% greater than the untreated substrate.

$$V\frac{dc}{dt} = Qc_I - Qc + \frac{Vc_s}{2k_s}\left(\operatorname{sech}^2\left(\frac{t-r_s}{k_s}\right)\right) - Vr_b ct$$

Eqn. 1-1

2 Introduction

This thesis investigates the application of coconut shell fragments within a fluidised bed to sustain biological denitrification where the coconut shell fragments not only provide the substratum[1] for the biological process, but also the only source of organic carbon. This research is applicable to the denitrification of a water source high in nitrate.

It has been shown that higher biological reaction rates can be achieved via the use of biological fluidised beds, which intensify the biological reaction rates of attached growth bioreactors (biological reactors) through the accumulation of a high concentration of biomass.

This research is different from the current research in this field, since the coconut shell substratum in the fluidised bed, provides the only organic carbon source for the bacteria. Current biological denitrification design relationships are therefore unable to be applied to this situation.

Biological denitrification utilises bacteria to denitrify aqueous nitrates in the absence of oxygen. The denitrifying bacteria are anaerobic respirators, that use nitrate and/or nitrite as electron acceptors for the oxidation of organic compounds when oxygen is absent, producing nitrogen gases (N_2, NO, and N_2O). The microbial reduction of nitrate to gaseous nitrogen products is termed dissimilatory denitrification or nitrate respiration. Generally denitrification is considered to be an anoxic process, occurring in the presence of nitrate and the absence of molecular oxygen.

Most of the experience with biological denitrification in drinking water has been in Europe. These denitrification units are primarily anoxic biological granular media filters and fluidised-bed reactors. As in most potable water sources, the water is low in organic carbon and requires the addition of an organic carbon source for denitrification to occur. Methanol has frequently been applied; however ethanol and acetic acid have also proved to be effective due to their comparative low cost and reduced toxicity (Bosman and Hendricks, 1981).

---

[1] Substratum is the material on which the bacteria lives and grows. In this case the coconut shell fragments are the substratum.

While the operating costs of a biological denitrification reactor is substantially cheaper than other physicochemical alternatives, the majority of the operating cost is associated with the consumption of carbon source (e.g.: methanol). Therefore the application of a bioreactor that utilises substratum to supply the organic carbon source may have several advantages including a financial benefit over the current options.

Other researchers (Volokita et al., 1996) have demonstrated that the denitrification of drinking water using newspapers and cotton as the carbon source is possible. Their experiments packed laboratory-scale columns with shredded newspapers or unprocessed short fibre cotton to provided the sole chemical and physical substrate for the microbes. Their series of experiments examined the use of the simple cellulose component as the source of organic substrate required by the bacteria. Since cellulose is a basic component of all plant materials, it is an abundant and renewable resource.

This thesis is the merging of two technologies; biological denitrification using fluidised bed reactors and an organic cellulose source to sustain biological denitrification; in this case fragmented coconut shells. The advantages of the using the coconut shell include not only its inert nature, high cellulose content, and that the material has demonstrated its suitability in fluidised beds.

However the key of the research is to degrade the coconut shell sufficiently to release enough cellulose to support the biotic processes. Two forms of laboratory reactors were utilised in this research in which parallel studies were untaken. Initially a series of 6L batch reactors evaluated nine pretreatment techniques to promote greater release of the cellulose from the coconut shell fragments. In total 36 pretreatment batch reactor trials were undertaken, of which the pretreated substrate was utilised in 12 denitrification batch reactor trials.

The baseline denitrification batch reactor trial, to which all other trials were compared, utilised untreated substrate. The substrate that presented the greatest hydrolysis rate and potential to maintain denitrification was then applied to the laboratory scale fluidised bed reactor.

Like the batch reactor trials, the fluidised bed reactor trials were conducted in parallel. Two laboratory scale reactors were utilised, in which the physical and chemical characteristics were identical. Only the pretreatment of the substrate differed. Direct comparisons of the

performance of the two reactors showed that while the untreated substrate was able to sustain denitrification, the pretreated substrate improved the ability of coconut shell fragments to denitrify.

This thesis is arranged in to the following six major sections:

Chapter 3. Theory of biological fluidised beds, denitrification, coconut shells, cellulose and lignocellulose, and the enzymatic hydrolysis of cellulose;

Chapter 4. Experimental equipment and methodology adopted, including a description of the two reactor forms utilised in this research;

Chapter 5. Results, discussions and analysis of the pretreatment batch reactor trials;

Chapter 6. Results, discussions and analysis of the denitrification batch reactor trials;

Chapter 7. Results, discussions and analysis of the denitrification fluidised bed reactor trials;

Chapter 8. Recommendations.

3 Theory

3.1 Biological Fluidised Beds

A fluidised bed occurs when a fixed bed of particulate solids typically resting on a grid plate is brought to a liquid-like state by an upward flowing liquid. A biological fluidised bed is a fluidised bed where the particulate solids in the fluidised state provide the substratum for the biofilm to adhere. However, the surface accumulation does not necessary remain uniform in time or space.

Biological fluidised bed processes have the ability to intensify the biological reaction rates of attached growth bioreactors (biological reactors) through the accumulation of a high concentration of biomass. The results from laboratory and field pilot plants have consistently shown technical advantages of utilising fluidised beds over most other suspended and supported growth biological reactors.

Traditionally bioreactors such as the fixed bed reactor tend to suffer from clogging – where the growth of bacteria is sufficiently large to block the pore spaces between the packed medium. This, in turn, increases the hydraulic shear stresses in the adjacent pore pathways. If the shear stresses are sufficiently great, the bacteria attached to the support media is sheared off, resulting in channels in the media where no biofilm is attached. The flow tends to pass through these channels thereby decreasing the efficiency of the reactor. As indicated in Table 3-1, the current practice is to backwash rigorously the filter medium in fixed bed reactors in order to remove a proportion of the immobilised biomass.

Fluidised bed reactors offer superior performance compared to complete-mix and fixed bed biofilm reactors. The biofilm is evenly distributed throughout the reactor, while the liquid regime of a fluidised bed offers all the advantages of a plug-flow reactor. Since the media is in a turbulent fluidised state, clogging does not occur. Instead, the hydraulic conditions remain symmetrical in the reactor – where the support particles order themselves in terms of relative density vertically up the reactor (i.e. the larger, denser particles settle near the bottom and the lighter, less dense particles rise to the top of the bioreactor).

Table 3-1 Comparison of Different Biofilm Support Reactors		
	Fixed/Expanded Beds	***Fluidised Beds***
Biomass control	Backwashing	Continuous particle removal and cleaning
Biomass recovery	Washings collected in humus tank	At high concentration external to reactor
Bed biomass attached to substratum	Variable	Constant (variable if there is periodic particle removal)
Reactor performance (e.g.: carbon removal)	Variable	Steady (variable if there is periodic particle removal)
Design	Requires prediction of the variation of the bed biomass hold-up with time	Requires prediction of the variation of the bed-particle biomass hold-up with time

(Source: Cooper and Atkinson, 1981).

Traditional bioreactors, such as fixed or expanded beds, tend to operate with variable biomass concentrations, due to the periodic backwashing of the biomass into humus collection tanks. As Table 3-1 indicates, fluidised beds are able to operate with a constant concentration of biomass in the reactors.

3.1.1 The History of Biological Fluidised Bed Bioreactors

The development of water and wastewater biological treatment systems utilising a fluidised bed of biomass can be traced back to the 1940s in England with research conducted by Pugh (1945). Researchers at Manhattan College in New York, at the U.S.EPA Municipal Environmental Research Laboratory (MERL) in Cincinnati, and at the Water Research Centre in Medmenham, England, can be credited for the initial application of media-based biological fluidised bed reactors to water and wastewater treatment in the early 1970s.

As a result of the research conducted, Manhattan College researchers applied for a U.S. patent in 1972 for a biological fluidised bed process to "denitrify wastewater". Their research in the early 1970s through to the 1980s primarily focused on sand as the fluidised bed media. However, they did consider other media, including anthracitic coal and activated carbon.

Despite the evidence of 'prior art' by Pugh in 1945, a patent was granted to MERL in 1974 based on their 1972 application. The patent is not specific to the media employed (e.g., sand or granular activated carbon [GAC]). In 1976 and 1977 additional biological fluidised bed process and apparatus patents were granted to the Manhattan group for nitrate reduction and oxidation of organics.

3.1.2 Hydrodynamics of Fluidised Beds

Fluidisation occurs when a fixed bed of particles is brought from a resting state to a liquid-like state by an upward flowing gas or liquid (superficial fluid). When the fluidised superficial velocity exceeds that of a certain limiting value $u_{mf,}$ then the particulate solids are kept in suspension or in a fluidised state. At this point the fluid behaves like a liquid, in that heavy objects will sink whereas light objects will float.

When a liquid is utilised to fluidise a bed, the bed will expand uniformly (homogeneous fluidisation) when the superficial fluid velocity exceeds the minimum fluidising velocity, u_{mf}. The fluidisation of a gas, by contrast, is often characterised by the presence of solid free bubbles (heterogeneous fluidisation).

Bubbles in gas fluidised beds coalesce rapidly; as a result, the local mean bubble volume increases with increasing height above the gas distributor. In narrow columns the mean bubble diameter quickly approaches that of the column. The resulting state of fluidisation is referred to as a slugging bed, where the bed is characterised by the column diameter, rather than the bubble volume. Similarly, the bubble rise volume is a function of the column diameter.

The point of minimum fluidisation is where the bed makes the transition from a fixed to a fluidised bed. The minimum fluidising velocity, u_{mf}, can be determined directly by measuring the drop in pressure in the bed Δp as a function of the superficial fluid velocity u (Werther, 1983) (Figure 3-1). The measurement should be carried out with the bed in the fluidised bed regime initially in order to ascertain reproducibility of results.

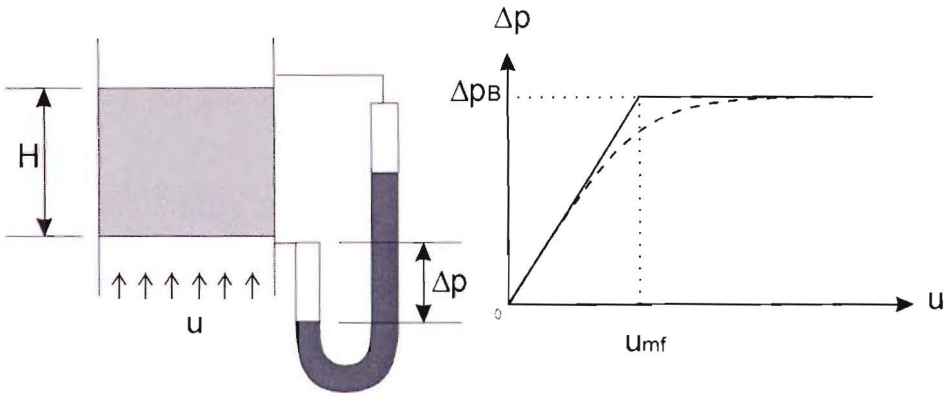

Figure 3-1 Definition of Minimum fluidisation velocity (u_{mf})

$$\Delta p = 150\frac{H_{mf}}{g}\frac{1}{D_p{}^2}\frac{(1-\varepsilon_{mf})^2}{\varepsilon_{mf}^3}\eta u_{mf} + 1.75\frac{H_{mf}}{g}\frac{(1-\varepsilon_{mf})}{\varepsilon_{mf}^3}\frac{\rho_f}{D_p}u_{mf}^2$$

Eqn. 3-1

Equals the fluidised bed pressure drop:

$$\Delta p_B = \frac{\text{mass x gravitational acceleration - buoyancy of the bed particles}}{\text{cross - sectional area of bed}}$$
$$= \frac{A_t H_{mf}(1-\varepsilon_{mf})(\rho_s - \rho_f)g}{A_t}$$

Eqn. 3-2

Werther (1983) development the following equation for minimum fluidisation velocity:

$$u_{mf} = 7.19(1-\varepsilon_{mf})\nu S_v\left[\sqrt{1+0.067\frac{\varepsilon_{mf}^3}{(1-\varepsilon_{mf})^2}\frac{(\rho_s-\rho_f)g}{\rho_f\nu^2}\frac{1}{S_v^2}}-1\right]$$

Eqn. 3-3

Where:

u_{mf}	[ms^{-1}]	superficial minimum fluidisation velocity
Δp	[Nm^{-2}]	pressure drop across the bed
u	[ms^{-1}]	superficial fluid velocity
S_v	[m^{-1}]	surface area of all particles in the bed divided by volume of all particles

ε_{mf}	[-]	mean void fraction in the state of minimum fluidisation
η	[$kgm^{-3}s^{-1}$]	viscosity of fluidising liquid/gas
H_{mf}	[m]	expanded bed height
ρ_f	[kgm^{-3}]	fluidising liquid density
ρ_s	[kgm^{-3}]	apparent density of bed particles
A_t	[m^2]	cross-sectional area of the bed
ν	[m^2s^{-1}]	kinematic viscosity of the fluidising liquid

An alternative methodology for evaluating the minimum fluidisation velocity was proposed by Leva (1959). Leva (1959) considered the effect of the transition from a fixed bed to the fluidised bed. In this transition, the velocity of the individual free falling particle is one of the main variables determining this relationship.

$$u_{mf} = 1.58 \times 10^{-4} \frac{D_p^{1.82}}{\nu^{0.88}} \left(\frac{\rho_s - \rho_f}{\rho_f} \right)^{0.94}$$

Eqn. 3-4

Where:

ν	[m^2s^{-1}]	kinematic viscosity
D_p	[m]	diameter of the particles

From Eqn. 3-3 and Eqn. 3-4 it is possible to obtain an estimate of the typical superficial fluid velocity required to fluidise a bed of homogeneous particles. However a bed of mixed particle buoyancies (particles with a variation in particle size and/or density) will require a different minimum fluidisation velocity to maintain fluidisation to that of the bed of homogeneous particles. A decreased in particle buoyancy correlates to a greater superficial velocity required to suspend the particles.

3.1.3 Fluidisation Regimes

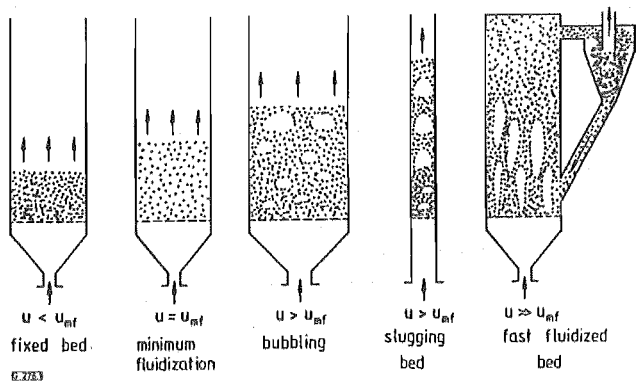

Figure 3-2 Fluidised bed regimes (reproduced from Werther, 1983).

As the superficial fluid velocity exceeds u_{mf}, bubbles form (Figure 3-2, where bubbling, slugging are characteristics of fluidisation by a gas). These bubbles coalesce rapidly; as a result, the local mean bubble volume increases with increased height in the column. In narrow columns the means bubble diameter soon approaches that of the column diameter. This condition is referred to as the slugging bed regime. In this regime, the column diameter governs the bubble rise velocity, rather than the bubble volume.

At very high velocities the individual bubbles are no longer discernable. The bed surface is no longer sharply defined, as bed material is quickly lost. In general, fast fluidisation beds can be maintained by recirculation of entrained solids.

3.2 Denitrification

Nitrogen can exist in seven oxidation states; the compounds of interest to this research take the following forms:

-III	O	I	II	III	IV	V
NH_3	N_2	N_2O	NO	NO_2^-	NO_2	NO_3^-

Figure 3-3 The oxidation states of the common oxidised forms of nitrogen

Denitrification is the process of converting nitrate (NO_3^-) to elemental dinitrogen (N_2). The microbial reduction of nitrate to gaseous dinitrogen is termed *dissimilatory denitrification* or *nitrate respiration*. Generally denitrification is considered to be an anoxic process, occurring in the presence of nitrate and the absence of molecular oxygen. The bacteria are chemoheterotrophic; hence they source energy from redox reactions, source carbon for growth and electron donors from organic compounds. The denitrifying bacteria are anaerobic respirators that use nitrate and/or nitrite as electron acceptors for the oxidation of organic compounds when oxygen is absent, producing nitrogen gases, (N_2, NO, and N_2O), in turn. Payne (1981) suggested that denitrification proceeds through a series of four steps, from nitrate to nitrogen gases.

Nitrate $NO_3^- \longrightarrow NO_2^- \longrightarrow NO \longrightarrow N_2O \longrightarrow N_2$ Nitrogen gas

Figure 3-4 The four steps of the denitrification process (Payne, 1981).

Surprisingly, most of the organisms known to denitrify are not strictly anaerobes, but rather are a form of facultative organisms, which under anoxic conditions use nitrate as a final electron acceptor for anaerobic respiration (Green et al., 1994). Gayle et al. (1989) discovered that most investigators consider oxygen as an inhibitor of denitrification. Some species have been reported to denitrify in systems with oxygen tensions as high as 0.2 bar[2].

Any denitrifying system has four basic components:

1. electron donors in aqueous solution;
2. one of the appropriate nitrogen oxides as the electron acceptor;
3. the bacteria; and
4. a lowered oxygen tension.

Mineral nutrients, pH, and temperature are also influential elements. Almost any sort of organic matter will serve as the electron donor for some denitrifying micro-organism. Animal, plant, or even industrial organic materials ranging from manure and straw to phenolics will provide a supporting base for denitrification in a variety of environments.

---

[2] 1bar is equivalent to 0.9869 atm, where 1 atm is the pressure of 10.4 m of water (@35°C).

In nature a hierarchy exists amongst the terminal electron acceptors used in bacterial respiration. Oxygen has precedence over any nitrogen oxide. Denitrification is a "second choice" mechanism for the denitrifiers. The exclusion requirement of oxygen[3] before the bacteria turns to an alternative form of respiration varies significantly due to the variety of micro-organisms that are able to denitrify.

Typically, the synthesis of denitrifying enzymes is repressed in the presence of O_2. The activity of these denitrifying enzymes is also inhibited by O_2; the rate of inhibition, however, is not known. Once produced, the denitrifying enzymes will continue to function in certain bacteria for some time after exposure to an aerobic environment.

3.2.1 Nitrogen Cycle

Nitrogen constitutes 79% of the earth's atmosphere, occurring almost entirely in the inert form of the gas, dinitrogen (N_2). The atmospheric nitrogen pool contains other compounds of nitrogen, such as nitrogen oxides, ammonia, and aerosols of nitrate and nitrite, but these constitute only a minuscule fraction of the pool.

The diagram of the nitrogen cycle, shown in Figure 3-5, illustrates the relationships between the various forms of nitrogen compounds. Nitrogen exists primarily in an inanimate state, as N_2 in the atmosphere or as nitrate ion (NO_3^-) in the soil or ocean. Biological systems acquire the nitrogen by reducing it to the ammonium ion (NH_4^+), and incorporating it into an organic linkage as amino or amido group (via the ammonification process). The reduction of NO_3^- to NH_4^+ occurs in green plants, various fungi, and certain bacteria in a two-step metabolic pathway known as nitrate assimilation. While dinitrogen can be transformed by large electrical storms in the form of nitric acid, this is insignificant in comparison to the rate removed by nitrogen-fixing bacteria. The formation of NH_4^+ from N_2 gas is termed *nitrogen fixation.*

---

[3] The absence of oxygen (or anoxia) is a requirement of some bacteria, which are often able to reduce nitrate in the presence of low concentrations of oxygen. Terai and Mori (1975) noted that *Pseudomonas denitrificans* stopped reducing nitrate in the presence of more than 0.2 mg/L of oxygen.

Nitrogen fixing is an exclusively prokaryotic[4] process. Although some plants are dependant on nitrogen fixing, this is achieved by a symbiotic relationship with certain bacteria. No animals are capable of nitrogen fixing or nitrate assimilation, so they totally depend on plants and micro-organisms for the synthesis of organic nitrogenous compounds, such as amino acids and proteins, to satisfy their requirement of this essential element of life.

Animals release excess nitrogen in a reduced form, either as NH_4^+ or as organic nitrogenous compounds such as urea. The release of N occurs both during life and as a consequence of microbial decomposition following death. Various bacteria return the reduced forms of nitrogen back to the environment by oxidising them. The oxidation of NH_4^+ to NO_3^- by nitrifying bacteria[5] provides their sole source of chemical energy for their life processes. Nitrate is eventually returned back to the atmosphere as dinitrogen as a result of the metabolic activity of denitrifying bacteria. These bacteria are capable of accepting NO_3^- as electron acceptors in the place of O_2 in energy-production pathways. Collectively these bacteria deplete the level of nitrogen, an important natural fertiliser in soil that might otherwise be available. However, these bacteria are utilised in wastewater treatment plants to reduce the load of combined nitrogen that might otherwise enter streams, lakes, and estuaries.

---

[4] *Prokaryotic* refers to bacteria that has its genetic material not enclosed in a cell nucleus.

[5] These nitrifying bacteria are typically chemoautotrophs.

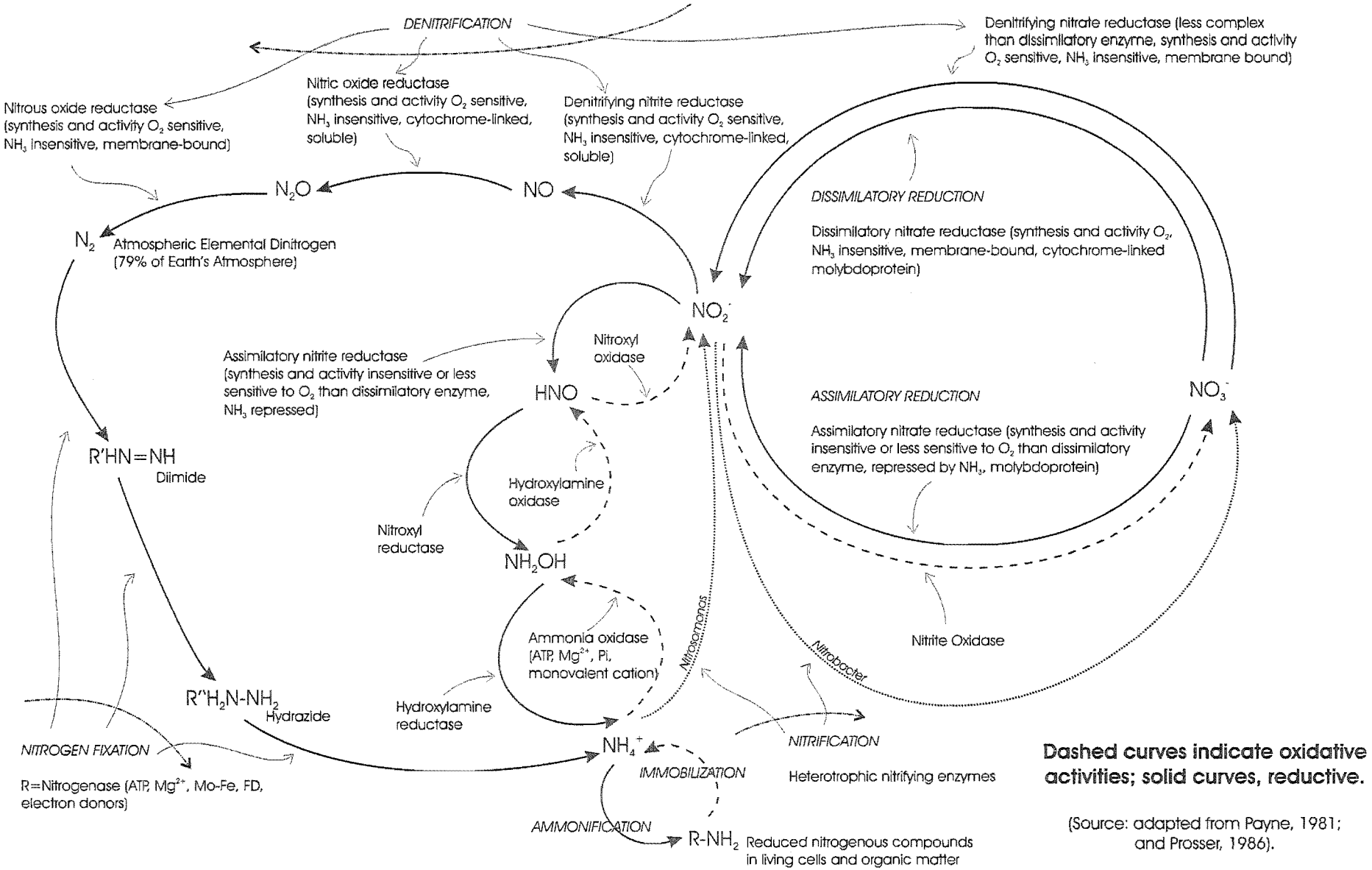

Figure 3-5 A synoptic depiction of the nitrogen cycle.

3.2.1.1 The Enzymology of Nitrogen Fixing

Less than 1% of the inorganic N incorporated into organic compounds by organisms can be attributed to nitrogen fixation (Garrett and Grisham, 1999); however, this process is the only direct biological access to the reservoir of N_2 in the atmosphere. Nitrogen fixing involves the reduction of dinitrogen gas (N_2) via an enzyme system only known to occur in prokaryotic cells. The process centres on the behaviour of the nitrogenase enzyme, which catalyses the following reaction:

$$N_2 + 8H^+ + 8e^- \rightarrow 2NH_3 + H_2$$

Eqn. 3-5

Despite the wide diversity of bacteria in which nitrogen fixation takes place, all N_2-fixing systems are nearly identical, and all have four fundamental requirements:

1. the enzyme nitrogenase;
2. a strong reductant, such as reduced ferredoxin;
3. ATP; and
4. O_2 free conditions.

In the nitrogenase reaction (Figure 3-6), electrons from reduced ferredoxin pass to the nitrogenase reductase, which serves as the electron donor to nitrogenase, the enzyme that actually catalyses N_2 fixation. Electron transfer from nitrogenase reductase to nitrogenase takes place through docking of nitrogenase reductase and the transfer of electrons.

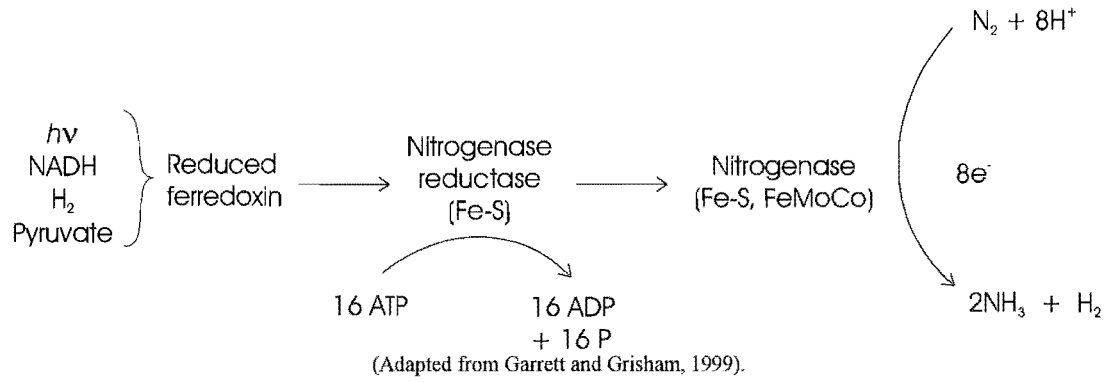

(Adapted from Garrett and Grisham, 1999).

Figure 3-6 The nitrogenase reaction

Depending on the bacterium, electrons for N_2 reduction may come from light (*hν*), NADH, hydrogen gas, or pyruvate. The primary electron donor for the nitrogenase system is reduced

ferredoxin. Reduced ferredoxin passes the electrons directly to nitrogenase reductase. A total of six electrons are required to reduce N_2 to 2 NH_3, and another two electrons are consumed in the obligatory reduction of $2H^+$ to H_2. Nitrogenase reduction transfers electrons to nitrogenase one electron at a time. N_2 is bound at the critical FeMoCo prosthetic group of nitrogenase until all the electrons and protons are added (as outlined in Nitrogen Fixation process, Figure 3-6). FeMeCo is a Fe(iron) Mo(molybdenum) cluster or co-factor of the nitrogenase complex.

Nitrogenase is a rather slow enzyme, reducing only three molecules of nitrogen gas per second. Because its activity is so weak, nitrogen-fixing cells maintain large amounts of nitrogenase so that their requirements for reduced N can be met. As much as 5% of the cellular protein may be nitrogenase.

3.2.1.2 The Enzymology of Nitrification

Nitrification is the process of converting ammonium to nitrate and the bacteria (nitrifiers) obtain energy for growth in the process. Ammonia is often added to soil, but little NH_3 is found there. Studies have shown that in soil ammonia is rapidly oxidised to nitrate; this is the primary source of nitrogen for non-fixing plants. The oxidation of NH_3 is carried out by two groups of nitrifying bacteria.

One group, the *Nitrosomonas*, convert NH_3 to nitrite, with O_2 as the oxidising agent

$$NH_3 + {}^3/_2\, O_2 \longrightarrow NO_2^- + H_2O + H^+ \quad \Delta G^\circ = -278\ kJ/mol$$

Eqn. 3-6

The other group, *Nitrobacter*, oxidise nitrite to nitrate.

$$NO_2^- + \tfrac{1}{2}\, O_2 \longrightarrow NO_3^- \quad \Delta G^\circ = -73.2\ kJ/mol$$

Eqn. 3-7

Both reactions are exothermic and exergonic: the first involves the oxidation of nitrogen from –III to +III states, and the second is a two-electron oxidation from +III to +V . A number of electrons are removed from the inorganic donors (NH_3 and NO_2^-) and transferred to oxygen along specialised transport chains linked to ATP generation sites (Hooper, 1978).

Both groups of bacteria are chemoautotrophs, since the energy required to reduce CO_2 to carbohydrate and other carbon compounds is supplied by the oxidation of NH_3 to NO_2^- or NO_2^- to NO_3^-.

The term *nitroso*, as in *Nitrosomonas*, refers to the capacity of the bacteria to oxidise ammonia into nitrous acid (which appears as NO_2^- under physiological conditions). The bacteria make use of a stepwise series of enzymatically catalysed events outlined below:

$$NH_3 + \tfrac{1}{2} O_2 \longrightarrow [NH_2OH]$$

$$[NH_2OH] \longrightarrow [HNO] + 2H^+$$

$$[HNO] + \tfrac{1}{2} O_2 \longrightarrow HNO_2$$

Eqn. 3-8

The intermediates, hydroxylamine [NH_2OH] and nitroxyl [HNO], are thought to be enzyme-bound during the transition phase.

In the *Nitrobacter*[6], cytochromes[7] a + a_3 are reduced by electrons derived from nitrite oxidation. Figure 3-7 shows that the electrons are then transferred from the reduced cytochrome a + a_3 level to oxygen, producing ATP in the process (Payne, 1981). NO_2^- is oxidised, eventually resulting in the reduction of oxygen to water

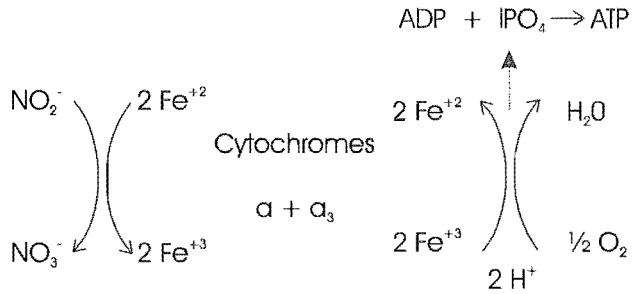

Figure 3-7 The electron transfer chain of *Nitrobacter*.

---

[6] The prefix *nitro* indicates that the bacteria with this term are able to generate nitric acid, which under normal physiological conditions is found as NO_3^-.

[7] Cytochromes are proteins involved in the electron transport chain, and contain heme prosthetic groups, which function by carrying or transferring electrons. The heme iron is converted from Fe^{2+} to Fe^{3+} and back.

3.2.1.3 The Enzymology of Nitrate Assimilation

Nitrate is the most abundant form of nitrogen in the soil. Plant and soil organisms have developed an ability to utilise this anion as the nitrogen source for their growth and development. Higher order plants and organisms, after taking up NO_3^-, must reduce it to NH_3 before the nitrogen can be assimilated. Nitrate assimilation is the process of absorbing nitrate-nitrogen into nitrogenous compounds in cellular proteins.

This process occurs in two steps (as indicated in Eqn. 3-9). Two-electrons are required to reduce nitrate to nitrite, which is catalysed by nitrate reductase, followed by the six-electron reduction of nitrite to ammonium, which is catalysed by nitrite reductase.

$$NO_3^- + 2H^+ + 2e^- \longrightarrow NO_2^- + H_2O$$

$$NO_2^- + 8H^+ + 6e^- \longrightarrow NH_4^+ + 2H_2O$$

Eqn. 3-9

Nitrate assimilation is the predominant means by which green plants, algae, and many organisms acquire nitrogen. The pathway of nitrate assimilation accounts for over 99% of the inorganic nitrogen assimilated into organisms.

Nitrate Reductase

The nitrate reductase takes electrons provided by NADH through a series of enzyme steps to reduce nitrate to nitrite (Figure 3-8, adapted from Garrett and Grisham, 1999).

Figure 3-8 Nitrate Reductase.

A pair of electrons are transferred from NADH via the enzyme-associated sulfhydryl (-SH) groups, FAD, cytochrome b_{557}, and MoCo to nitrate, reducing it to nitrite. The brackets [] indicate that these protein-bound prosthetic groups constitute an electron transport chain

between NADH and nitrate. Where MeCo is a Mo(molybdenum) cluster or co-factor of the nitrate reductase complex

Nitrite Reductase

Six electrons are required to reduce NO_2^- to NH_4^+ (Figure 3-9, adapted from Garrett and Grisham, 1999). Photosynthetic organisms obtain these electrons from six molecules of photosynthetically reduced ferredoxin (Fd_{red}), while other bacteria use another readily available reducing agent such as NADH.

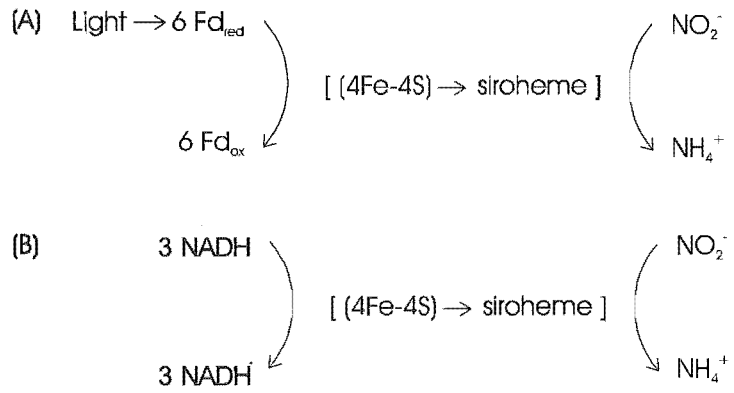

Figure 3-9 Nitrite Reductase.

As Figure 3-5, demonstrates, nitroxyl (HNO) and hydroxylamine (NH_2OH) intermediates are involved in this reduction. Prosser (1986) indicated that these intermediates are enzyme bound; however, some debate about the existence of the nitroxyl (HNO) as an intermediate exists (Conn et al., 1987).

3.2.1.4 The Enzymology of Denitrification

Nitrate dissimilation or denitrification is the process of converting the nitrate ion back to elemental dinitrogen. Microbes that reduce the nitrate to the gaseous dinitrogen are actually using the nitrate for respiration; hence this process is often called dissimilatory denitrification.

Various reductases are involved in the dissimilation of the nitrate ion to elemental dinitrogen. Figure 3-5 illustrates the current thinking with regard to the denitrification process. However, there is debate about the presence of nitric oxide as an intermediate. Nitric oxide has been measured in small quantities during denitrification experiments (Nömmik, 1956; Cady and Bartholomew, 1963; Fillery, 1979).

Nitrate Reductase

The term *nitrate reductase* is often used in a singular sense, but there are a number of enzymes that achieve nitrate reduction. Dissimilatory nitrate reductases are classified into three subgroups, according to their physical and physiological properties. The first is enzymes produced by aerobic bacteria that can grow facultatively both by fermentation and respiration under anaerobic conditions. The anaerobic respiration occurs when oxygen is absent and the cell substitutes nitrate as the terminal oxidant. The nitrate reductase involved is complex and is tightly bound in the cytoplasmic membrane (Wientjes et al., 1979).

The second group has the capacity for cytochrome-linked nitrate reduction. These bacteria carry out this process at the substrate-level. However, oxygen inhibits the functioning of this nitrate reductase.

The third group, ferment nitrate. The nitrate is not the "true" substrate for the fermentative reductase activity; rather, it is thought that the nitrate reduction is no more than a fortuitous event from which the bacteria can profit if nitrate is encountered.

Dissimilatory nitrate reducing bacteria in both of the facultative and the obligatory anaerobic groups may accumulate and tolerate nitrite without further reduction (Buchanan and Gibbons, 1974). Alternatively, they may reduce it to ammonia – some species do so only if no other source of nitrogen is available for growth, while other species may reduce it irrespective of the nitrogen supply.

Payne (1981) (Figure 3-10) noted that the denitrifying nitrate reductase is strongly bound in the cytoplasmic membrane, the groups within [ ] are involved in the reductions, but the interaction between them is unknown. Denitrifying nitrate reductase contain similar molecules to those of the respiratory nitrate reductase (such as iron, labile sulphide, and molybdenum) but in lower fractions[8]. The molecular weight of the intact enzyme was estimated to be 193,000 molecular units (Forget, 1974).

---

[8] A "lower fraction" is in terms of atoms per mole of protein.

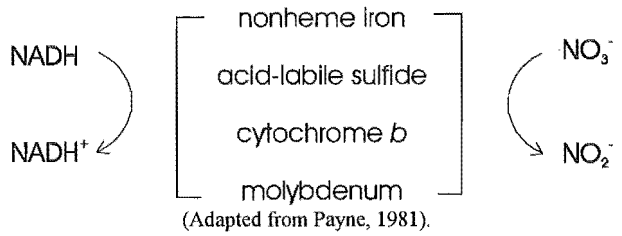

(Adapted from Payne, 1981).

Figure 3-10 The dissimilatory nitrate reductase.

John and Whatley (1970) and Verseveld et al. (1977) conducted experiments into the electron transport chain characteristics of anaerobically grown *Pseudomonas denitrificans* cells. Their research suggested that two phosphorylation sites exist in the electron transport chain, and found that one of the electron transport chain phosphorylation sites was sensitive to nitrite concentrations greater than 0.01M in the medium. This observation has been used to explain the sensitivity of denitrifiers to nitrite.

The data consistently shows that electrons are directed along the chain through a b-type cytochrome to nitrate reductase and hence onto nitrate, while only passing one phosphorylation site, that of site I. Reduction of either nitrite or nitrous oxide is assumed to send electrons past sites I and II. Site I was particularly sensitive in the experiments with more than 0.01M nitrite in the medium, which can be used to explain the sensitivity of many denitrifiers to nitrite.

John and Whatley (1970) noted that if the initial substrate contains excessive quantities of nitrate, it results in an unavoidable and large accumulation of nitrite. This accumulation of nitrite may slightly damage the cells and may account for a persistent accumulation of nitrous oxide – since the nitrite reductase process will become the rate limiting step.

Nitrite Reductase

Denitrifying nitrite reductase are enzymes that reduce the nitrite ion to nitric oxide (NO) (Payne, 1981). Payne defined the denitrifying nitrite reductase as a series of biochemical components that transfer electrons to ultimately reduce the nitrate. These components include flavoprotein that serves as an oxidant for NADH. The copper protein azurin is reduced as a result, which in turn contributes electrons to the c-d cytochrome so it can donate electrons to oxygen and carbon monoxide as well as nitrite, as demonstrated in Figure 3-11.

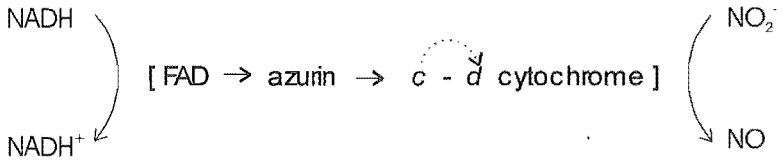

Figure 3-11 The dissimilatory nitrite reductase (adapted from Payne, 1981).

Reduction of Nitric Oxide

Nitric oxide (NO) is reduced to nitrous oxide (N_2O). The quantity of nitrous oxide released during denitrification is highly dependent on the physical and chemical composition of the media supporting the denitrification.

The electron transport chain linked to NO reductase is not fully understood. Miyata (1971) suggested the following scheme (Figure 3-12) where lactate or ascorbate serves as a physiological electron donor.

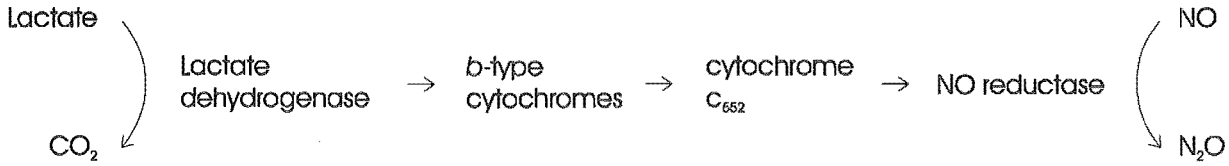

Figure 3-12 The reduction pathway of Nitric Oxide to Nitrous Oxide as proposed by Miyata (1971).

As indicated earlier, the presence of the NO intermediate is uncertain; conflicting research has supported and discounted the presence of NO. Averill and Tiedji (1982) proposed an alternative hypothesis that reconciled these contrasting observations. The hypothesis assumes that NO could form from the decomposition of a ferrous-nitrosyl complex, one of a series of bound intermediates they suggested could form during nitrite reduction to N_2O (Figure 3-13). This hypothesis is favoured for several reasons. First, there is chemical evidence to support the proposed reactions. Furthermore, this process provides a plausible explanation for the production and utilisation of NO during nitrite reduction. Finally, the reduction of nitrite to N_2O involves two electron steps and is consistent with other known biological reduction reactions coupled to phosphorylation and energy conservation.

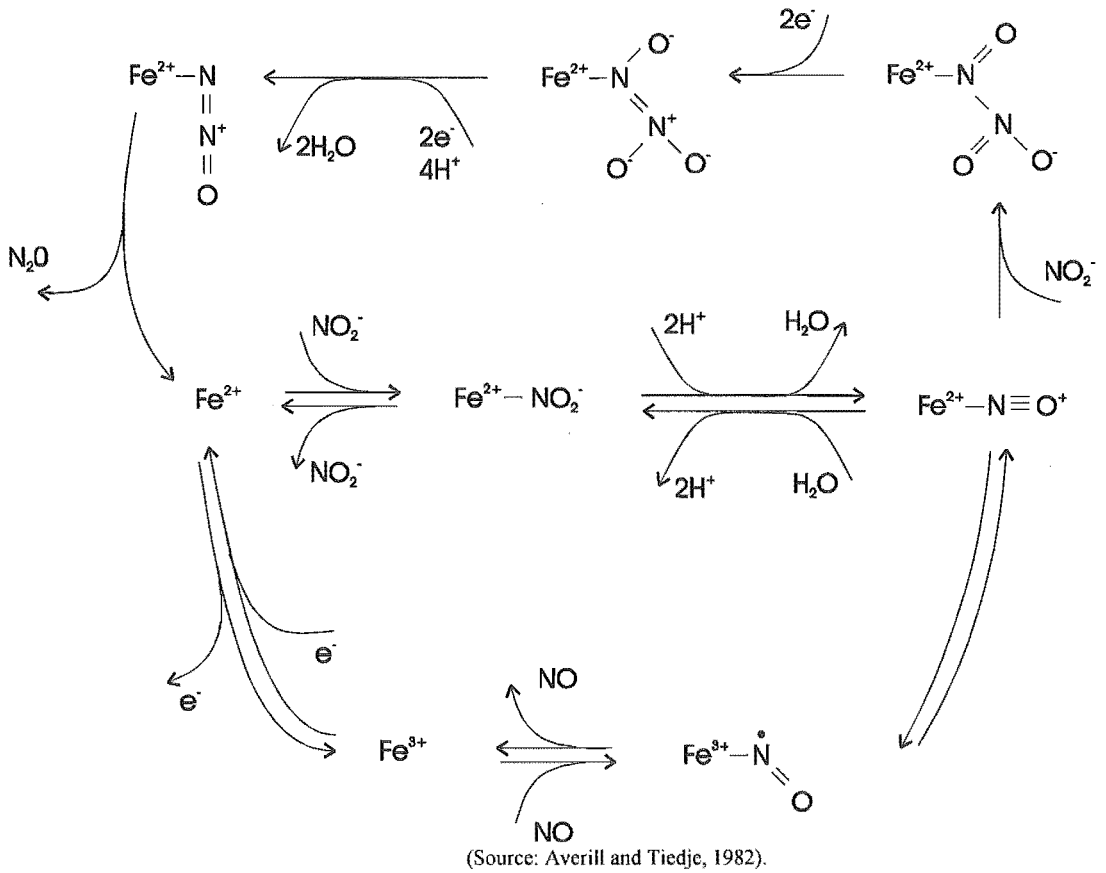

(Source: Averill and Tiedje, 1982).

Figure 3-13 Proposed pathway of nitrite reduction to nitrous oxide.

Reduction of Nitrous Oxide

Relatively little is known of the N_2O reductases in denitrifying bacteria. The enzyme is located on the bacterial membrane in *Pseudomonas perfectomarinus* and contains metal cofactors (Payne, 1973). The reduction of nitrous oxide (N_2O) forms the product of dinitrogen (N_2).

A comparative study by Koike and Hattori (1978) on the efficiency of various nitrogen oxides as electron acceptors for *Pseudomonas denitrificans* revealed that growth yields were proportional to the oxidation state. Cells grown anaerobically in a chemostat on a glutamate-minimal medium achieved 26.8 g dry wt/mol of nitrate converted to dinitrogen gas produced. The yield for nitrite utilisation was 16.9 g/mol, and that for nitrous oxide reduction was 8.8 g/mol. Koike and Hattori (1978) concluded that an increase in oxidation state corresponds to an increase in yield, which was linked to the concept that oxidation phosphorylation, was occurring at a similar extent to the oxidation state.

Federova et al. (1973) observed that the inclusion of acetylene would block the reduction of nitrous oxide by bacteria in the soil. The concentration required for complete blockage was 0.01 atm of acetylene, while lesser amounts inhibited the rate of reduction in proportion. The concept of using acetylene to block the reduction of nitrous oxide is often used to assess the denitrification rate by measuring the N_2O production.

3.3 Coconut Palm (Cocos nucifera)

The coconut palm has been called the "Tree of Life" because it is the source of many raw materials essential to traditional life-styles in the Pacific region. The leaves of the coconut palm are used for roofing and the production of mats; the trunk provides wood for furniture. The coconut meat is used as food, as animal feed, in the production of soap and cooking oil; the husks are used to produce ropes and mattresses; the shell is used to produce charcoal; and even the roots are used in dyes and traditional medicines.

The coconut is one of the most widely distributed crop plants and has a long history of cultivation in Asia, Africa, Latin America, and throughout the Pacific region, though its centre of origin is not known. Small coconut-like fossils, between one and 15 million years old, have been found in New Zealand (Cocos zeylandica) (Green 1991).

3.3.1 Botany

The palms (family *Palmae*) are among the most ancient woody plants. There are some 2,600 species, 600 of which are included in the subfamily *Cocoideae* to which the coconut (*Cocos nucifera*) palm belong. The genus *Cocos* at one time had over 60 species of palms assigned to it; today it is generally considered to be monotypic with *C. nucifera* being the sole species. However, different varieties and cultivars are recognised, and can be divided into two groups, the Tall coconuts and the Dwarf coconuts.

In strict botanical terms, *coconut* is not a tree, since its trunk is a stem, and it has no true bark, no branches, cambium[9] or secondary growth. The coconut palm is more closely related to the bamboos, reeds, and grasses.

The fruit of the coconut palm is not a real nut but a drupe: a fleshy fruit that develops from either one or several carpels[10] and contains one or more seeds. The seeds are enclosed by the hard protective endocarp of the fruit. Ohler (1984) outlined the development of the fruit of the coconut. After fruit-set, one of the ovules develops into a fruit, and the other two degenerate. First, the husk and shell grow mainly in size, not in thickness, and the cavity is filled with liquid. After about four months, the husk and shell become thicker and thicker; continuing to do so for about two months. About six months after fruit-set, the solid endosperm begins to form against the inner wall of the cavity, first at the apex and gradually extending toward the stalk end. This first layer is thin and gelatinous.

About eight months after fruit-set, the soft white endocarp, or shell, starts hardening and turning dark brown. This process also starts at the apex, reaching the stalk-end of the nut when it is almost ripe. At the same time, the nut's volume gets larger and its weight increases.

---

[9] Cambium is the plant tissue consisting of actively dividing cells and is responsible for increasing the girth of the plant, i.e. it causes secondary growth.

[10] The carpel is the female reproductive organ of a flower, typically consisting of a stigma, style, and ovary.

Toward ripening, the endosperm turns hard and white, covered on the outside by a brown testa firmly adhering to it, as indicated in Figure 3-14. At this stage, the endosperm can be gouged out of the nut by using a strong knife with considerable pressure. The loss of weight during the process of ripening is mainly due to the drying of the husk. The liquid in the cavity, the coconut water, decreases in volume and no longer fills the whole cavity.

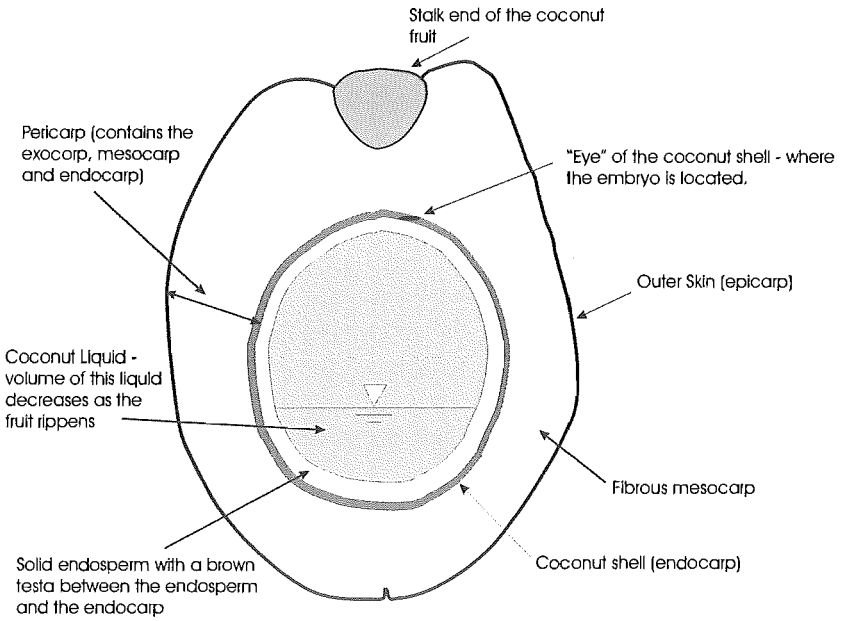

Figure 3-14 A cross-section of the fruit of a coconut palm.

The epicarp is about 0.1mm thick. The fibrous husk, or mesocarp, may vary in thickness from one to more than five cm at the base of the nut, and in some cases it may be up to 10 cm. The shell or endocarp is very hard and generally varies in thickness from 3 to 6 mm.

3.3.1.1 Coconut Shell

Coconut shells are similar in composition to the hardwoods, but have a higher lignin and lower cellulose content. Nathanel (1964) determined the dry basis composition of the coconut shell, reproduced in Table 3-2.

Table 3-2 Composition of Coconut Shell	
Lignin	36.51 %
Cellulose	53.06 %
Total pentosans	29.27 %
Ash	0.61 %

(Source: Nathanel, 1964).

The coconut shell is mainly used as a domestic fuel for making copra, and for the kitchen fire. The main commercial product made from the coconut shell is charcoal. The commercially available quantities, however, are relatively small.

The structure of the coconut shell is cellular and porous in composition. Activated granular carbon is often manufactured from coconut shell fragments as a direct result of these features (Figure 3-15). The coconut shell is favoured over other commonly utilised material, such as coal and wood, in the manufacture of activated carbon. This is because the coconut shell activated carbon has a higher volatile content, which produces a hard-granulated carbon with an even and large pore volume. It also has a higher density than wood or coal.

Many of the features of granular activated carbon derived from coconut shell make it operationally advantageous in a biological fluidised bed, as many of these features are inherent in the raw product.

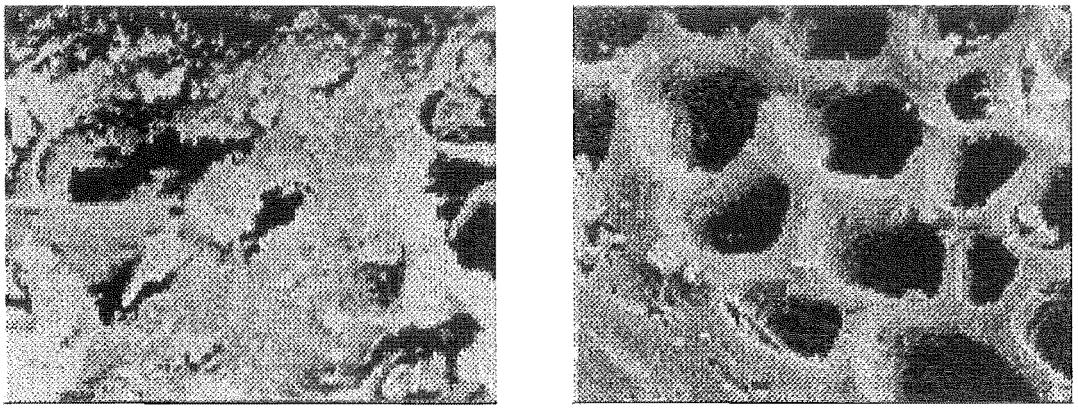

(A) (B)

Figure 3-15 The structure of the pores in a coconut shell

(A) carbonised coconut shell at X2000 magnification (B) activated carbon of a coconut shell at X3000 magnification. (Source: SafeLab, 2003).

3.4 Lignocellulose

The term *lignocellulose* (as indicated in Figure 3-16, reproduced from Zehnder, 1988) is used to collectively define the three major components of plant vascular tissue: cellulose, hemicellulose, and lignin. Lignocellulose may constitute as much as 89 to 98% of the dry weight of wood. The holocellulose (a collective term for the cellulose and hemicellulose component) is the largest fraction (63 to 78%) (Zehnder, 1988).

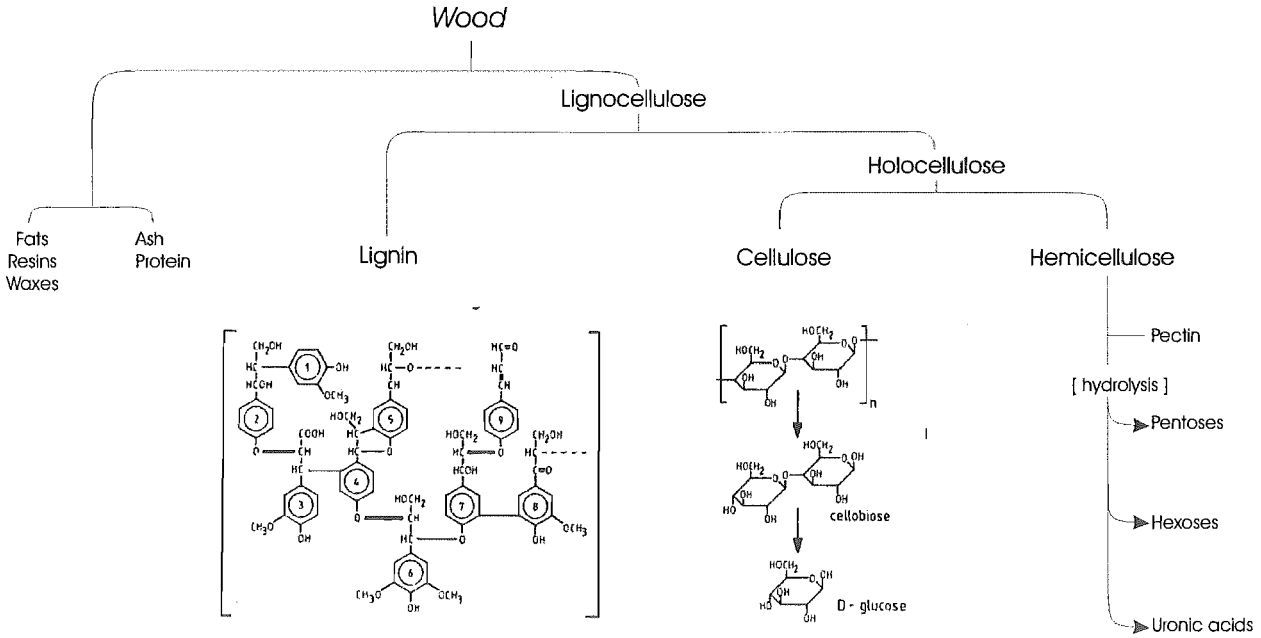

Figure 3-16 The major components of wood.

The components of lignocellulose are often considered together because the exact structure and bonding between the components is not fully understood. Lignin is known to surround cellulose physically and is not thought to be covalently linked to it (Zeikus, 1980). Other available data suggests that some type of chemical bond exists between other plant polysaccharides and lignin (Zehnder, 1988). The significance of such interactions and how they might affect the degradation of lignocellulose is not known.

3.4.1 Cellulose

Cellulose is a polysaccharide formed out of *D*-glucose (Dextrose glucose (or D-glucose) is particular isomer of glucose) units linked together into long molecular chains. Intra- and inter-chain hydrogen bonding of the cellulose chains leads to the crystalline state of cellulose. Depending on the origination of the bonds between the glucose units will determine the product of the glucose chain. As Figure 3-17 demonstrates α-amylose is product of α(1-4) bonds between *D*-glucose units. These bonds are naturally bent – the bending of this polymer ultimately forms a helical shape. Whilst cellulose contains β(1-4)-glycosidic bonds to link the glucose units, resulting in an alternating (or flip) in glucose units leading to the extended ribbon structure of cellulose chains.

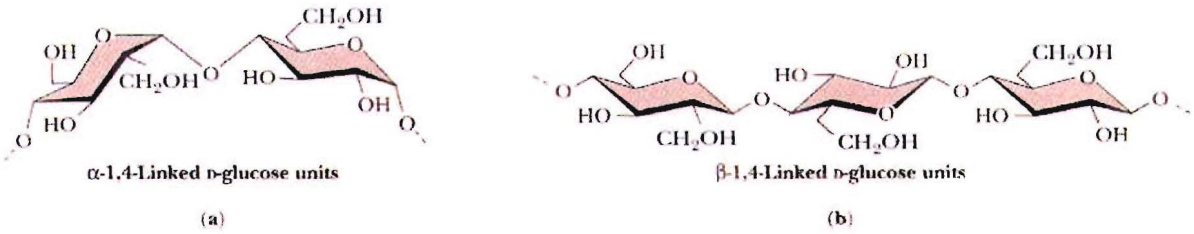

Figure 3-17 Structural difference between (a) α(1-4) bonds and (b) β(1-4)-glycosidic bonds.

The structure of cellulose has four common forms – one form, determined by X-ray and electron diffraction data, and is shown in Figure 3-18 (Source: Garrett and Grisham, 1999). The cellulose chains are rotated so that intrachain hydrogen bonding (red dashed line) occurs along the cellulose ribbon. Flat sheets of cellulose are formed when the cellulose ribbons lie side by side attached by interchain (green dashed line) hydrogen bonding. These sheets are then laid on top of each other, in a way such that the chains are staggered, allowing intersheet (blue dashed line) hydrogen bonding. The resulting structure offers significant strength and stability.

Given its strength, most animals cannot digest cellulose to any significant degree. Ruminant animals (cattle, deer, giraffes, and camels) are the exception because the bacteria that live in the rumen secrete the enzyme cellulase, β–glucosidase, which is effective in the hydrolysis of

cellulose. Similarly, termites and shipworms can digest cellulose because their digestive tracts also contain bacteria that secrete cellulase.

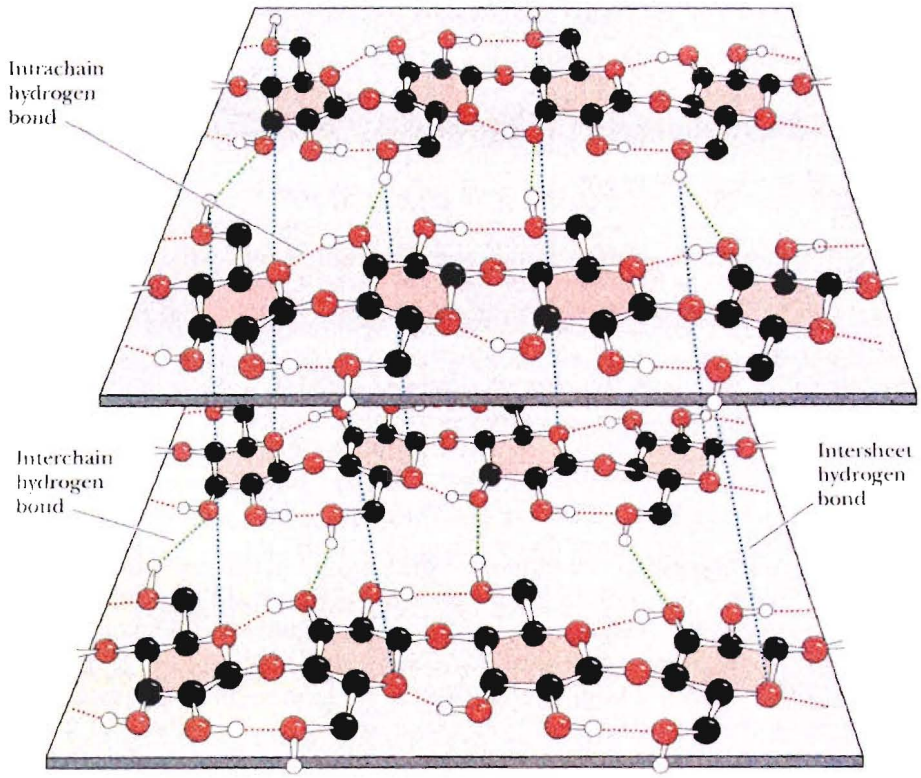

Figure 3-18 The crystalline structure of cellulose

Cellulose makes up to 90% of cotton fibres, but only about 45% of typical wood cell walls (Cowling, 1975). The cellulose in cotton and wood is similar in structure. Cotton fibres are formed independently, and contain no intercellular material, while wood fibres are in a form of cohesive 3D structure whose integrity is determined by the large amount of intercellular substance. Figure 3-19 shows how the typical cross-section of woody material is constructed of various wood cells.

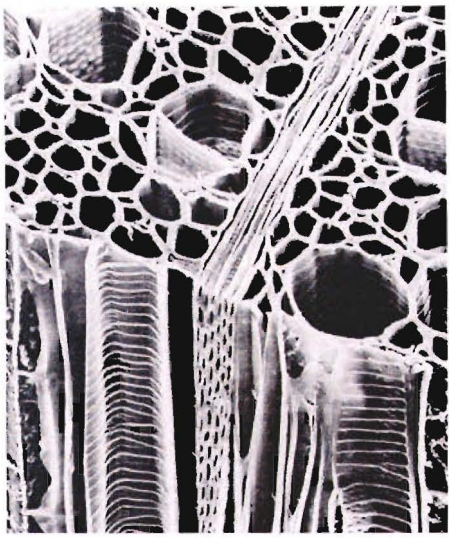

(Source: Panshin and De Zeeuw, 1980).

Figure 3-19 Scanning electron microscope view (350x) of wood

Both cotton and wood fibres have a thin primary wall that surrounds the relatively thick secondary wall. The secondary wall typically consists of three layers. The cellulose molecules in each layer are orientated in different directions. Within each layer of the secondary wall, the cellulose constituents are bound together into long slender bundles call microfibrils. Figure 3-20 displays a model of a portion of the woody cell wall, cut away to show the helical organisation of the microfibrils in the secondary wall. The true intercellular substance is the middle lamella (ML), and adjacent to these is the primary walls (PR). The secondary walls are composed of the outer (S1), middle (S2), and the inner (S3) layers – these are distinguished by the orientation of the microfibrils within each layer.

Within each microfibril the linear molecules of cellulose are bound laterally by hydrogen bonds (as indicated in Figure 3-18).

When the microfibrils are isolated from cell walls by chemical extraction to remove the polysaccharides in which they are imbedded, hydrolysis of the undisrupted microfibrils mostly yields sugars other than glucose. These strongly absorbed chains of sugars are thought to be xylan, mannan, xylogucan, or glucomannan, all intermixed with glucan.

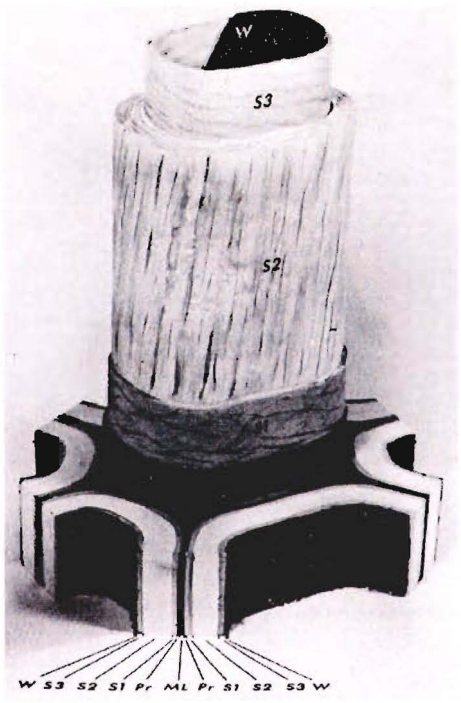

(Source: Panshin and De Zeeuw, 1980).

Figure 3-20 Model of a portion of the woody cell wall.

However, when cellulose is treated with strong sulphuric acid and titrated back to pH 3, the microfibrils fall into short rods which still have the same structure of cellulose, and on hydrolysis yield no sugar other than glucose (Dennis and Preston, 1961). Preston (1986) noted that the microfibrils are always imbedded in a matrix of other polysaccharides and, in some tissues, with compounds such as lignin. The chemical nature of the polysaccharides varies from tissue to tissue, and species to species, but they all consist of chains that are rod-shaped.

3.4.2 Lignin

Lignin is among the most complex natural polymers. Lignin-derived carbon is highly resistant to degradation and, due to its association with cellulose as lignocellulose, impedes the turnover of large quantities of organic carbon. Lignin decomposition is therefore considered to be the rate-limiting step in the biological carbon cycle (Zehnder, 1988).

Research on the degradation of lignocellulose has focused on an understanding of the aerobic mechanism while relatively little attention has been given to microbial degradation under anaerobic conditions. Aerobic degradation of lignin is known to require highly oxidative

conditions, and it has now been established that oxygen is not needed for the biodegradation of aromatic monomers (Evans, 1977), including those derived from lignin.

Lignin is the second most abundant naturally occurring polymer (second to cellulose), and is located primarily in the cell walls of vascular plants. Lignins are irregular phenylpropane bipolymers that make up approximately 20-30% of the available polymeric content of hardwood tree stems. Lignin performs a number of functions essential to the life of plants, such as an energy storage system, a permanent bonding agent between cells, and a waterproofing agent.

3.4.3 Lignocellulosic Degradation

Lignocellulosic biomass (Figure 3-16) is mainly composed of cellulose, hemicellulose, lignin, and ash. The biomass is resistant to enzymatic hydrolysis because of the lignin content (Young and Rowell, 1986) and the crystalline structure of cellulose. Some pretreatments designed to overcome the resistance of the lignocellulosic structure have already been developed, such as ball milling, steam explosion, and alkali treatment, but these methods tend to be costly.

3.4.3.1 Pretreatments

Mechanical grinding, a typical physical pretreatment, not only decreases the crystallinity of cellulose (Fan et al., 1980) but also increases the surface to volume ratio, thus making cellulose more susceptible to hydrolysis. Non-mechanical physical treatments such as steam explosion and high-energy irradiation have been extensively investigated. Interest recently focused on steam explosion, where the raw material is first heated with high-pressure steam and then instantaneously exposed to atmospheric pressure. The resulting steam explosion breaks the alpha and beta allyl ether bonds, and renders lignin soluble in methanol and ethanol solutions (Playne, 1984; Marchessault et al., 1982).

The biological degradation of lignocellulosics is one of the most important parts of the biological carbon-oxygen cycle. There are four groups of micro-organisms that can degrade lignocellulose: white-rot fungus, brown-rot fungus, soft-rot fungus, and bacteria. Although the degradation rate of lignin in particular is low, the process is comparatively low-cost.

3.5 *Enzymatic Hydrolysis of Cellulose*

The application of enzymes to hydrolyse cellulosic materials is yet another technique that has been developed and has shown promise (Humphrey, 1979 cited in Fan et al., 1989). This technique is favoured because the enzymatic reaction can be carried out under relatively mild conditions. Humphrey (1979, cited in Fan et al., 1989) and other researchers (Mandels et al. 1974) showed that the hydrolysis rate decreases gradually with time. This reduction has been attributed to the production of inhibitors that affect the adsorption of cellulase, the heat and shear inactivation of cellulase, or the decreased susceptibility of the residual cellulose. However, Tanaka et al. (1978) and Mukataka et al. (1983) demonstrated that the hydrolysis rate of cellulose was reduced by agitation

Enzymatic hydrolysis of cellulose degrades cellulose to glucose. This is a heterogeneous catalytic reaction in which the insoluble reactant cellulose is hydrolysed by a soluble catalyst in the enzyme. Both structural features of the cellulose and the form of the enzyme action control the rate of this reaction.

The hydrolysis of native cellulose occurs at a slow rate, and therefore pretreatment prior to hydrolysis is essential to enhance the rate of hydrolysis.

3.5.1 Basic Mechanism of Enzymatic Hydrolysis of Cellulose

Walker and Wilson (1991) summarised the complex system of reactions involved in the enzymatic hydrolysis of cellulose. The system involves the following steps:

1. transfer of enzymes from the bulk aqueous phase to the surface of the cellulose particle;
2. adsorption of the enzymes and formation of enzyme-substrate complexes (ES);
3. hydrolysis of cellulose – resulting in formation of cellodextrins, glucose and cellobiose;
4. transfer of the cellodextrins, glucose and cellobiose, from the surface of the cellulosic particle to the bulk aqueous phase; and
5. hydrolysis of the cellodextrins and cellobiose into glucose in the aqueous phase.

The adsorption of the enzymes and the formation of the enzyme-substrate complexes are considered to be critical steps in the enzymatic hydrolysis of cellulose (Mandels et al., 1971;

Fan and Lee, 1983). Fan and Lee (1983) noted that these steps are influenced by the structural features of the cellulose, the mode of interaction between the cellulase and the cellulose fibre, the nature of the cellulase employed, and the enzyme's susceptibility to product inhibition.

3.5.2 Physical Properties of Cellulase

3.5.2.1 Molecular Weights of Cellulase Components

The molecular weights of various enzyme components range from 5,300 to 76,000 molecular weights (Lee and Fan, 1980). Whitaker et al. (1954, cited in Fan et al., 1987), during their characterisation of a particular cellulase molecule, determined that the cellulase enzyme was asymmetrical – they assessed the molecular weight at approximately 63,000 molecular weights. The smaller particles (molecular weights) measured by Lee and Fan (1980) are thought to possibly represent subunits of normal enzymes.

Whitaker et al. (1954, cited in Fan et al., 1987), during their studies, determined that the enzymatic molecule was cigar shaped approximately 200 Å long and 33 Å wide at its widest point. While the size of the enzyme appears to vary depending on the source micro-organism (Cowling, 1975), the average size tends to be similar to that determined by Whitaker et al. (1954, cited in Fan et al., 1987).

3.5.3 Effect of Cellulase on Cellulose Fibres

Before native cellulose undergoes attack by cellulase, the material exhibits a change in its physical properties. The cellulose undergoes transverse cracking, a loss in tensile strength, lowering of the degree of polymerisation, increased moisture uptake capacity and alkali absorption, and ultimately fragments into short separable fibres (Lee & Fan, 1980).

3.5.4 Properties and Mode of Cellulase Biodegradation

Native cellulose in crystalline form is insoluble in water and its structure and complexity renders it resistant to the hydrolytic action of enzymes. In cellulolytic organisms, several components form the cellulase complexes which hydrolyse the cellulosic substrates.

In 1957 Reese E.T. et al. proposed the (C_1-C_x) hypothesis to explain the mechanism of cellulase hydrolysis of cellulose. This hypothesis involves two enzyme components. The first, C_1, activates or deaggregates the cellulose chains in preparation for the attack by the next hydrolytic component of the cellulase complex. The second component, C_x, hydrolyses these partially degraded cellulose chains, and any soluble derivatives of cellulose. However, highly ordered substrates are not attacked.

3.5.5 Structural Features that Influence the Rate and Extent of Hydrolysis

The structural features of the lignocellulosic substrate influence the rate and extent of cellulose hydrolysis (Stone et al., 1969; and Fan et al., 1980). The structural features of lignocellulosic materials that govern the susceptibility to enzymatic degradation include:

i. the moisture content and swelling of the fibre;
ii. the size and diffusivity of the cellulolytic enzymes and other molecules involved (i.e. possible coenzymes) relative to the size of the capillaries and pores spaces between the microfibrils;
iii. the degree of crystallinity of the cellulose;
iv. the unit cell dimensions of cellulose, including the cell length and surface area;
v. the conformation and steric rigidity of the anhydroglucose units;
vi. the degree of polymerisation of the cellulose;
vii. the nature of the substance in which the cellulose is associated; and
viii. the nature, concentration, and distribution of substituent[11] groups.

The two structural features that have been identified as the most important are surface area and crystallinity (Fan et al., 1980).

---

[11] *Substituent groups* are groups that replace another in a substitution reaction. Like the following example in for the reaction for bromethane with hydroxide:

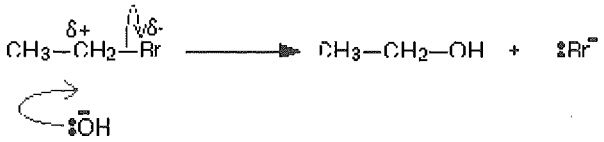

3.5.5.1 Degree of Swelling of the Cellulose Fibre:

The properties of wood and cellulose are profoundly influenced by water. The volumetric swelling of wood in water varies from 9 to 21.1%, depending on the type of wood (Browning, 1963). The expanded capillary structure results in a significant increase in the surface area of the cellulose fibre, and the total area of the swollen material may result in a 100-fold increase in the total area of dried material. This enlarges the fine structure of the material, rendering the substrate more accessible to cellulolytic enzymes. This also facilitates diffusion of extracellular enzymes.

3.5.5.2 Crystallinity of Cellulose:

As outlined earlier, one of the most important structural features that affect the rate of enzymatic hydrolysis is the degree of crystallinity of cellulose. Crystallinity occurs in many forms: in the glucose unit scale, individual glucose units combine to form sheets of ribbons that are hydrogen bonded together into a crystalline form (Figure 3-18). The crystallinity of native cellulose is experimentally determined with an X-ray diffractometer. The X-ray crystallinity index provides a measure of the fraction of crystalline material to the total cellulose. The higher the crystallinity index the greater the crystalline content. Dunlap et al. (1976) analysed the data reported by Baker et al. (1957) and found a relationship between the cellulose crystallinity and digestibility of cotton linter and wood cellulose (Figure 3-21).

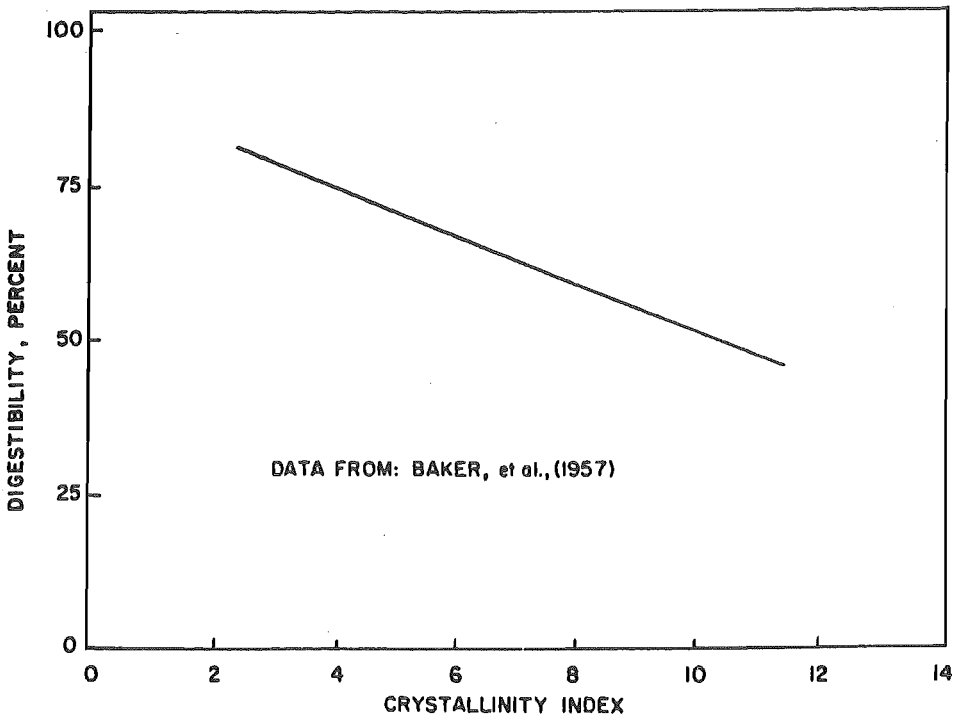

(Source: Fan et al., 1987).

Figure 3-21 Digestibility of cotton linters and wood cellulose against X-ray crystallinity index

In a similar study, Norkrans (1950, cited in Fan et al., 1987) and Walseth (1952, cited in Fan et al., 1987) found that the cellulolytic enzymes degrade the more readily accessible amorphous cellulose, but the enzymes were unable to access the crystalline portions. They observed an increase in crystallinity during enzymatic hydrolysis of cellulose. It is possible that with depletion of the highly accessible material, the substrate becomes more crystalline, thereby offering more resistance to further hydrolysis (Reese et al., 1950, cited in Fan et al., 1987).

3.5.5.3 Extraneous Material – Lignin

Lignin, in combination with partially crystalline cellulose (as found in wood) is one of nature's most biologically resistant materials. Micro-organisms are prevented from degrading the cellulose by the presence of the lignin. While the structure of lignin is well understood, the nature of its association with polysaccharides in wood remains unknown. Three main theories exist regarding the form of the association:

(a) hydrogen bonding between the constituents;

(b) covalent chemical bonds; and

(c) encrustation, thereby preventing easy access by enzymes molecules

Several well-developed methods are available to bring about the disintegration of the cellulose-lignin association, with chemicals that decompose lignin, leaving the cellulose largely intact. These processes are technically called pulping or digestion. The processes are often discounted due to the costs, and the pretreatment process also poses a number of technical problems, e.g., recovery of pulping chemicals and safe disposal of waste chemicals.

Fan et al. (1981) observed that the hydrolysis rate of wheat straw increased substantially with an increase in the extent of delignification (up to about 50% delignification); beyond this, the hydrolysis rate only increased slightly.

3.5.5.4 Capillary Structure of Cellulose

As alluded to earlier, the susceptibility of cellulose to enzymatic hydrolysis is determined primarily by the accessibility of cellulolytic enzymes. Direct physical contact between the enzymes and the substrate molecules of cellulose is a prerequisite to hydrolysis (Fan et al., 1980). This process requires the diffusion of the enzymes into the complex matrix structure of cellulose. Therefore, any structural feature that limits the accessibility of enzymes to cellulose will reduce the extent of cellulose hydrolysis.

The capillary structure of woody material like coconut shell, as utilised in this research, is accessible to water and hydrogen ions. The majority of the cellulose is, however, completely inaccessible to enzymes and, hence, the amorphous material in the wood tends to be slow to hydrolyse. At the same time, these materials tend to have a high degree of swelling (Lee, 1966). An increase in swelling results in an increase in the pore size, typically beyond the critical size necessary for enzyme molecules to penetrate.

The capillary structure of cellulose relative to the size and diffusivity of each cellulolytic enzyme is the most significant structural feature. Direct physical contact between the enzyme and substrate is required before the formation of the enzyme-substrate complex. Ultimately, this complex decomposes and yields the reaction product. It is expected that the rate of this reaction should be a function of the surface area of the cellulosic fibres that is defined by the size, shape, and surface properties of the microscopic capillaries within the fibre, relative to the size, shape, and diffusibility of the cellulolytic enzymes.

The capillary voids in cellulosic fibres come in two forms:

1. gross capillaries – these are physical structures visible under a light microscope, such as the cell lumina, pit apertures, and pit-membrane pores. These voids range in size between 200Å and 10 microns in diameter.

2. cell wall capillaries – such as the spaces among the microfibrils and those among the cellulose molecules in the amorphous regions. These are less than 200Å in diameter (as per Figure 3-22).

The total surface area exposed in the gross capillaries is fairly large, approximately 2 x 10^3 cm^2 per gram of wood or cotton. This is several orders of magnitude smaller than the total surface area exposed within the cell wall capillaries, which is approximately 3 x 10^3 cm^2 g^{-1} (Cowling, 1963). The area exposed on the gross capillary surfaces of one gram of wood or cotton is sufficient to accommodate about 3 x 10^{15} randomly oriented enzyme molecules 200 Å x 35 Å. This is equivalent to 3mg of enzyme protein per gram of wood or cotton.

The cutting or grinding of the wood would produce a considerable additional contact surface between the cellulose and enzyme. Figure 3-22 shows that the pulping of Black Spruce wood substantially increases the mean and distribution of the cell wall capillaries.

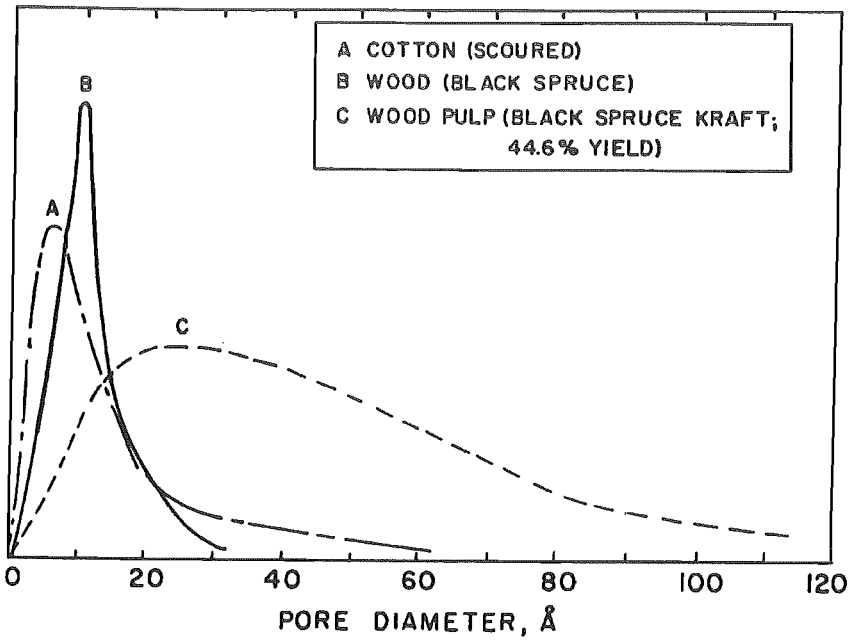

(Source: Cowling and Brown, 1969)

Figure 3-22 The relative frequency distribution of pore diameters of three cellulosic materials

The increase in median and maximum pore sizes during pulping is due in part to the removal of lignin and hemicellulose from the cell wall capillaries.

Since the dimension of cellulolytic enzyme molecules range from 24 to 77 Å in diameter, with an average dimension of 33 Å (Cowling, 1975 and Lee & Fan, 1980), these molecules would be expected to diffuse readily within the gross capillaries and act on cellulose molecules exposed on the surface of these capillaries. As Figure 3-22 indicates, only a small fraction of the cell wall capillaries in water-swollen wood are large enough to allow penetration of most of the cellulolytic enzyme molecules. Hence, cellulolytic enzymes are likely being physically excluded from all but the cell wall capillary. These capillaries are required to enlarge to render them further accessible to the enzymes, either by further swelling or via some other mechanism.

3.5.6 Pretreatment Methods

The proposed coconut shell media, like other hardwoods, exhibits higher ordered packing of cellulose in crystalline regions. This limits chemical reactions to primarily external surfaces of the media. In addition, the lignocellulosic structure of the cell walls within the media ensures that the biodegradation is very slow.

Many different pretreatments have been attempted to enhance the rate and degree of cellulosic hydrolysis in lignocellulosic material. These pretreatments are broadly classified as physical pretreatment, chemical pretreatment, and biological pretreatment according to the principal process on the substrate.

3.5.6.1 Physical Pretreatments

Physical pretreatments are further classified into two general categories, mechanical and non-mechanical pretreatments. Physical forces applied in mechanical pretreatments can subdivide lignocellulosic material into fine particles that are highly susceptible to acid or enzymatic hydrolysis. These smaller particles have a large surface-to-volume ratio, thus rendering cellulose more accessible to hydrolysis. Mechanical grinding also causes reduction in crystallinity, while the non-mechanical forms of physical pretreatments cause decomposition of lignocellulosic material by exposing it to harsh external forces other than mechanical ones.

Milling and Grinding

Ball milling: Ball milling of lignocellulosics and cellulose is an effective method for enhancing enzymatic hydrolysis. The shearing and compressive forces of the ball milling process cause a reduction in crystallinity, a decrease in the mean degree of polymerisation, an increase in bulk density, and a decrease in particle size (Mandels et al., 1974).

Although ball milling is an effective pretreatment method, this technology is often ignored as it is impractical on a large scale because of the lengthy pretreatment time and the cost of processing

Two-roll Milling: This method is commonly practised in the rubber and plastics industries for grinding raw materials, and it has been applied to lignocellulosics primarily to increase their digestibility. The mill consists of two cast-iron surface rolls placed horizontally with an adjustable roll clearance to control the degree of milling.

Two-roll milling decreases the crystallinity and the degree of polymerisation; nevertheless, its effects on lignin are not well understood. The susceptibility of enzymatic attack is controlled by the clearance between the mill rolls and the process time. According to Spano et al. (1977), as the clearance between the rolls decreases and the processing time increases, the susceptibility of a substrate to hydrolysis increases.

Hammer Milling: A hammer mill comprises a rotor with a set of hammers attached. As the rotor turns, the hammers impact on the substrate against a breaker plate. Hammer milling has been applied as a form of lignocellulosic pretreatment. Mandels et al. (1974) measured the effect of hammer milling on the digestibility of newspaper and found a slight increase in susceptibility to digest the hammer-milled newspaper over that of untreated newspaper.

Colloid Milling: A colloid mill consists of two disks set close to each other revolving in opposite directions while the substrate slurry is passed between them. Pretreatment by means of colloid milling has been attempted, and Mandels et al. (1974) obtain modest improvements in the susceptibility of cellulose to be digested. They concluded that the high operational costs make this pretreatment uneconomical on a large scale.

Vibro Energy Milling: Vibro energy milling is similar to ball milling except that the mill is vibrated instead of being rotated. Vibro energy milling provides effective size reduction and increases in digestibility of lignocellulosics (Millet et al., 1979). Pew (1957) observed that vibratory milling of spruce and aspen wood markedly enhanced their susceptibility to enzymatic hydrolysis.

Pyrolysis

Pyrolysis is the chemical decomposition occurring as a result of high temperatures. Pyrolysis has been investigated as a process by which to increase the susceptibility of cellulosic material to hydrolysis. Above 300°C, cellulose rapidly decomposes to produce gaseous and tarry compounds, which leave a small amount of char residue upon evaporation. At intermediate temperatures, however, decomposition proceeds slowly and relatively few volatile products are formed.

In the presence of oxygen, pyrolytic depolymerisation, oxidation, and dehydration are accelerated. Depolymerisation occurs more slowly in an inert atmosphere, but the formation of unwanted by-products of oxidation and dehydration are also retarded. Moreover, the addition of a zinc chloride catalyst has been reported to cause decomposition of pure cellulose at a much lower temperature.

Fan et al. (1981a) observed a negligible change in the crystallinity index and surface area of Solka Floc upon pyrolysis pretreatment at 170°C in an air or helium atmosphere.

High Energy Radiation

The digestibility of cellulose and lignocellulosics is enhanced by high-energy radiation (Beardmore, 1980; Millett and Baker, 1975). The irradiation of pure cellulose results in oxidative degradation of the molecules and dehydrogenation, as well as the destruction of anhydroglucose units to yield dioxide and cellulose chain cleavage (Millett, 1970, cited in Fan et al., 1987). Fan et al. (1980, cited in Fan et al., 1987) found that gamma irradiation was very effective in increasing the crystallinity index. The resulting increase in the surface area was due to extensive depolymerisation. They observed that the hydrolysis rate increased only after the dosage exceeded a certain level.

Dunlap and Chiang (1980) noted that irradiation appears to be strongly species selective; for example, the digestion of aspen carbohydrate is essentially complete after an electron dosage of 10^8 rad, while spruce was only 14% digestible at this dose.

High Pressure Steaming

High pressure steaming is a pretreatment method where the substrate is treated with steam under pressure at high temperatures and generally without any addition of chemicals. This process cleaves the acetyl groups and provides an acidic medium conducive to hydrolytic action.

Nesse et al. (1977) investigated this form of pretreatment to manure fibres. These fibres were autoclaved for 5, 10, and 30 minutes at temperatures ranging from 130 to 200°C. It was found that the optimum steam treatment was at 30 minutes at 175°C.

Extrusion and Expansion

Two pretreatments similar to high pressure steaming are moist-heat expansion (extrusion) and dry-heat expansion (popping). Brenner et al. (1977) pretreated newspaper by the extrusion technique for acid hydrolysis and obtained significant improvements in cellulose hydrolysis. They suggested that extrusion may be a promising pretreatment method for acid hydrolysis.

Microwave Treatment

Ooshima H. et al. (1984, cited in Fan et al., 1987) subjected rice straw and bagasse[12] to microwave irradiation, and found that enzymatic hydrolysis was enhanced markedly by this pretreatment. They found that the enzymatic hydrolysis rate for pretreated bagasse was 3.2 times that of the untreated bagasse.

3.5.6.2 Chemical Pretreatments

Chemical pretreatments are typically used to remove the lignin surrounding the cellulose, and to destroy its crystalline structure. Traditionally the paper industry has been pulping the

---

[12] Bagasse, derived from sugar cane, is a typical cellulosic waste product, and contains on a dry matter basis about 40% cellulose, 27% hemicellulose, 20% lignin, and 13% water-soluble substances (Playne, 1984).

cellulosic material for delignification with the aim of producing high strength, long fibre paper products. However, these processes are deemed to be overly severe and expensive for pretreatment of lignocellulosics.

Alkalis

Sodium Hydroxide: Dilute NaOH treatment of lignocellulosic material causes swelling, leading to an increase in the internal surface area, decrease in the degree of polymerisation, decrease in the crystallinity, separation of structural linkages between lignin and carbohydrates, and disruption of the lignin structure (Fan et al., 1987). Various substrates respond differently to sodium hydroxide treatment. Feist et al. (1970, cited in Fan et al., 1987) observed that the digestibility of softwoods with high lignin content increased slightly with NaOH pretreatment, while the digestibility of some hardwoods and other lignocellulosic materials with low lignin content increased significantly upon NaOH treatment.

Ammonia: This pretreatment for increasing the digestibility of straw was first patented by Lehmann in 1905 (cited in Fan et al., 1987). Moore et al. (1972, cited in Fan et al., 1987) treated aspen with liquid ammonia and found that the percentage yield of reducing sugar as glucose increase from 11% for untreated aspen to approximately 36% for NH_3 treated aspen. This increase was attributed mostly to the swelling in water subsequent to the pretreatment.

Ammonium Sulphite: Ammonium sulphite has been employed mainly in conventional pulping processes. The shredded material is treated with $(NH_4)_2SO_3$ under high pressure and elevated temperature. The resultant pulp has a residual lignin content of 15% and a dietary energy equivalent of medium quality hay.

Acids

Acids serve primarily as catalysts for hydrolysis of cellulose rather than as reagents for pretreatment (Brenner et al., 1977). Acid hydrolysis of cellulose on an industrial scale was started during the First World War. While various acids have been utilised to improve the hydrolysis process, their performance is variable. Sulphuric acid (Tsao et al., 1978, cited in Fan et al., 1987) and phosphoric acid (Walseth, 1952, cited in Fan et al., 1987) have been demonstrated to improve the hydrolysis process.

Sulphuric Acid: Tsao et al. (1978, cited in Fan et al., 1987) pretreated lignocellulosics with sulphuric acid. The resultant pentose fraction was separated by a mild acid while the remaining residue was dried and mixed with concentrated acid (70-80%) to dissolve the cellulose, which eventually was precipitated from the solution by the addition of methanol. This precipitated cellulose was amorphous and could be easily saccharified by acid or enzymatic hydrolysis.

Hydrochloric Acid: Rice straw was pretreated with 3% HCl at 130°C for 4 hours by Han and Callihan (1974). Compared to the control, the cell yield of the bacteria grown on the treated substrate decreased.

Phosphoric Acid: Walseth (1952, cited in Fan et al., 1987) investigated the possible pretreatment of cellulose with phosphoric acid. Phosphoric acid (85%) was used to saturate the samples for two different periods of time, 10mins and 2 hrs. The substrates obtained were swollen and amorphous and hence were highly reactive to enzymatic degradation.

<u>*Gases*</u>

Chlorine Dioxide: Chloride dioxide is an active agent of the chlorite pulping technique. By passing ClO_2 through a bed of dried and ground wheat straw, Sullivan and Hershberger (1959) determined that the maximum increase in the *in vitro* digestibility of treated wheat straw was 43% more than the untreated wheat straw. They postulated that the increase was attributable to decomposition of lignin by chlorine and its oxides.

Nitrogen Oxides: A pulping scheme involving nitrogen oxides was investigated by Brink et al. (1974). It gave a rapid rate of delignification and a higher overall sugar yield than conventional pulping processes at comparable lignin contents. These results indicate that nitrogen oxides may provide an effective pretreatment for enzymatic hydrolysis.

Ozone: In an ozone pretreatment of wheat straw, Fan et al. (1982) obtained a drastic increase in the biodegradability of cellulose. Ozone was observed to attack both lignin and carbohydrates, though the reaction rate of carbohydrate was slower.

Other oxidizing agents

Hydrogen Peroxide: The action of H_2O_2 with Fe^{2+} as a catalyst causes cotton cellulose to oxidise and decompose to CO_2 (Halliwell, 1961). This reaction is thought to be similar to what takes place when brown-rot fungus degrades lignocellulosics.

Peracetic Acid: Fan et al. (1981b) obtained a significant increase in the digestibility of wheat upon peracetic acid pretreatment. This increase was attributed to extensive delignification by this pretreatment.

Cadoxen: Cadoxen is an alkaline solution containing ethylene diamine and water. This solution can readily dissolve cellulose and can be reprecipitated into a soft floc by adding excess water. This pretreatment has the disadvantage of solvent toxicity and high cost (Burgess and Binnie, 1990).

CMCS: CMCS is composed of sodium tartrate, ferric chloride, sodium sulphite, and sodium hydroxide solution. The CMCS solvent dissolves cellulose that precipitates easily by adding excess water. CMCS dissolves less cellulose than cadoxen, but it is non-toxic.

3.6 References

Averill B.A., and Tiedje J.M. (1982) Hypothesis: The chemical mechanism of microbial denitrification, FEBS Letters.

Aylward G., and Findlay T. (1994) SI Chemical Data, 3rd Edition, Jacaranda Wiley Ltd, Milton, Australia, pp. 180

Beardmore D.H. and Fan L.T., Lee Y-H (1980) Gamma-ray irradiation as a pretreatment for the enzymatic hydrolysis of cellulose, Biotechnological Letters, Vol. 2, pp. 435-438

Brenner W. et al. (1977) In: New approaches for the acid hydrolysis of cellulose. Dept. of Appl. Sci., New York Univ., NYU/DAS-77-30, New York

Brink D. L et al. (1974) In: Abstracts of papers of the 167th Amer. Chem. Soc. Meeting, Los Angeles, Ca., March 31-April 5

Browning B.L. (1963) The chemistry of wood, Interscience, New York, 429 p.

Buchanan, R. E. and Gibbons N. E. (1974) Bergey's Manual of Determinative Bacteriology, 8th ed., Williams & Wilkins, Baltimore.

Burgess, H. D. and Binnie N. E. (1990) The Development Of A Research Approach To The Scientific Study Of Cellulosic And Ligneous Materials, JAIC 1990, Vol. 29, No.2, pp. 133-152

Cady F.B., and Bartholomew W.V. (1963) Investigations of nitric oxide reactions in soils., Soil Sci. Soc. Am. Proc., Vol 27, pp. 546-549

Conn E.E., and Stumpf P. K., Bruening G., Doi R.H. (1987) Outlines of Biochemistry 5/E. John Wiley & Sons, New York, 693p.

Cooper P.F. and Atkinson B.(1981) Biological Fluidised Bed Treatment of Water and Wastewater. Ellis Horwood Publishers, Chichester, England

Cowling E.B. (1963) In: Advances in enzymatic hydrolysis of cellulose and related material, Reese E.T. editor, Pergamon, New York, pp. 1

Cowling E.B. (1975) Physical and chemical constraints in the hydrolysis of cellulose and lignocellulosic materials, In: Biotechnol. & Bioeng. Symp., editor Wilke C.R., No. 5, John Wiley & Sons, New York, pp. 163-181

Cowling E.B., and Brown W. (1969) In: Cellulases and Their Applications, Adv. Chem. Ser., Eds. Hajny GJ & ET Reese, Vol. 95, pp. 152

Dennis D.T., and Preston R.D. (1961) Constitution of cellulose microfibrils, Nature, Vol. 191, London, pp. 667-668

Dunlap C.E., and Chiang L.C. (1980) In: Cellulose degradation – a common link, Shuler M.C. editor, CRC Press, New York

Dunlap C.E., and Thomson J., Chiang L.C.(1976) Treatment processes to increase cellulose microbial digestibility, AIChE Symposium Series 72, Vol. 158, pp. 58

Ergun S. (1952) Fluid flow through packed columns. Chemical Eng. Process, Vol. 48, No. 2, pp. 89-93

Evans, W.C. (1977) Biochemistry of the bacterial catabolism of aromatic compounds in anaerobic environments., Nature (London), Vol. 270, pp. 17-22

Fan L T., and Lee Y-H, Beardmore D.H. (1981) Communication with editor: The influence of major structural features of cellulose on rate of enzymatic hydrolysis, Biotechnol. Bioeng., Vol. 23, pp. 419-424

Fan L.T., and Lee Y.H. (1983) Kinetic studies of enzymatic hydrolysis of insoluble cellulose: derivation of a mechanistic kinetic model. Biotechnol. Bioeng., Vol. 25, pp. 2707-33

Fan L.T., and Lee Y-H, Beardmore D.H. (1980) Major chemical and physical features of cellulosic materials in substrates for enzymatic hydrolysis, In: Adv. Biochem. Eng., Vol. 14, Fiechter A. editor, Springer, New York, pp. 101-117

Fan L.T. et al. (1982) In: Fiechter A. (ed) Adv Biochem Eng, Vol. 23, Springer, Berlin Heidelberg New York, pp. 157

Fan L.T., and Gharpuray M.M., Lee Y.H. (1987) Cellulose Hydrolysis, Springer-Verlag, New York. 198p.

Federova M.K., and Mileklina E.I., Ilyukhina N.I. (1973) Possibility of using the "gas exchange" method to detect extraterrestrial life: identification of nitrogen-fixing organisms. Akad. Nauk SSr Izvestia Ser. Biol., Vol. 6, pp. 797-806

Fillery I.R.P. (1979) Denitrification in soils under low oxygen or anaerobic environments. Diss. Abstr. Int., Vol. B40, pp. 1529

Garrett R. H. and Grisham C. M. (1999) Biochemistry, Second Edition. Saunders College Pub. Harcourt Brace College Pub., Florida, U.S.A. 1273p.

Gayle B. P., and Boardman G. D., Sherrard J. H., Benoit R. E. (1989) Biological denitrification of water. ASCE, J. Enviro. Engrg. Vol. 115, No. 5, Oct. pp. 930-943

Green A.H. (1991) Coconut productions: present status and priorities for research, World Bank technical paper, Washington, U.S.A.

Green M., and R. E. Loewenthal, M. Schnitzer, S. Tarre. (1994) Denitrification of drinking water – a biological evaluation. Water SA, Vol. 30, No. 3, July, pp. 223-230

Hach Company (1997) Water Analysis Handbook, Loveland, Colorado, U.S.A., 1309p.

Halliwell G (1961) The action of cellulolytic enzymes from Myrothecium verrucaria, Biochem. J., Vol. 79, pp. 185-192

Han Y.W., and Callihan C.D. (1974) Cellulose fermentation: effect of substrate pretreatment on microbial growth, Appl. Microbiol., Vol. 27, No. 1, pp. 159

Hooper A.B. (1978) Nitrogen oxidation and electron transport in ammonia-oxidising bacteria. In: Microbiology-1978, D. Schlessinger editor, ASM Publications, Washington, pp. 299-304

Koike I., and Hattori A. (1975) Energy yield of denitrification: An estimate from growth yield in continuous cultures of Pseudomonas denitrificans under nitrate, nitrite and nitrous oxide-limited conditions. J. Gen. Microbiol., Vol. 88, pp. 11-19

Lee G.F. Jr (1966) Physical factors affecting enzymatic hydrolysis of cellulose, M.Sc. Thesis, Syracuse Univ., Syracuse N.Y. 69p.

Lee Y-H., and Fan L.T. (1980) Properties and mode of action of cellulase, In: Adv. Biochem. Eng., editor Fiechter A., Vol. 17, Springer-Verlag, New York, pp. 101-129

Leva M. (1959) Fluidization, McGraw-Hill, N.Y., pp. 327.

Leva M., Shirai T., and C. Wen (1956) La prevision de debut de la fluidisation des les lits solides granulaires. Genie Chim., Vol. 75 pp. 33-42

Mandel M. and Reese E.T. (1965) Inhibition of cellulases. In Annual Review of Phytopathology, Vol. 3, ed. J G. Horseford & K.F. Baker. Annual Review, Inc., Palo Alto, pp. 85-102

Mandels M., and Hontz L., Nystrom J. (1974) Enzymatic hydrolysis of waste cellulose, Biotechnol. Bioeng., Vol. 16, pp. 1471-1493

Mandels M., and Hontz L., Nystrom J. (1974) Enzymatic hydrolysis of waste cellulose, Biotechnol. Bioeng., Vol. 16, pp. 1471-1493

Mandels M., and Kostick J., Parizek R. (1971) The use of adsrobed cellulase in the continuous conversions of cellulose to glucose. J. Polyer Sci., Vol. C(36), pp. 445-59

Marchessault R.H., and Coulombe S., Morikawa H., Robert D., (1982) Can. J. Chem., Vol. 60, pp. 2372

Millett M.A. and Baker A.J. (1975) Pretreatments to enhance chemical, enzymatic and microbiological attack of cellulosic materials, In: Biotechnol. & Bioeng. Symp., Wilke C.R. editor, No. 5, John Wiley & Sons, New York, pp.193-219

Miyata M. (1971) Studies on Denitrification. XIV. The electron donating system in the reduction of nitric oxide and nitrate. J. Biochem. (Tokyo) Vol. 30, pp. 205-213

MSDS (2004) Sodium Azide July 18th, http://www.jtbaker.com/msds/englishhtml/s2906.htm

Mukataka S., and Tada M., Takahashi J. (1983) J. Ferment. Technol. Vol. 61 pp. 615

Nathanel W.R.N. (1964) Coconut Shells as Industrial Raw Material, Coconut Bulletin, Vol. 18, No. 3-4, pp. 163-183

Nesse N and Wallick J., Harper J.M. (1977) Pretreatment of cellulosic wastes to increase enzyme reactivity, Biotechnol. Bioeng., Vol. 19, pp. 323-336

Nömmik H. (1956) Investigations on denitrification in soil., Acta Agric. Scand., Vol. VI 2, pp. 195-228

Ohler J.G. (1984) Coconut, tree of life., FAO Plant Production and Protection Paper No. 57, Food and Agriculture Organisation of the United Nations, Rome.

Panshin A.J., and de Zeeuw C. (1980) Textbook of Wood Technology, 4th Ed., McGraw-Hill, New York, 722 p.

Payne W.J. (1973) Reduction of nitrogenous oxides by microogranisms. Bacteriol. Rev., Vol. 37, pp. 409-452

Payne W.J. (1981) Denitrification, John Wiley & Sons, New York, 214 p.

Pew J.C. (1957) Properties of powered wood and isolation of lignin by cellulytic enzymes, TAPPI (Technical association of the pulp and paper industry), Vol. 40, pp. 553-558

Playne M.J. (1984) Increased digestibility of Bagasse by pretreatment with Alkalis and steam explosion, Biotechnol. Bioeng., Vol. 26, pp. 426-433

Preston R.D. (1986) Natural Celluloses, In: Cellulose: structure, modification, and hydrolysis, Young R.A., and Rowell R.M. ed., John Wiley & Sons, New York, U.S.A. pp. 3-27

Prosser J. I. (1986) Nitrification, Special Publications of the Society for General Microbiology, Vol. 20, Oxford: IRL Press

SafeLab (2003) C-100 Impregnated Carbon Filters, http://www.ssfelab.co.uk/filters.pdf

San Diego Earth Times On-Line (2000) Sodium azide in car airbags poses a growing environmental hazard, August, http://www.sdearthtimes.com/et0800/et0800s9.html

Spano L., and T. Tassinari, C. Macy, and E. Black. (1977) Pretreatment And Substrate Evaluation For The Enzymatic Hydrolysis Of Cellulosic Wastes, U.S. Environmental Protection Agency, Washington, D.C., EPA-600/7-77/038

Sullivan J.T. and Hershberger T.V. (1959) Effect of Chlorine Dioxide on lignin content and cellulose digestibility, Science, Vol. 130, pp. 1252-1252

Tanaka M., and Takenawa S., Matsuno R., Kamikubo T. (1978) Some factors affecting cellulose degradation with Pellicularia filamentosa cellulases, J. Ferment. Technol., Vol. 56, pp. 108

Volokita, M., and Belkin S., Abeliovich A., Soares M. (1996) Biological Denitrification of Drinking Water using Newspaper, Wat. Res. Vol. 30, No. 4, pp. 965-971

Walker L.P., and Wilson D.B. (1991) Enzymatic Hydrolysis of Cellulose: An Overview; in Enzymatic Hydrolysis of Cellulose, Walker L.P. and Wilson D.B. ed., Elsevier Science Publishers Ltd, England, pp. 3-14

Weast R.C. (1976) Handbook of Chemistry and Physics, 57th Edition, CRC (Chemical Rubber Company) Press, Cleveland, U.S.A.

Werther J. (1983) Fundamentals of fluidized bed technology. German Chemical Eng. Vol. 6, pp. 228-235

Wientjes, F.B. and Kolk A. H. J., Nanninga N., Riet J. Van'T (1979) Respiratory nitrate reductase: Its localization in the cytoplasmic membrane of Klebsiella aerogenes and Bacillus licheniformis. Eur. J. Biochem., Vol. 95, pp. 61-67

Young R.A., and Rowell R.M. (1986) Cellulose: structure, modification, and hydrolysis. John Wiley & Sons, New York, U.S.A. 379p.

Zehnder A.J.B. (1988) Biology of anaerobic microorganisms. John Wiley & Sons, Inc., New York, U.S.A., pp. 872

Zeikus J.G. (1980) Fate of lignin and related aromatic substrates in anaerobic environments. In: Lignin biodegradation: microbiology chemistry and potential applications, T.K. Kirk, T. Higuchi and H.-m. Chang eds., CRC Press, Boca Raton, Fla., pp. 101-109

4 Experimental Equipment and Methodology

4.1 Experimental Equipment

The experimental trials were conducted in the Environmental Control Rooms located in the Environmental Engineering Laboratory at the University of Canterbury.

All the experiments were conducted in an ambient air temperature of 35°C and room humidity of 25%.

This research utilised two lab scale vessels to conduct two series of parallel studies. The first and second set of trials were conducted in 6L batch reactors comprising an Erlenmeyer flask, magnetic stirrer and other sundry equipment to allow fluid and gas samples to be taken. The third series of experimental trials were conducted in two 11.3 L purpose-built fluidised bed reactors.

4.1.1 Crushing of Coconut Fragments

To reduce the shells of the coconut to a manageable size, a combination of manual hammering and mechanical grinding was utilised. The coconut shell was reduced to 30mm trapezoidal shapes by hammer and then fed into a mechanical grinder.

The mechanical grinder employed (Baukneckt SK1, 1.1kw) progressively ground the coconut shell in a chamber till it passed the fragments through either a 10, 8, or 4mm sieve. The 4mm sieve was not utilised as the superficial fluid velocity of the resultant product was difficult to control, and the low yield of useable material as the grinder sieve size decreased.

The grinder product contained a significant proportion of fines. These were dry sieved off through a 2mm stainless steel sieve to yield the final product utilised in this research.

4.1.2 Batch Reactors

Each batch reactor consisted of a 6L Erlenmeyer flask placed on a magnetic stirrer to ensure the fluid within the reactor remained homogeneous (Figure 4-1).

A rubber stopper with sampling tubes was used to isolate the reactor from the outside environment. The sampling tubes and stopper arrangement was constructed out of soft rubber with three stainless steel tubes (2 mm I/D) penetrating through the rubber into the reactor at predetermined lengths. The length of the tubing allowed fluid to be sampled from the bottom of the flask. While the remaining tubes terminated in the headspace of the reactor, allowing gas samples to be taken from second tube, whilst the third tube was connected to a balloon containing an inert gas (helium). The gas would replace any displaced fluid or gas taken from the reactor.

The positive pressure of the helium balloon prevented the unwanted entry of atmospheric gases (in particular oxygen) into the reactor during the trials.

Plastic syringes (60 mL) were used to draw off the fluid samples via a 16-gauge needle (as demonstrated in Figure 4-1). A slow withdrawal rate was required ($\approx$ 5 mL/sec) to ensure that any gases in the fluid were not pulled out of the solution by the negative pressure in the syringe. When excessive negative pressure was applied, small gas bubbles formed on the side of the syringe.

Trial studies comparing the measured DO in the reactor directly to that obtained by drawing the fluid via the elevated sample tube and syringe showed that the variation in oxygen concentration was minimal, in the order of 3% (Appendix A).

The trial studies identified that as the rate of withdrawal increased; more oxygen was lost during the withdrawal process. This loss is thought to be due to the formation of small bubbles (observed) as a result of the negative pressure within the syringe.

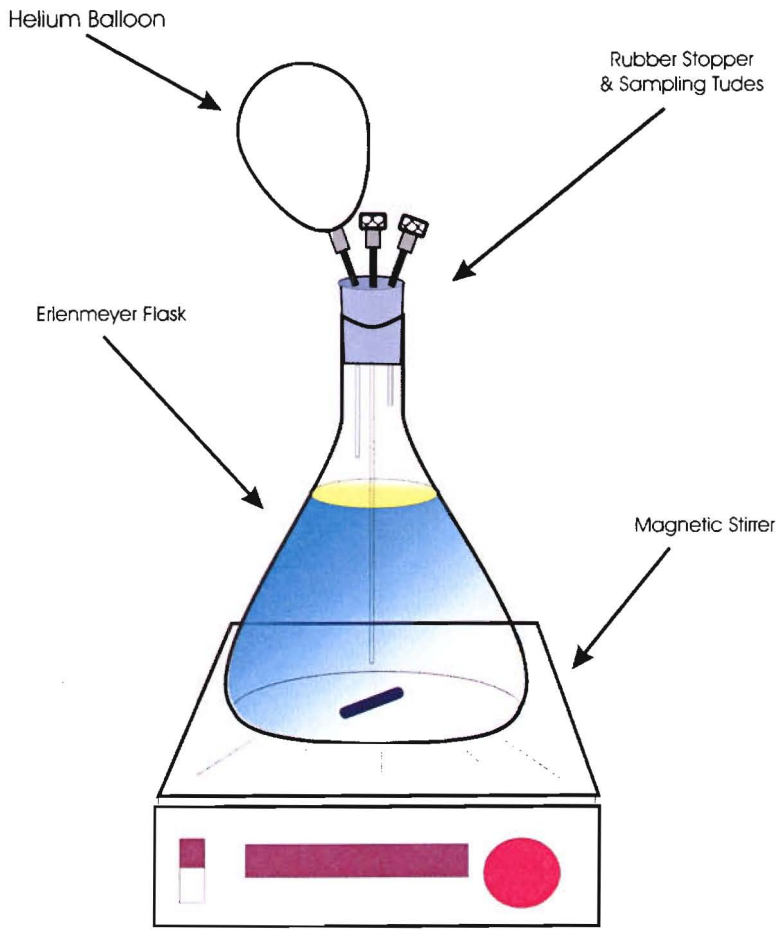

Figure 4-1 Schematic of the configuration of batch reactor

The magnetic stirrer ensured adequate mixing/interchange of the reactor fluid. During the denitrification batch reactor trials the rate of stirring was limited to ensure that adequate fluid exchange occurred yet the fluid velocities were not excessive to inhibit any extra-cellular enzymatic processes or even denaturantion of the enzymes (Schmid, 1979). The stirrer tended to operate at 50-100 rotations/min.

4.1.3 Fluidised Bed Reactor

Two FBR reactors were constructed, to allow two parallel trials to operate on the same influent feed. The FBR reactor was an 86mm tube with a diffusion chamber and settling chamber. The pumped recycle (superficial fluid) maintained the coconut shell fragments in a fluidised state.

4.1.3.1 Configuration of the Fluidised Bed Reactor

The fluidised bed reactor comprises seven major components, as illustrated in Figure 4-2:

- influent storage tank
- influent dosage pump
- recycle pump
- fluidised Bed Reactor (FBR), which comprises the following subunits:
    - diffusion chamber
    - reactor column
    - settling chamber
- treated effluent tank

A common influent feed tank to the two FBRs was used, comprising of an 80L HDPE tank in which the influent was mixed and stored. As summarised in Table 4-7, tap water was augmented with nitrate and nutrients, and was typically produced in batches that would feed two reactors for approximately 25 days.

A dedicated Masterflex L/S Tubing Pump (7553-85, 1-100 rpm), with an EasyLoad Tubing Pump Head (7518-00) fed the influent to the reactors. The influent entered the bioreactor and mixed with the internal recycle on the inlet side of the internal recycle pumps.

The rate of influent was controlled by the selection of the pump tube diameter and the speed and duration of pumping. To achieve an adequate and controllable influent flow rate, the influent pump was pulse operated. An Allen-Bradley MicroLogix 1000 Programmable Logic Controller (PLC) was utilised to control this process. While the PLC was capable of monitoring analogue and digital inputs, these functions were not utilised. Instead, the internal timer function was used to determine the period that the dosage pump would operate. The PLC offered the advantage of operating the dosage pumps at distinct switching cycles, while allowing for easy monitoring and change of the programme mid-stream via an RS232 connection to a personal computer.

The recycle pump was responsible for maintaining the coconut fragments in a suspended state. Unfortunately, a common recycle pump was unable to be sourced for this experiment. Two different pumps with similar pump curves were utilised (both were manufactured by Davis Pumps, Reactor #1: 0.124HP, 2650rpm, and Reactor #2: 0.17HP, 2850rpm). Both pumps were fixed speed pumps, and the uncontrolled discharge was excessive; thus, both were throttled back via a knife valve until they both discharged at the same rate and provided a similar fluidised bed depth.

The FBR reactor was constructed in three parts: the diffusion chamber, the FBR reactor tube, and a settling chamber. Table 4-1 below provides a summary of the FBR reactor dimensions. The reactor tube was constructed from 85mm (ID) laboratory glass tube (4mm wall thickness).

Table 4-1 Physical Characteristics of the Fluidised Bed Reactor

	Length	Volume
Settling Chamber	500 mm	0.24 L
Reactor Tube	1400 mm	7.04 L
Diffusion Chamber	300 mm	4.08 L
Total	2200 mm	11.26 L

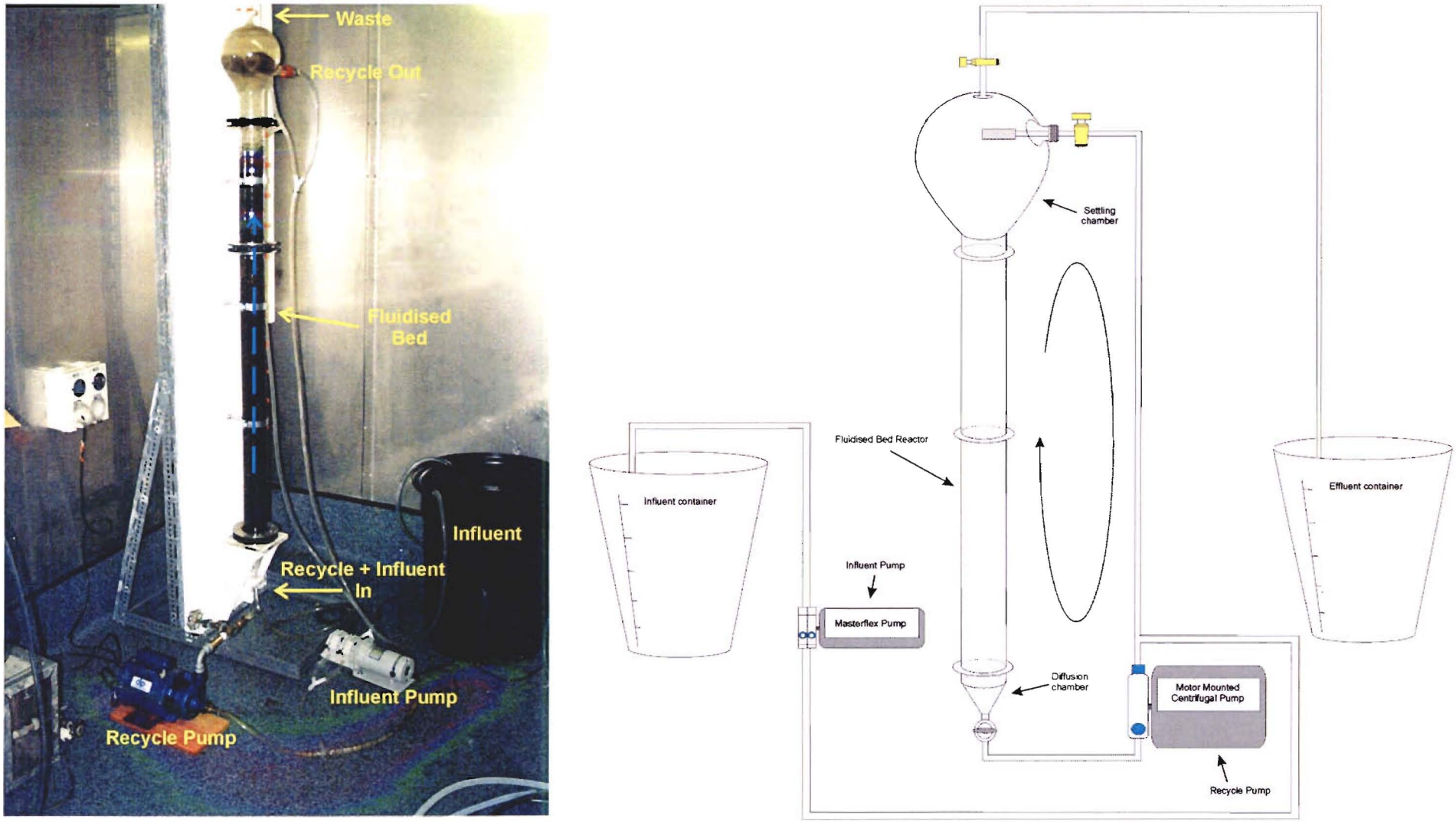

Figure 4-2 Schematic of the configuration of the fluidised bed reactor.

To prevent the inflow into the reactor column acting like a jet and flushing the bed material from the reactor column, a diffusion chamber was provided. The gradual increases in cross-sectional areas, in conjunction with the set of Perspex and stainless steel diffusers, ensured the upflow was evenly distributed across the reactor column.

It was necessary to make the bioreactor modular to allow for periodic dismantling and cleaning. The two-part construction of the reactor column allowed for a variety of possible column heights. In the initial scoping investigation into this project, it was thought that it would be necessary to change the length (hence volume/HRT) of the reactor, but that option was not required.

To ensure that only the superficial fluid is recycled, a settling chamber-recycle filter arrangement was incorporated. The settling chamber was designed so that the superficial fluid velocity declined as the cross-sectional area of the chamber increased. A majority of the suspended matter would fall out of suspension and settle back into the reactor column. To prevent fragments of the substratum entering the recycle line and potentially blocking the line or damaging the recycle pump, a stainless steel gauze filter was constructed around the recycle intakes.

4.1.3.2 Design of the Fluidised Bed Reactor

Design considerations

The primary design consideration was balancing the superficial fluid velocity required to maintain a bed fluidisation while ensuring that the fluid velocity was not excessive as to strip the biomass from the substrate and/or disrupt the biological enzymatic processes.

Another design consideration was the requirement of providing effective mixing of the influent with the superficial fluid. This was achieved by pumping the influent feed into the recycle line downstream of the recycle pump. Turbulent mixing provided by the centrifugal recycle pump, in conjunction with natural diffusion within the reactor and the coconut fragments provided, would achieve effective mixing.

The final design was determined by following the consideration and assessment of the following design parameters:

- hydraulic retention time
- height of the reactor column
- height of the fluidised bed zone
- amount of bed expansion
- distribution of substratum/substrate particulate diameter (representative diameter)
- dosage rate (nutrients, DO, nitrates)
- substratum/substrate density
- effect of biomass on the substratum/substrate density
- kinematic viscosity of the superficial fluid

As outlined in Section 3.1.2, the ratio of the superficial fluid velocity to the superficial fluid velocity at the onset of fluidisation (u/u_{mf}) determines the state of the fluidised bed. This ratio was the most important design parameter, and many of the other design parameters were dependant on this ratio.

The design process involved evaluating the interaction between these variables and developing a suitable reactor configuration that was consistent with the available material sizes (i.e. reactor tube diameters, tube lengths and pump flow rates etc.). The primary design variable, the superficial fluid velocity, was applied to an analytical model of the physical processes occurring within the reactor to assess the effect on an idealised substrate and attached biomass.

The two design equations outlined in Chapter 3.1 on Biological Fluidised Beds (Eqn. 3-3 Werther, 1983, and Eqn. 3-4 Leva, 1959) were applied to evaluate the superficial fluid velocity required to maintain the bed in a fluidised state (Appendix B).

Once a suitable design velocity and the cross-sectional area of the reactor are determined, the minimum flow rate can be evaluated. In turn allows the recycle pump flow rate envelop to be determined. A further safety factor of 2 was then applied, to allow some redundancy in the design and compensate for unforeseen head losses. The selection of the safety factor of 2 is consistent with the selection of fluidisation pumps in full scale operations, which vary from 1.5 to 3.0 .

While a variable speed pump would have been ideal, a fixed speed pump with a valve to throttle the flow was utilised. The pumps operated could deliver a flow of 2 L/s at a total head of 2m.

Fluidised Bed Reactor Material Selection

Several materials were considered in the construction of the fluidised bed reactor tubes. The materials that were thoroughly assessed included uPVC, mPVC, glass, and acrylic or polycarbonate tubing. Ultimately, glass was selected due to its wear characteristics, transparency, and inert nature. While glass appears to be the ideal material, the fabrication of the fluidised bed reactor required specialised skills, and the brittle nature of glass and lack of tensile strength were issues that were overcome during the course of the research.

Fortunately the Chemistry Department at the University of Canterbury employs skilled glass blowing technicians who were able to fabricate the necessary equipment for this research project.

Size constraints of the laboratory and the inevitable handling of the equipment required the fluidised bed reactor design to be modular, with the reactor divided into manageable sections. A glass flanged connection was provided for each of the modular elements.

Since glass is brittle and offers little tensile strength, special attention in the detailing of the flange-to-flange connection was required. To maintain a water-tight seal it was necessary to supply sufficient compressive force to hold the flanges together; any uneven point load on the flange had the potential to crack the flange, as experienced a couple of times during the development of the flange seal.

The solution adopted was to sandwich a RTV-Latex-RTV layer between the two surfaces of the flanges. This layer allowed in the order of a 1 mm differential settlement between the flanges while still maintaining a watertight seal. The self-weight of the column was insufficient to hold the flanges together and therefore it was necessary to use a clamp, which involved screwing together four half-circle stainless plates offset by 90 degrees. A soft rubber washer ensured that an even load was applied to the flange, while the stainless steel screws tapped into the bottom plates applied the compressive force that held the flanges together (Figure 4-3).

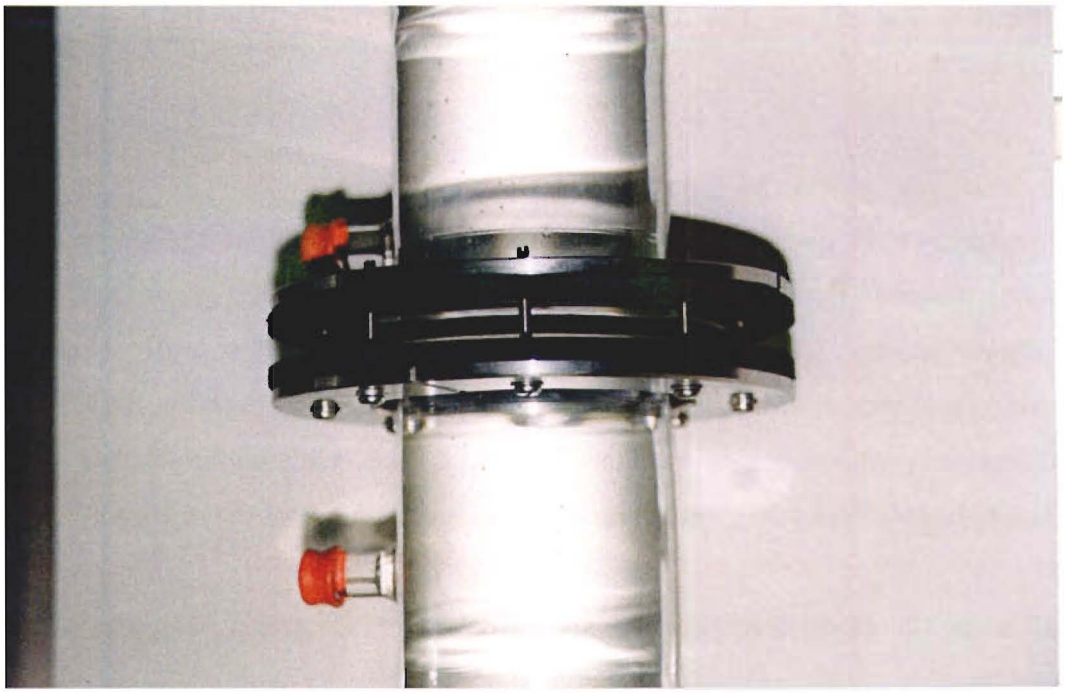

Figure 4-3 Connection detail between the flanged reactor sections.

Tubing Material Selection

A combination of PVC and HDPE tubing was used. PVC tended to be used where flexibility was required, e.g.: attaching to the valves on the inlet and outline connections of the reactor and the pump whilst 16mm HDPE tubing provided the internal recycle pipework.

Issues Encountered with the Design:

Below is a summary of several of the problems identified with the design during the construction and initial operation:

While the initial calculations (Appendix B) determining the recycle pump selection were adequate to maintain the media in suspension, the head losses associated with the entry and exit conditions in the fluidised bed reactors and other associated fittings (bends, diffusers, filters) were not fully appreciated. As a result larger recirculation pumps were installed.

The flanged reactor connection (Figure 4-3) between the glass flanges of the reactor components was developed through a series of trial and breakages. The final solution (with the stainless steel clamps) ensured that the RTV-Latex-RTV seal did not leak once the reactor was operational.

During the operation of the two fluidised bed reactors it was difficult to maintain a similar influent dose to the two reactors, especially when the dosage pumps were operating at low RPM (revolutions per minute). This was overcome by the use of the PLC outlined earlier, and by periodic dosing of the reactors at a higher RPM.

4.2 Inoculum source

The inoculum was a mixed culture sourced from decomposed woody material that showed evidence of termite or wood bore attack. Prior to the selection of this source of bacteria, various sources of mixed cultures were evaluated (Appendix C). The two sources that showed initial promise were those from a woody-material mentioned above, and that from a compost-derived soil. The woody-derived bacteria provided a greater denitrification rate to that of the compost-sourced bacteria and this mirrored the results of Volokita et al. (1996).

The mixed bacteria inoculum was grown from a woody material exhibiting decay, including evidence of termite and/or borer attack. Since the intestinal track of termites contains cellulase producing bacteria in order to decompose the cellulose in the wood, it was thought that some of the termite/borer faeces within the woody material may also contain bacteria capable of denitrifying.

Both the denitrification batch reactor and fluidised bed reactor trials were dosed with the same inoculum.

To minimise the lag time required to acclimate the inoculated bacteria in the denitrification trials, the mixed culture bacteria was stored and maintained in similar environmental conditions as those of the denitrification reactor trials. The bacteria were isolated from the outside environment and maintained in an anoxic environment, with regular feeding of essential nutrients, together with glucose and nitrates to maintain their viability.

4.3 Chemical/Physical Assessment

The DO was measured in a 60mL BOD bottle. The fluid collected in the syringe was carefully injected into the bottle ensuring minimal oxygen entrainment. A YSI (Yellow Stone Instruments) 57 and 58 model DO meter in conjunction with a YSI 5700 series BOD bottle

DO stirrer probe with high sensitive (0.0005" thick, FEP Teflon) membrane allowed measurement to be taken directly from the 60mL bottle. The high sensitive membranes were adopted due to the reactors operating in an anoxic regime, and as a result the DO readings were often below 1mg/L.

During the course of this research two pH meters were utilised. Initially, an EDT Instruments RE357Tx microprocessor pH meter was used, and ultimately replaced with a Hach SensIon3 (Model 51750-60) pH meter. While the meter changed, the same brand of the pH probe, a Hanna Instruments (HI 1230B) BNC pH, was used.

Both the DO and pH were measured directly in the 60 mL BOD bottle, whereas other chemical parameters such as nitrate and COD were chemically assessed once the samples had been filtered. An unfiltered sample typically contained many fine particulate materials, either bacterial flocs or minute fragments of the coconut shell, which had the potential to affect the chemical assessment.

To eliminate the influence these particulate materials may have on the chemical tests, all samples were first passed through a 1.2μm glass fibre (Whitman GF/C) filter before undergoing the chemical tests summarised in Table 4-2.

A comparative assessment of the performance of the 1.2μm filter paper was conducted (Appendix D). The assessment demonstrated that in this application 1.2μm filter paper resulted in a 5.4% greater COD in the filtrate than that of 0.45μm filter paper. This error margin was considered acceptable, and application of the 1.2μm filter paper was considered consistent with the approach adopted by other researchers in the field (Volokita et al., 1996).

The chemical parameters in this research were assessed via spectrophotometric techniques. The chemical of interest was chemically reacted with a reagent powder pillow (or vial), and the resultant colour intensity of the reaction was then measured with a HACH DR/2000 Spectrophotometer.

The procedures and reagents utilised were consistent with those outlined in the Hach Water Analysis Handbook 3rd Edition (Hach Company, 1997) or the Standard Methods 20th Edition

(APHA 1999). All the reagents were typically in the form of premixed test tubes or reagent powder pillows (Table 4-2) manufactured by Hach.

Table 4-2 Spectrophotometric Techniques for the Hach DR2000 Spectrophotometer

Test	Hach Method	Summary of Method	Wavelength (nm)	Range
NO_3^--N	8039	Cadmium metal reduces nitrates in the sample to nitrite. The nitrate ions react in an acidic medium with sulfanilic acid to form an intermediate diazonium salt. This salt couples with gentistic acid to form an amber-coloured product.	410	0-30mg/L
NO_2^--N	8507	Nitrite reacts with sulfanilic acid to form an intermediate diazonium salt. This couples with chromotropic acid to produce a pink complex.	507	0-0.3mg/L
NH_3-N	8155	Ammonia combines with chlorine to from monochloramine. This reacts with salicylate to form 5-aminosalicylate. In turn, it is oxidised in presence of a sodium nitroprusside catalyst to form a blue-coloured compound. The colour is masked by excess reagent to give it a green colour.	655	0-0.5mg/L
PO_4^{3-}	8048	Orthophosphate reacts with molybdate in an acid medium to produce a phosphomolybdate complex. Ascorbic acid reduces the complex to give molybdenum a blue colour.	890	0-5mg/L
COD *	8000	Sample digested for 2 hours with potassium dichromate. Oxidised organics reduce dichromate to green chromic ion.	620	0-1500mg/L

* APHA 1999 colorimetric reflex method was ultimately applied.

While the HACH DR20000 provides a method for measuring the COD of a water/wastewater (Hach method 8000, Table 4-2), it was elected instead to follow the COD Colorimetric Reflux Method from Standard Methods 20th Edition (APHA 1999). This method is a closed dichromate reflux digestion technique calibrated to operate in the range of 0-800mg/L at a wavelength of 620nm, and proved a cost effective alternative suitable for this research.

4.4 Pretreatment Batch Reactor Methodology

Each experimental run was comprised of six batch reactors. The 6L batch reactors outlined in Section 4.1.2 were utilised in these experiments. The parameters monitored in this set of experiments included the hydroxide ion concentration in the form of pH, DO, and COD, all as a function of time.

In total, thirty six (36) reactors were evaluated. Sodium Azide was added to some of the later experiments to control the growth of unwanted bacteria and fungi that was observed within a couple of the earlier trials.

200g of substrate (coconut shell fragments) were added to each flask, augmented with 6L of deionised water.

The frequency of sampling and testing varied, with a greater sampling rate (every 1 or 2 hours) occurring at the beginning of each experiment. By the end of the experimental run the sampling frequency was every 2 days. The length of the experimental runs were in the order of 10-14 days, but varied from a few hours to 20 days. Each experimental run was terminated once the rate of COD hydrolysis had achieved a steady rate.

During the course of the pretreatment experiments, it was observed that clouding was occurring in some reactors, in conjunction with a sudden and unexpected reduction in the chemical parameters COD and DO. This indicated the presence of bacterial activity within the reactors. To remove this unwanted biological presence, some of the later experimental runs were dosed with sodium azide.

Sodium azide (NaN_3) is toxic to some bacteria and fungi; however the metabolism is thought to be similar to cyanide (CN^-) (Garrett and Grisham, 1999). In that the azide ion disrupts the metabolic process, and inhibits oxidative phosphorylation (Cruz et al., 1994).

4.4.1 Pretreatment Parameters Investigated

In this set of investigations, a series of 36 trials were conducted. Each trial considered a combination of three parameters as outlined in Table 4-3. Two of these parameters were physical in nature, namely variability in crushed particle size distribution, and the substrate drying technique, while the other parameter was the chemical pretreatment undertaken: either soaking the substrate in an alkali or acid.

Table 4-3 Pretreatment Parameters		
Physical Parameters	1. Crushing	2-10mm particle distribution 2-8mm particle distribution
	2. Heat Treatment (substrate dying technique):	Air dried @ 30°C, and zero % humidity Oven dried @ 105°C, and zero % humidity
Chemical Parameter	3a. Alkalis	Deionised Water NaOH, initial pH = 9 NaOH, initial pH = 12 NaOH, initial pH = 14 Lime, initial concentration 50mg/L Lime, initial concentration 100mg/L Lime, initial concentration 500mg/L
	3b. Acids	HCl, initial pH = 2 HCl, initial pH = 4 H_2SO_4, initial pH = 2 H_2SO_4, initial pH = 3 Acetic Acid, initial pH = 3 Acetic Acid, initial pH = 5 Propionic Acid, initial pH = 3 Propionic Acid, initial pH = 5

Crushed Substrate:

The influence of crushed particle size distribution on COD liberation involved the consideration of two grain size distributions. If the mass of substrate used in each series of experiments was kept similar and the particulate material was homogenous in size, it follows that a smaller particle size would have a greater surface area per mass of substrate. It is also likely that the rate and/or the amount of COD released will be a function of the amount of surface area. An increase in the surface area results in the greater solid-fluid contact, in turn increasing the probability that the organic matter could be hydrolysed.

The decision to utilise a distribution of shell fragments was made for pragmatic reasons. No technique was available to readily fragment the coconut shell into homogenous-sized particles. The yield of coconut shell fragments was low, with 27% and 43% of the mass being wasted (i.e. 27% of the original mass of the unfiltered $2 \leq x \leq 10$ mm distribution was rejected, along with 48% of the $2 \leq x \leq 8$ mm distributions). A further reduction in upper distribution would have resulted in further wasted matter (i.e. particle and dust <2mm).

In Section 3.1, Eqn. 3-4 indicates that as the diameter of the particles decreases in size, the minimum velocity required to suspend the particles in a fluidised bed would decrease proportionally. Therefore, a distribution of particles with the same density but differing diameters would order itself vertically in the fluidised bed. The large particles at the bottom act like a fluidised bed, with the smaller particles at the top tending to act like individual particles. If the velocity of the superficial fluid is sufficiently great, then the smaller particles will be swept away with the fluid. For this reason, the distribution's lower limit was set to that of 2mm. This was a practical limit as well, since the lab scale fluidised bed had stainless steel gauze partitions restricting the movement of the particles to within the column. If the distribution limit was set any lower, there was a possibility that the substrate could enter the recycle pipework and pump. This would be an unfavourable outcome, as it can introduce mass balance errors, and has the potential to damage the pump.

The upper limit of the distribution was restricted by the mechanical grinder employed (Baukneckt SK1, 1.1kw), as this grinder only had provision to grind and pass material through either a 10, 8, or 4mm sieve. The 4mm sieve was discounted due to the superficial fluid velocity constraints indicated above, and the low yield of useable material as the grinder sieve size decreased.

The grinder product contained a significant proportion of fines (Figure 4-4). These were dry sieved off through a 2mm stainless steel sieve to yield the final product utilised in this research.

The $2 \leq x \leq 10\text{mm}$ and $2 \leq x \leq 8\text{mm}$ particle distributions, expressed in Figure 4-4, once ground and filtered, varied in particle size grading. The $2 \leq x \leq 8\text{mm}$ distribution is predominantly in the 2.36 to 4 mm particle size, while the $2 \leq x \leq 10\text{mm}$ distribution is predominately 4.75 to 8 mm. The net result is that each particle distribution offers a similar order of magnitude of surface area per gram of substrate, as represented in Table 4-4 below.

Table 4-4 Surface Area of Particle Distributions

Sieve Size (mm)			*Particle Distribution (mm)*			
			% within the Range		Surface area/gm (mm^2/gm) [(a)]	
Upper	Lower	Ave	2<x<8	2<x<10	2<x<8	2<x<10
10	9.5	9.75				
9.5	8	8.75		2.6		15
8	4.75	6.375	1.5	50.2	12	404
4.75	4	4.375	14.1	18.0	164	211
4	3.35	3.675	30.6	10.3	427	143
3.35	2.36	2.855	44.1	14.3	793	257
2.36	2	2.18	9.7	4.7	228	110
2	1.18	1.59				
1.18	0.6	0.89				
0.6	0	0.3				
			100	100	1624	1140

[(a)] Based on the assumption that the particles are spherical and the density of the coconut is $1170 kg/m^3$ (as derived in Appendix E).

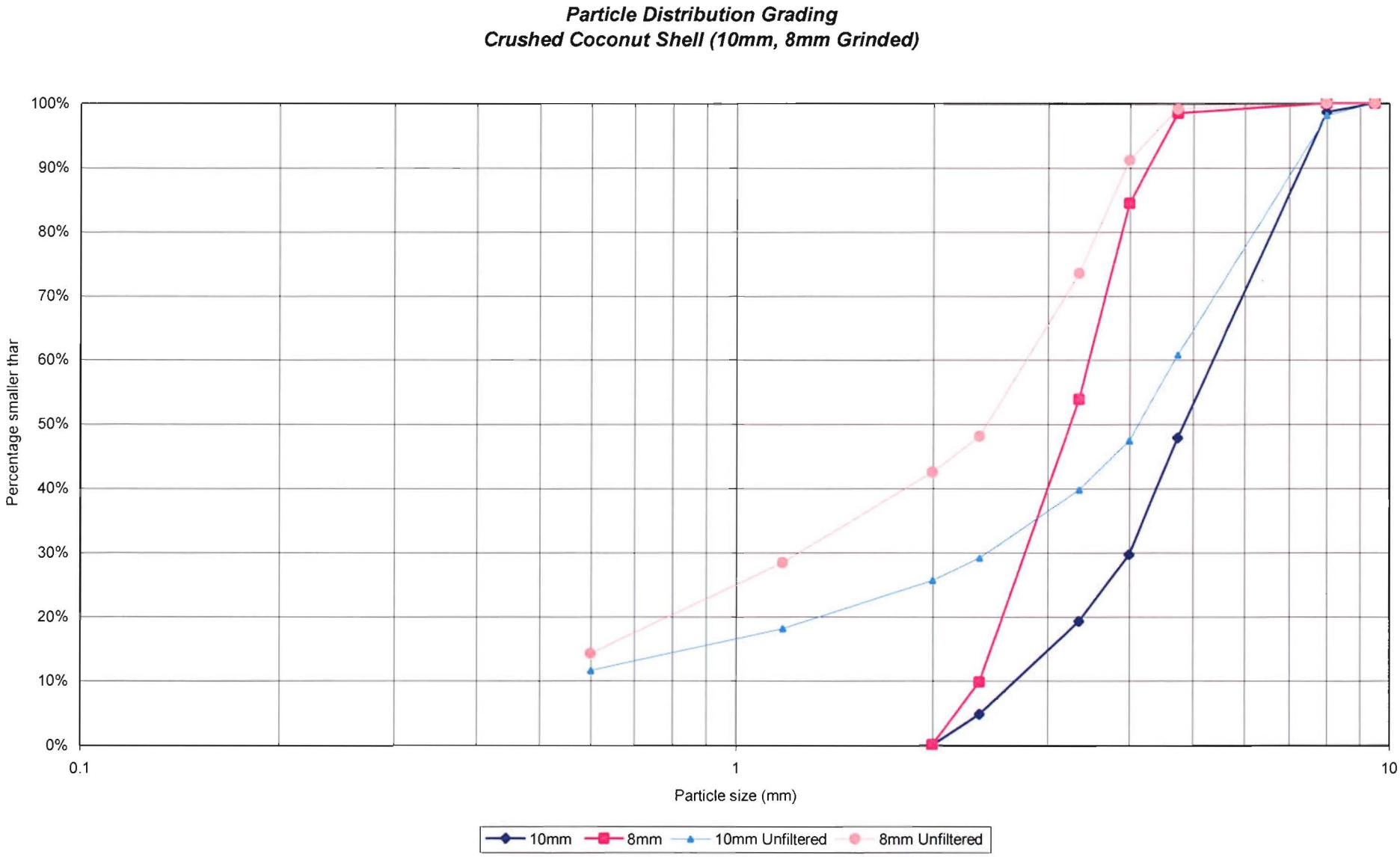

Figure 4-4 Particle size distribution profiles of the 8mm, and 10mm substrates.

Heat Treatment:

The other form of physical pretreatment considered was that of heat. Two extremes were considered to see if heat treatment would break down the bonds within cellulose, or degrade the lignocellulose structure sufficiently to allow preferential cellulose degradation.

In the course of washing and cleaning the substrate prior to application, the material was dried. Two drying temperatures were utilised to expel the moisture from the substrate, as well as to treat the substrate:

Oven Dried: an oven set at 105°C +/- 10°C at zero % humidity, and
Air Dried: an incubator operating at 30°C +/- 2°C at zero % humidity.

Not only was the effect of heat energy investigated, but the sudden application of heat to a saturated substrate could result in some form of steam or thermal expansion. The expansion of the water within the porosity of the substrate was considered as a possible mechanism to expand or increase the porosity at a micro-scale as well as possibly disrupting the cellulose crystallinity on a macro-scale.

With the structure and crystallinity of the substrate damaged or disrupted, the material would be susceptible to preferential hydrolysis in the damaged regions and there would be an increase in the internal surface area of the substrate. This would ultimately increase the available substrate able to be hydrolysed and should result in a measurable increase in COD.

Sodium Hydroxide:

Fan et al. (1987) conducted a literature review of the application of sodium hydroxide to increase the hydrolysis and digestibility of lignocellulosic matter. They noted that dilute NaOH treatment resulted in the swelling of the material and, in turn, an increase in internal surface area, reduction in crystallinity, and separation of the structural linkages between lignin and any carbohydrate (in the case of coconut shell the primary carbohydrates of interest is cellulose and its polymer unit glucose). Different lignocellulosic materials respond differently to sodium hydroxide treatment, as noted by Feist et al. (1970, cited in Fan et al., 1987) who found that the lignin content would control the rate and amount of digestion of the wood.

Due to the physical constraints of the small laboratory scale batch trials, it was decided not to continuously monitor and control the pH in the reactor. Instead, the initial hydroxide concentration in the reactor was set to a predetermined value and the changes in DO, COD, and pH as a function of time and the initial conditions of the reactor were monitored.

A range of initial hydroxide ion concentrations was considered. The hydroxide ion concentration should correlate to the rate of COD released, as identified by Fan et al. (1987). The range of initial hydroxide ion concentrations considered included initial pH values of 9, 12, 14 and that of deionised water.[13]

Lime:

Lime is the common name for calcium hydroxide. Calcium hydroxide has a low solubility, in the order of 0.12g of solute per 100g of water at 25°C, which dissociates into its elemental calcium and hydroxide ions. As outlined above, the hydroxide ion has been linked to increased digestibility and/or hydrolysis of cellulose. The dissociation of calcium hydroxide provides a convenient supply of these ions under normal conditions.

Lime is a cheap and readily available material that could provide a source of hydroxide ions to disrupt the structure of lignocellulosic materials. To determine whether lime also disrupts the lignocellulosic structure, three initial solutions of lime were considered.

The three initial conditions examined were all cases of complete dissociation of the solute (initial condition - 50mg/L, 100mg/L, and 500mg/L of calcium hydroxide), where the solubility of Lime is 1200mg/L (SI Chemical Data, 1994).

Acids:

Brenner et al. (1977) identified that acids serve primarily as catalysts during hydrolysis of cellulose, rather than as a reagent when utilised in pretreatment. Their findings would suggest that little or no COD would be released during the pretreatment process. However, it is

---

[13] Deionised water was degassed, resulting in a reduction in pH and alkalinity. The initial pH was measured in the order of 6.5

possible that acids are capable of disrupting the structure of the lignocellulosic material sufficiently to favour greater rates of enzymatic degradation, as would occur in denitrification batch trials.

Two inorganic acids (HCl and H_2SO_4) and two organic acids (acetic and propionic acid) were considered. Two initial pH concentrations were evaluated to determine if the acid concentration had an influence on the rate of hydrolysis and later enzymatic degradation, as summarised in Table 4-5. The Alphanumeric identification sequence adopted identifies the sequence of the batch by the numerical value; the subsequent letter (a-f) signifies which reactor the trial was conducted in. Nine of the thirty six trails were duplicates or an earlier trial, as outlined in Table.

Table 4-5 Pretreatment Reactor Numbering Reference Table

		Air Dried		Oven Dried
		2-8mm	2-10mm	2-10mm
Deionised Water	pH = 7[1]	1e‡, 1f‡	1a‡, 1b‡, 6a†	1c‡, 1d‡
NaOH	pH = 9		3d, 6d†	
	pH = 12		3c, 6e†	
	pH = 14		2c, 6c†	
Lime	50 mg/L	8a†‡, 8e†‡	8f†	
	100 mg/L	8b†		
	500 mg/L	8c†‡, 8d†‡	5a‡, 5b‡, 6f†	
H_2SO_4	pH = 2		5e‡, 5f‡, 6b†	
	pH = 3		5c‡, 5d‡	
HCl	pH = 2		4e‡, 4f‡	
	pH = 4		4c	
Acetic Acid	pH = 3		7a, 7b†	
	pH = 5		7c	
Propionic Acid	pH = 3		7d, 7e†	
	pH = 5		7f†	

† indicates that 500mg/L Sodium Azide has been added to the batch reactor for this experiment.

‡ indicates that the reactor was part of a duplicate trial

[1] a nominal value of pH=7 was elected for deionised water.

4.5 Denitrification Batch Reactor Methodology

The purpose of the Denitrification Batch Reactor trials was to evaluate the pretreatment substrates and identify which substrate was best suited for biological denitrification.

In total twelve reactor trials were conducted. Eleven of the reactors were used to study various combinations of pretreated substrate, as to determine the suitability or otherwise of the pretreatment technology to promote denitrification.

As outlined above, the substrates for the denitrification batch trials came from the preceding pretreatment trials. During the recovery of the substrate, mass was lost in the course of the washing/cleaning processes that were conducted between the end of the pretreatment investigations and the start of the Denitrification Batch Reactor Trials. To eliminate the possible inaccuracy associated with the differences in mass between trials, all analyses are normalised with respect to the substrate mass.

Each experimental run was comprised of six batch reactors. The 6L batch reactors outlined in Section 4.1.2 were utilised in these experiments. The parameters monitored in this set of experiments included the hydroxide ion concentration in the form of pH, DO, and COD, all as a function of time.

The procedure for obtaining samples and assessing their chemical properties was similar to that outlined in the pretreatment batch reactor study. However, a greater variety of chemical parameters were assessed. COD, NO_3-N, NO_2-N, NH_3-N and PO_4^{3-} were assessed as outlined in Table 4-2 while DO and pH were measured with non destructive instruments (refer to Section 4.3).

4.5.1 Composition of Denitrification Batch Reactor Nutrient Fluid

Hiscock et al. (1991) noted that the availability of nutrients is an important requirement to sustain cell growth. Large amounts of essential elements (such as C, H, O, N, P, and S) are necessary for biosynthesis, while various other minerals (such as K, Na, mg, Ca, and Fe) are required in minor quantities, as well as trace concentrations of certain metals (such as Mn, Zn, Cu, Co, and Mo). Average cellular composition suggests that a C:N:P ratio of about 50:10:1 is

required for biosynthesis (Fagerbakke, 1996). However, additional organic carbon is necessary for denitrification due to the chemotrophic nature of the bacteria utilised in this series of experimental trials.

As mentioned earlier, it is envisaged that the availability of organic carbon would be the nutrient to limit the biosynthesis processes within the batch reactors. To ensure that no other chemicals/nutrients would adversely affect the processes, adequate quantities of the other nutrients were supplied. Hence excess phosphate was available, in excess of that minimum requirement for biosynthesis outlined by Fagerbakke (1996).

The primary nutrients (H, O, N, and P) would be expected to be sourced from either the hydrolysis of the coconut shell fragments or the augmented phosphate and nitrate. The minor minerals were added to the fluid in the concentrations outlined in Table 4-6. Trace metals such as Mn, Zn, Cu, Co, and Mo were assumed to be sourced from domestic tap water.

Table 4-6 Chemical Composition of the Denitrification Fluid

Nutrient	*Concentration*	*Source*
NO_3-N	200 mg/L	$NaNO_3$
PO_4^{3-}	3 mg/L	Na_2HPO_4
Cycloheximide	2.5 mg/L	$C_{15}H_{23}NO_4$
Trace nutrients		
Na	2.34 mg/L	Na_2HPO_4
Mg	0.05 mg/L	$MgCl_2.6H_2O$
K	0.05 mg/L	KNO_3
Fe	0.01 mg/L	$FeCl_2$

As can be seen from Table 4-6, Cycloheximide ($C_{15}H_{23}NO_4$) was applied to the denitrification reactor, primarily because of its fungicidal characteristics. Since the inoculum came from a natural source, it would invariably contain many fungal spores. This was evident by the formation of a white haze in some of the earlier trials that were conducted without the inclusion of cycloheximide in the reactor.

Volokita et al. (1996), in their studies of denitrification using newspaper, had used similar concentrations to prevent any fungal growth. Data about the toxicity of cycloheximide is sparse; however, animal studies have indicated that it may be very toxic by ingestion (IPCS,

1993). Marino and Gannon (1991) used cycloheximide to eliminate protozoan (and fungal) predators from bacterial samples in their studies. Their results agree with Whiffen (1948) who tested 12 bacterial species including *E. coli* and noted that none were inhibited by concentrations of up to 1 mg cycloheximide/mL. These previous studies suggest that cycloheximide is an effective fungicide and protozoacide that does not detrimentally inhibit denitrification bacteria.

4.5.2 Denitrification Batch Reactor Establishment

A six-step procedure was followed to establish the conditions favourable in the denitrification batch reactors. The initial step involved washing the coconut shell fragments under a tap. During the next step, the coconut shell fragments were completely saturated with water (under vacuum[14]) the fragments in deionised water for 4 hours. As the pressure decreased, any atmospheric gases that were present in the substrate were displaced.

As a result of the bubbles forming from within the substrate, any minute fragments previously formed during the crushing or pretreatment process would migrate out of the pores of the fragmented coconut shell.

Prior to filling the denitrification reactor, the fragments were again rinsed, but at all times the substrate was keep saturated.

The fourth step involved combining the now saturated substrate with the denitrification/nutrient fluid (Table 4-6) in an Erlenmeyer flask. The completely stirred reactor was provided by way of a magnetic stirrer and bar as demonstrated in Figure 4-1.

The fifth step involved displacing the atmospheric gases from the headspace in the reactor(s) with inert helium. The removal of oxygen in particular from the atmospheric gases prevented the possible recharging of oxygen into the liquid phase, hence eliminating any possible oxygen tension to the biological process.

---

[14] The fragments saturated whilst 90 kPa below atmospheric pressure to aid the process.

Fluid was withdrawn from the reactor via a syringe that penetrated the rubber seal attached to the fluid sample tubing.

The denitrification batch reactors differed from the earlier pretreatment trials in that the fluid volume was only 4L for the denitrification trials, while 6L was utilised during the pretreatment trials. The rationale behind the reduction in fluid volume was to increase the concentration of the COD response/release in the denitrification trials. It was expected that an increased release in COD would correspond to a greater increase in the rate of denitrification within the reactor.

DO measurements were conducted in a 60mL BOD bottle (as shown in the foreground of Figure 4-1). To preserve the volume within the reactor, the sample was reinjected into the reactor once the DO measurement had been conducted.

Once all of the constituents were added to the reactor, with the exception of the inoculum, the reactor was left to acclimate for two days and during this time all of the chemical properties were monitored. The purpose of the two days was to allow the substrate and reactor fluid to reach equilibrium, so as to overcome (via dilution) any adverse conditions or toxicity associated with the pretreated coconut fragments.

The final step, prior to the start of the batch trial, was to inject 60mL of bacterial inoculum into the reactor. It should be noted that the inoculum was maintained in a batch reactor that was feed the same concentration of nutrients and nitrate as the batch reactors, organic carbon was sourced from coconut fragments within the reactor and supplementary glucose. Hence the injected bacterium should be acclimated to a denitrification batch reactor process.

To prevent the possibility of stale fluid in the sample tubes introducing some bias/error into the chemical analysis, the sample tubes were flushed with reactor fluid a couple of times before the samples were collected.

Time $t = 0$ was deemed to be the point at which the bacteria were added to the reactor. The reactor(s) were then monitored for the next 13 to 31 days. Initially sampling occurred daily, but in the longer experimental runs the frequency of sampling was reduced to every second day after day 5, and then further reduced to every third day from day 13 onwards.

Some of the later experiments were operated in two regimes. During the first regime (comprising the first eight or nine days) the headspace was left open to the atmosphere. The second regime (from day eight or nine) had the dissolved oxygen in the fluid and headspace gases stripped from the reactor (with helium gas as outlined earlier), and the reactors were then operated in an anoxic state.

The rationale behind the variation in the atmospheric conditions was to assess, and then eliminate the possible influence of DO being preferentially consumed instead of nitrate during the denitrification process. With the reactors open to the atmosphere, it was possible that the atmospheric oxygen would constantly replace any DO consumed by the bacteria. Removing this influence allowed for a more realistic assessment of the viability of the denitrifying bacteria as well as providing a more accurate means of assessing the hydrolysis of organic carbon (via the rate of denitrification).

In the course of the pretreatment investigations it was determined that air-dried substrates offered greater hydrolysis potential compared to those of oven-dried substrates. However, the same investigations were able to differentiate the rate of hydrolysis between the two particle distributions considered (2-8mm, and 2-10mm). In this series of trials, air dried and 2-10 mm graded substrates were utilised.

4.6 Denitrification Fluidised Bed Reactor Methodology

Like the batch reactor trials, the fluidised bed reactor trials were conducted in parallel trials. Two laboratory scale reactors were utilised, in which the physical and chemical characteristics were identical. Only the pretreatment technique applied to the substrate within the reactors differed.

The two reactors operating in parallel allowed direct comparisons to be made between the performance of the pretreated substrate and that of the untreated substrate. The nitrate and hydraulic loading were stepped up and down during the course of the experiment. From the reactor's response it was possible to evaluate the recovery and/or capacity of the reactor to manage the corresponding change in influent condition.

Typically each trial would last 7 to 10 days, while some of the trials were left to operate for 19 to 25 days. The longer duration trials provided an insight into the medium to long term suitability of the treatment process sustain biological denitrification.

4.6.1 Chemical Composition of Influent Feed Fluid:

The chemical composition of the influent feed (Table 4-7) was similar to that utilised in the denitrification batch reactors. The major difference between these two series of experiments was that the fluidised bed reactor trials were conducted with varying nitrate dosages and rates of feeding (Table 4-7).

Cycloheximide and trace nutrients (concentrations as outlined in Table 4-7) were injected into the reactors to prevent the growth of fungi and protozoa within the reactor, while the trace nutrients were provided to ensure that only nitrate and/or organic carbon liberated from the substrate would be the rate-limiting nutrients in the trial.

Table 4-7 Chemical Composition of the Denitrification Feed Fluid Utilised in the FBR.

Nutrient	*Concentration*	*Source*
NO_3^--N	10.7 to 98.5 mg/L	$NaNO_3$
PO_4^{3-}	3 mg/L	Na_2HPO_4
Cycloheximide	2.5 mg/L	$C_{15}H_{23}NO_4$
Trace nutrients		
Na	>2.34 mg/L	Na_2HPO_4
Mg	0.05 mg/L	$MgCl_2.6H_2O$
K	0.05 mg/L	KNO_3
Fe	0.01 mg/L	$FeCl_2$

4.6.2 Process Performance Monitoring:

The range of chemical parameters monitored was similar to that in the earlier denitrification batch reactors. The DO and pH were measured with the meters outlined earlier (section 4.3). The COD, Nitrate, Nitrite, Ammonia, and Phosphate concentrations were chemically assessed with a Hach DR/2000 spectrophotometer utilising the procedures outlined previous in Table 4-2.

To trace the growth of the biomass within the fluid phase, periodic measurements of Standard Total Coliform and Faecal Coliform colony counts were conducted. These tests followed the membrane filter procedures outline in Standard Methods (APHA, 1999) method 9222 B and 9222 D respectively.

The evaluation of some bio-kinetic properties was undertaken, such as the Total Cellulase Activity – using filter paper (Commission on Biotechnology (IUPAC)), and the DEA or Denitrifying Enzyme Activity – using the acetylene blocking technique (Methods of Soil Analysis [ASA, 1982] Method 47). However, the applications of these techniques were found to be unsuitable for the assessment of biological denitrification occurring in a fluidised state, due to the insensitivity of the tests as to the low concentrations and/or activity of the enzymes present in the samples.

The hydraulic residence time (HRT) of these trials was in the order of 1 to 117 days (as per Table 4-9). To provide effective monitoring of the processes daily measurements were on most parameters. However, some parameters, such as the flow rate, phosphate, nitrite, and ammonia concentrations were assessed less frequently at 2-day or greater intervals (Table 4-8).

Table 4-8 Parameter testing frequency

Parameter	*Influent*	*Reactor*
DO	2-5 day interval	Daily
pH	2-5 day interval	Daily
Temperature		Daily
COD		Daily
NO_3^--N	2-5 day interval	Daily
PO_4^{3-}	4-10 day interval	1-2 day interval
NO_2^--N		≥2 day interval
NH_4^+-N		≥2 day interval
Flow rate	2-5 day interval	

4.6.3 Testing Schedule:

A total of thirty eight distinct trials were conducted within the fluidised bed reactors. Half of the trials (as summarised in Table 4-9) were conducted with a lime pretreated substrate, while the other trials utilised an untreated substrate.

To assess the relative treatment improvement offered by the lime pretreated substrate, the two reactors were operated in parallel. One reactor contained the untreated substrate, while the other utilised the lime pretreated substrate.

Since the mechanical crushing procedure resulted in a significant production of coconut shell dust, most of the pores in the shell had become clogged with this dust. Extensive washing of the substrate prior to its application was necessary to remove this contaminating influence. The procedure for removing this dust involved rinsing the material with tap water though a sieve, then leaving it to soak for 24 hours before repeating the process three times.

Once cleaned, the lime pretreated substrate was soaked in a 6L Erlenmeyer flask with a supersaturated solution of lime (slaked lime or $Ca(OH)_2$). In the earlier pretreatment batch reactors, 500 mg/L of calcium hydroxide was used to treat 200 mg of coconut shell fragments. This dose was scaled up in proportion to the mass of the substrate within the reactor (being 2.14 kg), hence:

$$\frac{2.14kg}{0.2kg} \times 500mg/L \times 6L = 31.95g \text{ of lime was dissolved in the 6L of water}$$

The lime-substrate slurry was continuously mixed for twenty-four hours in an Erlenmeyer flask. An extensive washing regime, as outlined above, was followed to remove any attached lime or readily soluble COD for the substrate. Excess lime and lime induced hydrolysed COD had the potential to adversely influence the trials. Lime could affect the biological processes (i.e. precipitate out reactive phosphate from the reactor, and/or detrimentally affect the hydroxide ion concentration in the reactor). Eliminating the lime-hydrolysis released COD allows for direct comparisons of the enzymatic-induced hydrolysis to be drawn between the two substrates.

Each reactor contained 2.14 kg of crushed coconuts shell fragments. This equates to a bed depth of 1 metre, assuming that 30% of bed expansion was achieved once the reactor reached its operational fluidised state. At rest 2.14 kg of substrate equates to a reactor bed depth of 890 mm or a volume of 5.05 L. In its operational state the bed depth was measured initially at 1065 mm but settled at 980 mm (volume of 5.56 L) within a few days.

Nineteen variations of nitrate loading, hydraulic loading, and fluidised bed treatment were evaluated as represented in Figure 4-5. The initial series of trials considered the higher nitrate and hydraulic loading; however, it became apparent that a HRT lower than three days was unsustainable due to hydraulic flushing, and hence the majority of the trials in Table 4-9 were above this threshold.

Table 4-9 Summary of Testing Regime

Reactor	*Nitrate Load*	*Hydraulic Load*	*HRT*	*Duration*	*Reactor*	*Nitrate Load*	*Hydraulic Load*	*HRT*	*Duration*
FBR 1-1, 6th April 2000, No pretreatment					FBR 1-2, 6th April 2000, Lime pretreatment				
(a)	Reactor pulsed with 50 mg/L NO_3^--N			4 – 14d	(a)	Reactor pulsed with 50 mg/L NO_3^--N			4 – 14d
(b)	5.18 mg/hr	0.465 L/hr	1.01 d	14 – 22d	(b)	6.52 mg/hr	0.584 L/hr	0.80 d	14 – 22d
(c)	0.10 mg/hr	0.008 L/hr	58.5 d	22 – 28d	(c)	0.12 mg/hr	0.010 L/hr	46.8 d	22 – 28d
(d)	1.79 mg/hr	0.155 L/hr	3.02 d	28 – 36d	(d)	2.24 mg/hr	0.195 L/hr	2.40 d	28 – 36d
FBR 2-1, 16th May 2000, No pretreatment					FBR 2-2, 16th May 2000, Lime pretreatment				
(a)	Reactor pulsed with 100mg/L NO_3^--N, no substrate			0 – 3d	(a)	Reactor pulsed with 100mg/L NO_3^--N, no substrate			0 – 3d
(b)	Reactor pulsed with 400mg/L glucose			3 – 6d	(b)	Reactor pulsed with 400mg/L glucose			3 – 6d
FBR 3-1, 24th May 2000, No pretreatment					FBR 3-2, 24th May 2000, Lime pretreatment				
(a)	1.4 mg/hr	0.073 L/hr	6.42 d	0 – 10d	(a)	1.7 mg/hr	0.085 L/hr	5.51 d	0 – 10d
(b)	Ran out of influent			10 – 13d	(b)	Ran out of influent			10 – 13d
(c)	3.5 mg/hr	0.111 L/hr	4.22 d	13 – 29d	(c)	3.3 mg/hr	0.101 L/hr	4.64 d	13 – 29d
FBR 4-1, 24th July 2000, No pretreatment					FBR 4-2, 24th July 2000, Lime pretreatment				
(a)	4.2 mg/hr	0.111 L/hr	4.22 d	0 – 9d	(a)	3.8 mg/hr	0.101 L/hr	4.64 d	0 – 9d
(b)	3.5 mg/hr	0.111 L/hr	4.22 d	9 – 24d	(b)	3.2 mg/hr	0.101 L/hr	4.64 d	9 – 24d
(c)	5.8 mg/hr	0.111 L/hr	4.22 d	24 – 35d	(c)	5.3 mg/hr	0.101 L/hr	4.64 d	24 – 35d
FBR 5-1, 9th October 2000, No pretreatment					FBR 5-2, 9th October 2000, Lime pretreatment				
(a)	6.0 mg/hr	0.089 L/hr	5.26 d	0 – 17d	(a)	5.6 mg/hr	0.081 L/hr	5.78 d	7 – 15d
					-	Reactor down – no dosage			15 – 21d
(b)	4.0 mg/hr	0.089 L/hr	5.26 d	17 – 49d	(b)	3.7 mg/hr	0.081 L/hr	5.78 d	21 – 49d
FBR 6-1, 19th December 2000, No pretreatment					FBR 6-2, 13th December 2000, Lime pretreatment				
(a)	0.6 mg/hr	0.026 L/hr	18.0 d	0 – 7d	(a)	0.5 mg/hr	0.022 L/hr	21.3 d	0 – 7d
(b)	1.1 mg/hr	0.030 L/hr	15.6 d	7 – 14d	(b)	1.0 mg/hr	0.023 L/hr	20.4 d	7 – 14d
(c)	1.9 mg/hr	0.020 L/hr	23.4 d	14 – 22d	(c)	1.8 mg/hr	0.019 L/hr	24.6 d	14 – 22d

Table 4-9 Summary of Testing Regime									
Reactor	*Nitrate Load*	*Hydraulic Load*	*HRT*	*Duration*	*Reactor*	*Nitrate Load*	*Hydraulic Load*	*HRT*	*Duration*
(d)	0.3 mg/hr	0.004 L/hr	117 d	22 – 27d	(d)	0.4 mg/hr	0.004 L/hr	117 d	22 – 27d
(e)	2.2 mg/hr	0.026 L/hr	18.0 d	27 – 50d	(e)	2.0 mg/hr	0.023 L/hr	20.4 d	27 – 50d

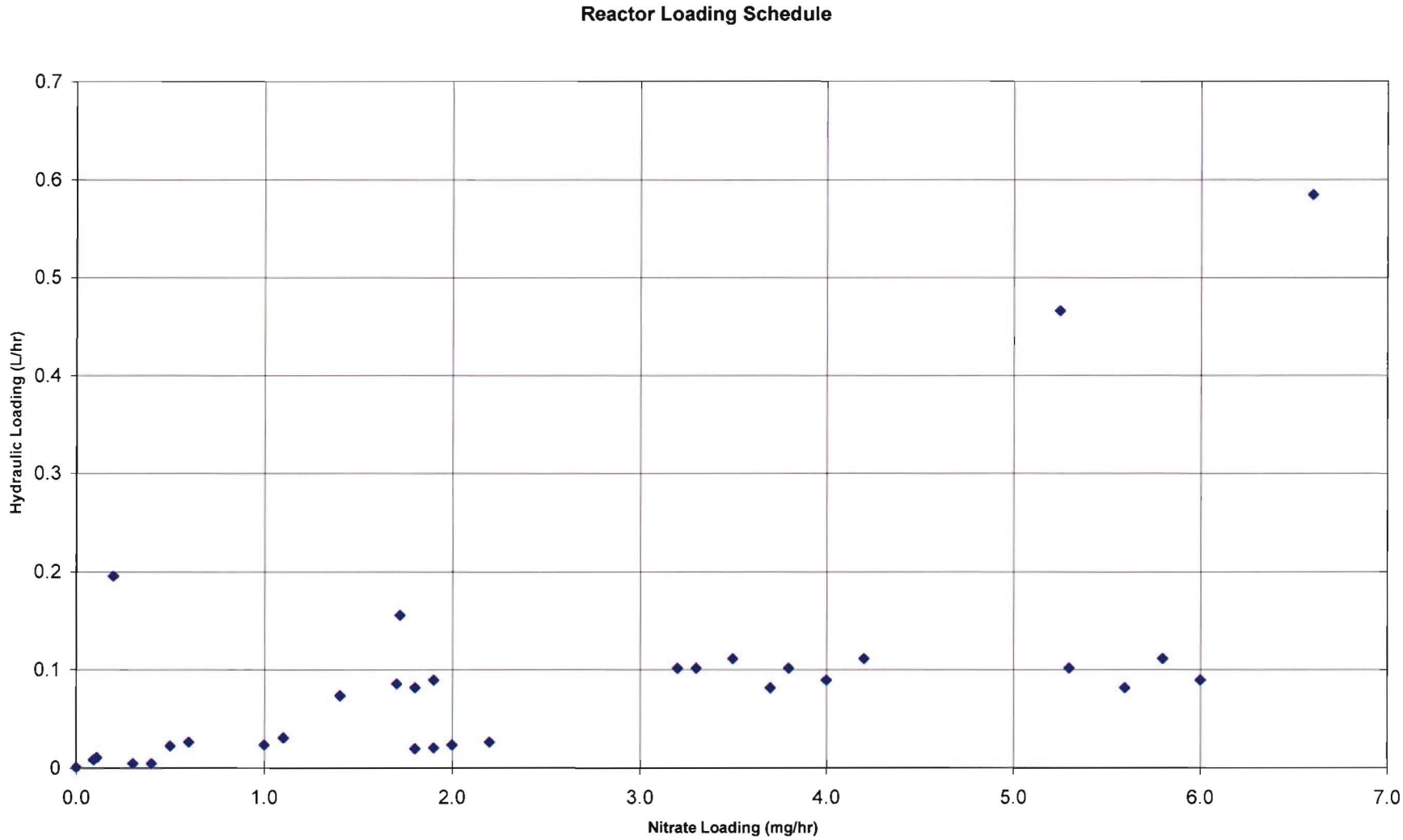

Figure 4-5 Nineteen combinations of nitrate and hydraulic loads were evaluated in the FBR trails.

4.7 References

APHA (1999) Standard Methods for the examination of water and wastewater. 20th Edition, American Public Health Association, Washington.

ASA (1982) Methods of soil Analysis, Part 2. Chemical and Microbiological Properties. No. 9, Second Edition, American Society of Agronomy (ASA), pp. 1011-1026

Aylward G., and Findlay T. (1994) SI Chemical Data, 3rd Edition, Jacaranda Wiley Ltd, Milton, Australia, 180p.

Brenner W. et al. (1977) In: New approaches for the acid hydrolysis of cellulose. Dept. of Appl. Sci., New York Univ., NYU/DAS-77-30, New York

Cruz N, and Alvarez X, Berg R.D., Deitch E.A. (1995) Bacterial translocation across enterocytes: results of a study of bacterial-enterocyte interactions utilizing Caco-2 cells, Shock. , Jan (1), pp. 67-72.

Fagerbakke K.M., and Heldal M., Norland S. (1996) Content of Carbon, Nitrogen, Oxygem, Sulfur and Phosphorous in Native Aquatic and Cultured Bacteria, Aquatic Microbial Ecology, Vol. 1, No. 1, pp. 15-27

Fan L.T., and Gharpuray M.M., Lee Y.H. (1987) Cellulose Hydrolysis, Springer-Verlag, New York. 198p.

Garrett R. H. and Grisham C. M. (1999) Biochemistry, Second Edition. Saunders College Pub. Harcourt Brace College Pub., Florida, U.S.A. 1273p.

Hiscock, K.M., and Lloyd, J.W., Lerner, D.N. (1991). Review of natural and artificial denitrification of groundwater, Wat. Res., Vol. 25, No. 9, p. 1099-1111

IPCS (1993) Cycloheximide ICSC, 17th July 2004 http://www.inchem.org/documents/icsc/icsc/eics0244.htm

Leva M. (1959) Fluidization, McGraw-Hill, N.Y., pp. 327.

Marino R.P. and Gannon J.J. (1991) Survival of Faecal Coliforms and Faecal Streptococci in Storm Drain Sediment, Water Resources, Vol. 23, No. 9, pp. 1089-1098

Schmidt R.D. (1979) Stabilized soluble enzymes, in: Advanced in Biochemical Engineering, A. Fiechter, ed., Vol. 12, Springer-Verlag, New York, p. 41-118

Volokita, M., and Belkin S., Abeliovich A., Soares M. (1996) Biological Denitrification of Drinking Water using Newspaper, Wat. Res. Vol. 30, No. 4, pp. 965-971

Werther J. (1983) Fundamentals of fluidized bed technology. German Chemical Eng. Vol. 6, pp. 228-235

Whiffen A.J. (1948) The production, assay, and antibiotic activity of actidone, and antibiotic form *Streptomyces griseus.* Journal of Bacteriology, Vol. 56, pp. 283-291

5 Pretreatment Batch Reactor Trials

5.1 Introduction

The extent and rate of biological activity occurring within a reactor is influenced by many factors, and one of the most significant is the availability of organic carbon. Since this research sources the organic carbon from the coconut fragments that provide the medium on which bacteria are to grow, there is very little operational control of this parameter. Some initial exploratory trials conducted at the start of this research suggested that the availability of readily soluble organic matter (COD) might be the rate-limiting variable influencing the rate and extent of all biological processes. Hence, this section of the research is focussed on finding the conditions that maximise the availability of organic carbon from the coconut shell fragments.

As mentioned in Section 3.4, the composition of a coconut shell is in excess of 53% cellulose (Nathanel, 1964). Cellulose is a readily degradable polysaccharide that consists of a long unbranched chain of glucose units. Since glucose units are readily consumed by bacteria, it is proposed that glucose is the major source of organic carbon for the heterotrophic denitrifying bacteria utilised in later stages of this research.

With high concentrations of nitrate contamination, organic carbon is often the rate limiting nutrient for denitrification; therefore, an increase in the rate of hydrolysis of cellulose is expected to correspond to an increase in the rate of denitrification. The Chapter 3 indicated several pretreatment methods that have been utilised to promote greater hydrolysis of the cellulose. Many require significant investment in machinery and often a considerable operational budget.

Mechanical physical pretreatments apply some form of physical force to the substrate to reduce its size, and possibly reduce the crystallinity of the material. The mechanical grinder utilised processed two particle distributions, $2 \le x \le 10mm$ and $2 \le x \le 8mm$. Several operating conditions constrained the selection of particle size distribution to these two distributions. As the upper limit of the particle range decreases, there is a corresponding increase in the mass of material that falls into the dust/grain <2mm regime. Reducing the upper limit from 10mm to 8mm resulted in a 17% increase in the dust/grain <2mm. This

increase is due to the increase in the grinding time required to reduce the size of the particles. An increase in time spent in the grinder resulted in greater damage to the particle. Each impact resulted in further production of dust and minute fragmentation. A 50% increase in grinding time was required to grind to the lower particle range.

Furthermore, to maintain an effective fluidised bed (in later stages of the research) the particle distribution needed to be greater than 2mm, and evenly distributed. However, narrower particle distributions were not considered feasible due to the waste and the volume of raw material necessary for manufacture.

Other non-mechanical physical pretreatments were not considered due to the specialised nature of the equipment required to conduct these tests. As mentioned, the focus of the research was to determine a low technical technique to biologically denitrify a potable water supply, not to revaluate physical pretreatment techniques.

Chemical pretreatments typically remove the lignin surrounding the cellulose, increasing the rate and amount of degradation of cellulose within the material. Both alkali and acid chemical pretreatments were considered. The alkalis investigated were sodium hydroxide and lime, while the acids were sulphuric acid, hydrochloric acid, acetic acid, and propionic acid. In the Section 3.5.6 it was noted that hydroxide ions in dilute quantities cause lignocellulosic materials to swell, which often results in the separation of the structural linkages between lignin and carbohydrates. In contrast, acids serve as catalysts for hydrolysis of cellulose rather than as a reagent for pretreatment.

5.2 Results

5.2.1 The Hydrolysis of Coconut Shell Fragments in the Presence of Deionised Water

The application of deionised water to stimulate the hydrolysis of coconut shell fragments was considered as the baseline trial, against which all the other chemical pretreatments were evaluated. A total of seven experiments were conducted with deionised water and small variations in the physical treatment processes enabled a comparative evaluation of the

performance of the drying technique, the influence of particle size distribution on the rate, and amount of organic matter able to be hydrolysed from the coconut shell fragments.

A graphical presentation of the various combinations of physical pretreatments with deionised water is presented in Figure 5-1. This figure includes a pretreatment trial that contained sodium azide (NaN_3), and a trial in which the substrate was oven dried. Significantly, all of these trials displayed an initial COD concentration in the range of 35-150 mg/L. While every attempt was made to clean the substrate prior to its placement in the reactor, it is highly likely that the source of the soluble COD released is due to minute dust fragments trapped in and on the substrate, then liberated within the turbulent environment of the batch reactor.

During the first two days of the trial, four of the five combinations displayed a substantial increase in COD within the batch reactor increases. This rise in COD is attributed to the hydrolysis of the organic matter in and on the substrate. It is assumed that the hydrolysis liberates glucose units into solution, hence the COD assessed is a direct measure of the quantity of glucose in solution.

By day two, the COD values in reactors 1a ($2 \le x \le 10mm$), 1e ($2 \le x \le 8mm$), and 1c ($2 \le x \le 10mm$, Oven dried) peaked. From day two onwards, they fluctuated and eventually reached a steady state with a similar COD value of about 110 mg/L.

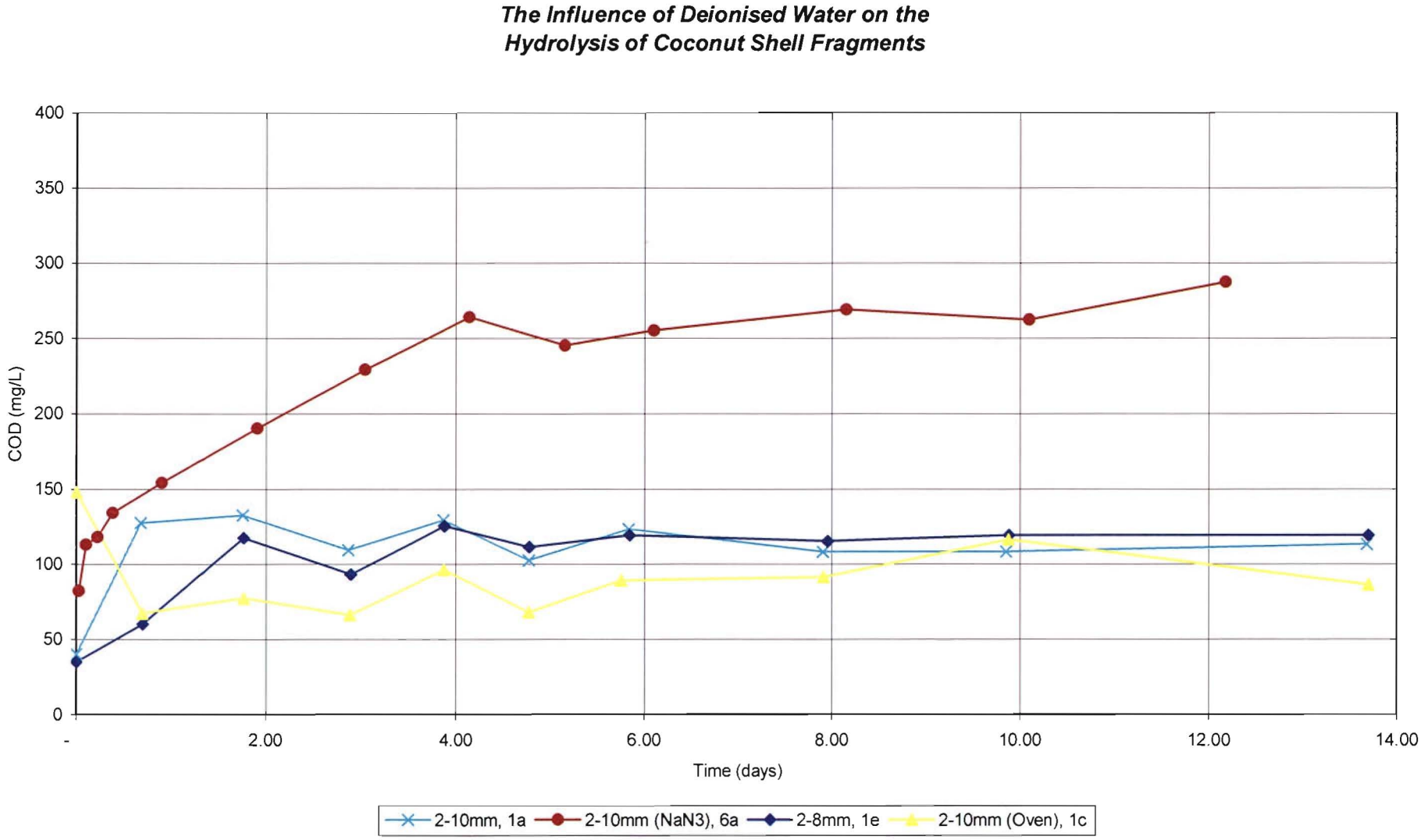

Figure 5-1 The Hydrolysis of coconut shell fragments by deionised water.

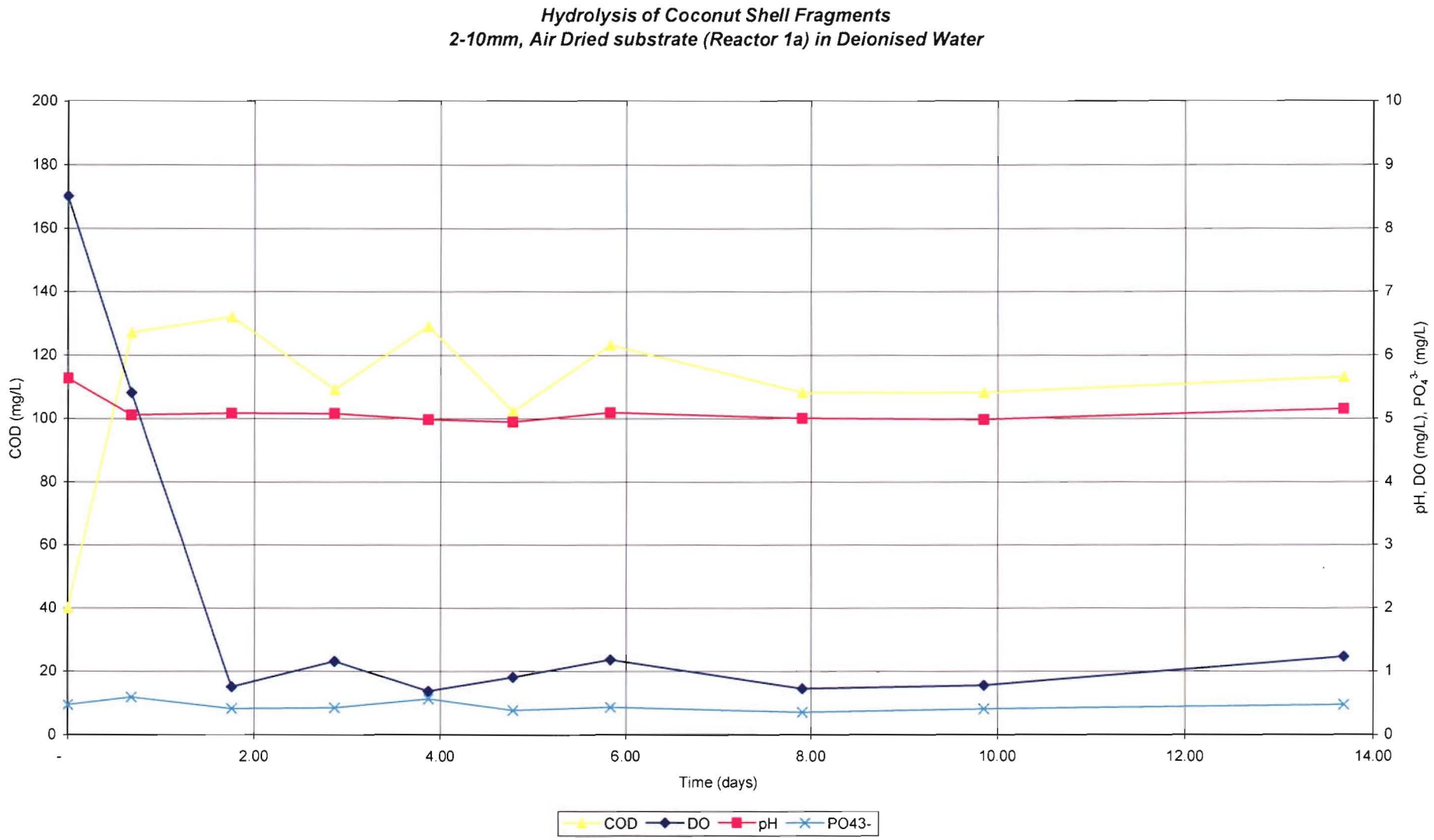

Figure 5-2 Hydrolysis of coconut shell fragments (2-10mm) following air-drying and pretreated in deionised water (Reactor 1a).

Both reactors showed fluctuations in COD from day two, which suggests that a process was consuming the organic matter within the reactor. Since neither the pretreatment reactors nor the substrate were sterilised, it is highly feasible that heterotrophic bacteria was introduced and was able to survive in the low nutrient, high DO environment, hence the observed consumption of COD and DO within the reactor.

Figure 5-2 (Reactor 1a) supports this hypothesis. The bacterial metabolism of the COD coincided with a reduction in DO (7.6mg/L of oxygen was consumed). This observation in conjunction with the fluctuation in COD in the reactor from day two to day six could be explained by the following:

1. variability in the COD test is in part associated with the confidence interval of the COD test +/- 7.7% (as evaluated in the uncertainty analysis in Appendix F), or
2. possibly bacterial metabolism.

In the course of the pretreatment batch trials, it was thought that bacterial growth occurring within the reactor was influencing the process. This is due to the fluctuations in soluble COD and DO in the reactors and, in some experimental trials, the fluid in the reactors turned a cloudy tannin colour.

More specifically, the COD might be released in an ongoing process but, as it is simultaneously released, it is being consumed by heterotrophic bacteria. The overall result may be either an increase or decrease in the COD measured in the bulk solution, depending on the relative rates of COD release verses COD consumption.

In one extreme case (Figure 5-3, this photo was taken on day eight of the trial), bacteria growth was observed to form a slimy floc attached to the sampling tube and in cloudy flocs in solution.

Membrane filtration of these reactors indicated that the bacteria were predominantly in the coliform group. Dilutions of 1 mL in 500 resulted in colonies too numerous to count. However, some of the membrane filtration tests showed no evidence of coliform type bacteria but were predominantly non-coliform. Again, dilution of 1mL in 500 resulted in colonies to numerous too count.

Figure 5-3 Pretreatment Batch Reactor 1f, coconut shells (2-8mm, air dried) in deionised water.

In later trials, sodium azide was added to minimise the effect of bacterial and fungal growth (clouding) and the result was apparent in, reactor trial 6a (Figure 5-1). The sodium azide treated substrate released 141% more COD than those of the untreated reactors.[15]

From day one to day six, the sodium azide augmented reactor profile (of reactor 6a), continued to have a measurable increase of COD in solution while the other reactors in Figure 5-1 had a

[15] The COD released, excluding the initial COD release that occurs in the first few hours, resulted in the sodium azide treated reactor releasing 111% more COD than those reactors without treatment by NaN_3.

static concentration of soluble COD in solution. From day six onwards the rate of COD increase for the sodium azide augmented reactor tended to plateau off.

As mentioned earlier, the majority of the increase in COD is attributed to the hydrolysis of the cellulose on the coconut shell substrate. This is supported by the shape of the sodium azide augmented deionised water pretreatment trial (Figure 5-1, 6a). The sudden rise in soluble COD in the first few hours of the trial is due to the solubilisation of organic dust on the surface and inside the pores of the coconut shell. The increase in soluble COD in the next few days is attributed to hydrolysis of the cellulose sites on the coconut shell. As the number of available sites declines the rate of COD hydrolysis plateaus until it reaches a horizontal asymptote.

5.2.2 Results of the Hydrolysis of Substrate by Hydrochloric Acid

Three hydrolysis pretreatment reactors were operated with hydrochloric acid as the only form of pretreatment on the fragmented coconut shells. Two different concentrations of hydrochloric acid were considered. Two reactors (4e and 4f) were operated with an initial pH=2, which equates to 1×10^{-2} moles/L of hydrochloric acid, while the other reactor (4c) had an initial concentration of 1.4×10^{-4} moles/L of hydrochloric acid or pH=3.74 (to simplify the descriptive analysis, this has been defined as pH=4).

Figure 5-4 below illustrates the COD hydrolysis profile of the hydrochloric acid pretreatments as well as that of the baseline scenario (deionised water + sodium azide, 6a). The hydrochloric acid pretreatment profiles exhibited similar characteristics as before in that all had an initial increase in COD during the first 12-24 hours, and all reached a COD release plateau at day five. The reactors without the sodium azide additive all reach the COD level of about 110mg/L, while reactor 6a (with NaN_3) had a greater initial release and continued to hydrolyse the coconut shell fragments at a rate much greater than the other reactors, eventually levelling off at a COD value of 260mg/L by day five.

The results of this set of experiments indicate that pretreatment of coconut shells with hydrochloric acid offers no advantage in the liberation of molecular organic matter from the coconut shells during the hydrolysis process. This is evident in Figure 5-4 where the hydrochloric acid pretreatment reactors show a similar final COD release value to that of deionised water (1a).

It is probable that the highly acidic environment of the hydrochloric acid reactors (in particular reactor 4f with its initial pH=2.0) would be toxic to bacteria. Table 5-1 supports this hypothesis, since minimal or no bacterial activity occurred in the low pH reactors. That is, the DO concentration in reactors with minimal or no bacterial activity remains static or exhibited a gradual decline, as per reactors 4f (HCl, pH = 2) and 6a (Deionised water + NaN_3). Since minimal or no bacterial activity was occurring in these reactors, any COD hydrolysed would not be consumed by the bacteria.

A comparison of the HCl, pH = 2 reactor to that of the deionised water + sodium azide reactor indicates that the COD hydrolysis induced by hydrochloric acid is 41.8% of that released by deionised water. This observation supports the theory that hydrochloric acid has a detrimental influence on the rate and amount of organic matter hydrolysed from coconut shell fragments.

This observation could be due to the fact that highly acidic conditions have low concentrations of hydroxide ions. The probability that hydroxides are present at a potential hydrolysis site on the coconut shell is then considered to be low, hence the low rate of hydrolysis.

Table 5-1 Dissolved Oxygen (mg O_2/L) Concentration within the Hydrochloric Acid Pretreatment Reactors

Time (days)	t = 0	t = 1	t = 2	t = 5	t = 8
Deionised Water (1a)	8.50	4.00*	0.75	0.90	0.73
HCl pH = 4 (4c)	9.20	3.95	3.65	2.63	1.98*
HCl pH = 2 (4f)	9.20	7.00	7.05	7.10	7.05*
Deionised Water + NaN_3 (6a)	9.00	6.55	6.05*	5.90	5.75

* Denotes that this value has been determined by interpolation.

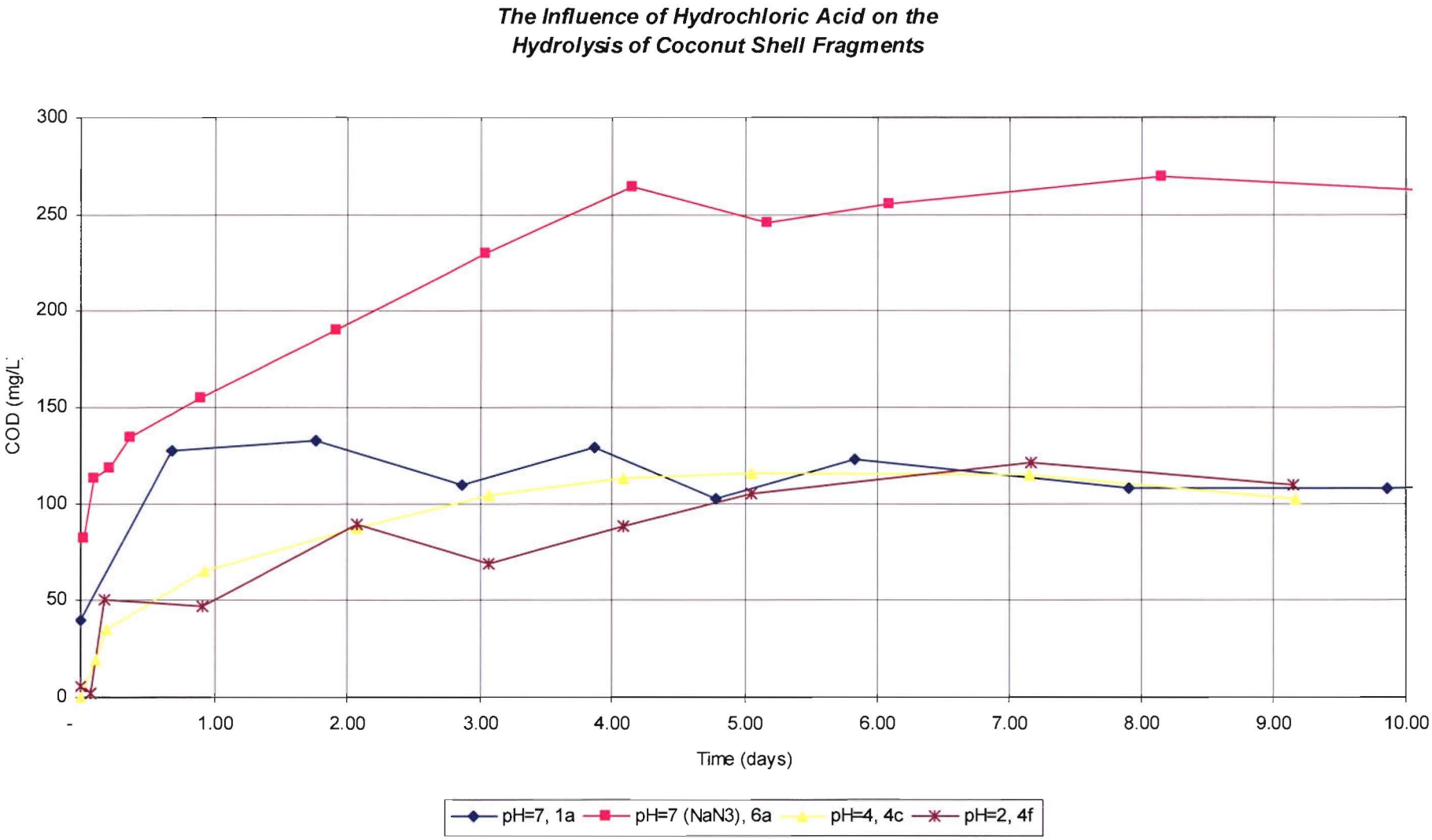

Figure 5-4 Hydrolysis of coconut fragment substrate by Hydrochloric acid.

5.2.3 Results of the Hydrolysis of Substrate by Sulphuric Acid

Two concentrations of sulphuric acid were considered. Three trials operated with an initial concentration of $6.6x10^{-3}$ moles/L of H_2SO_4 (nominal pH = 2), and two with $5.4x10^{-4}$ moles/L of H_2SO_4 (nominal pH = 3). One of the pH = 2, reactors (6b) was augmented with sodium azide, to remove the possible influence of bacteria growth and/or metabolism. Figure 5-5 below outlines the hydrolysis profile of this pretreatment technique and, as expected, indicates that an initial release in COD occurs in the first 10 hours. The rate of COD release then remains constant within the reactor until day five, after which the amount of COD released plateaus.

The shape and eventual plateaus of reactors 5d and 5f (without sodium azide) are similar, with the reactors eventually plateauing at 138mg/L and 109mg/L respectively. In contrast, reactors 6a (pH=7, NaN_3) and 6b (pH=2, NaN_3) achieved solubilised COD values almost double that of the reactors without sodium azide. Reactor 6a plateaued at 258mg/L, and reactor 6b at 195mg/L.

Table 5-2 summarises the rate of COD hydrolysis that occurs between the initial COD release (t = 1 day) and the COD plateau (t = 5 days). The rate of COD released from the substrate due to the sulphuric acid solution was 18.3mg/L/day and 12.9mg/L/day for the reactor with an initial pH=3 (5d) and reactors with initial pH=2 (average 5f and 5e) respectively. Reactor 6b (initial pH=2, 500mg/L NaN_3) exhibited a similar rate of COD release of 21.0 mg/L/day to that of the deionised and sodium azide treated reactor (reactor 6a), 26.1mg/L/day.

Table 5-2 The Rate of COD Hydrolysis due to Sulphuric Acid Pretreatment

	Distribution Size	Reactor	t_1 (day)	COD_{t1} (mg/L)	t_2 (day)	COD_{t2} (mg/L)	Rate of COD release (mg/L/day)	
pH = 7, NaN_3	2-10mm	6a	0.10	113	5.16	245	26.1	
pH = 2, NaN_3	2-10mm	6b	0.02	70	4.93	173	21.0	
pH = 3	2-8mm	5d	0.05	6	4.91	95	18.3	
pH = 2	2-8mm	5f	0.00	10	4.91	69	12	Ave.
pH = 2	2-8mm	5e	0.32	7	4.90	70	13.8	12.9

The variation between the initial release in COD between the sodium azide treated reactor (pH = 2, 6b) and the untreated reactors (pH = 2, 5f and 5e) could be attributed to variation in the degree of cleaning of the substrates prior to pretreatment. It is possible that a varying degree of soluble material remained on the substrate after the cleaning process. Table 5-3 compensates for this effect by assuming that the initial COD hydrolysis is primarily attributable to the solubilisation of minute material remaining on the substrate after the cleaning process. Hence, the initial release that occurs in the first 10 hours has been subtracted from the profile, resulting in a virtual COD hydrolysis profile.

The virtual COD technique compensates for the initial COD release, thought to be as a result of minute fragments of COD bound in the substrate. Effectively the start of the COD hydrolysis results are offset by the initial COD release and the data records compensated by the initial offset and demonstrated in Table 5-3 and Figure 5-6. This technique is similar to the "virtual origin" concept utilised to assess momentum and buoyant hydraulic plumes.

This technique is considered valid since the long-term suitability of this pretreatment technique is of interest, and any short-term gains in COD such as the initial COD release are not sustainable.

Table 5-3 Virtual COD Hydrolysis (mg/L) as a result of Sulphuric Acid Pretreatment

	Particle Size Distribution	*Reactor*	*t = 0*	*t = 1*	*t = 5*	*t = 8*
pH = 7, NaN_3	2-10mm	6a	0	37	113	134
pH = 2, NaN_3	2-10mm	6b	0	25	105	123
pH = 3	2-8mm	5d	0	35	92	113
pH = 2	2-8mm	5f	0	29	48	73

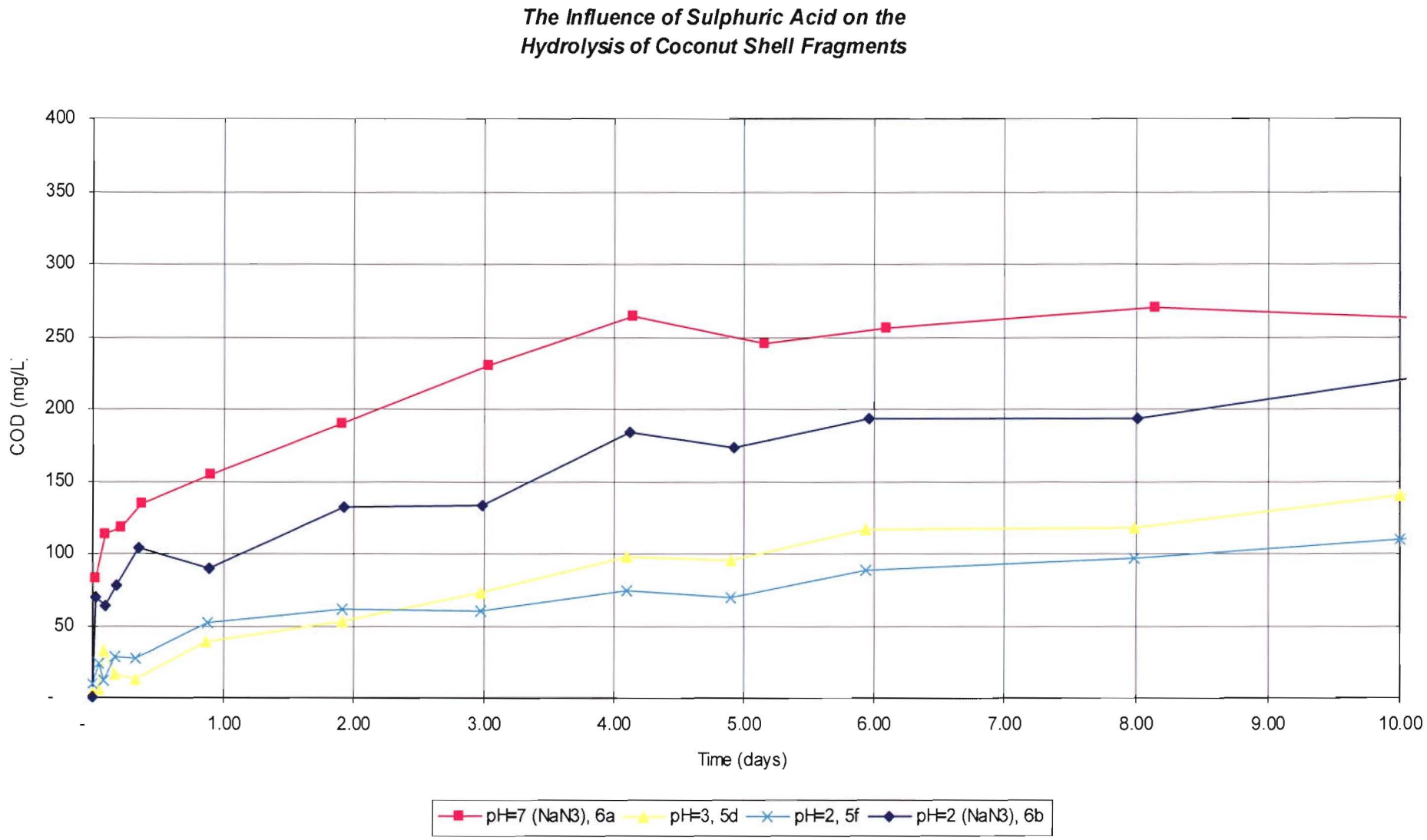

Figure 5-5 Hydrolysis of coconut shell fragments by Sulphuric Acid.

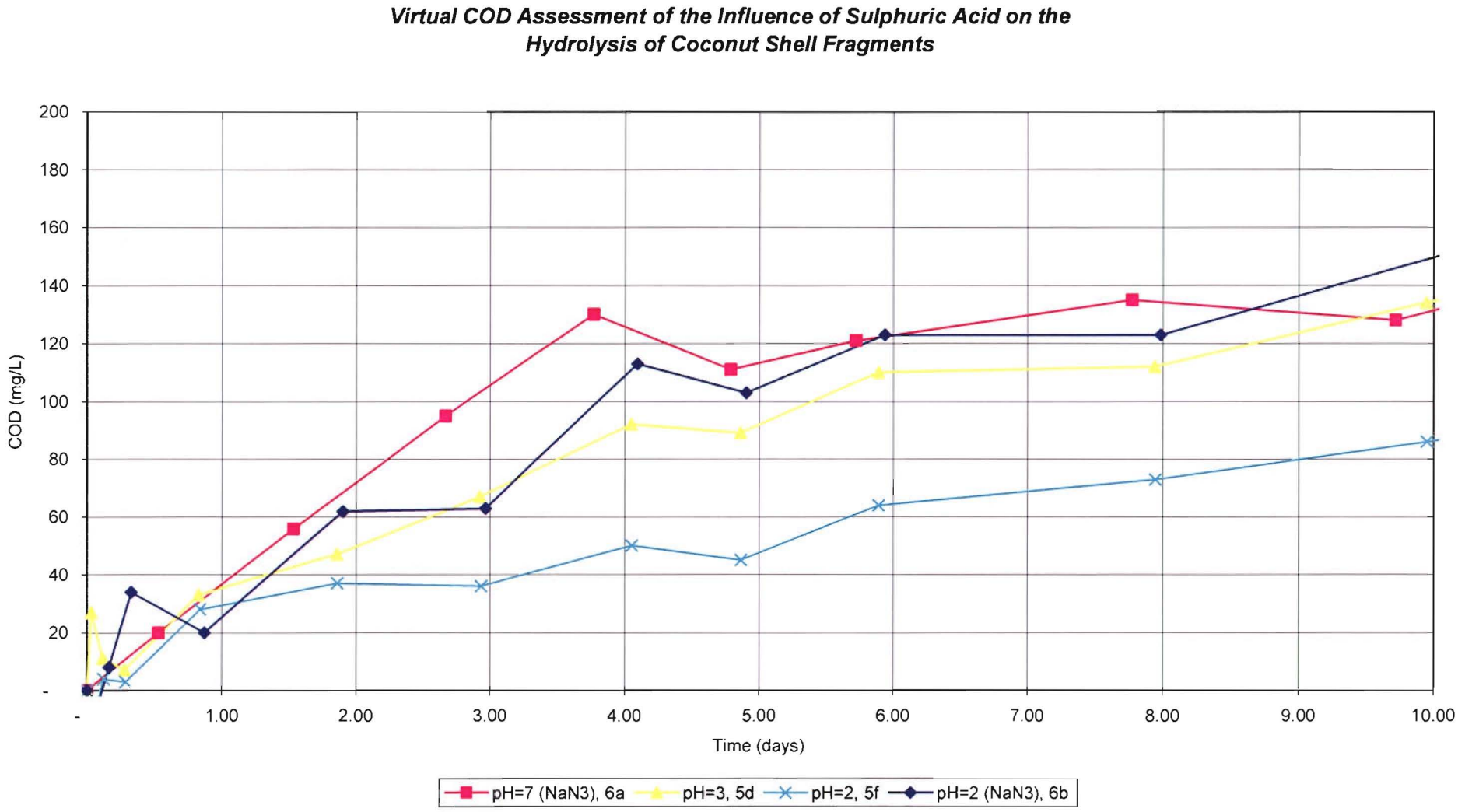

Figure 5-6 Virtual COD assessment of Figure 5-5 (Influence of Sulphuric Acid on the Hydrolysis of Coconut Shell Fragments)

Two comparisons can be drawn from Table 5-3, the first being that the lower the initial pH, the lower the amount of COD hydrolysis that occurs, which is evident by the comparisons between reactors 6a, and 6b at days 5 and 8, and reactors 5d, and 5f at days 5 and 8. The second comparison, between reactor 5f (pH=2, 2-8mm) and reactor 6b (pH=2, 2-10mm, NaN_3), indicated that reactor 6b releases greater COD due to hydrolysis. This is probably due to the influence of NaN_3 but may also be due to the influence of the large particle distribution range. That is, it should be remembered that the larger, 2-10mm particle distribution has a slightly lower surface area per gram of substrate when compared to the 2-8mm particle distribution (Table 4-4).

5.2.4 Results of the Hydrolysis of Substrate by Acetic Acid

Both acetic and propionic acid are carboxylic acids and therefore coupled to these acids is a chemical oxygen demand associated with the concentration of the acid. Appendix G outlines the dissociation calculations and oxidation reactions used to assess the COD of acetic and propionic acid, summarised in Table 5-4.

Table 5-4 Theoretical Oxygen Demand of Organic Acids Utilised in Pretreatment

	Nominal pH	*Molar Concentration*	*Theoretical COD*
Acetic Acid CH_3COOH	pH = 3, (7a, 7b)	5.854×10^{-2} moles	3747 mg/L
	pH = 5, (7c)	1.575×10^{-5} moles	1 mg/L
Propionic Acid CH_3CH_2COOH	pH = 3, (7d, 7e)	7.512×10^{-2} moles	8413 mg/L
	pH = 5, (7f)	1.741×10^{-5} moles	2 mg/L

The COD test (Standard Methods, APHA 1999) is limited in the amount of organic matter it is capable of oxidising, equivalent to a COD reading of 0-800 mg/L O_2. Since some of the carboxylic acids utilised have associated COD values in the thousands, the COD sample required diluting. Uncertainty analysis conducted in Appendix F, as applied in Table 5-5 indicates that the standard error expected of the COD of pH =3 acetic acid reactor would be ±1Std Dev. = 8.7% or ±326 mg/L.

Table 5-5 Standard Deviation Expected from the Theoretical Chemical Oxygen Demand Test of Organic Acids Utilised in Pretreatment				
	Nominal pH	*Theoretical COD*	*Std. Dev.%*	*Std. Dev.*
Acetic Acid CH_3COOH	pH = 3, (7a, 7b)	3747 mg/L	8.95%	326 mg/L
	pH = 5, (7c)	1 mg/L	8.7%	-
Propionic Acid CH_3CH_2COOH	pH = 3, (7d, 7e)	8413 mg/L	8.95%	732 mg/L
	pH = 5, (7f)	2 mg/L	8.7%	-

The band of uncertainty (equivalent to ±1 standard deviation) associated with reactors 7a and 7b (Acetic acid, pH = 3) in Figure 5-7 suggests that no measurable hydrolysis of the substrate occurred. That is, since the maximum COD released from this pretreatment process is expected to be in the same order as one standard deviation of the theoretical oxygen demand, it is difficult to distinguish the COD due to hydrolysis amongst the natural variability attributed to the COD measurement technique. Fortunately, the lower acidic reactors had a background COD of 1 mg/L (due to the acetic acid, pH = 5) and therefore any change in COD due to hydrolysis is not hidden by the uncertainty in the test itself.

Figure 5-7 shows that the lower concentration of acetic acid (7c) exhibits a similar COD profile to that of the untreated substrate (Reactor 6a). Closer analysis (Figure 5-8) shows that the profiles are practically identical, indicating that the initial COD hydrolysis that occurs in the first several hours is responsible for the 52 mg/L COD offset between reactors 7c and 6a, observed in Figure 5-7.

Unlike the hydrochloric and sulphuric acids, higher concentrations of acetic acids do not seem to hinder the hydrolysis of coconut shell fragments, as evident in both Figure 5-7 and Figure 5-8. These figures illustrate that the acetic acid pretreatment (pH = 5) offers similar hydrolysis ability to that of deionised water. In comparison, hydrochloric acid (Figure 5-4) and sulphuric acid (Figure 5-5) have less ability to hydrolyse as the pH of the acid drops.

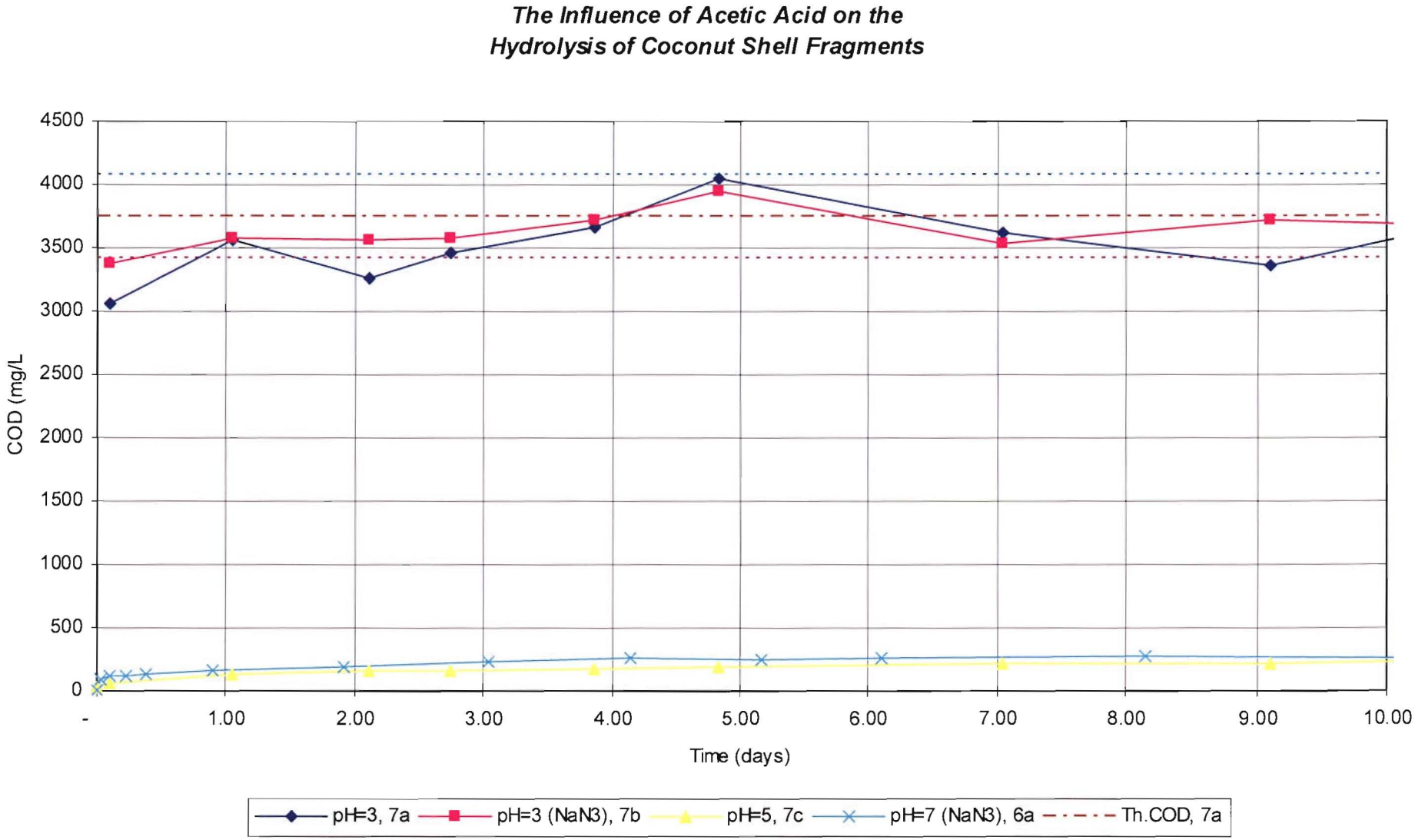

Figure 5-7 The influence of acetic acid pretreatment technique.

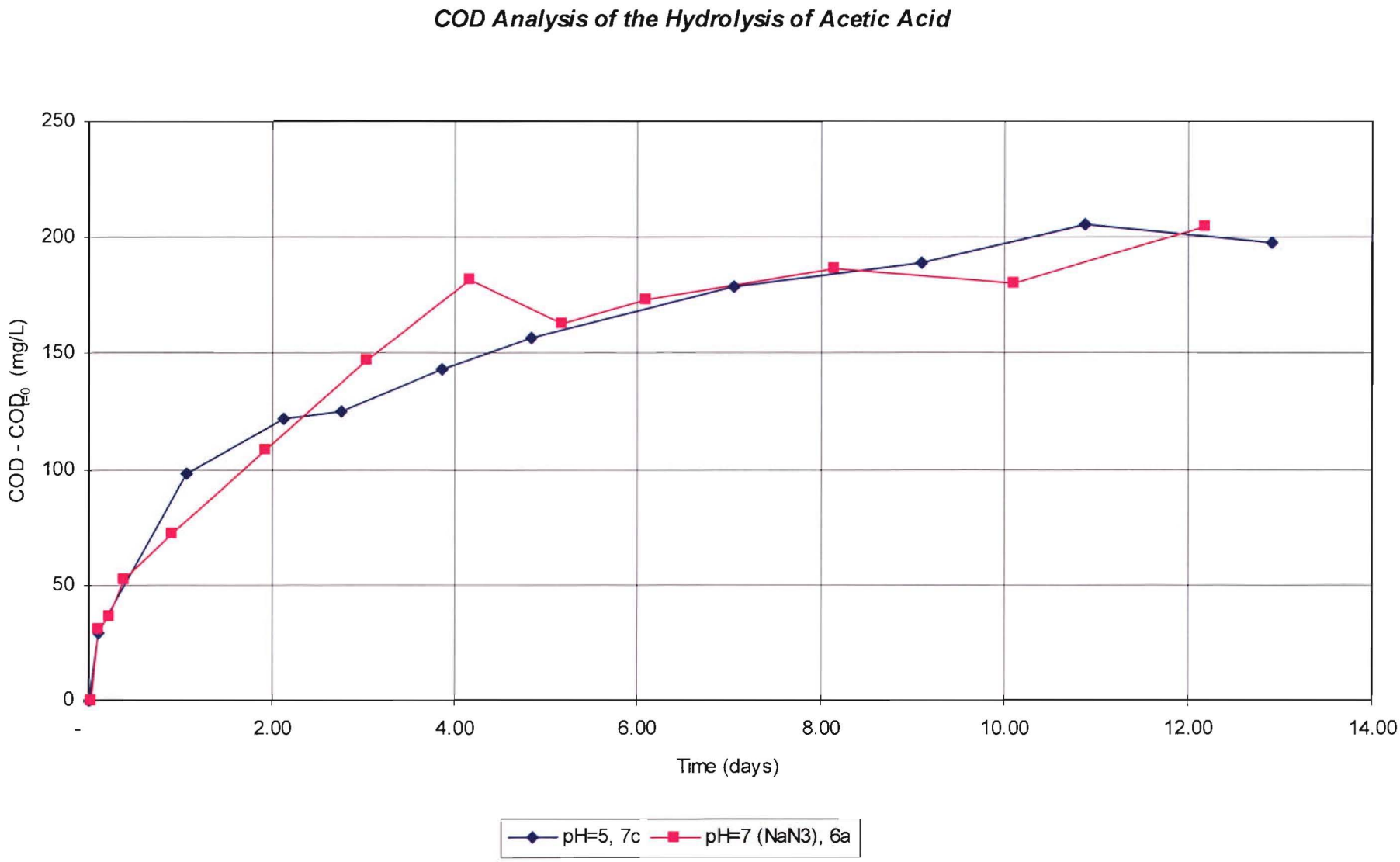

Figure 5-8 The COD analysis of the acetic acid (pH=5) as a hydrolysis pretreatment reagent.

5.2.5 Results of the Hydrolysis of Substrate by Propionic Acid

Since propionic acid is also a carboxylic acid, the COD test suffers from the same limitations outlined above in Section 0. High concentrations of propionic acid (pH = 3), shown in Figure 5-9, have COD profiles that do not exceed the ±1 standard deviation limit that the COD uncertainty analysis (Appendix G) indicate. Therefore, it is not possible to support any claim that propionic acid has a capability similar to that of deionised water in the hydrolysis of coconut shell fragments.

Unfortunately, the lower concentration of propionic acid (pH = 5, reactor 7f) also cannot be used to support any claims. Within this reactor there is an unexplained initial offset in the COD. Analysis of the COD demand of the organic acid, summarised in Table 5-4, suggests that the COD profile should be elevated by 2mg/L; however, the actual COD profile of reactor 7f in Figure 5-9 has an offset on the order of 1000mg/L. Even compensating for the initial offset via virtual COD analysis (Figure 5-10) provides inconclusive results. The initial increase in COD of reactor 7f could be due to experimental error, such as contamination of the reactor prior to addition of the substrate and propionic acid

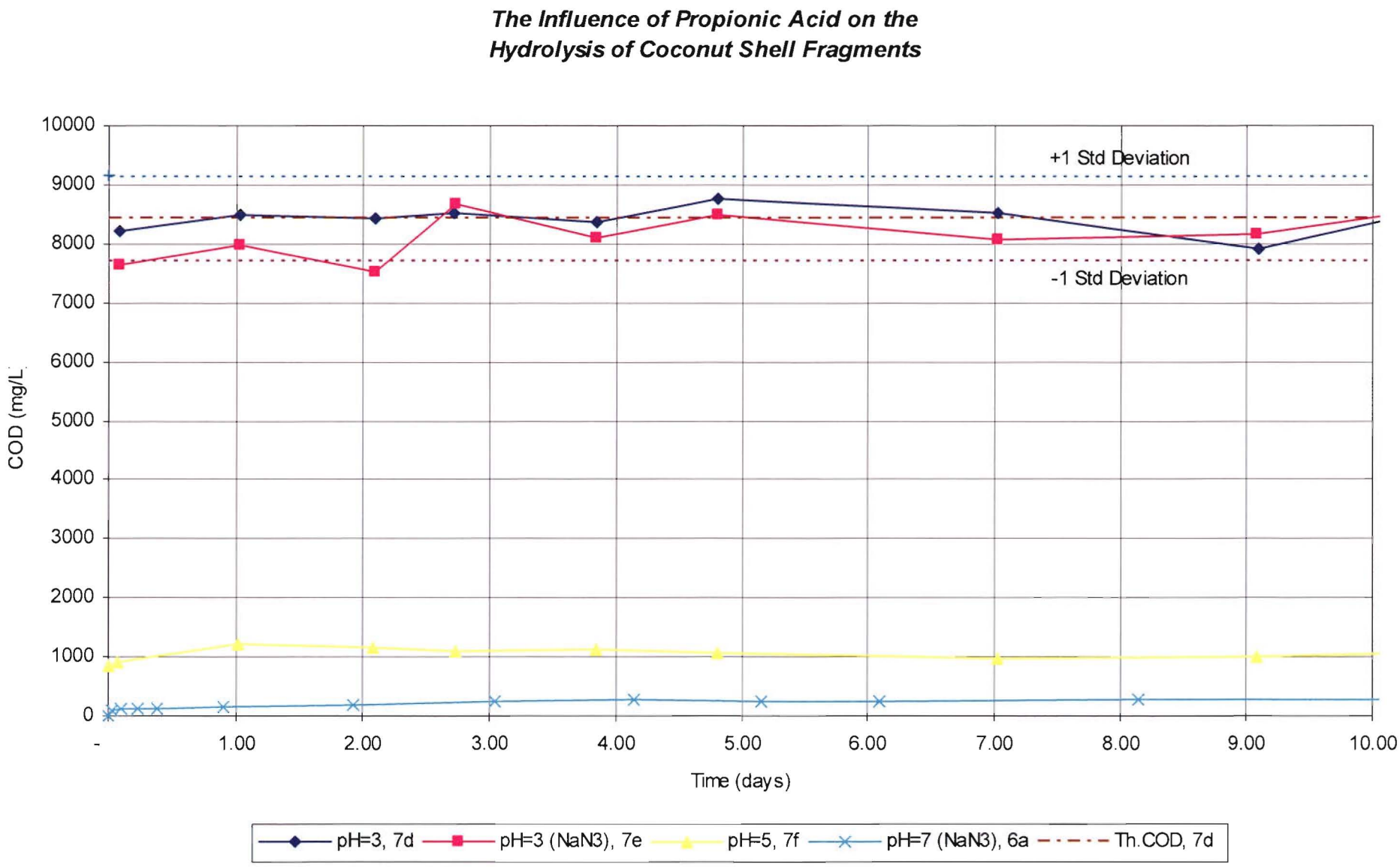

Figure 5-9 Influence of propionic acid on the hydrolysis of coconut shell fragments

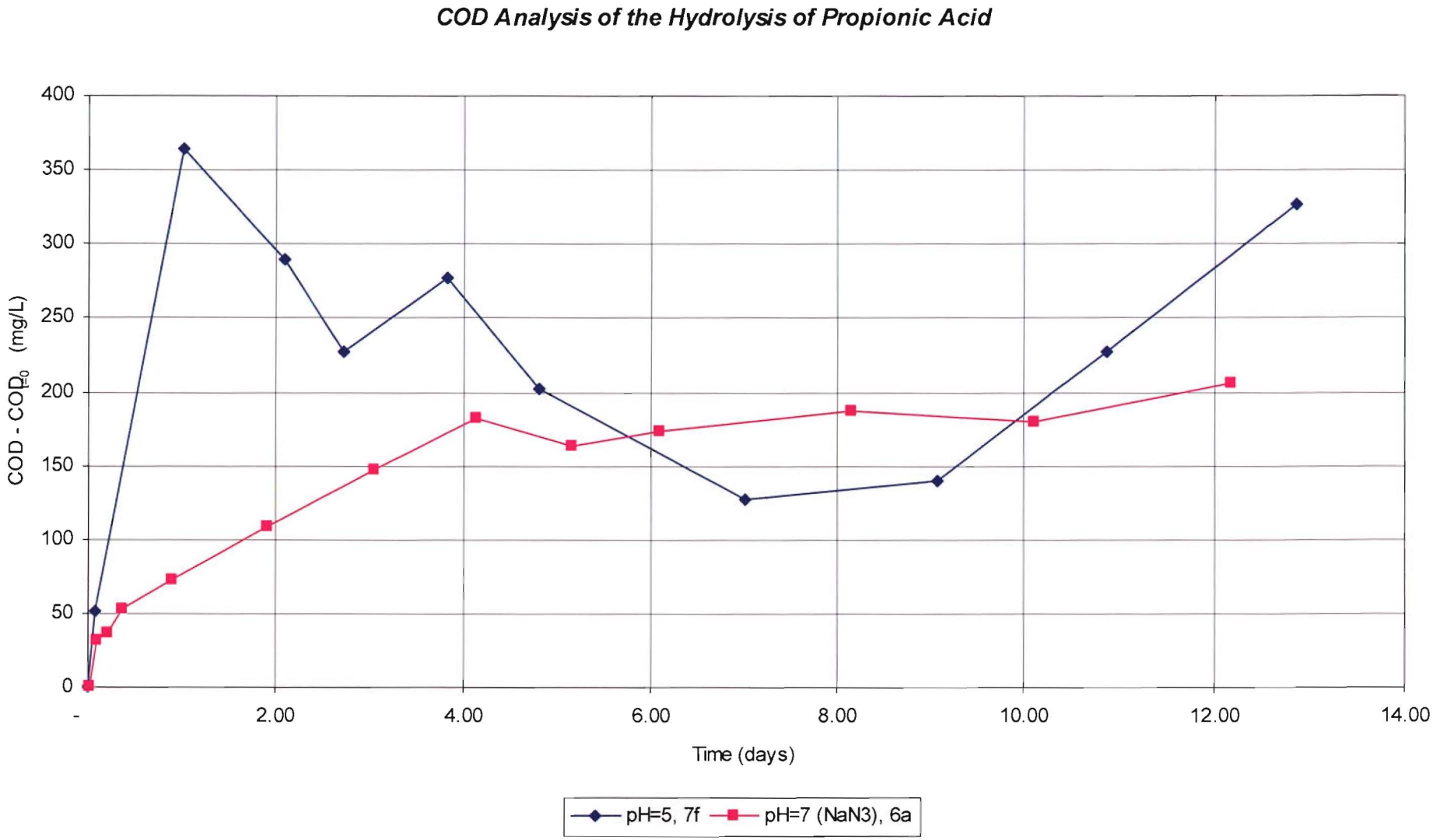

Figure 5-10 The COD analysis of propionic acid (pH=5) as a hydrolysis pretreatment agent.

5.2.6 Results of the Hydrolysis of Substrate by Sodium Hydroxide

The previous trials with acid pretreatments show that as the pH of the pretreatment dropped, the rate of organic hydrolysis decreased. Therefore, alkaline pretreatments such as sodium hydroxide and lime, may show an increase in the rate of organic hydrolysis.

Figure 5-11 summarises the COD hydrolysis profile of coconut fragments treated with sodium hydroxide. As suspected, all the profiles display rates of hydrolysis greater than those of the baseline condition, deionised water + NaN_3 (reactor 6a). In addition, the profiles have similar characteristics to those of previous chemical pretreatments, with an initial increase in soluble COD in the first four hours (in this case on the order of 50 to 150mg/L). Some of the trials eventually reached a COD plateau.

Table 5-6 The influence of Sodium Hydroxide Concentration on the Rate of COD release due to hydrolysis

Initial concentration of NaOH	*COD solubilisation Rate*		
	Reactor Conc./day [1] *(mg/L/day)*	*Released/day* [2] *(mg/day)*	*Released/day/gm substrate* [3] *(1/day)*
pH = 9, 3d	78	313	1.57
pH = 12, 3e	221	886	4.43
pH = 14, 2c	3389	13555	67.78
pH = 7 (NaN_3), 6a	30	118	0.59
pH = 12 (NaN_3), 6e	106	426	2.13
pH = 14 (NaN_3), 6c	895	3578	17.89

[1] A measure of the rate of change of the COD concentration within the reactor.

[2] A measure of the amount of COD released in the reactor per day.

[3] A normalised measure of the rate of COD released per mass of substrate within the reactor.

The initial rate of COD release began to decline from day 0.5. The time at which the plateau was reached would vary with the concentration of hydroxide ions. That is, in some cases the plateau point was not reached as the chemical pretreatment continued to hydrolyse the coconut shell fragments within the timeframe allotted to the experiment. At the lower concentrations of NaOH (pH = 7 reactor 6a, and pH = 9 reactor 6d), however, COD release plateaued after day

two in the case of pH=12 and pH=9 trails. Both Figure 5-11 and Table 5-6 show that as the initial concentration of NaOH present increases, there is a corresponding increase in the rate and quantity of soluble COD released. The rate of COD released in Table 5-6 is determined to be the change in COD between the initial release and eventual plateau.

As previously identified by Feist et al. (1970, cited in Fan et al. 1987), the digestibility of hardwoods increased significantly with NaOH treatment. Similarly, the application of NaOH on coconut shell fragments helped digest or hydrolyse chemically oxidisable material from the fragments. It is assumed that the hydrolysed form is cellulose that is readily degraded into glucose units that have the potential to be readily consumed by denitrifying bacteria.

While the hydrolysis of the coconut shells resulted an increase in COD in solution, a complementary reduction in hydroxide ions was observed, as demonstrated in Figure 5-12.

The change in reactor pH for the NaOH pretreatment was distinct to that of the earlier pretreatments (acids and those with deionised water), in that the earlier pretreatments trials did present in any movement in the reactor pH during the experimental trials.

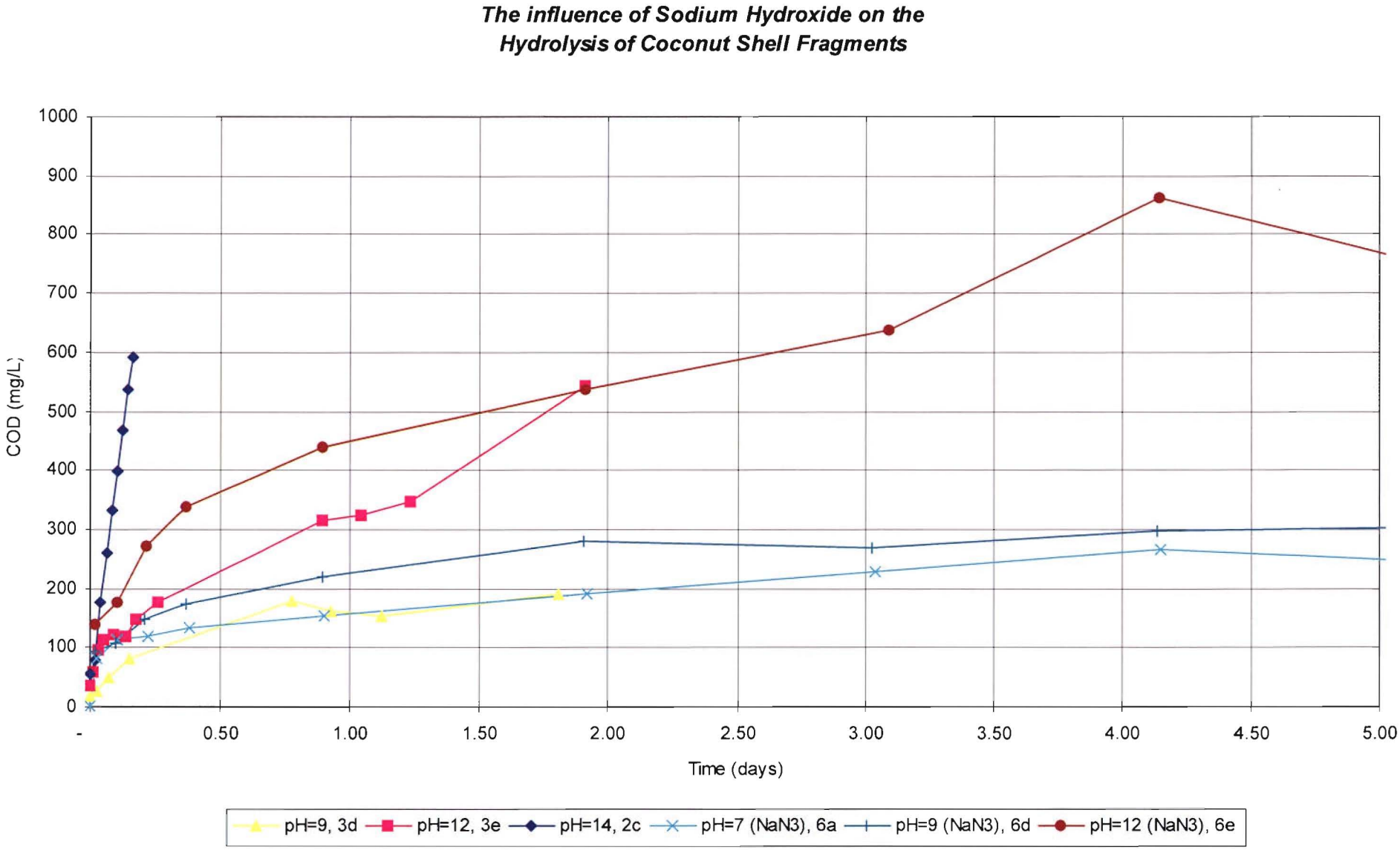

Figure 5-11 The hydrolysis of shell fragments by sodium hydroxide.

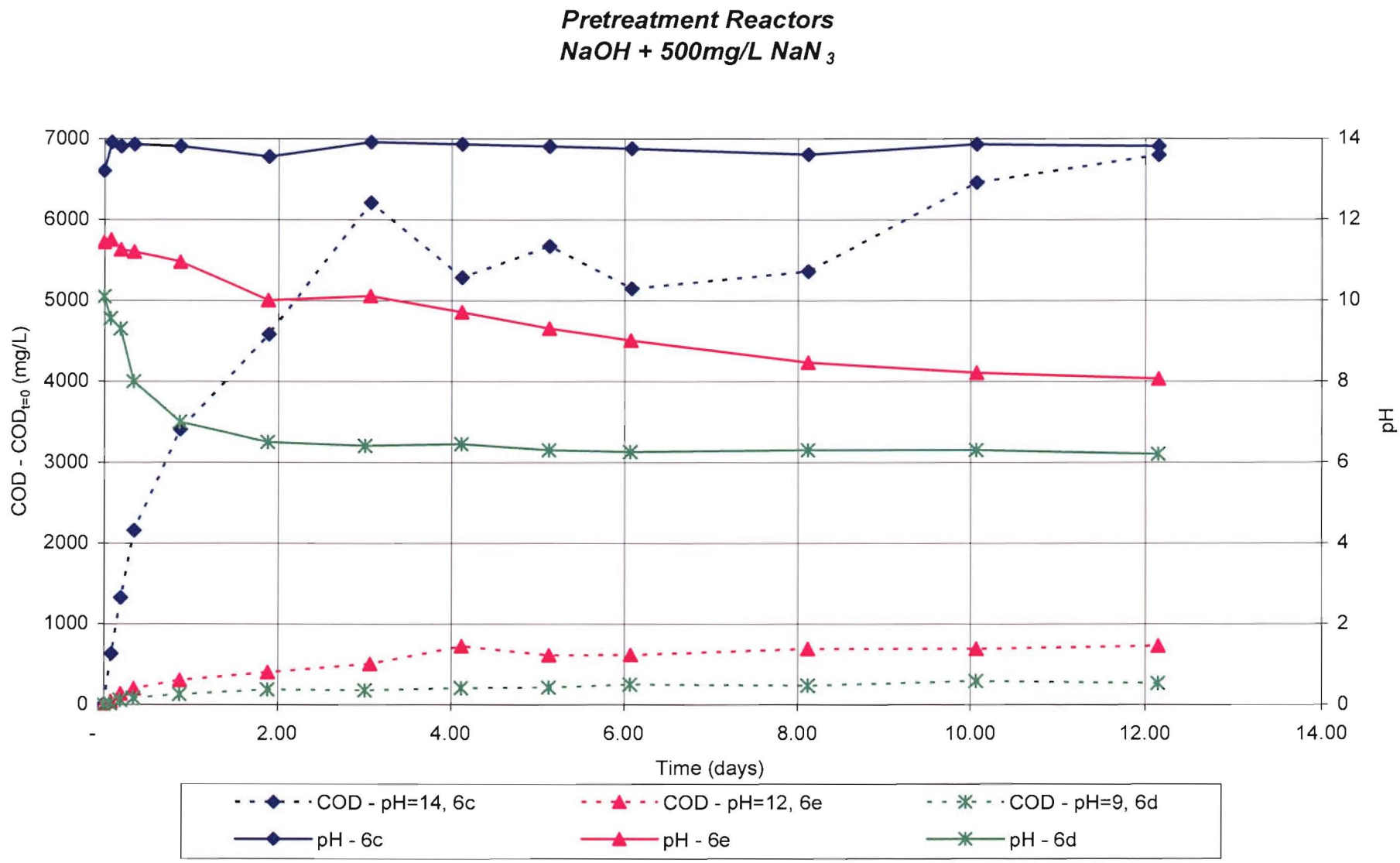

Figure 5-12 Comparison of the COD released and the pH value of the NaOH pretreatment trails.

5.2.7 Results of the Hydrolysis of Substrate by Lime

The previous section indicated that hydroxide ions participate in the hydrolysis of organic matter from coconut shell fragments. The three concentrations of lime added to the reactors (50, 100 and 500 mg/L) dissociate into the corresponding concentrations of hydroxide (Table 5-7).

Table 5-7 Hydroxide Concentrations due to the Dissociation of Calcium Hydroxide [$Ca(OH)_2$]

Concentration of Calcium Hydroxide	*Concentration of hydroxide ions present in solution*			
	Theoretical Initial pH	*m.moles OH/L*	*m.moles OH in reactor*	*m.moles OH / gm of substrate*
50mg/L	10.8	1.33	5.32	2.66×10^{-2}
100mg/L	11.1	2.60	10.4	5.20×10^{-2}
500mg/L	11.6	10.9	43.6	0.218

The differing concentrations of calcium hydroxide revealed (Figure 5-13) an increase in the extent and rate of COD hydrolysis with increasing hydroxide in the solution. However, the relationship was non-linear. A 8-fold increase in hydroxide ions from 50 to 500 mg/L as indicated in Table 5-7; correlated to a 13.5x increase in the hydrolysis rate, and a 5.5x increase in the COD released into solution (Table 5-8).

The COD profiles in Figure 5-13, like the profiles in the other pretreatment studies, undergo three phases: an initial increase in COD, a COD plateau, and a transitional phase between the initial COD release and the COD plateau. The changeover point at which the COD profile goes from the transition to plateau phase observed in Figure 5-13 is summarised in Table 5-9. Correlating these time intervals with the pH within the reactor in Figure 5-14, Table 5-9 indicates that the cessation of calcium hydroxide induced hydrolysis occurs when the pH within the reactor reaches pH = 8.2 – 9.0. At this point the concentration of hydroxide ions is insufficient to continue providing a readily available source of cellulose molecules.

Table 5-8 The Rate and Extent of the COD Hydrolysis due to Calcium Hydroxide

Concentration of Calcium Hydroxide		*COD (mg/L) Released*		*Rate of Increase (mg O_2 /L / day)*	*Amount of COD Release(t=2→8d)*
		t = 0 days	*t = 2 days*		
50mg/L + NaN_3	8e	0	29	6.4	49
100mg/L + NaN_3	8b	0	85	4.8	37
500mg/L + NaN_3	6f	0	379	103	103
500mg/L	5a	0	80	None	None
pH = 7 + NaN_3	6a	0	108	37.7	79

As outlined earlier, sodium azide augmentation to the reactors suppresses the consumption of COD within the reactor, as evident in the comparison (Table 5-8) between the two $Ca(OH)_2$ at 500mg/L reactors (5a, and 6f). This is, due to the toxic nature of sodium azide to bacteria, Reactor 6f has a substantially higher amount of COD in solution than Reactor 5a (Figure 5-13 and Table 5-8).

Table 5-9 Correlation between the Start of the Plateau Phase and the Reactor pH

Concentration Calcium Hydroxide	*Transition – Plateau Phase Intersection*	*pH Range*
500 mg/L	t = 8 – 10 days	8.5 – 8.3
100 mg/L	t = 2 – 4 days	9.4 – 8.4
50 mg/L	t = 1 – 3 days	9.1 – 7.9

Table 5-8 indicates that the baseline condition (reactor 6a) offers a greater rate and extent of hydrolysis of the substrate than the 50mg/L and 100mg/L calcium hydroxide concentrations. The reason for this is uncertain, but if it is assumed (as explained in Section 5.2.10) that the hydrolysis process consumes hydroxide ions and that the dissociation of small concentrations of calcium hydroxide is immediate, then it is possible that the majority of hydroxide ions are actually consumed immediately (within the first few hours).

Evidence supporting this can be drawn from Figure 5-14, where the pH decreases over time as the rate of COD in solution also decreases. Figure 5-14 shows that with greater reduction in pH, the greater the amount of COD released into solution.

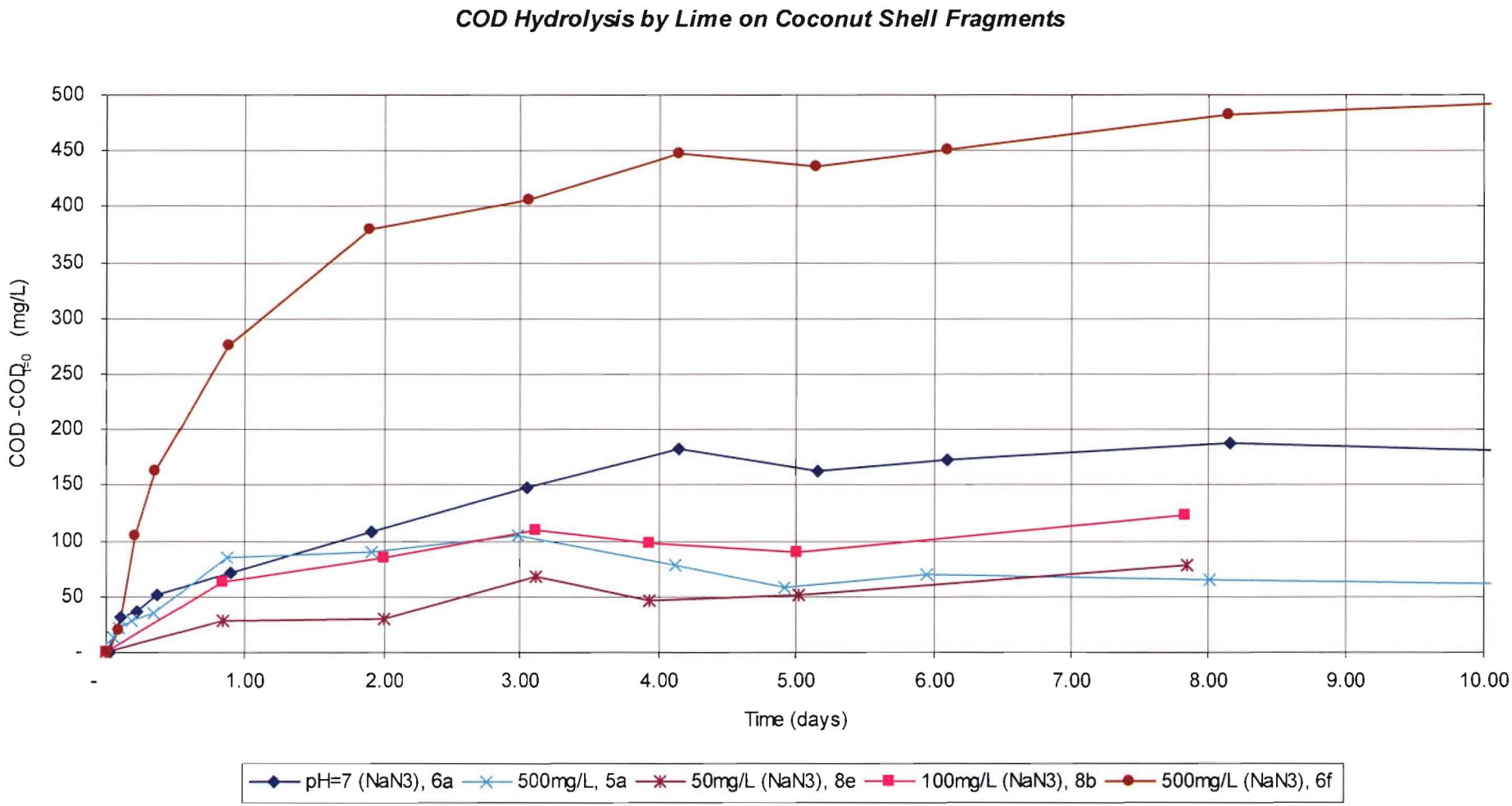

Figure 5-13 The COD hydrolysis of coconut shell fragments by calcium hydroxide.

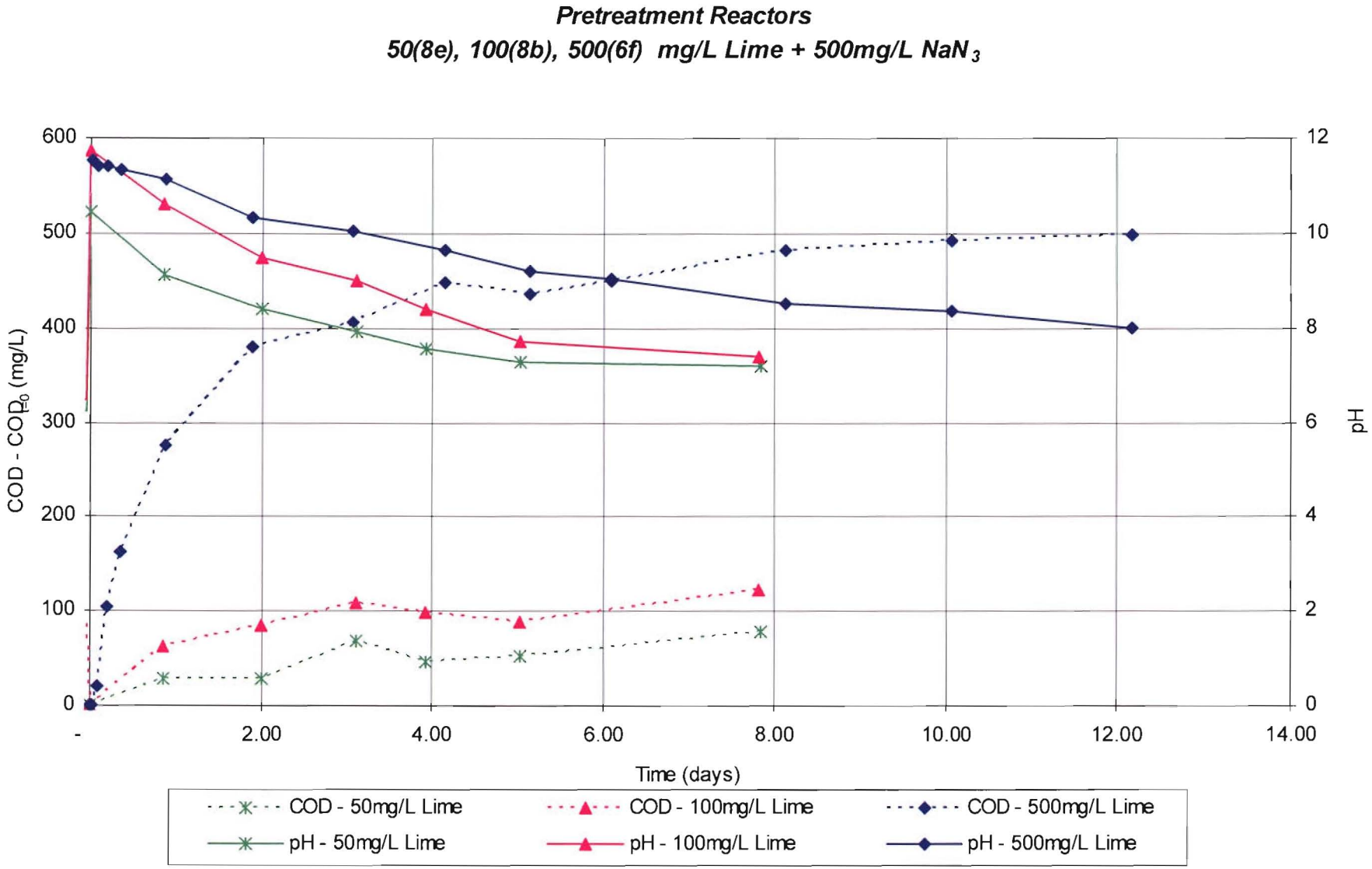

Figure 5-14 A comparative plot between the COD released and the acidity within the reactor for Lime pretreatment of coconut shell fragments.

5.2.8 The Influence of Heat Treatment on the Rate of Hydrolysis

During the cleaning of the coconut fragments it was necessary to dehydrate them as well to allow for an accurate measurement of the dry weight. This process also allowed the opportunity to investigate the possible influence that heat temperature of the fragments may have on the rate of hydrolysis.

Elevated temperatures have the potential to effect the degradation of the lignocellulose structure of the coconut fragments. Nesse et al. (1977) experimented with steam under pressure, while Brenner et al. (1977) applied a technique of moist heat expansion to increase hydrolysis of cellulose.

Thus, increasing the temperature of drying had the potential to improve the rate of hydrolysis in coconut shell fragments.

Two drying temperatures were considered, these were:

1. Air Drying: 30°C at zero % humidity
2. Oven Drying: 110°C at zero % humidity

The result of several trials of these drying temperatures is represented in Figure 5-15. This figure shows that neither temperature treatment resulted in an improvement or increase in long term hydrolysis, evident by the horizontal COD profiles from Day 2 onwards. However, in the short term (0 to 2 days) the 30°C drying treatment did result in a greater initial release. The 30°C treatment resulted in an increase in the order of 30 mg/L, while surprisingly the 110°C treatment resulted in a 60 mg/L reduction in COD during the same period (0 to 2 days).

A possible explanation for the reduction in organic carbon release at 110°C could be in part due to the combustion of the readily soluble organics on the fragments. The 110°C treated fragments were noticeably blacker in colour than the 30°C – consistent with incomplete combustion.

Figure 5-15 does show that no gain in organic hydrolysis is achieved by increasing the drying temperature. This resulted in the remaining shells for the rest of the trials being dried at 30°C at zero % humidity.

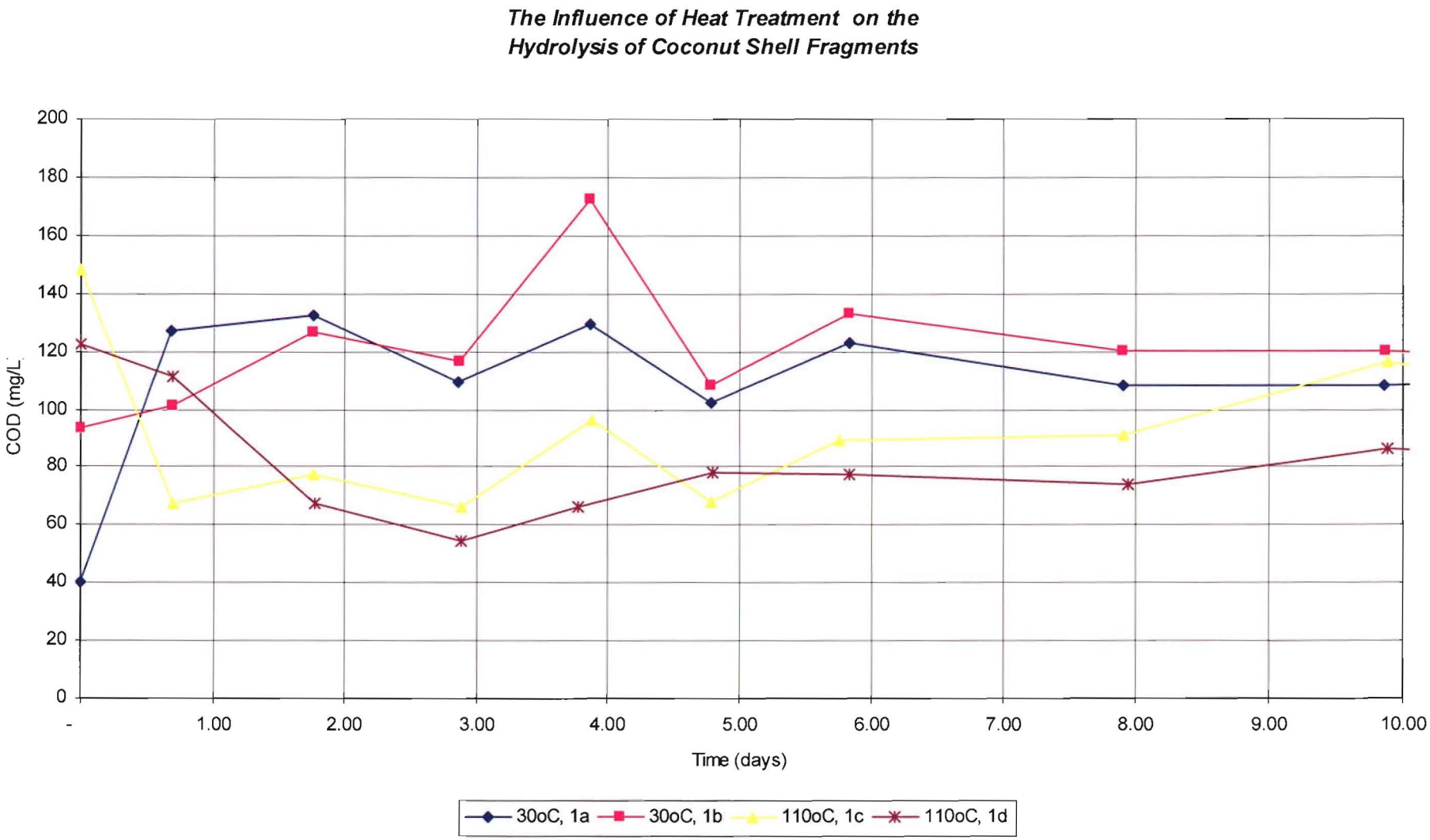

Figure 5-15 Influence of heat treatment of the coconut shell fragments on the rate of hydrolysis of organic carbon.

5.2.9 The Influence of Particle Size on the Rate of Hydrolysis

As summarised in Table 4-5, two particle size distributions were evaluated:

1. $2 \leq x \leq 10mm$ or defined as 2-10mm;
2. $2 \leq x \leq 8mm$ or defined as 2-8mm

The same stock of crushed coconut shell fragments was sieved into two particle distributions, as per the sieve analysis in Figure 4-4. Analysis of the nominal surface area per gram of substrate, Table 4-4, indicated that the smaller distribution $2 \leq x \leq 8mm$ has 42.5% greater surface area per gram of substrate. It seemed logical therefore that the rate of COD release would be substantially greater than that of the $2 \leq x \leq 10mm$ distribution on a per gram basis.

Comparisons of the 2-10mm ($2 \leq x \leq 10mm$) and the 2-8mm ($2 \leq x \leq 8mm$) distributions of deionised water treated substrates previously shown in Figure 5-1 provides no evidence that the COD release was greater for the 2-8mm, indeed there appears to be no discernable difference in COD hydrolysis between the two distributions.

Pretreatment studies with 50mg/L and 500mg/L of lime also considered the influence of variable particle sizes on the hydrolysis rate. The COD profiles of these two concentrations forms two distinct groups when graphically presented (Figure 5-16). The upper group characteristic profile results from the hydrolysis induced by 500mg/L of lime; the lower group is induced by 50mg/L. It is apparent that within each group, the profiles of the 2-8 mm and 2-10 mm are essentially the same.

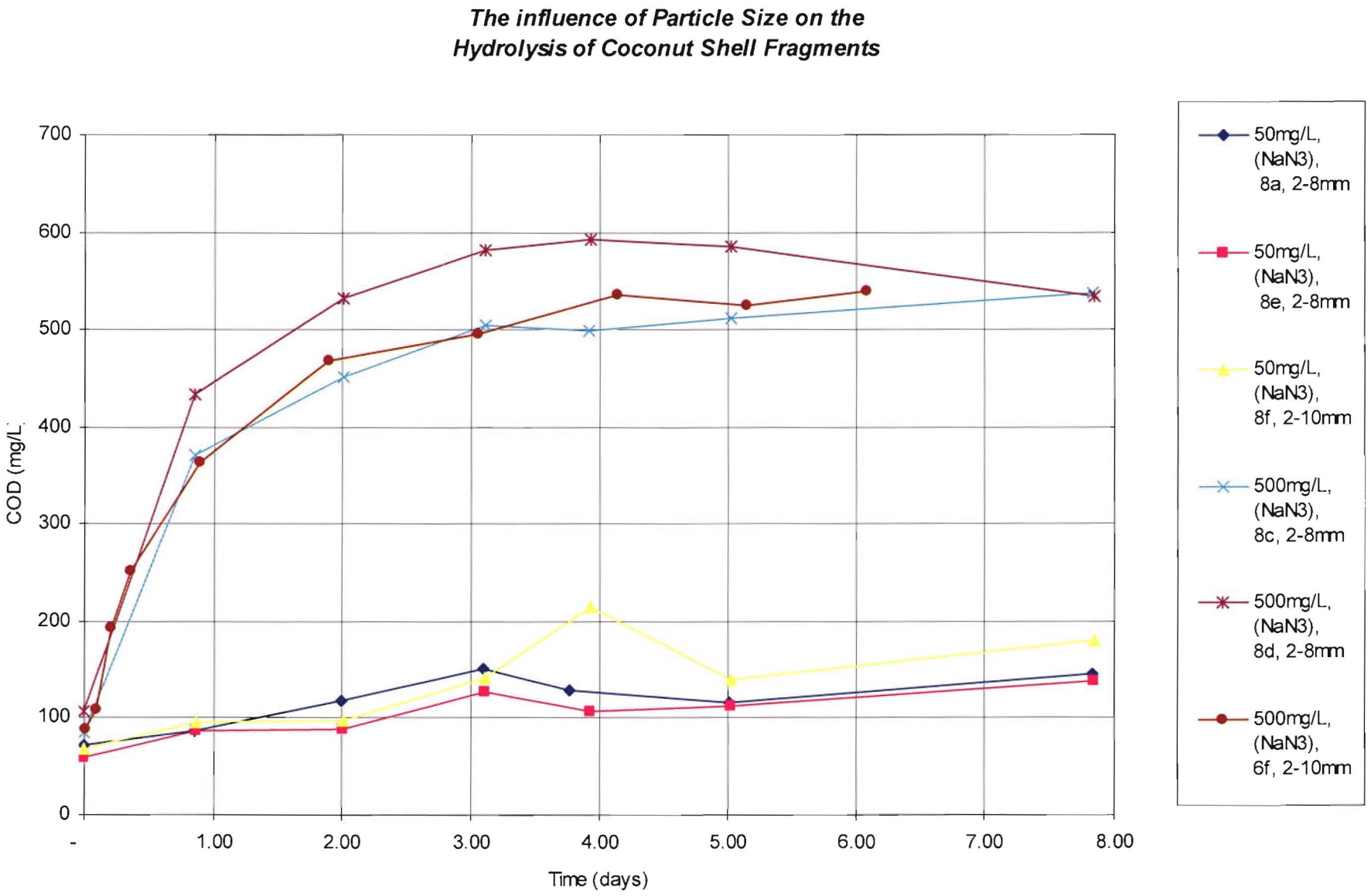

Figure 5-16 The influence of particle size on the hydrolysis of lime treated coconut shell fragments.

5.2.10 Alkaline Hydrolysis and Alkali Cellulose

The increased COD release into solution as a result of the NaOH and lime pretreatment is thought to be as the result of Alkaline Hydrolysis. Alkaline Hydrolysis is defined as the cleaving of a molecule (in this case it is assumed to be cellulose) into two by the addition of a water molecule in a solution with a pH > 7 (as demonstrated in Figure 5-17). The hydrolysis process is the complementary reaction to the formation of cellulose (via a series of dehydration synthesis reactions). As Figure 5-17 indicates that the ions for a H_2O molecule will splits the cellulose molecule at the *β-1-4* bond.

In the laboratory hydrolysis reactions require a catalyst, as typically the cleaved molecule is less polar than the very polar water molecule. Hydrolysis reactions in the presence of high concentrations of hydrogen or hydroxide ions are said to be acid-catalysed or base-catalysed (alkaline hydrolysis) respectively (Chang and Cruickshank, 2005). Since no increase in COD release was observed in the presence of an acid, whilst NaOH and Lime laboratory trials demonstrated an increase in COD release into solution, suggests that the hydrolysis favours alkaline hydrolysis.

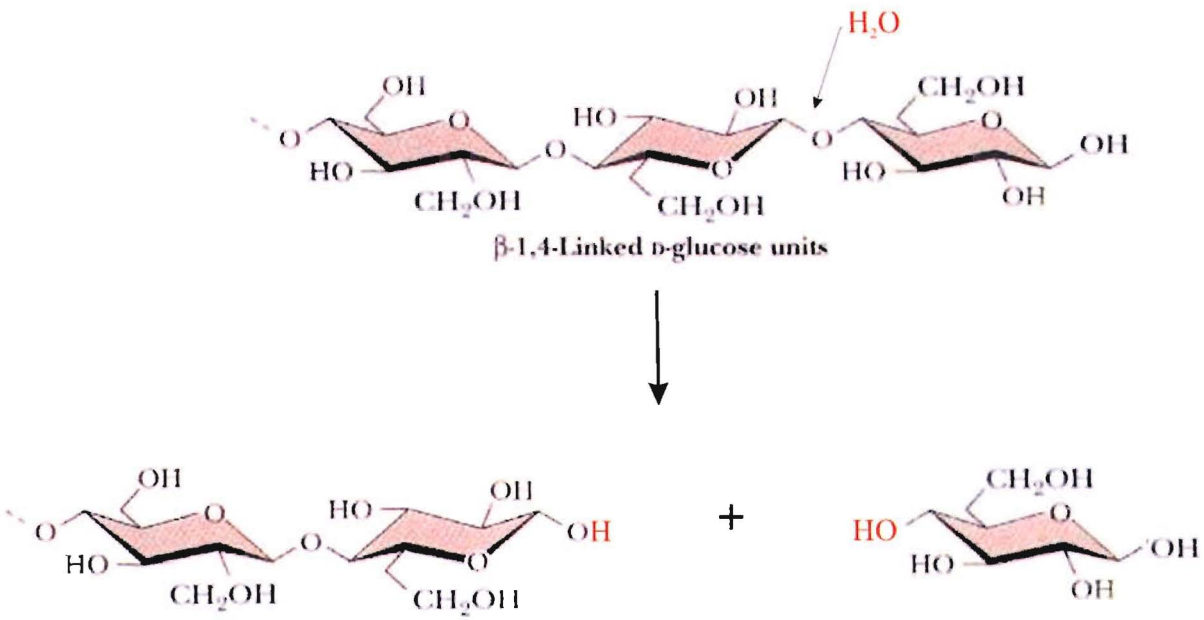

Figure 5-17 Hydrolysis of the cellulose molecule.

As observed in the NaOH and Lime trials the COD released into solution increased with increasing hydroxide concentration (alkalinity). However a complementary reduction in the reactor pH (hydroxide concentration) was observed. As Figure 5-17 indicates, the hydrolysis process consumes both H^+ and OH^- ions in equal quantities and does not contribute to a reduction in reactor alkalinity.

However Lindgren (2000) noted that for cellulose to be able to react and hydrolyse, the hydrogen bonds in the crystalline form (Figure 3-18) need to be ruptured to a high extent. This can be achieved in the presence of concentrated sodium hydroxide, but will remove a lot of the hydroxyl hydrogen from the cellulose, thus forming alkali cellulose (Eqn. 5-1).

$$\text{Cellulose - OH} + \text{NaOH} \rightleftharpoons \text{Cellulose - O}^-\text{Na}^+ + \text{H}_2\text{O}$$

Eqn. 5-1

It is thought that a similar reaction will occur in the presence of Lime [$Ca(OH)_2$]. Instead of the formation of the alkoxylate ion ($-O^-Na^+$) a $-O^-CaOH^+$ ion is formed (Eqn. 5-2).

$$\text{Cellulose - OH} + \text{Ca(OH)}_2 \rightleftharpoons \text{Cellulose - O}^-\text{CaOH}^+ + \text{H}_2\text{O}$$

Eqn. 5-2

5.2.11 Analysis of Pretreatment Batch Reactor Studies:

As has been observed, the shape and form of the COD release profiles were similar to that of Figure 5-18. The profile of the COD release is that of a rectangular hyperbolic (1-exponential) function.

Rectangular hyperbolic functions have two distinct asymptotic regions: at $t \to 0$ and $t \to \infty$. In the case of the COD profile, the amount of COD within the reactor is smallest at $t = 0$, while the gradient or rate of COD hydrolysis is greatest as $t \to 0$. The rate of hydrolysis declines with time until the maximum soluble COD release is achieved at $t \to \infty$, at which time the hydrolysis rate is essentially zero.

These characteristics are visible in Figure 5-18. At $t = 0$ the COD released by the substrate after addition of the lime is zero, but quickly increases over the day. By day two, the rate of

release has slowed, and eventually the release peaks with the effective cessation of any further organic hydrolysis by day 5-8

The equation modelling the soluble COD release profile in Figure 5-18 has the following generalised form:

$$COD = COD_u\left(1 - e^{-kt}\right)$$

Eqn. 5-3

Where:

COD_u	is the ultimate value of COD released by the substrate as $t \to \infty$
COD	COD within the reactor
k	the rate of COD solubilisation coefficient
t	time since the addition of both the substrate and pretreatment reagent to the reactor

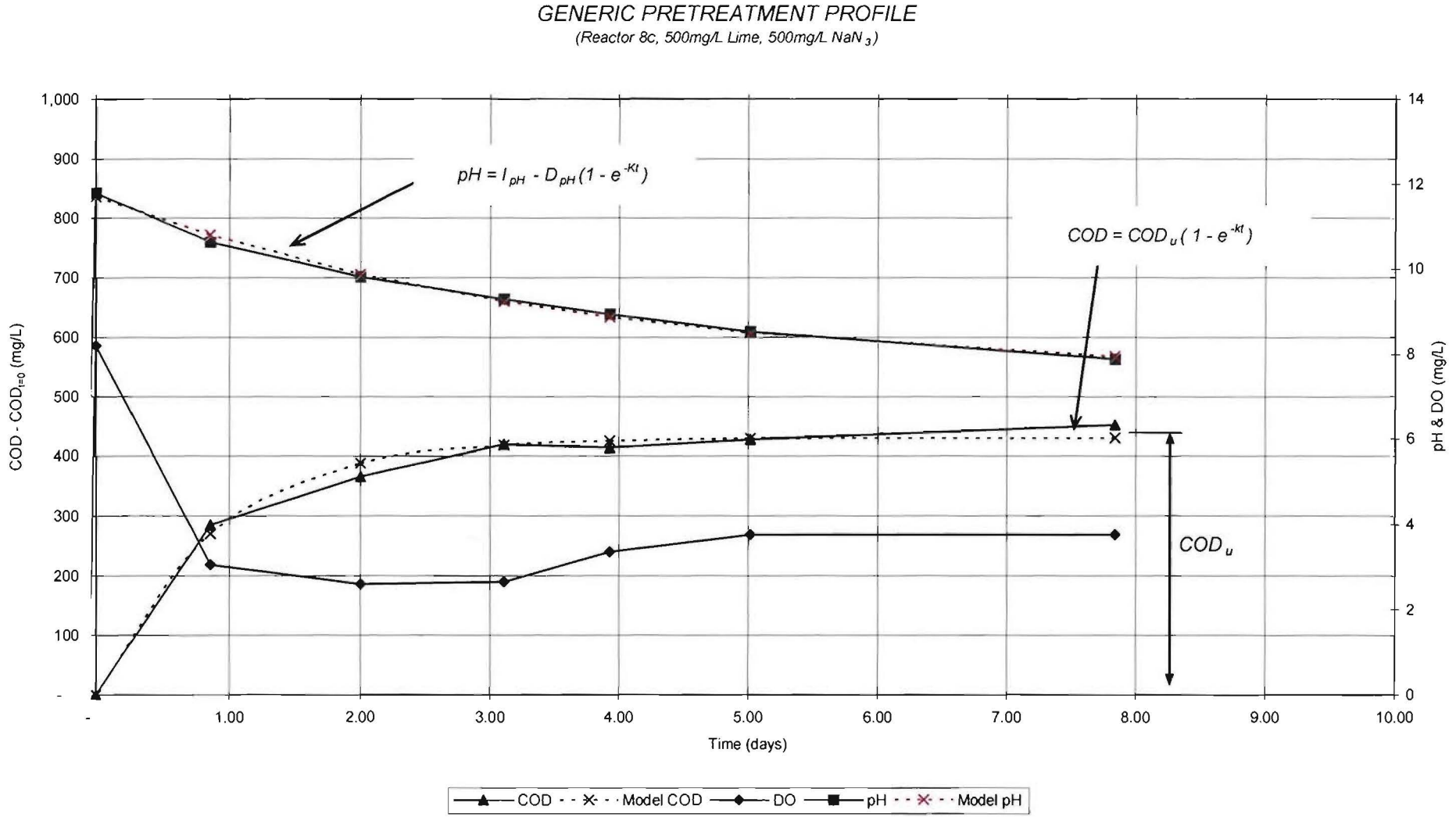

Figure 5-18 A typical pretreatment profile. Rectangular hyperbolic functions model the actual soluble COD and pH profiles exhibited in this trial.

When Eqn. 5-3 is normalised by the term COD_u, the asymptotic value for COD as $t \to \infty$, we get:

$$\frac{COD}{COD_u} = 1 - e^{-kt}$$

Eqn. 5-4

The parameters k and COD_u define the particular shape of the soluble COD profile. The COD_u parameter specifies the location of the horizontal asymptote, i.e. the maximum COD release. While in graphical terms the k parameter defines the curvature of the COD profile, an increase in k relates to a greater rate of COD release over a short timeframe. Conversely, a smaller k value equates to a slower and prolonged COD hydrolysis rate. The dimensionless nature of the kt term suggests that the k parameter is a time-scaling variable, whereby the $\frac{COD}{COD_u}$ profiles are all similar except the time scale is either stretched or compressed by the factor k (Figure 5-19).

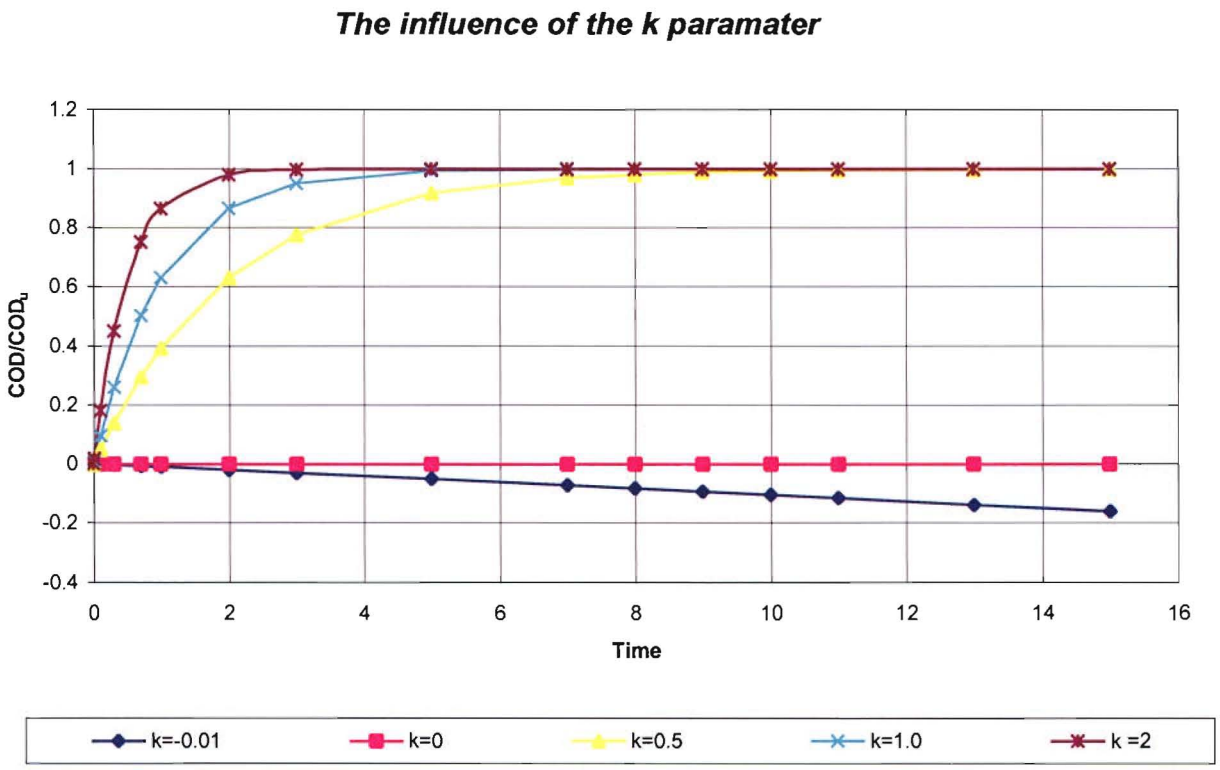

Figure 5-19 Evaluation of the effect the k parameter has on the rectangular hyperbolic function.

Figure 5-18 also models the pH within the reactor. Like the COD profile, the pH within the reactor follows a rectangular hyperbolic (Eqn. 5-5) function. As alluded to earlier, the hydrolysis process consumes hydroxide ions, resulting in a reduced pH value (Section 5.2.10). The amount of hydroxide ions present and the rate of their consumption are greatest at $t \to 0$, eventually tailing off at $t \to \infty$.

$$pH = I_{pH} - D_{pH}(1 - e^{-Kt})$$

Eqn. 5-5

Where:

pH a measure of the hydrogen ions concentration within the reactor and by association the hydroxide ion concentration.

I_{pH} the initial pH in the reactor (at $t \to 0$)

D_{pH} the drop in pH in the reactor between $t \to 0$ and $t \to \infty$

K coefficient for the rate of consumption of the hydroxide ion

t time since the addition of the substrate and pretreatment reagent to the reactor

The K parameter is similar to the k parameter in that it is a time-scaling term of the process. A larger positive K value equates to a greater rate in hydroxide consumption; conversely, a smaller K value indicates that the process occurs at a slower rate.

All thirty-six pretreatment batch trials had the COD and pH parameters evaluated with models based on best-fit analyses. These results are summarised in Appendix H. From these results, correlation between the effects of pH on the COD release can be summarised.

Of particular interest is the influence of the hydroxide ion source chemical pretreatments (i.e. Lime and NaOH). For these pretreatments, Figure 5-20 indicates that there is a strong correlation between the initial reactor pH (I_{pH}) and the net release of COD.

The relationship is shown in Figure 5-20:

$$COD_u = 0.0355e^{0.8072 I_{pH}}$$

Eqn. 5-6

Since I_{pH} is a logarithmic measure of the pH, and the COD_u scale in Figure 5-20 is logarithmic, Eqn. 5-6 can be rearranged into the following:

$$\log(COD_u) = \log(0.0355) + \log(e^{0.8072 I_{pH}})$$

and knowing that: $\log(x) = \frac{\ln(x)}{\ln(10)}$

then:

$$\log(COD_u) = \log(0.0355) + \frac{\ln(e^{0.8072 I_{pH}})}{\ln(10)}$$

$$\log(COD_u) = 0.35 I_{pH} - 1.45$$

Eqn. 5-7

or

$$COD_u = \frac{[H^+]^{-0.35}}{28.2} \text{ or } COD_u = \frac{10^{4.9} \times [OH^-]^{0.35}}{28.2}$$

Eqn. 5-8

Eqn. 5-8 indicates that the amount of soluble COD released into solution is proportional to the hydroxide ion concentration to the power of 0.35. This suggests that low concentrations of hydroxide ions correlate to a low COD release, as indicated in Figure 5-20 where the reactor with an initial pH = 7 would be expected to release only 10mg/L of COD.

However, this relationship was not valid when the reactor pH < 10. Figure 5-21 demonstrates that the pretreatment process, independent of the chemical reagent, results in a COD release in the order of 130mg/L. Therefore, the Lime or NaOH pretreatment with an initial pH < 10 would be expected to follow a similar relationship.

The variability in COD release in Figure 5-20 and Figure 5-21 is assumed to be due in part to the release of minute fragments from the substrate, in conjunction with the inherent error associated with the COD test (Appendix F). Although every effort was made to ensure that the substrate was adequately washed prior to application, it is feasible that some of the COD

measurement can be attributed to dust fragments remaining in or on the substrate. In addition, the magnetic stirrer bar within the reactor provided mechanical energy that resulted in visible collisions of the substrate. These collisions could have resulted in further fragmentation and damage of the substrate, ultimately releasing more minute soluble organic fragments.

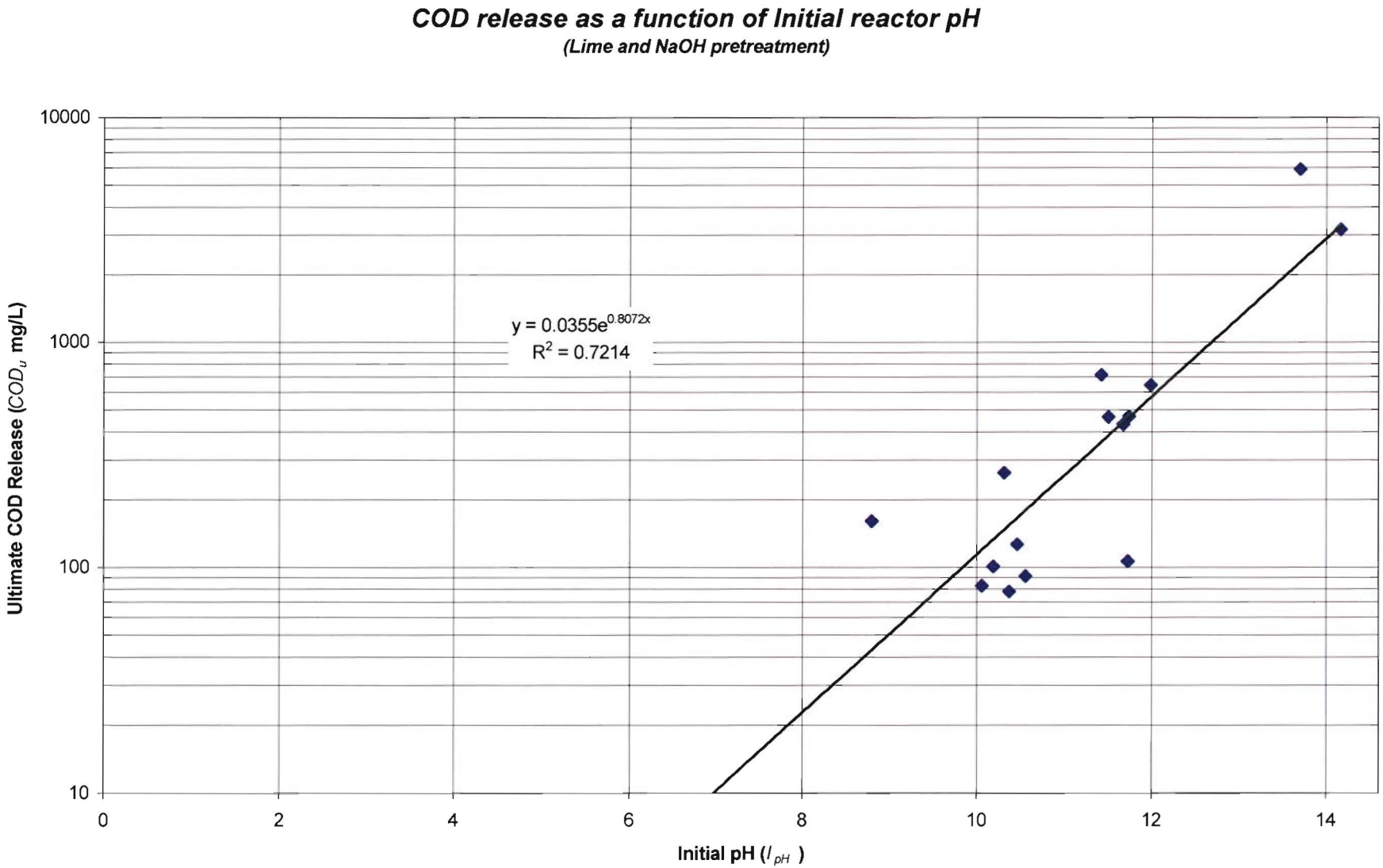

Figure 5-20 The influence of initial reactor pH on the ultimate release of COD, via lime and NaOH chemical pretreatment.

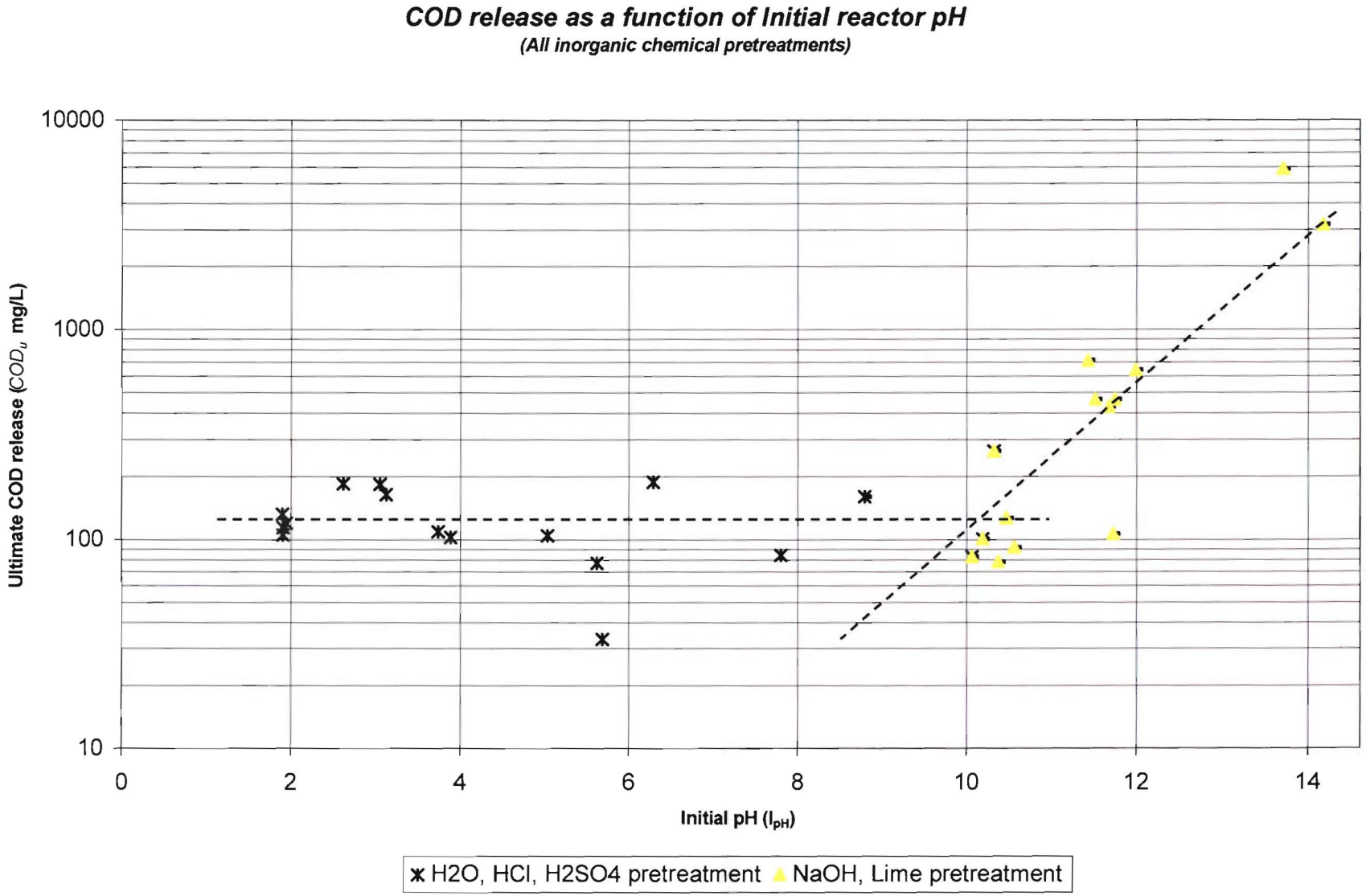

Figure 5-21 The influence of initial reactor pH on the ultimate release of COD induced by all inorganic pretreatments assessed.

5.3 Conclusions

1. The pretreatment batch trials showed signs of heterotrophic bacteriological consumption of COD. In later trials, sodium azide was injected into the reactors to prevent bacterial growth from affecting the assessment of organic carbon (COD). Comparable reactors treated with sodium azide to prevent bacterial growth observed a 141% greater release of COD than those reactors without.

2. COD release of untreated reactors (with sodium azide) exhibited a sudden release of organic carbon in the first few hours of the trial, followed by a gradual release over the following four days. The sudden release is attributed to the soluble organic dust on the surface or within the pores of the coconut shell fragments

3. Hydrochloric acid with an initial hydroxide concentration of pH = 2.0 demonstrated no improvement in the release of organic carbon from coconut shell fragments compared to the baseline treatment (deionised water).

4. In the sulphuric acid pretreatment batch reactors, the more acidic the initial reactor, the lower the COD hydrolysis observed during the trial.

5. The uncertainty associated with the COD measurement of the reactor COD for the acetic acid and propionic acid treatment had the potential to mask any release due to hydrolysis of the coconut shell fragments. If any hydrolysis did occur, the rate and quantity was insufficient to exceed the uncertainty associated with the COD measurement technique.

6. Treating the coconut shell fragments with sodium hydroxide resulted in an improvement in the rate of COD release attributed to hydrolysis of the organic carbon within the fragments. Increasing the initial concentration of sodium hydroxide resulted in an increase in the rate of hydrolysis and hence COD release. A similar result was observed with calcium hydroxide.

7. The COD concentration profile of sodium hydroxide and calcium hydroxide pretreatments exhibits a bi-linear relationship: an initial sudden release of organic carbon followed by a reduced plateau.

8. Reagents with low concentrations of hydroxides, such as acids, showed no improvement in the rate of hydrolysis, while reagents with high hydroxide concentrations (i.e. sodium hydroxide and calcium hydroxide) showed improved COD releases associated with hydrolysis.

9. During the hydroxide pretreatments, it was noted that with the onset of hydrolysis-induced COD release, the pH in the reactors would rapidly decrease. This is most likely the result of the formation of alkali cellulose, in which the hydroxyl hydrogen from the cellulose is substituted with either a sodium ion in the case of the NaOH pretreatment or with a $CaOH^+$ ion with the Lime pretreatment.

$$\text{Cellulose - OH} + \text{NaOH} \rightleftharpoons \text{Cellulose - O}^-\text{Na}^+ + \text{H}_2\text{O}$$

$$\text{Cellulose - OH} + \text{Ca(OH)}_2 \rightleftharpoons \text{Cellulose - O}^-\text{CaOH}^+ + \text{H}_2\text{O}$$

10. Elevated temperatures during the coconut fragment cleaning phase did not result in an improvement in the rate of COD hydrolysis.

11. Two particle size distributions were evaluated $2 \le x \le 10mm$ and $2 \le x \le 8mm$. Whilst the $2 \le x \le 8mm$ distribution contained a greater surface area per gram of substrate (42.5%) than the $2 \le x \le 10mm$ distribution, there appears to be no discernable difference in COD hydrolysis between the two distributions.

12. The batch reactors that resulted in a gain of COD within the batch reactor exhibited a COD release profile that had the following generalised form:

$$COD = COD_u\left(1 - e^{-kt}\right)$$

The pH profile had the following form:

$$pH = I_{pH} - D_{pH}(1 - e^{-Kt})$$

13. The lime and NaOH chemical pretreatment resulted in the following specific relationship between COD_u (ultimate COD released) and I_{pH} (initial reactor pH).

$$COD_u = 0.0355e^{0.8072I_{pH}}$$

The COD_u for the other pretreatment reagents (HCl, H_2SO_4, and deionised water) was independent of the initial reactor pH (Figure 5-21).

5.4 References

APHA (1999) Standard Methods for the examination of water and wastewater. 20th Edition, American Public Health Association, Washington.

Aylward G., and Findlay T. (1994) SI Chemical Data, 3rd Edition, Jacaranda Wiley Ltd, Milton, Australia, 180p.

Brenner W. et al. (1977) In: New approaches for the acid hydrolysis of cellulose. Dept. of Appl. Sci., New York Univ., NYU/DAS-77-30, New York

Chang R. and Cruicksnak B. (2005) Chemistry, 8th Ed., McGraw-Hill, New York, 1088p.

Lindgren Å. (2000) Use of Multivariate Methods and DOE to Improve Industrial-Scale Production Quality of Cellulose Derivative, J. Chemometrics, Vol. 14, pp. 657-665

Nathanel W.R.N. (1964) Coconut Shells as Industrial Raw Material, Coconut Bulletin, Vol. 18, No. 3-4, pp. 163-183

Nesse N and Wallick J., Harper J.M. (1977) Pretreatment of cellulosic wastes to increase enzyme reactivity, Biotechnol. Bioeng., Vol. 19, pp. 323-336

6 Denitrification Batch Reactor Trials

6.1 Introduction

In this section, the pretreated substrates from the previous chapter were evaluated as to their ability to supply an organic carbon source and maintain biological denitrification. The objective of this section of the research was to encourage the release of organic carbon from the substrate. However the uncontrolled and unmanaged COD accumulation has its associated concerns, in a potable water supply excess COD in downstream unit process or reticulation system was result in unwanted bacterial and/or algae growth.

The process of releasing organic carbon and its accumulation within the reactor is masked somewhat by the consumption of the carbon by the bacteria. Therefore, a comparative measure of the performance of the substrate was undertaken by means of the rate and extent of denitrification that occurred within the batch reactors.

To ensure that organic carbon was the only limiting nutrient for these trials, adequate concentrations of nitrate, phosphorous, iron, and other trace elements were provided. Nitrate, in excessive concentrations has been observed to inhibit biological processes (Glass and Silverstein [1999] reported that inhibition of activated sludge denitrification occurred when wastewater nitrate concentrations were greater than 300 mg/L NO_3^--N). As a consequence the initial concentration in the denitrification batch reactors was set at 200 mg/L NO_3^--N.

In total twelve reactor trails were conducted. Table 6-1 provides a comparative summary of each denitrification reactor, and the corresponding pretreatment reactor(s) from which the substrate was sourced. To eliminate the possible inaccuracy associated with the differences in mass between trials, all analyses are normalised with respect to the substrate mass.

Table 6-1 Correlation between Denitrification and Pretreatment Reactors					
Reactor	*Weight of dry Coconuts (g)*	*Net Surface Area (mm^2)*	*Volume of fluid added (@ 20°C) (L)*	*Corresponding Pretreatment Reactor*	
1 DR a	101.51	115737	4.00	NIL	Untreated
1 DR b	104.56	119214	4.00	5a/5b	Lime 500 mg/L
1 DR c	103.31	117789	4.00	6f	Lime 500 mg/L + NaN_3
1 DR d	85.13	97061	4.00	6c	NaOH pH=14
1 DR e	93.44	106536	4.00	2c	NaOH pH=14 + NaN_3
1 DR f	102.70	117093	4.00	4e/4f	HCl pH=2
2 DR a	101.51	115737	4.00	3d	NaOH pH=9
2 DR b	104.56	119214	4.00	4e/4f	HCl pH=2
2 DR c	103.31	117789	4.00	4c/4d	HCl pH=4
2 DR d	85.13	97061	4.00	3c	NaOH pH=12
2 DR e	93.44	106536	4.00	5a/5b	Lime 500 mg/L
2 DR f	102.70	117093	4.00	7c	Acetic Acid pH=5

6.2 Results

6.2.1 Denitrification of Untreated Substrate

As shown in Figure 6-1, only one trial was conducted with an untreated substrate. This substrate was washed as per the other pretreated substrates; however, this sample did not experience any other form of physical or chemical treatment to improve the rate of hydrolysis of organic carbon prior to its application in this trial.

During the first eight days of this trial, substantial accumulation of COD was observed (Figure 6-1). Since the COD measurement is essentially the difference between the hydrolysis of the coconut fragments (i.e. COD release) and the consumption of the organic carbon (bacterial metabolism), the observed increase in COD indicates that the hydrolysis of the coconut fragments exceeded the bacterial metabolic consumption.

Since fragmented coconut shell was the only source of organic matter in the reactor any increase in COD was a direct result of hydrolysis of the coconut shell fragments.

During the initial eight days, no noticeable increase in COD was observed, however a decrease in DO occurred. The COD measurement of 86 mg/L at day eight is most likely the result of analytical error. During this same period the hydrolysis of the coconut corresponded to a reduction in reactor pH from 7.05 to 6.07. This reduction is consistent with the observation in Chapter 5, in which the pH reduced (as the result of hydroxide ion consumption) during the hydrolysis of coconut fragments, however an excess of soluble COD would be expected.

The next sample record at day ten shows a drop in COD to 16 mg/L, with a corresponding reduction in DO to 1.25 mg/L. From day ten to the day twenty-eight, whilst COD accumulation was not significant, the observed rate of accumulation within the reactor was in the order of 1.7 mg of COD/L/day. During this period the DO never dropped below 1.0 mg/L. It should be noted DO concentrations greater than 0.2 mg/L have been identified to have inhibitory effects on denitrification (Kapoor and Viraraghavan 1997, Gayle et al. 1989); hence, it is highly unlikely any denitrification occurred in the batch reactor during this time.

The nitrate profile in Figure 6-1 confirms the absence of denitrification during this trial, which would normally be expected were the depleted oxygen concentration in the reactor below 1.0 mg/L. The initial nitrate concentration was initially assessed at 192 mg/L nitrate-nitrogen, and by the end of the trial was 194 mg/L. During this trial the nitrate concentration varied between 180-200 mg/L, with an average concentration of 190 mg/L, which is consistent with the precision associated with the spectrophotometric technique (+/- 5% or +/- 9.5 mg/L).

The assessment of hydroxide ion consumption during the hydrolysis of coconut organic matter indicated that from day zero to ten, and from day ten to day twenty-eight, similar concentrations of hydroxide ions were consumed, most likely as the result of the hydrolysis of the coconut fragments (Table 6-2).

Table 6-2 Hydroxide consumption of reactor 1DRa

Time	*pH*	*[OH]*
0 day	7.05	1.12×10^{-7}
10 days	6.16	1.45×10^{-8}
28 days	5.78	6.03×10^{-9}

Period	*Reduction in [OH]*
0 – 10 days	9.76×10^{-8} moles
10 – 28 days	8.42×10^{-8} moles

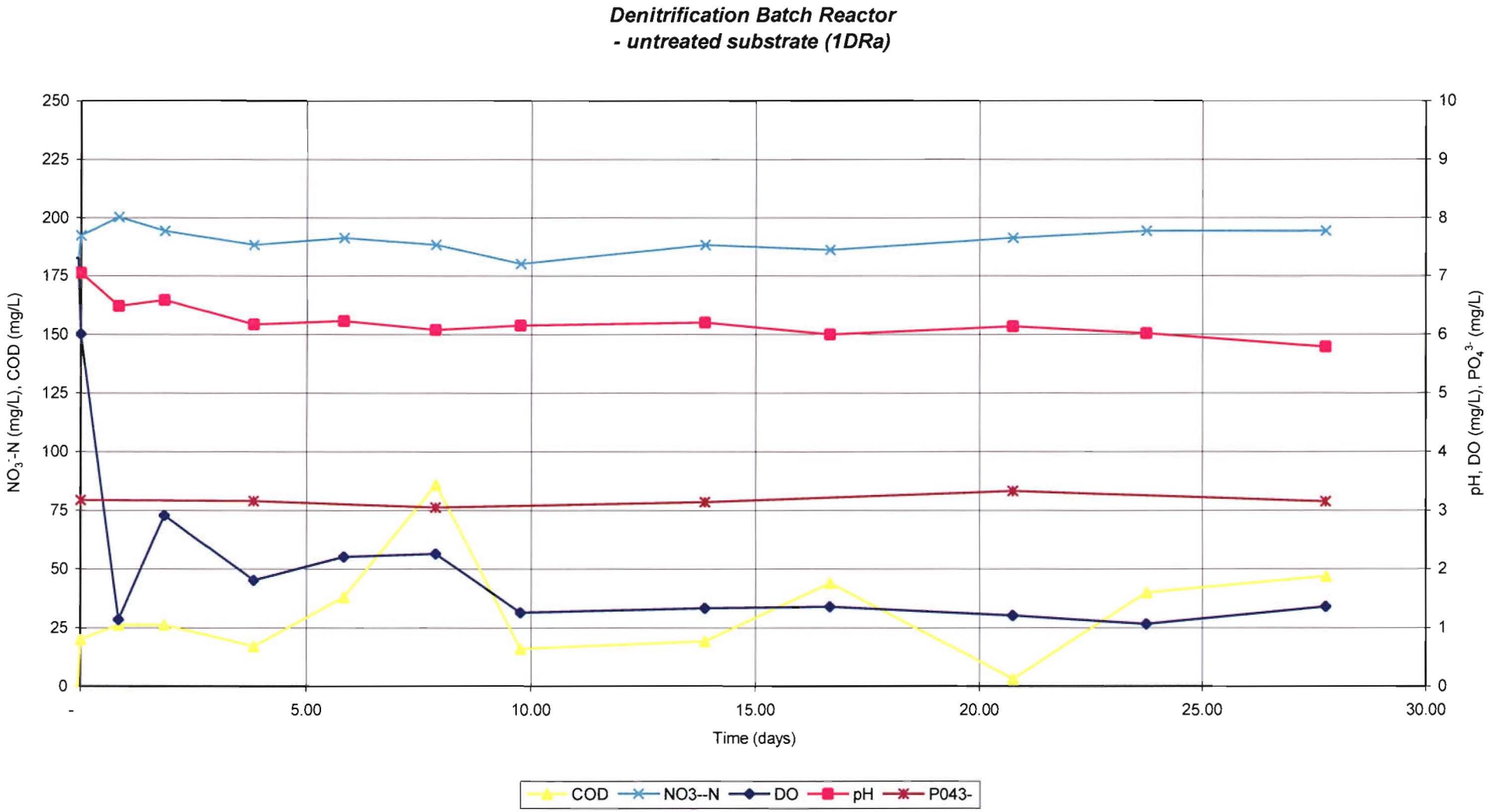

Figure 6-1 Denitrification batch trial of utilising untreated substrate.

6.2.2 Denitrification of Acetic Acid Pretreated Substrates

Only one of the twelve denitrification reactors in this series of experimental trials utilised the acetic acid pretreated substrate (reactor 2DRf). This reactor was one of the later experimental trials in this series, in which the atmosphere within the reactor was modified part way through the trial. During the first nine days the reactor was open to the atmosphere, followed by an anoxic period in which atmospheric gases, including oxygen, were displaced (i.e. degassed) from the liquid and the headspace with inert helium.

Figure 6-2 indicates that the initial DO concentration 7.45 mg/L dropped to 3.2 mg/L during the first 24 hours, but in next eight days the DO recovered from 2.2 mg/L to 5.4 mg/L. This recovery in DO suggests recharging of the fluid phase from atmospheric oxygen. Under ideal conditions the partial pressure of atmospheric oxygen at 35°C correlates to a 7.9 mg/L DO concentration (Appendix I), hence some form of oxygen recharging would be expected, as observed.

Denitrification requires anoxic conditions to allow for the preferential consumption of nitrate; hence, the reactor was degassed and sealed from the outside atmosphere. This adjustment resulted in the DO concentration reducing from 5.4 mg/L to 1.7 mg/L. During the following 24 hours the DO concentration continued to decline to 0.7 mg/L and remained at this value until the conclusion of the experimental trial. The observed reduction in DO from 1.7 mg/L to 0.7 mg/L suggests that aerobic respirations occurred until the DO concentration was insufficient to maintain the process.

It was expected that if denitrification were to occur, it would most likely happen in the anoxic regime when the DO was below 1 mg/L. However, no evidence of denitrification was observed during the period that the reactor was anoxic (i.e. t =9 days to t = 13 days) as evident by no reduction in NO_3^--N. The inability of this reactor to denitrify may be due to other environmental conditions (i.e. the acidic condition of the reactor during that regime). Mayo and Noike (1994) noted that the growth rate of most micro-organisms is at the maximum when the pH value nears neutral and falls quickly at high and low pH values. While the pH of this trial was not excessively acidic, it may have participated in limiting the rate of denitrification if any denitrification had occurred.

During the first nine days of the trial, the batch reactor became more acidic. The initial pH of the reactor was 7.5; however, by day nine a concentration of pH = 5.4 was observed. During the anoxic period the pH concentration recovered slightly such that by day thirteen the reactor concentration was pH = 6.2. It is possible that during the pretreatment process some acetic acid or hydrogen ions diffused into the pores of the coconut fragments. Sufficient quantities were absorbed that when the substrate was re-suspended in the reactor the hydrogen ion concentration would eventually peak at $10^{-5.5}$ moles/L.

Assuming that the hydrogen ion concentration peak of $10^{-5.5}$ moles/L is wholly attributed to that of diffused acetic acid, the corresponding COD due to the acetic acid would be insignificant (as the calculations in Appendix G suggest). Hence, it is a valid assumption that all the COD measurements are solely attributed to the hydrolysis of the organic matter.

From day six to nine, while the reactor was still open to the atmosphere, the rate of biological activity was thought to have plateaued. The cessation of a growth phase would explain the corresponding increase in available COD as well as the reactive phosphate within the reactor remaining effectively static during this period.

From day three, the DO in the reactor recovered at a rate of 0.29 mg/L/day. With the reactor open to the atmosphere for the majority of this trial, atmospheric oxygen dissolved back into solution as defined by Henry's and Graham's Laws.

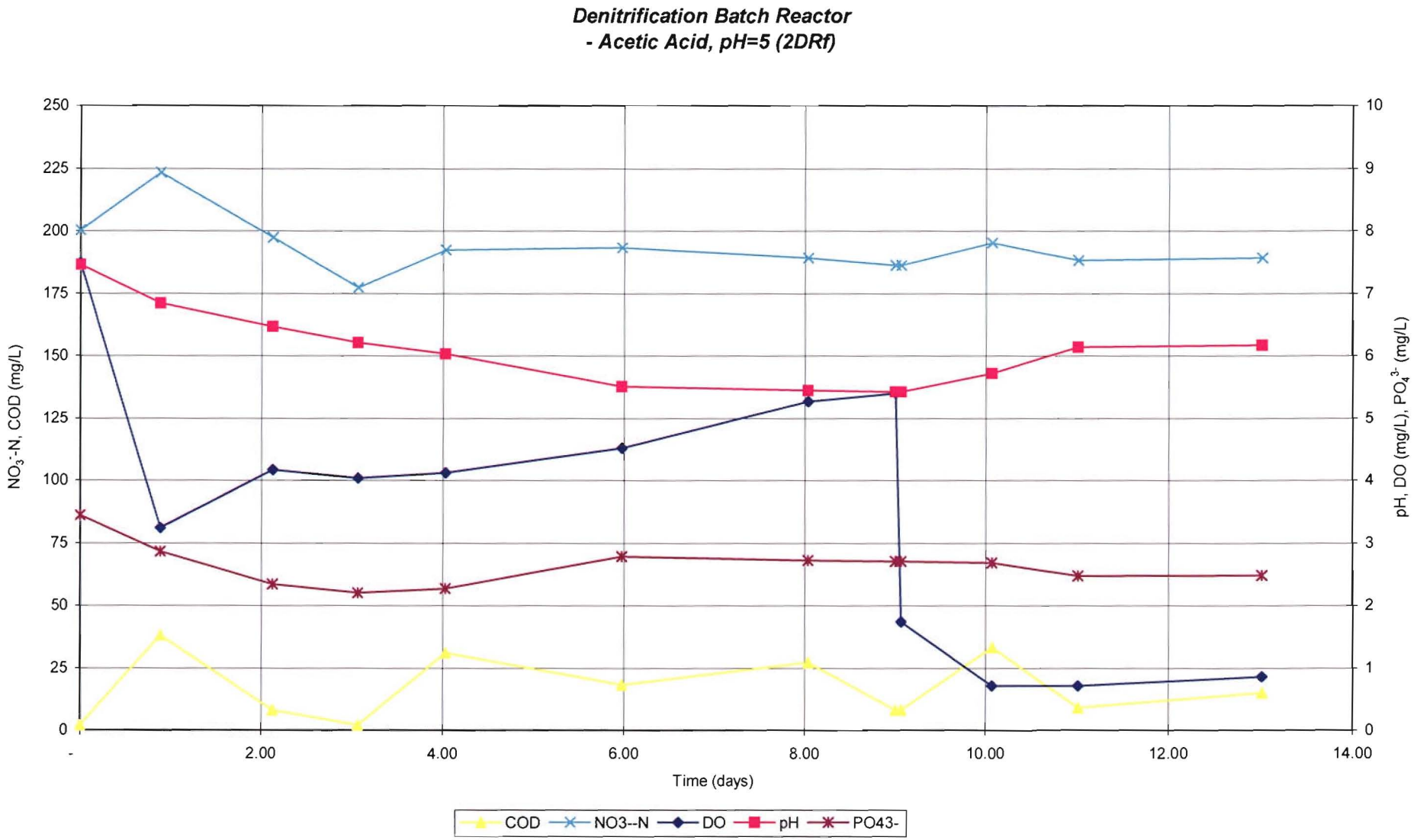

Figure 6-2 Denitrification batch reactor utilising acetic acid pretreated substrate.

The parameter that appears most likely to influence the presence and rate of biological activity within the reactor is the availability of organic carbon. The COD profile drifted around 25 mg/L, peaking at 38 mg/L at day one, and dropping to 2 mg/L by day three. While the assessment of the organic component in this reactor (via measurement of the COD parameter) suggested that there was sufficient organic carbon to allow some form of biological process to occur, the biological process seemed to decline or cease after day three, as evident by the DO recovery.

The evidence of any biological activity occurring during the anoxic regime is slim. The drop in DO from 1.7 mg/L after degassing to 0.7 mg/L 24 hours later, and the 8% reduction in reactive phosphate during this regime is the only supporting evidence of biological activity. It was expected that the mixed culture of facultative denitrification bacteria injected into the reactor would show evidence of denitrification once the DO fell below the 1 mg/L threshold, but no denitrification was observed in this regime (as shown by no decline in nitrate levels).

Acetic acid pretreatment therefore offers no significant increase in COD accumulation compared to that of the untreated substrate. As a result, denitrification never occurred within the reactor, hence acetic acid pretreated substrate is not recommend as a feasible technique to encourage denitrification, due to the treatment's inability to provide readily available organic carbon from the treated coconut shell fragments.

6.2.3 Denitrification of Hydrochloric Acid Pretreated Substrate

As outlined in Table 6-1, three reactors trials were conducted with a substrate that had been pretreated with hydrochloric acid. One of these reactors was operated in an anoxic state (1DRf), with the other two (2DRb, 2DRc) operated in conditions similar to 2DRf (acetic acid denitrification batch reactor), where the reactor was left vented to the atmosphere for the first eight days, followed by degassing and a further five days in an anoxic condition. All three of these reactors exhibited similar characteristics, and the chemical profile of reactor 2DRd (Figure 6-3) has been included as the best representation of the processes that were occurring in these trials.

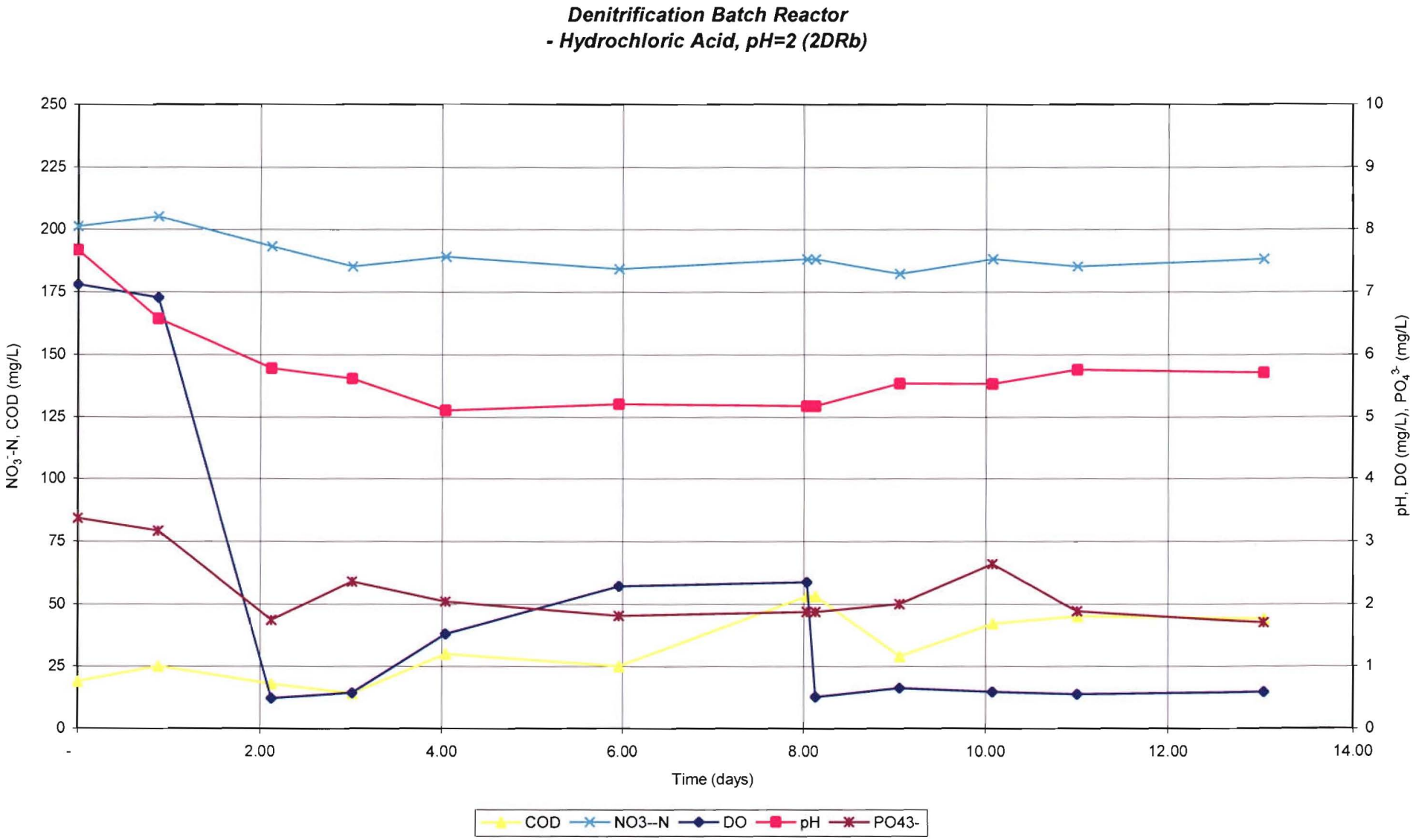

Figure 6-3 Denitrification batch reactor utilising hydrochloric acid pretreated substrate

The DO profile during the first eight days showed evidence the reactor entered an anoxic regime sometime after the first 24 hours, even though the reactor was exposed to the atmosphere. An anoxic regime was maintained until day four. While the nitrate appeared to reduce during this period, the observations were within the experimental error confidence internal (+/- 20 mg/L). The lack of denitrification is thought to be primarily due to the low C:N ratio, observed to be in the order of 1:20. As a general rule, every gram of nitrate that is denitrified requires four grams of BOD (Rittmann and McCarty (2001) cited in Safferman et al. (2004)).

The laboratory results recorded an increase in the hydrogen ion concentration in the reactor until the end of the anoxic phase ($\approx t = 4$ *days*), at which point the reactor hydrogen ion concentration peaked at $10^{-5.1}$. It is highly feasible that such an adverse acidic environment resulted in the cessation of the anoxic process. Henze et al. (1995) noted that pH = 7.5 is the optimum pH for heterotrophic denitrification processes; hence, the biological process could become stressed and degrade in efficiency as the reactor became more acidic.

The cause of the reactor acidification could be due to re-suspension of the HCl pretreatment reagent, similar to the mechanism described in Section 6.2.2.

At day eight the reactor was degassed and isolated from the atmosphere. This change in condition corresponded to a DO drop from 2.34 mg/L to 0.5 mg/L. Reducing the DO tension would be expected to stimulate nitrate respiration, and would be expected to correlate to a change in the denitrification rate. During this period the bacteria consumed only 1.7 mg/L of phosphate, the reactor hydroxide concentration recovered to pH = 5.7, and the average COD in the reactor was 44.3 mg/L and did not fall below 29 mg/L. The reactor showed no measurable sign of nitrate consumption.

The observations summarised above tend to suggest the bacteria ceased to respire once the adverse acidic conditions reached pH = 5.1. The gradual increase in reactor acidity is possibly due to the release of hydrogen ions from within the coconut fragments. The degassing of the reactor showed no measurable improvement in the capacity of the pretreated substrate to denitrify. Therefore, hydrochloric acid pretreated substrate is not favoured as a pretreatment technique.

6.2.4 Denitrification of Sodium Hydroxide Pretreated Substrate

Four reactors were operated with sodium hydroxide-treated substrate (Table 6-1). Two were operated in an anoxic environment (1DRd, 1DRe) and two were initially left open to the atmosphere and then degassed at day eight (2DRa, 2DRd). The chemical profiles of reactors 1DRd (Figure 6-4) and 1DRe (Figure 6-5) are shown. Both were pretreated with pH = 14 sodium hydroxide with the substrate in reactor 1DRe also dosed with sodium azide to eliminate any possible fungal growth.

6.2.4.1 Reactor Trial 1DRd and 1DRe

Both reactors 1DRd and 1DRe were closed to atmospheric gases and the headspace gases were purged from the reactor and replaced with inert helium gas. Unlike the previous experimental trials, the reactor fluid was not degassed as it was assumed, and later confirmed, that the biological process would readily consume the DO resulting in an anoxic environment.

At day zero (Figure 6-4), the inoculum was injected into the reactor, at which time the reactor DO concentration was 6 mg/L. Three days earlier (*t = -3 days)*, with only the substrate and nutrients in the reactor, the DO concentration was 8.2 mg/L. The change is attributed to the combined effect of equalisation between the DO in the fluid phase and atmospheric oxygen concentration on one hand and possible bacterial DO consumption on the other hand. Since neither the reactor nor the substrate was thoroughly sterilised, it is possible some bacteria might have entered the reactor prematurely. This error was deemed acceptable for two reasons. First, it is the medium-term suitability of the substrate that is of particular interest and, second, it is highly unlikely that the initial bacteria would out-compete the high concentration of acclimated mixed culture.

As outlined in Figure 6-4, this reactor demonstrates three distinct regimes. The first spans from 0 to 8 days, the second from day 8 to 14, and the third from day 14 until the end of the trial.

Twenty-four hours after the injection of inoculum, the mixed culture bacteria had consumed 4.6 mg/L of the DO, which remained static for the next five days at 1.35 mg/L. During this initial six-day period the pH reached a high of 8.97. Like the pretreatment studies in the

previous chapter, a high pH corresponded to increased COD release from the substrate. In excess of 100 mg/L of COD was released during this period, with the concentration of the reactor assessed at 65 mg/L initially and 165 mg/L at the end of the period. Bacteria were consuming the organic matter (COD) during this period over the course of aerobic respiration, hence the conversion of reactive phosphate to new cells and/or bio-P reserves and the corresponding drop of phosphate in the reactor from 3.36 mg/L at day zero to 2.73 mg/L at day seven.

By day six the DO concentration had fallen below 1.35 mg/L, and the corresponding rate of nitrate removal at this stage was 1.9 mg/L/day. From day six until day fourteen the DO continued to decline to approximately 0.9 mg/L, coinciding with an increase in the nitrate removal rate (3.1 mg/L/day) primarily attributed to the denitrification process.

In the third regime (day 14 to 30), the rate of COD accumulation in the reactor was relatively consistent, and accumulated COD at a rate of 8.5 mg/L/day (r^2 = 0.90). This is an advantageous situation, as the premise of this research is that the availability of organic carbon is suspected to be the primary rate-limiting parameter influencing the rate and extent of denitrification. However, in a full scale application, carbon release, in excess of the amount able to be consumed during the denitrification process, would result in a high COD in the effluent. This would be expected to cause problems downstream, in particular the formation of unwanted biological growth in piping networks or, if the water were chlorinated, the possible formation of carcinogenic trihalomethanes.

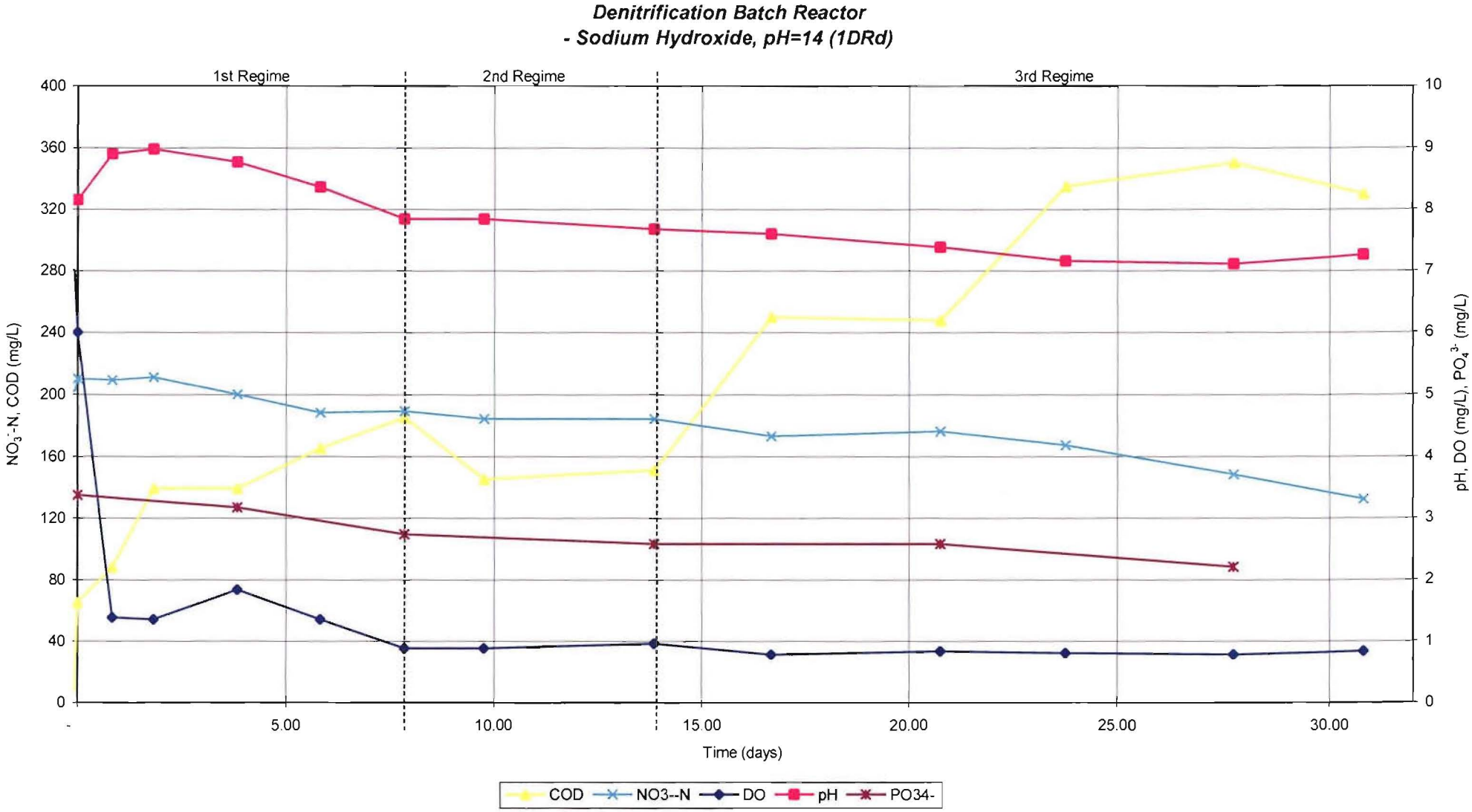

Figure 6-4 Denitrification batch trial utilising sodium hydroxide pretreated substrate. Initially treated pH = 14.

These trials demonstrate (as shown in Figure 6-4) that as the organic carbon increased due to hydrolysis, a corresponding decline in the hydroxide concentration within the reactor occurred. In trial 1DRd, the pH dropped from 8.36 to 7.68 in the course of eight days (from day six to day fourteen). An increase in biological density was observed as the reactor became cloudy, occurring concurrently with a phosphate concentration decline.

In the third regime (day fourteen till day thirty one) the DO concentration was consistently below 0.9 mg/L (averaged 0.83 mg/L), and like the 2nd regime, maintained a relatively high rate of denitrification (3.1 mg/L/day). During this regime the reactive phosphate concentration was observed to fall from 2.57 mg/L at day fourteen to 2.2 mg/L at day twenty-eight.

The reactor hydroxide ion concentration continued to decline during this regime until day twenty-four, at which time the reactor pH plateaued at 7.18. This plateau corresponded to a similar plateau for the COD profile. The fact that the COD and the pH concentration plateaued at the same time provided further evidence to support the argument that the COD hydrolysis and the consumption of hydroxide ions are linked.

The substrate utilised in Figure 6-5 was first treated with sodium azide, and it is possible that some sodium azide may have re-suspended in the denitrification reactor, killing off the inoculum. Evidence of this is presented in Figure 6-5, as the drop in reactor DO during the first two days seemed to halt and reversed itself in the following four days. That is, the DO dropped from 7.5 mg/L at day zero to 1.05 mg/L by day two, only to recover to 2.8 mg/L four days later.

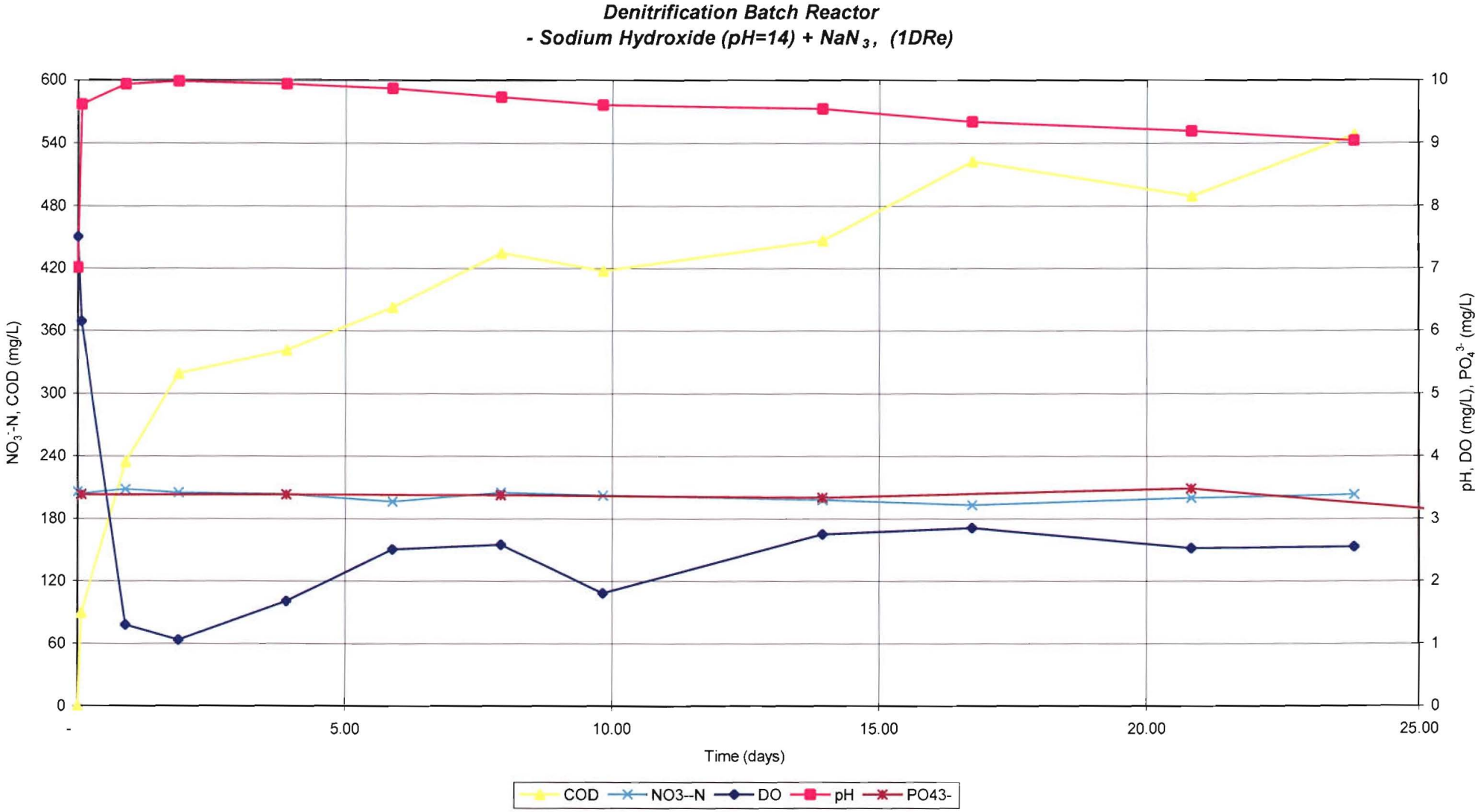

Figure 6-5 Denitrification batch reactor using sodium hydroxide pretreated substrate. Substrate also treated with sodium azide.

The stable profiles of the nutrients phosphate and nitrate were further evidence of the cessation of bacterial activity in the reactor. Neither of these two nutrients showed any sign of biological consumption. The absence of bacterial activity is thought to have removed the variability in the pH and accumulated COD profiles (as previously observed in Figure 6-4).

Comparisons of the accumulated soluble COD profiles in Table 6-3 indicate that the rate of COD accumulation of the two sodium hydroxide treated substrates (pH = 14) were similar. However, reactor 1DRd showed the three distinct regimes of COD accumulation.

It would be expected that reactor 1DRe (with sodium azide) would have a greater rate of COD accumulation over reactor 1DRd because of the inhibition of bacterial metabolism; however the two reactors exhibited similar rates of COD accumulation.

Both reactors exhibited a decline in hydroxide ions during the trial. During the course of the trial the reduction of hydroxide ions in reactor 1DRd was approximately 1.0×10^{-7}, while in reactor 1DRe a 1.0×10^{-4} reduction in hydroxide ions was observed.

Table 6-3 Comparison of COD accumulation with change in reactor pH

	1DRe	1DRd (NaOH pH = 14)			
	(NaOH pH=14 + NaN_3)	As a whole ($0<t<31$)	1st Regime ($0<t<8$)	2nd Regime ($8<t<14$)	3rd Regime ($14<t<31$)
COD	$COD = 9.68\,t + 321$	$COD = 8.49\,t + 92.35$	$COD = 13.94\,t + 83.14$	$COD = -4.52\,t + 207.77$	$COD = 10.47\,t + 44.13$
COD* (Normalised)	$\frac{COD}{M/V} = 415 \times 10^{-6} t +$ 13.7×10^{-3} $r^2 = 0.90$	$\frac{COD}{M/V} = 399 \times 10^{-6} t +$ 4.34×10^{-3} $r^2 = 0.90$	$\frac{COD}{M/V} = 655 \times 10^{-6} t +$ 3.90×10^{-3} $r^2 = 0.87$	$\frac{COD}{M/V} = -213 \times 10^{-6} t +$ 8.85×10^{-3} $r^2 = 0.414$	$\frac{COD}{M/V} = 492 \times 10^{-6} t +$ 2.07×10^{-3} $r^2 = 0.79$
pH	$pH = -0.35t + 9.95$	$pH = -0.055t + 8.62$	*No Relationship Observed*	$pH = -0.034t + 8.11$	$pH = -0.031t + 8.07$
pH* (Normalised)	$\frac{pH}{M/V} = -1.50 \times 10^{-6} t +$ 0.426×10^{-3} $r^2 = 0.83$	$\frac{pH}{M/V} = -2.58 \times 10^{-6} t +$ 0.405×10^{-3} $r^2 = 0.80$	*No Relationship Observed*	$\frac{pH}{M/V} = -1.60 \times 10^{-6} t +$ 0.381×10^{-3} $r^2 = 0.88$	$\frac{pH}{M/V} = -1.46 \times 10^{-6} t +$ 0.379×10^{-3} $r^2 = 0.76$

Where:

$$\text{Normalisation Factor} = \frac{M}{V} = \frac{\text{mass substrate}}{\text{volume of fluid in reactor}} \text{ (mg/L)}$$

Eqn. 6-1

The Normalisation Factors for the Denitrification Batch Reactor trials are tabulated in Appendix J. The Normalisation Factor for Reactor 1DRe and 1DRd are 23,360 mg/L and 21,282 mg/L respectively.

6.2.5 Denitrification of Lime Pretreatment Substrate

As demonstrated previously (Section 6.2.4), lime [calcium hydroxide, $Ca(OH)_2$] is another source of hydroxide ions when hydrated. The pretreatment trials with lime showed rates of organic carbon (COD) accumulation similar to those of the sodium hydroxide trials.

Since the mechanism for degrading the substrate with lime is similar to that of sodium hydroxide, it follows that the denitrification rate of lime pretreated substrates might be similar to the denitrification rate of sodium hydroxide pretreated substrates.

Three reactors were operated with lime-treated substrates. Two of these (1DRb and 2DRe) contained substrates treated with 500 mg/L of lime, while the third reactor (1DRc) contained substrates pretreated with 500 mg/L of lime and 500 mg/L sodium azide.

The profile of Reactor 1DRb is shown in Figure 6-6. At day zero the reactor had an initial DO concentration of 7.15 mg/L, which dropped to 1.13 mg/L 24 hours after the addition of the inoculum. By day four the DO concentration was below 1 mg/L and remained constantly below this threshold until the end of the trial at day 28. The weighted average DO concentration in the reactor during the trial was 0.87 mg/L (Appendix K). During this period the amount of accumulated COD fluctuated widely, eventually settling at a value of 84 mg/L. There was minimal reduction of reactor hydroxide concentration as the pH fell from 7.33 at day zero to 6.8 by day 28.

The nitrate concentration reduced from 202 mg/L to 179 mg/L over the period, whilst the change is not significant it is probable that the change was as a consequence of nitrate-nitrogen consumption at a rate of 0.83 mg/L/day (cf. pH=14 NaOH, 1DRd equated to 1.9 mg/L/day). This reduced rate of consumption could be attributed in part to the oxygen tension on the denitrification process and/or lack of available soluble organic carbon in solution.

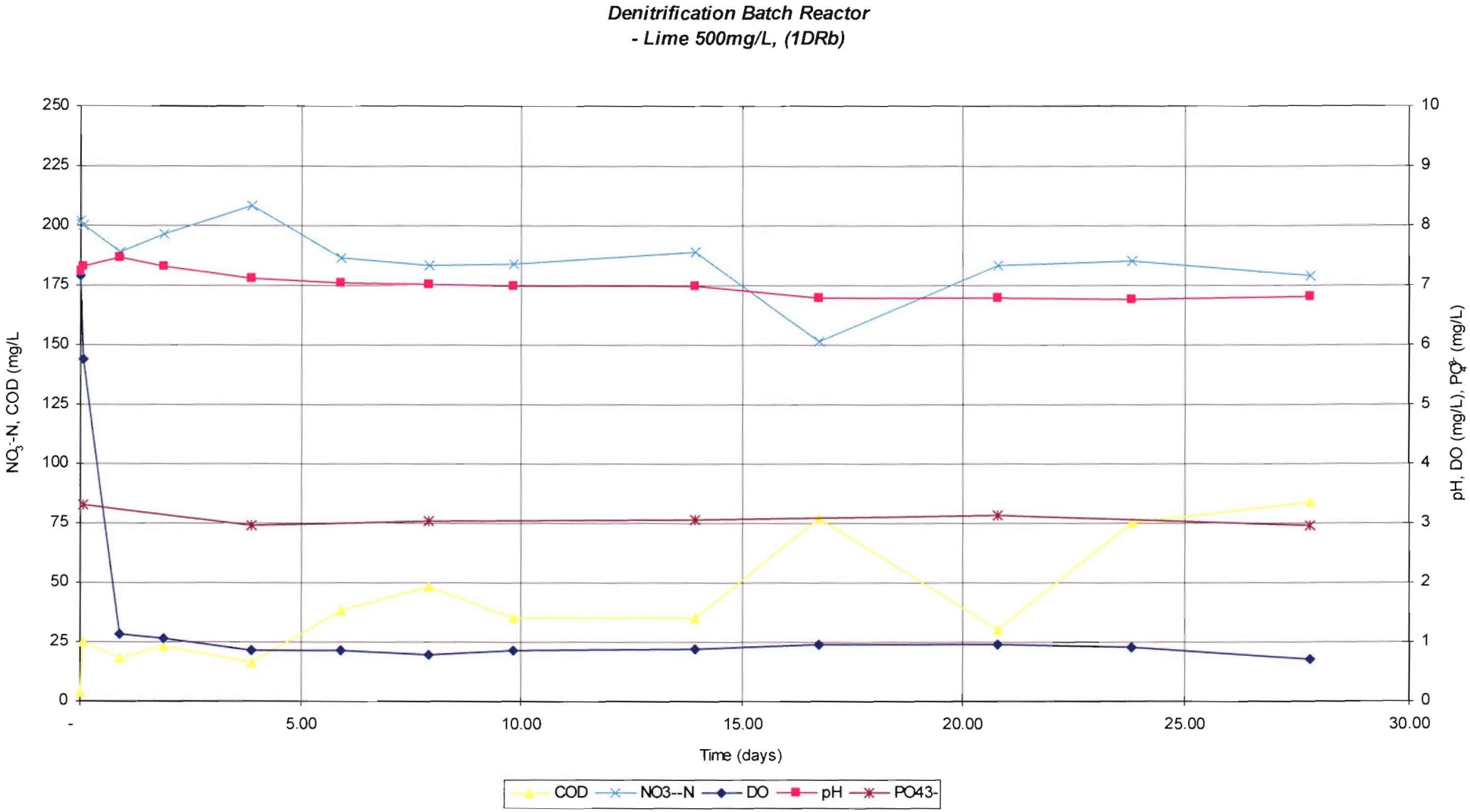

Figure 6-6 Denitrification batch trial utilising Lime pretreated substrate

The major difference between the sodium hydroxide pretreatment (Figure 6-4) and that of the lime pretreatment profiles (Figure 6-6) is the availability of organic carbon (COD). The rate of COD accumulation for the lime pretreated substrate was $COD = 2.03t + 19.4$ ($r^2 = 0.65$), while sodium hydroxide pretreated substrate exhibited a COD accumulation rate four times greater ($COD = 8.49t + 92.4$). Due to the large amount of COD (relatively speaking) it is highly unlikely that denitrification of the sodium hydroxide pretreated substrate was limited by any unavailability of organic carbon. However the comparatively low COD concentration in the lime treated reactors (Figure 6-6) supports the theory that the biological process may have been restricted by the limited availability of the organic carbon hence restricting the rate of denitrification.

The observations and comments made above suggest that the rate of denitrification is both a function of reactor DO and the availability of organic carbon. If the availability of organic carbon had not been limited then it would be expected that the rate of nitrate consumption (with a similar DO concentration) would be similar to that of the sodium hydroxide pretreated substrate (i.e. 1.9 mg/L/day of nitrate-nitrogen).

The pH profile showed minimal decline during this trial. Initially, the pH in the reactor was assessed at pH = 7.32 and, during the course of the trial, the pH reduced at a rate of $pH = -0.02t + 7.3$ ($r^2 = 0.82$). This gradual reduction in reactor hydroxide concentration (reflected by the declining pH) corresponded to a gradual accumulation of organic matter within the reactor.

The variability in the COD profile exhibited in Figure 6-6 supports the presence of some form of biological activity within the reactor. In the course of the pretreatment studies and analysis of the denitrification batch reactor trials, the reactors that were not dosed with sodium azide often exhibit this type of variability. By contrast, the reactors dosed with sodium azide tended to show a constant increase in COD accumulation without the scatter or variability that reactor 1DRb (Figure 6-5) demonstrates.

6.3 *Analysis of Denitrification Batch Reactor Studies*

This section of the research confirmed that several favourable conditions are required before denitrification will occur. When sufficient concentrations of nitrate and denitrifying bacteria are present in a reactor, then parameters such as the reactor DO concentration, availability of organic carbon, and reactor pH will determine whether denitrification will occur and/or the rate of denitrification. In particular, the rate of occurrence of denitrification observed in these trials was strongly influenced by the presence or absence of both readily available organic carbon and dissolved oxygen within the reactor.

6.3.1 Normalisation of Denitrification Batch Reactors

To allow comparisons to be drawn each trial needed to be normalised. For example, if the mass of organic carbon were to increase, a complementary increase in the rate of COD release might occur. Similarly, if the fluid volume were reduced whilst maintaining the same mass of organic carbon, then the relative concentration of COD within the reactor would increase. For these reasons, the process parameters assessed were normalised by the normalisation factor expressed in Eqn. 6-1, reproduced below.

$$\text{Normalisation Factor} = \frac{M}{V} = \frac{\text{mass substrate}}{\text{volume of fluid in reactor}} \text{ (mg/L)}$$

Where:

M	Mass of substrate in the reactor (mg)
V	Volume of fluid in the reactor (L)

The normalised behaviour of all the parameters evaluated in this section of the research is tabulated in Table 6-4 (the raw non-normalised reaction rates and normalisation factors are summarised in Appendix J).

An inspection of Table 6-4 indicates that the greatest rate of denitrification was achieved by reactor 1DRd (NaOH, pH=14) with a denitrification rate of 102 x 10^{-6} day^{-1} of NO_3^--N [16]. This corresponded to the second highest COD accumulation rate of 399 x 10^{-6} day^{-1} of COD. The reactor with the greatest accumulation of organic matter was that of reactor 1DRe (NaOH, pH=14, NaN_3). While reactor 1DRe and 1DRd were similar, reactor 1DRe had been dosed with sodium azide during the pretreatment trials to eliminate bacterial growth. The denitrification rate of this reactor had an order of magnitude less than that of reactor 1DRd.

The adverse effect of the sodium azide pretreated substrate is consistent with the observations that the residual sodium azide on the substrate may adversely affect the biological processes during the denitrification trials. It is thought that the sodium azide in low concentrations may retard the biological process, reducing the rate of organic carbon consumption and denitrification within the reactor – thus resulting in the greater rate of accumulation of the organic carbon and the slower reduction in nitrate from the reactor. Sutherland and Cook (1980) noted that sodium azide reduced the reaction rates of facultative anaerobic bacteria.

Of the twelve reactors trials conducted, eighteen data sets are collected. Where each data set was a distinct combination of pretreated substrate and dissolved oxygen state within the reactor, twelve of the dissolved oxygen states were anoxic, and the remaining six are classified as aerobic.

---

[16] The normalised reaction rates for COD, NO_3^--N, DO and PO_4^{3-} are expressed with the following: $\frac{mg}{L}\frac{1}{day}\frac{L}{mg} \equiv \frac{1}{day}$ while normalised reaction of pH is expressed in terms of $\frac{1}{day}\frac{L}{mg}$

Table 6-4 Evaluation of normalised reaction relationships for the denitrification batch reactors

Reactor		Substrate Pretreatment	$\frac{COD}{M/V}$	$\frac{pH}{M/V}$	$\frac{NO_3^- - N}{M/V}$	DO/(M/V) (Linear Approx.)	$\frac{PO_4^{3-}}{M/V}$
Anoxic Pretreated							
1DRa		Untreated	$11.0\times10^{-6}t + 41.3\times10^{-3}$	$-1.06\times10^{-6}t + 25.7\times10^{-3}$	$-1.34\times10^{-6}t + 7.53\times10^{-3}$	$-4.30\times10^{-6}\,t + 11.3\times10^{-3}$	$-0.24\times10^{-6}\,t + 12.4\times10^{-3}$
1DRb		Lime 500 mg/L	$83.4\times10^{-6}\,t + 0.639\times10^{-3}$	$-0.803\times10^{-6}\,t + 0.278\times10^{-3}$	$-32.8\times10^{-6}\,t + 7.50\times10^{-3}$	$-0.230\times10^{-6}\,t + 0.037\times10^{-3}$	$-0.230\times10^{-6}\,t + 0.12\times10^{-3}$
1DRc		Lime 500 mg/L + NaN_3	$82.5\times10^{-6}t + 1.33\times10^{-3}$	$-1.08\times10^{-6}t + .287\times10^{-3}$	$-26.4\times10^{-6}t + 7.67\times10^{-3}$	$0.0774\times10^{-6}\,t + 0.0353\times10^{-3}$	$-0.116\times10^{-6}\,t + 0.121\times10^{-3}$
1DRd		NaOH pH=14	$399\times10^{-6}\,t + 4.34\times10^{-3}$	$-2.58\times10^{-6}\,t + 0.405\times10^{-3}$	$-102\times10^{-6}\,t + 9.87\times10^{-3}$	$-0.230\times10^{-6}\,t + 0.037\times10^{-3}$	$-1.79\times10^{-6}\,t + 0.152\times10^{-3}$
1DRe		NaOH pH=14 + NaN_3	$415\times10^{-6}t + 13.7\times10^{-3}$	$-1.50\times10^{-6}t + 0.426\times10^{-3}$	$-11.1\times10^{-6}\,t + 8.73\times10^{-3}$	$2.53\times10^{-6}\,t + 0.066\times10^{-3}$	$.0.158\times10^{-6}\,t + 0.144\times10^{-3}$
1DRf		HCl pH=2	$62.3\times10^{-6}\,t + 1.42\times10^{-3}$	$0.234\times10^{-6}\,t + 0.18\times10^{-3}$	$-9.35\times10^{-6}\,t + 7.91\times10^{-3}$	$-0.818\times10^{-6}\,t + 0.0697\times10^{-3}$	$-0.896\times10^{-6}\,t + 0.12\times10^{-3}$
2DRa	*7<t<12*	NaOH pH=9	$-3.39\times10^{-6}t + 0.065\times10^{-3}$	$3.86\times10^{-6}t + 0.206\times10^{-3}$	$-10.1\times10^{-6}t + 4.33\times10^{-3}$	$31.5\times10^{-6}\,t + 0.697\times10^{-3}$	$0.355\times10^{-6}\,t + 0.717\times10^{-3}$
2DRb	*6<t<11*	HCl pH=2	$-0.115\times10^{-6}\,t + 1.63\times10^{-3}$	$3.79\times10^{-6}\,t + 0.181\times10^{-3}$	$13.3\times10^{-6}\,t + 7.00\times10^{-3}$	$0.191\times10^{-6}\,t + 0.0212\times10^{-3}$	$-2.03\times10^{-6}\,t + 0.0933\times10^{-3}$
2DRc	*7<t<12*	HCl pH=4	$44.3\times10^{-6}t + 0.39\times10^{-3}$	$-0.813\times10^{-6}t + 0.226\times10^{-3}$	$23.1\times10^{-6}t + 7.16\times10^{-3}$	$20.4\times10^{-6}\,t - 0.108\times10^{-3}$	$2.13\times10^{-6}\,t + 0.0643\times10^{-3}$
2DRd	*8<t<13*	NaOH pH=12	$206\times10^{-6}\,t - 0.803\times10^{-3}$	$1.27\times10^{-6}\,t + 0.302\times10^{-3}$	$1.27\times10^{-6}\,t + 8.55\times10^{-3}$	$3.89\times10^{-6}\,t + 0.0163\times10^{-3}$	$0.611\times10^{-6}\,t + 0.11\times10^{-3}$
2DRe	*9<t<13*	Lime 500 mg/L	$104\times10^{-6}t - 0.388\times10^{-3}$	$1.08\times10^{-6}t + 0.259\times10^{-3}$	$-12.2\times10^{-6}t + 8.07\times10^{-3}$	$8.05\times10^{-6}\,t - 0.0471\times10^{-3}$	$2.23\times10^{-6}\,t + 0.075\times10^{-3}$

Table 6-4 Evaluation of normalised reaction relationships for the denitrification batch reactors							
2DRf	*8<t<12*	Acetic Acid pH=5	$-10.2\times10^{-6}\,t + 0.735\times10^{-3}$	$7.28\times10^{-6}\,t + 0.156\times10^{-3}$	$2.88\times10^{-6}\,t + 7.35\times10^{-3}$	$..-6.62\times10^{-6}\,t + 0.104\times10^{-3}$	$-2.41\times10^{-6}\,t + 0.124\times10^{-3}$
Initial Aerobic Cond.							
2DRa	*0<t<7*	NaOH pH=9	$79.6\times10^{-6}t + 0.414\times10^{-3}$	$-4.41\times10^{-6}t + 0.257\times10^{-3}$	$-52.7\times10^{-6}t + 7.84\times10^{-3}$	$7.05\times10^{-6}\,t + 0.0996\times10^{-3}$	$-6.23\times10^{-6}\,t + 0.0871\times10^{-3}$
2DRb	*0<t<6*	HCl pH=2	$216\times10^{-6}\,t + 0.529\times10^{-3}$	$-3.63\times10^{-6}\,t + 0.214\times10^{-3}$	$-23.0\times10^{-6}\,t + 7.24\times10^{-3}$	$13.5\times10^{-6}\,t + 0.021\times10^{-3}$	$-1.11\times10^{-6}\,t + 0.0777\times10^{-3}$
2DRc	*0<t<7*	HCl pH=4	$15.6\times10^{-6}t + 0.652\times10^{-3}$	$-3.02\times10^{-6}t + 0.236\times10^{-3}$	$-32.5\times10^{-6}t + 7.19\times10^{-3}$	$3.29\times10^{-6}\,t + 0.0925\times10^{-3}$	$0.268\times10^{-6}\,t + 0.0709\times10^{-3}$
2DRd	*0<t<8*	NaOH pH=12	$85.9\times10^{-6}\,t + 0.556\times10^{-3}$	$-5.40\times10^{-6}\,t + 0.347\times10^{-3}$	$-122\times10^{-6}\,t + 9.30\times10^{-3}$	$-16.1\times10^{-6}\,t + 0.244\times10^{-3}$	$-3.38\times10^{-6}\,t + 0.143\times10^{-3}$
2DRe	*0<t<9*	Lime 500 mg/L	$39.7\times10^{-6}t + 0.466\times10^{-3}$	$-5.35\times10^{-6}t + 0.303\times10^{-3}$	$-78.1\times10^{-6}t + 8.43\times10^{-3}$	$-17.6\times10^{-6}\,t + 0.236\times10^{-3}$	$-3.81\times10^{-6}\,t + 0.124\times10^{-3}$
2DRf	*0<t<8*	Acetic Acid pH=5	$35.5\times10^{-6}\,t + 0.943\times10^{-3}$	$-7.45\times10^{-6}\,t + 0.285\times10^{-3}$	$-109\times10^{-6}\,t + 8.72\times10^{-3}$	$-10.1\times10^{-6}\,t + 0.149\times10^{-3}$	$1.24\times10^{-6}\,t + 0.104\times10^{-3}$

A negative rate parameter is indicative of that chemical being utilised or consumed during the course of the trial; conversely, a positive rate parameter indicates that the chemical is released.

Example: 2DRf $0<t<8$: $\frac{COD}{M/V} = 35.5\times10^{-6}\,t + 0.943\times10^{-3}$, 35.5×10^{-6} (day^{-1}) is the rate parameter for COD. In this case the parameter is positive indicating that COD was accumulating during the trial.

Notation: The normalised reaction rate R^{N}_{XXX} is defined as the rate variable, e.g.. 1DRa COD reaction relationship: $\frac{COD}{M/V} = 11.0\times10^{-6}t + 41.3\times10^{-3}$, where the normalised reaction rate $R^{N}_{COD} = 11.0\times10^{-6}$ (day^{-1}).

The presence of denitrification was defined as a decline in the nitrate concentration within the reactor, while in the absence of dissolved oxygen (i.e. below 1 mg/L). Of the 12 anoxic reactors that had a DO concentration profile that fell below 1 mg/L, only eight showed evidence of denitrification.

From Table 6-4, the greater normalised COD accumulation rate and nitrate reduction rate were associated with substrates that had been pretreated with a hydroxide ion releasing reagent (i.e. NaOH, lime, etc). Conversely, all of the acid treated substrates (with the exception of reactor 1DRf), demonstrated a lack of denitrification while in the anoxic environment. However, these same substrates, when utilised in an aerobic environment, recorded a measurable reduction in nitrate, which was thought to be nitrate assimilation rather than denitrification due to the aerobic nature of the batch reactor(s) during this phase.

6.3.1.1 Dissolved Oxygen Decay Profiles

The DO profiles of the batch reactors in this section of the research demonstrated an initial exponential decay profile. While Table 6-4 provides an evaluation of the normalised DO, the linear approximation is a simplistic model of the observed profiles. Hence, the following alternative normalised exponential analysis has been undertaken.

The general normalised form of the exponential decay function is expressed in Eqn. 6-2. The DO parameter has been normalised by the maximum DO reading in the data set (typically this occurs at $t = 0$ days). The variables (A, k, and C) were determined by evaluating the time-weighted best-fit trend for the data set (as demonstrated in Appendix L). Table 6-5 provides a tabular summary of normalised exponential variables for each trial/regime conducted in this series of experiments.

$$\frac{DO}{DO^*} = Ae^{-k_{DO}^N \bullet t} + C$$

Eqn. 6-2

Where:

DO^*	Maximum DO reading in the data set (mg/L)
A	Model variable (-)
k_{DO}^N	Exponential rate dependant variable (t^{-1})
C	Exponential variable (-)

Table 6-5 Normalised exponential parameters that model the DO profile in the denitrification batch reactors

	Reactor	A	k_{DO}^{N}	C
Anoxic Pretreatment Profile	1DRa	0.791	0.563	0.209
	1DRb	0.878	4.488	0.122
	1DRc	0.895	6.043	0.105
	1DRd	0.898	3.104	0.102
	1DRe	0.821	4.078	0.179
	1DRf	0.835	1.713	0.165
Anoxic Pretreatment Profile	2DRa	0.799	23.068	0.201
	2DRb	0.761	3.020	0.239
	2DRc	0.542	4.779	0.458
	2DRd	0.770	1.997	0.230
	2DRe	0.747	2.546	0.253
	2DRf	0.870	22.976	0.130
Aerobic Pretreatment Profile	2DRa	0.522	0.872	0.478
	2DRb	0.927	1.279	0.073
	2DRc	0.570	1.687	0.430
	2DRd	0.580	1.452	0.420
	2DRe	0.673	0.490	0.327
	2DRf	0.540	0.811	0.460

6.3.2 Generalised Parameter Dependence Relationships

COD Accumulation and Nitrate Reduction Rates

The results as presented in the earlier sections of this chapter demonstrated that as the COD in the reactor increases a corresponding reduction in reactor DO would occur while in the presence of bacteria. As expected, the presence of readily available COD in a normally COD-limited environment would stimulate bacterial growth, while conversely a low rate of COD accumulation is indicative of a reactor in which minimal bacterial activity is occurring, hence the minimal reduction in DO.

This relationship is graphically presented in Figure 6-7, where the increase in the accumulation of organic carbon in the fluid phase corresponded to a complementary increase in the DO reduction rate (k_{DO}^{N}). The data summarised in Figure 6-7 is sourced from the normalised COD accumulation rates tabulated in Table 6-4, and the DO reduction rate (the k_{DO}^{N} parameter) expressed in Table 6-5.

Figure 6-7 does not show a strong relationship between the COD accumulation and DO reduction, as the square of the Pearson product moment correlation coefficient (R^2) indicates. However, the batch reactors with the higher COD accumulation rates do correlate to batch reactor trials where the greatest DO reduction rate occurred, as would be expected.

The variation between the actual data set and the best-fit exponential representation of the relationship between the DO reduction rate and the COD accumulation rate (Figure 6-7) is thought to be associated with variations in the mass of bacteria present in the bioreactor and/or the pretreatment of the substrate directly influencing the biological process. The low R^2 value (0.2258) suggests that the relationship as expressed in Figure 6-7 and reproduced in Eqn. 6-3 is a rather simplistic assessment of the biological process.

$$R_{COD}^{N} = 6.12e^{3.2 \cdot k_{DO}^{N}}$$

Eqn. 6-3

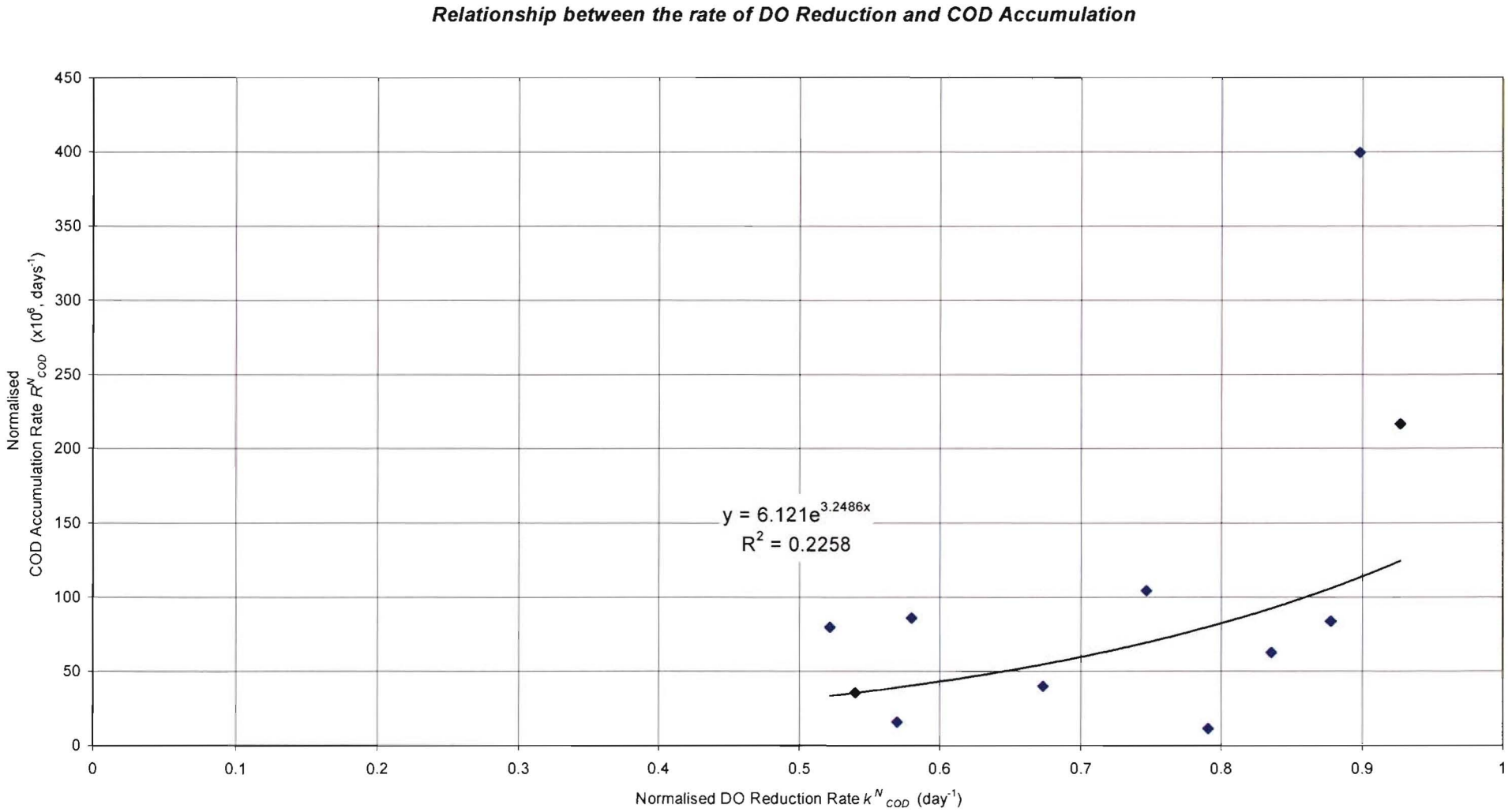

Figure 6-7 The relationship between the rate of DO reduction (k^N_{DO}) and the rate of COD accumulation (R^N_{COD}).

However the correlation between COD accumulation and denitrification rates as presented in Figure 6-8 indicates that there is a strong relationship between the rate of COD accumulation and nitrate consumption rate (reproduced in Eqn. 6-4). This figure also shows that the sodium azide-treated substrates exhibited a low rate of denitrification, independent of the amount of accumulated organic matter. Even though the data set in this figure is sparse, it follows the anticipated trend in that, for a biological process that is normally carbon limited, the greater the rate of COD accumulation the greater the rate of nitrate reduction due to biological denitrification.

$$R^{N}_{NO_3^- - N} = -0.26 R^{N}_{COD} - 2.9$$

Eqn. 6-4

Where:

$R^{N}_{NO_3^- - N}$ Normalised NO_3^--N reaction rate (day^{-1})

R^{N}_{COD} Normalised COD reaction rate (day^{-1})

pH and Nitrate Reduction Rates

While the optimum pH to promote denitrification is 6.3 (Payne, 1981), the experimental trials undertaken showed that during the course of the trial the reactors became more acidic. An increase in the rate of nitrate removal in the batch reactor was associated with a complementary increase in the rate of acidification of the reactor (Figure 6-9).

From Figure 6-9, the more negative the pH reaction rate[17] the greater the rate of nitrate removal. This observation is consistent with the model of hydroxide consumption associated with organic carbon release from the substrate. As the biological process is carbon-limited, an increase in organic carbon in the reactor will result in a complementary increase in the consumption of nitrate.

The data set presented in Figure 6-9, demonstrates that for the Lime and NaOH pretreated substrates, the following linear relationship (Eqn. 6-5) between the rate of nitrate consumption

---

[17] A negative normalised pH reaction rate indicates that the pH value in the reactor is reducing with time, ie. that the reactor is becoming more acidic

and pH reaction rate. However it should be noted that this data does not demonstrate a strong dependency between the two reaction rates, as the square of the Pearson product moment correlation coefficient (r^2) equates to 0.60 .

$$R^N_{NO_3^- - N} = 14.8 R^N_{pH} - 14.0$$

Eqn. 6-5

Where:

$R^N_{NO_3^- - N}$ Normalised NO_3^--N reaction rate (day^{-1})

R^N_{pH} Normalised pH reaction rate ($day^{-1} \bullet L/mg$)

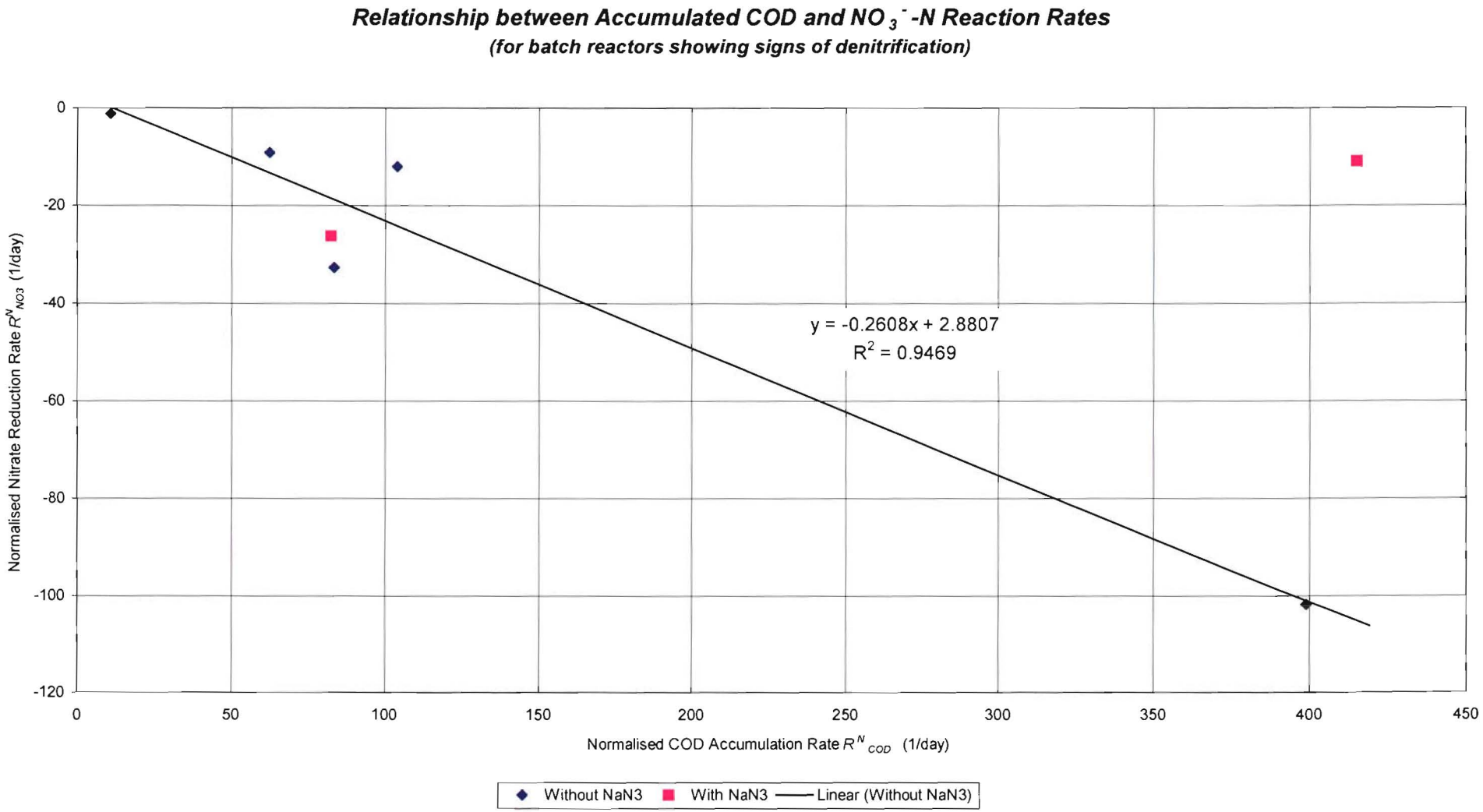

Figure 6-8 Correlation between the normalised NO_3^--N consumption and COD accumulation rate.

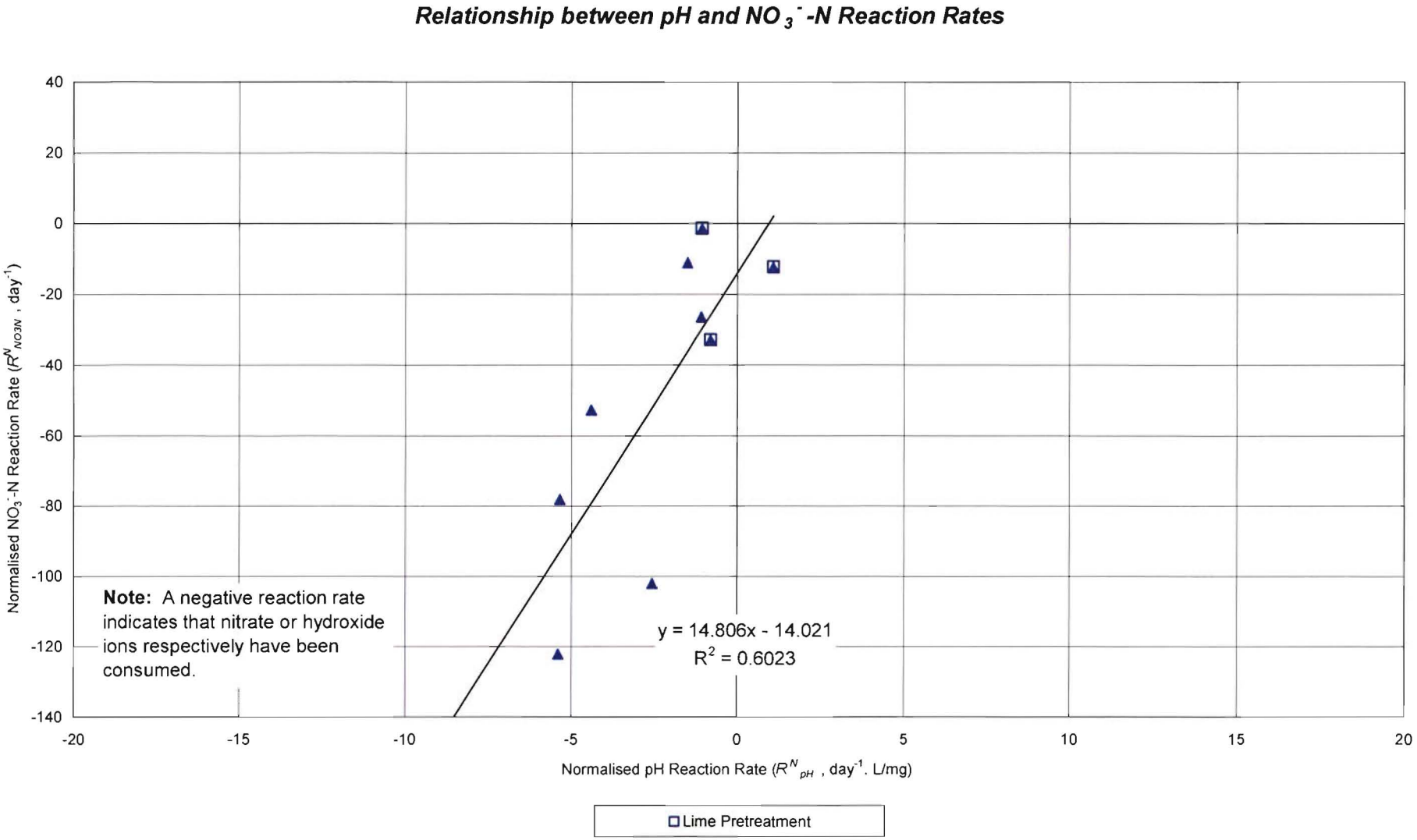

Figure 6-9 Comparative relationship between the normalised pH and NO_3^--N reaction rate (of Lime and NaOH pretreated substrate).

The reactors with substrate pretreated with a strong acid (i.e. HCl pH=2 or 4) demonstrated variable nitrate reduction rates performance. However the batch reactors operating in an aerobic state demonstrated relatively greater nitrate consumption with a complementary high rate of hydroxide ion reduction. This observation is not unexpected, as the denitrifying bacteria injected into the reactors are facultative, they will preferentially respire oxygen at a higher metabolic rate. The observed reduction in reactor nitrate is thought to be associated with the synthesis of new bacteria, while the reduction in hydroxide ions remains unknown.

Phosphate and Nitrate Reduction Rates

An assessment of the normalised nitrate reduction and the phosphate reduction rates summarised in Table 6-4, indicates that the dependency between these rates is weak (Figure 6-10). Notwithstandly, the greater the PO_4^{3-} reduction rate, the greater the nitrate reduction rate with the rates increase in proportion to each other.

The rate of PO_4^{3-} consumption did depend upon the history of the batch trial and/or substrate within it. That is, the trials that were initially operated aerobically and then followed by an anoxic regime tended to consume the PO_4^{3-} in the aerobic regime due to heterotrophic growth, only to release the PO_4^{3-} in the anoxic regime. Hence, the tendency that the greatest PO_4^{3-} consumption was associated with those reactors that were operated aerobically, while the reactors that exhibited minimal or negative PO_4^{3-} utilisation tended to be reactors in an anoxic regime.

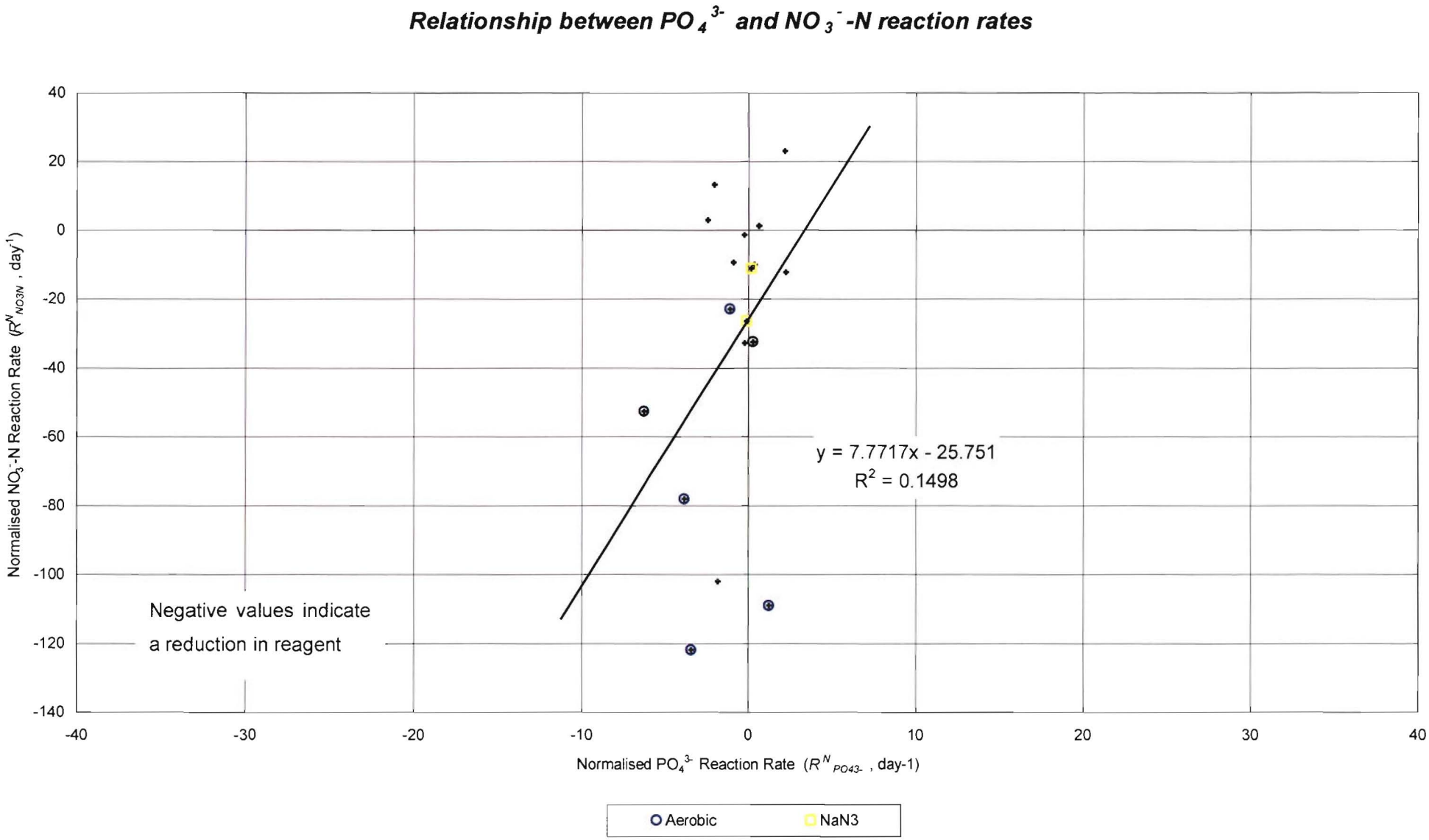

Figure 6-10 Comparative relationship between the normalised PO_4^{3-} and NO_3^--N reaction rates.

6.4 Discussions

6.4.1 Alkaline Induced COD Hydrolysis

As outline in Section 5.2.10, the hydrolysis of cellulose in the presence of sodium hydroxide and calcium hydroxide is thought to have resulted in the removal of many of the hydroxyl-hydrogen bonds from the cellulose molecule(s). Resulting in a reduction in the intrachain, interchain and intrasheet hydrogen bonds (Figure 3-18). Hence the cellulose in the coconut fragments is more susceptible to future enzyme hydrolysis.

A comparative assessment of the hydroxide pretreated substrates (Figure 6-11) demonstrates that the NaOH pretreated substrates release more COD into solution than the Lime pretreated substrates. However both substrates indicate that the rate of COD hydrolysis is greater than the observed rate of denitrification, resulting in the accumulation of the COD within the reactors.

The greater COD hydrolysis during the denitrification trail of the NaOH pretreated substrate compared to the Lime pretreated substrate is possible explained be the following:

1. During the alkaline hydrolysis process, an increased occurrence of the alkoxylate ions ($-O^-Na^+$) in the alkaline cellulose compared to the formation of $-O^-CaOH^+$ ions during the lime pretreatment. The increase in alkoxylate ions is expected to correlate to increase susceptibility to future hydrolysis;

2. The alkoxylate ion ($-O^-Na^+$) is more reactive that the $-O^-CaOH^+$;

3. Combination of 1. and 2.

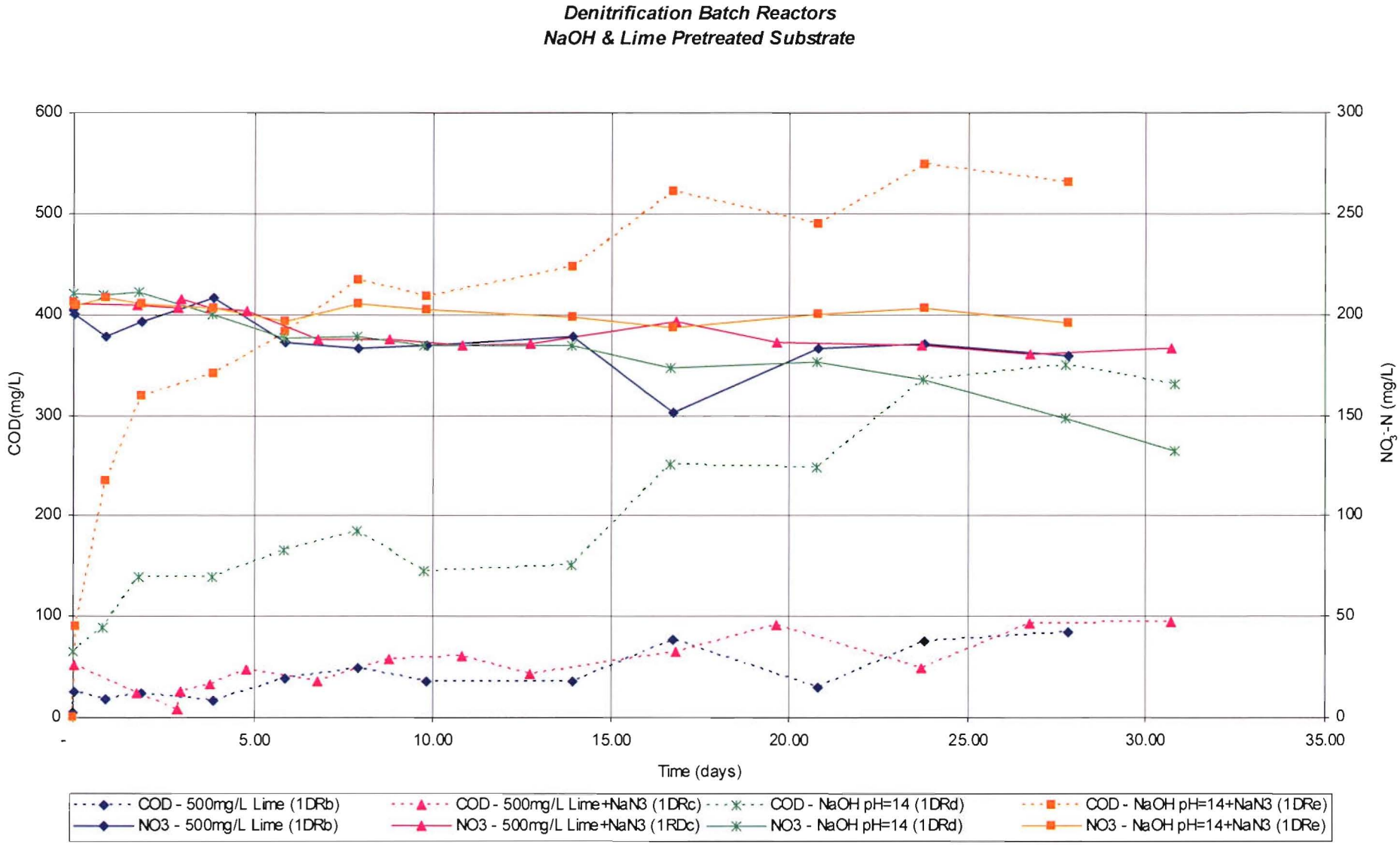

Figure 6-11 Comparison between the NaOH and Lime pretreated substrate Denitrification Batch Reactor trials.

It follows that as the cellulose fragments containing the $-O^-Na^+$ or $-O^-CaOH^+$ ions are liberated from the cellulose matrix, the ability of the cellulose structure to reacts and hydrolyse will reduce as the remaining intrachain, interchain and intrasheet hydrogen bonds limit the cellulose from further degradation.

Blank

Launch Internet Explorer Browser.lnk

6.4.2 Medium – Long Term Denitrification Viability

During the course of this section of the research, the short to medium-term viability (10-28 days) of the substrate to sustain biological denitrification was considered. Both the sodium hydroxide and lime-treated substrates showed signs of a further capacity to release organic carbon after the 28 day trial period (as indicated by the continued accumulation of organic carbon in the reactor, especially in the last few days of the trials).

However, it would be expected that the rate of organic carbon release would decline as the damaged section (containing $-O^-Na^+$ or $-O^-CaOH^+$ ions) of the cellulose were eventually liberated and consumed. It could be possible to then re-treat the substrate to recover its capacity to release further organic carbon, though this hypothesis was not tested in the scope of the research.

6.4.3 Preferred Substrate Pretreatment

Based on the results of the twelve reactor trials the hydroxide pretreated substrates (sodium hydroxide and lime) exhibited the greater ability to release COD and demonstrated the highest nitrate consumption (denitrification).

However sodium hydroxide was discounted as a feasible pretreatment technique due to the issues associated with a full-scale application of the technique. The caustic and hazardous nature of the sodium hydroxide would require a full-scale treatment facility to install specialised handling and storage facilities. The management and disposal of the spent aqueous sodium hydroxide is a particular issue that would need to be overcome. Many of the above issues can be easily managed were lime utilised.

The application of any full-scale technique tends to determined based on the favour Net Present Value (NPV) economic analysis. As the calculations below indicate the operational cost of the Lime pretreatment is less than a quarter than the sodium hydroxide pretreatment.

For the reasons outlined above the 500mg/L of Lime is the preferred pretreatment reagent to precede biological denitrification from coconut shell fragments.

NaOH, pH=12

Reagent cost $950/tonne or 0.095 ¢/gm, and 0.0219 mole/L of NaOH disassociates at 35°C result in pH=12. This equates to $0.83 /$m^3$ of NaOH solution

Lime, 500mg/L

Reagent cost $280/tonne or 0.028 ¢/gm, and 500gms of Lime required per 1m^3. This equates to $0.14 /$m^3$ of Lime solution.

6.5 Conclusions

1. The hydroxide based chemical pretreatment techniques (sodium hydroxide and lime) showed great promise as a treatment method to promote the release of organic matter. Not only did the chemicals improve the rate and amount of organic carbon released during the pretreatment process, but after the substrate had been washed and placed in the denitrification batch reactors, the substrate continued to release organic carbon. This was advantageous given that the biomass requires a readily available source of organic carbon to sustain biological denitrification.

2. The continued release of organic carbon from the hydroxide pretreated substrates could have resulted from damage to the cellulose during the pretreatment phase. In which the lost of many of the hydroxyl-hydrogen bonds from the cellulose molecule(s), resulted in a reduction in the intrachain, interchain and intrasheet hydrogen bonds. As a consequence the cellulose in the pretreated coconut fragments is more susceptible to future enzyme hydrolysis.

3. The long-term viability of the damaged/disrupted substrate was not fully assessed; however, in the short to medium-term (0-28 days) the substrate continued to release organic carbon in excessive quantities such that the organic carbon (COD) would accumulate in the denitrification reactor.

4. Sodium hydroxide is not favoured as a full-scale pretreatment technique to promote denitrification from coconut shells. Due to the hazardous (caustic) nature of sodium hydroxide and the requirement that special handling and storage facilities be

provided. More importantly, the operational costs of a sodium hydroxide pretreatment technique are more than four times that of the lime based pretreatment.

5. For the reasons outlined above rule out sodium hydroxide, the preferred pretreatment technique to promote biological denitrification is 500mg/L of Lime.

6. Since the lime-treated reactors were still carbon limited, they exhibited a lower rate of denitrification than those with sodium hydroxide-treated substrate, however, this can en an advantage, in that excessive release of organic carbon from the biological process can now be managed, thereby possibly eliminating COD breakthrough from the denitrification process or limiting the COD load on any downstream treatment processes.

7. The dissolved oxygen decay from the series of batch trials exhibited an exponential decay profile with the following generalised form:

$$\frac{DO}{DO^*} = Ae^{-k_{DO}^N \bullet t} + C$$

8. An assessment of the normalised reduction or accumulation rates in the denitrification batch trials presented a strong relationship between the normalised rate of nitrate reduction and normalised rate of COD accumulation, as reproduced below:

$$R_{NO_3^- - N}^N = -0.26 R_{COD}^N - 2.9$$

The follow relationships were observed, but the dependency between the normalised reaction rates were not as evident:

$$R_{NO_3^- - N}^N = 14.8 R_{pH}^N - 14.0$$

$$R_{COD}^N = 6.12 e^{3.2 \cdot k_{DO}^N}$$

and

$$R_{NO_3^- - N}^N = 7.77 R_{PO_4^{3-}}^N - 25.8$$

Eqn. 6-6

6.6 References:

Christchurch City Council (2000) Per. Conservation, Water Unit

Gayle B. P., and Boardman G. D., Sherrard J. H., Benoit R. E. (1989) Biological denitrification of water. ASCE, J. Enviro. Engrg. Vol. 115, No. 5, Oct. pp. 930-943

Glass C. and Silverstein J. (1999) Denitrification of High-Nitrate, High-Salinity Wastewater. Water Research Vol. 33, No. 1, pp. 223-229

Henze, M., Harremoës, P., La Cour Jansen, J. and Arvin, E. (1995). Wastewater Treatment: Biological and Chemical Processes. Springer, Heidelberg.

Mayo A.W. and Noike T. (1994) Response of Mixed Cultures of *Chlorella Vulgaris* and Heterotrophic Bacteria to Variation of pH, Water Science Technology, Vol. 30, No. 8, pp 285-294

Payne W.J. (1973) Reduction of nitrogenous oxides by microogranisms. Bacteriol. Rev., Vol. 37, pp. 409-452

Safferman S.I. and Burks B.D, Parker R. A. (2004) Carbon and Nitrogen Removal from On-Site Wastewater Using Extended-Aeration Activated Sludge and Ion Exchange, Water Environment Research, Vol. 75, No.5, pp. 404-412

Sutherland J.B. and Cook R.J. (1980) Effects of Chemical and Heat Treatments on Eythlene Production in Soil, Vol. 12, No. 4, pp 357-362

7 Denitrification Fluidised Bed Reactor Trials

7.1 Introduction

The previous denitrification batch reactor section showed that biological denitrification has a low process rate when using coconut as a substrate. This segment of the research evaluates the Fluidised Bed Reactor (FBR) process as a possible technique to improve the rate and capacity of the substrate to sustain biological denitrification.

In Chapters 5 and 6, the treatment of coconut shell fragments with a super saturated lime solution increased the rate of organic carbon hydrolysis. Since biological denitrification is carbon-limited, an increase in the rate of carbon hydrolysis should result in an increase in the rate of denitrification. A substrate capable of an improved rate of organic carbon hydrolysis, used in conjunction with a fluidised bed that has the potential to improve the operational performance of the bioreactor, suggests that a feasible biological denitrification technique is possible.

Thirty-one trials were conducted for this segment of the research. Two reactors were operated in parallel, one with the lime pretreated substrate and the other with untreated substrate. The focus was on the response these reactors exhibited to a variety of influent flow rates and nitrate conditions.

Naming Convention

The following reactor notation naming convention has been applied for this series of trials, the reactor number, and the particular series under consideration:

FBR *Y*-*X*(*z*)

Where:

Y numerical number, corresponding to the reactor series. In total 6 series were conducted

X numerical number corresponding to the particular reactor of interest (i.e. 1 or 2)

z alphabetic sequence corresponding to the trial under consideration

e.g.. Reactor one from the third series of the fluidised bed reactor trials (in particular trial "c") would have the following notation: FBR3-1(c)

As mentioned, lime pretreatment offered a similar increase in the rate of COD hydrolysis to that of sodium hydroxide. The lime-treated substrates utilised in this series of experiments were treated with a similar mass of $Ca(OH)_2$ to substrate as the denitrification batch reactor trials (500mg/L). The pretreatment methodology followed was detailed in Section 4.

7.2 Results

7.2.1 Fluidised Bed Reactor – Series 1

In the first series of fluidised bed reactor trials, eight experiments were conducted. Both reactors were commissioned on the 27th March 2000, with the first trial beginning on the 6th April 2000 (t = 0 days). Reactor 1 contained the untreated coconut shell substrate, while the lime-treated substrate was added to Reactor 2.

During the 10 days between the 27th March 2000 and the 6th April 2000, the hydraulic performance and reliability of the reactors were monitored. Only on the 6th of April 2000 had the fluidised beds had maintained a constant bed depth for three days that was deemed satisfactory to add the bacteria. At which time the bacterial inoculum was injected into FBRs both reactors. For the following fifteen days both reactors were closed to the atmosphere and influent was pumped into the reactors.

7.2.1.1 FBR1-X(a)

The purpose of two initial trials, FBR1-1(a) and FBR1-2(a), was to evaluate the performance of the fluidised bed reactor. Both reactors were pulsed with nitrate and the resulting decay in nitrate due to denitrification was observed.

On the 6th April 2000, 30mL of inoculum was injected into each reactor. Figure 7-1 shows that at $t=0$ days both reactors were close to anaerobic, with DO concentrations well below 1 mg/L. The initial COD concentrations were 163 mg/L and 440 mg/L within reactor 1 and 2 respectively. The difference in initial COD is attributed to increased hydrolysis as the result of the lime pretreatment on the substrate in reactor FBR1-2 that is, as both substrates had been placed in their respective reactors 10 days earlier (i.e. at $t=-10$ days), the lime-pretreated resulted in a greater release of COD, thought to be as a result of continued alkaline hydrolysis of the substrate.

From *t=0* to *t=4.2* days, both reactors were operated in a fluidised state, thus allowing the bacteria to acclimate to the new physical conditions. No denitrification occurred during this period due to the absence of any nitrate within the reactors. During the first four days of this trial, both reactors continued to accumulate organic carbon such that in Reactor 1 the COD concentration in the liquid had increased from 163 mg/L to 298 mg/L, while the concentration in reactor 2 had increased from 442 mg/L to 506 mg/L. At *t = 4.2* days, both reactors were pulsed with 570 mg of NO_3^--N, sufficient to increase the nitrate concentration in both reactors to approximately 50 mg/L NO_3^--N. An assessment of the two graphs presented in Figure 7-1 highlights that the denitrification rate for the lime-treated substrate was greater than that exhibited by the untreated substrate (11.58 mg/L/day compared with 7.06 mg/L/day for the untreated substrate). It should be noted that this assessment is crude due to the infrequent nitrate sampling conducted in this set of trials. As a consequence, the sampling frequency was increased for the remaining trials.

A few days after the addition of the nitrate, both reactors recorded a slight dip in COD concentration , which quickly recovered once the nitrate concentration approached zero. The COD dips corresponded to the period in which the nitrate consumption was its greatest, indicating that at stage of the trial, the rate of COD demand due to the denitrification process exceeds the ability of both substrates to supply COD.

The COD parameter is an assessment of the soluble COD in solution. By assessing the COD we are evaluating the summation of two processes, the first being the hydrolysis of organic carbon from the coconut shell fragments (releasing COD into solution), and the second being the biological consumption of COD (reduction in COD). This interaction is best demonstrated in FBR1-2(a), Figure 7-1.

In this figure it can be observed that the COD concentration in solution dipped 40 mg/L from *t=4* to *t=8* days. During this period the nitrate concentrations in the reactor reduced from 45 mg/L to practically zero. The biological denitrification that consumed the available nitrate as consumed COD. The dip in COD in solution, indicates that the rate of biological consumption exceeded the rate of COD release due.

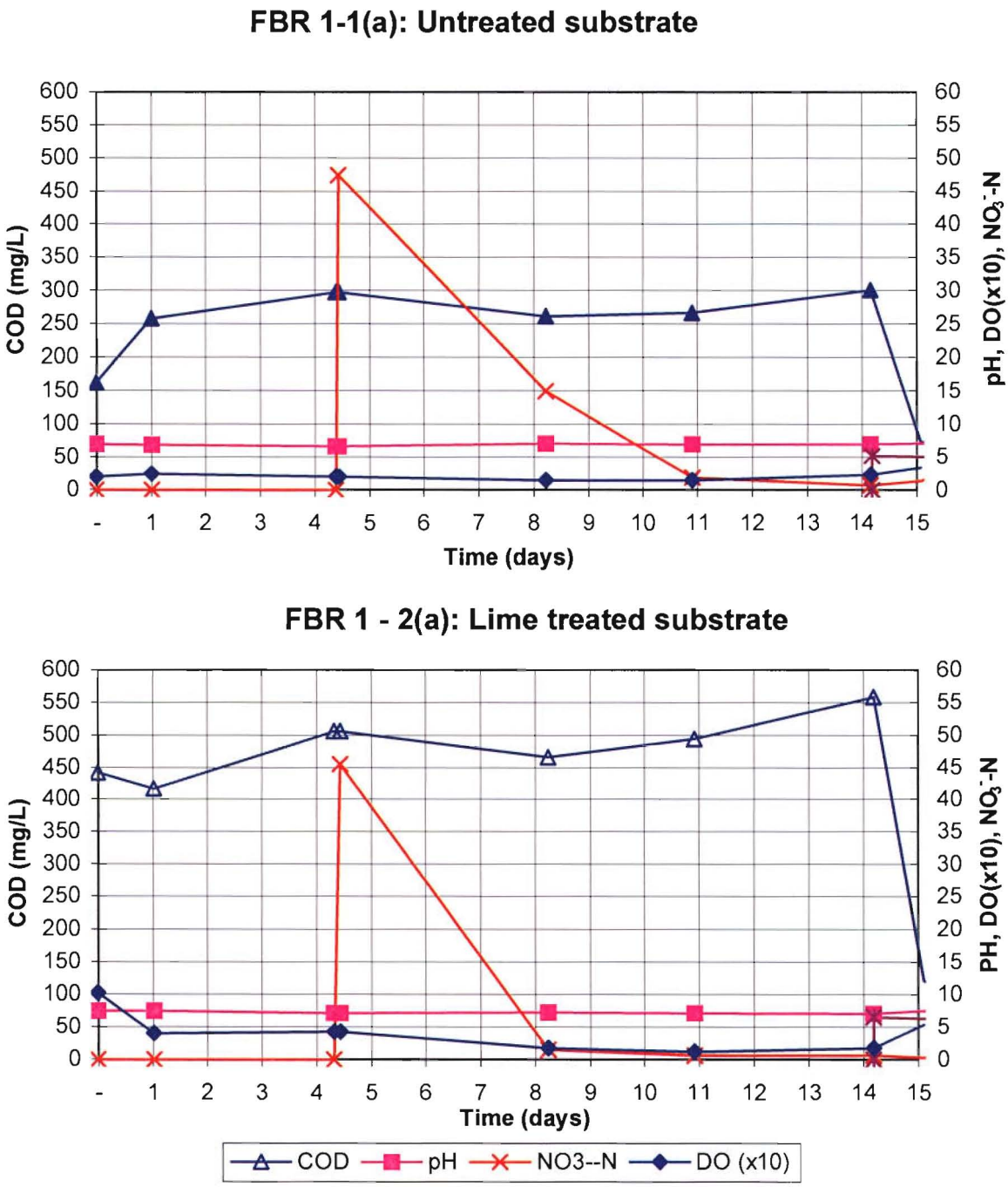

Figure 7-1 The acclimation phase of FBR 1-1(a) and FBR 1-2(a) respectively.

From t =8 to t = 14 the absence of biological consumption of COD due to the absence of readily available nitrate of dissolved oxygen for respiration, resulted in a nett gain of COD in the reactor as result of COD release.

7.2.1.2 FBR1-X(b)

The remaining FBR1-X(x) trials subjected the reactors to a series of three distinct hydraulic and nitrate loading conditions as outlined in Table 4-9. In the first of these conditions, FBR1-X(b) from *t=14* to *t=22* days, the nitrate was dosed at a rate of 5.25mg/hr and 6.60 mg/hr and a hydraulic load of 0.465 L/hr and 0.584 L/hr for reactor 1 and 2 respectively. An assessment of the reactors immediately following the start of trial (i.e. dosing) showed a marked increase in the nitrate concentration in both reactors (Figure 7-2 and Figure 7-3). During the first three days of this trial the nitrate concentration continued to accumulate at a rate of 2.04 mg/L/day for reactor 1 (Figure 7-2), while Reactor 2 (Figure 7-3) increased at a slightly lower rate of 1.44 mg/L/day.

The increase in nitrate within both reactors indicates that the reactor configuration and COD/substrate characteristics were unable to fully process the nitrate load. The inability to denitrify the nitrate was thought to be due in part to the hydraulic load placed on the reactors. The relatively high hydraulic load (24.5 hours HRT for Reactor 1 and 19.5 hours HRT for Reactor 2) had the effect of flushing out organic carbon from the reactors, as indicated by the drop in COD without the coincidental decrease in either nitrate or dissolved oxygen.

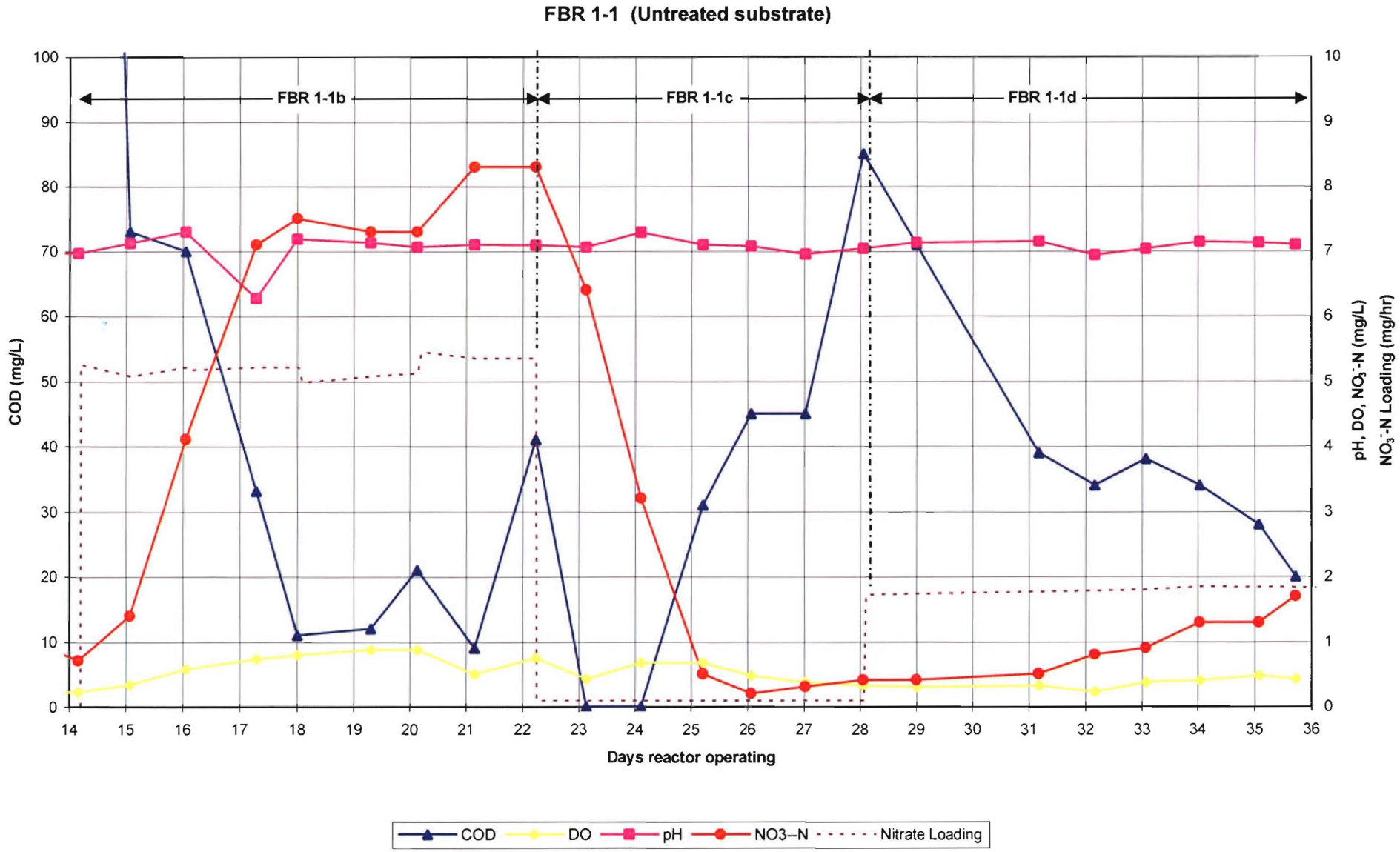

Figure 7-2 Denitrification Trial FBR1-1, the untreated substrate.

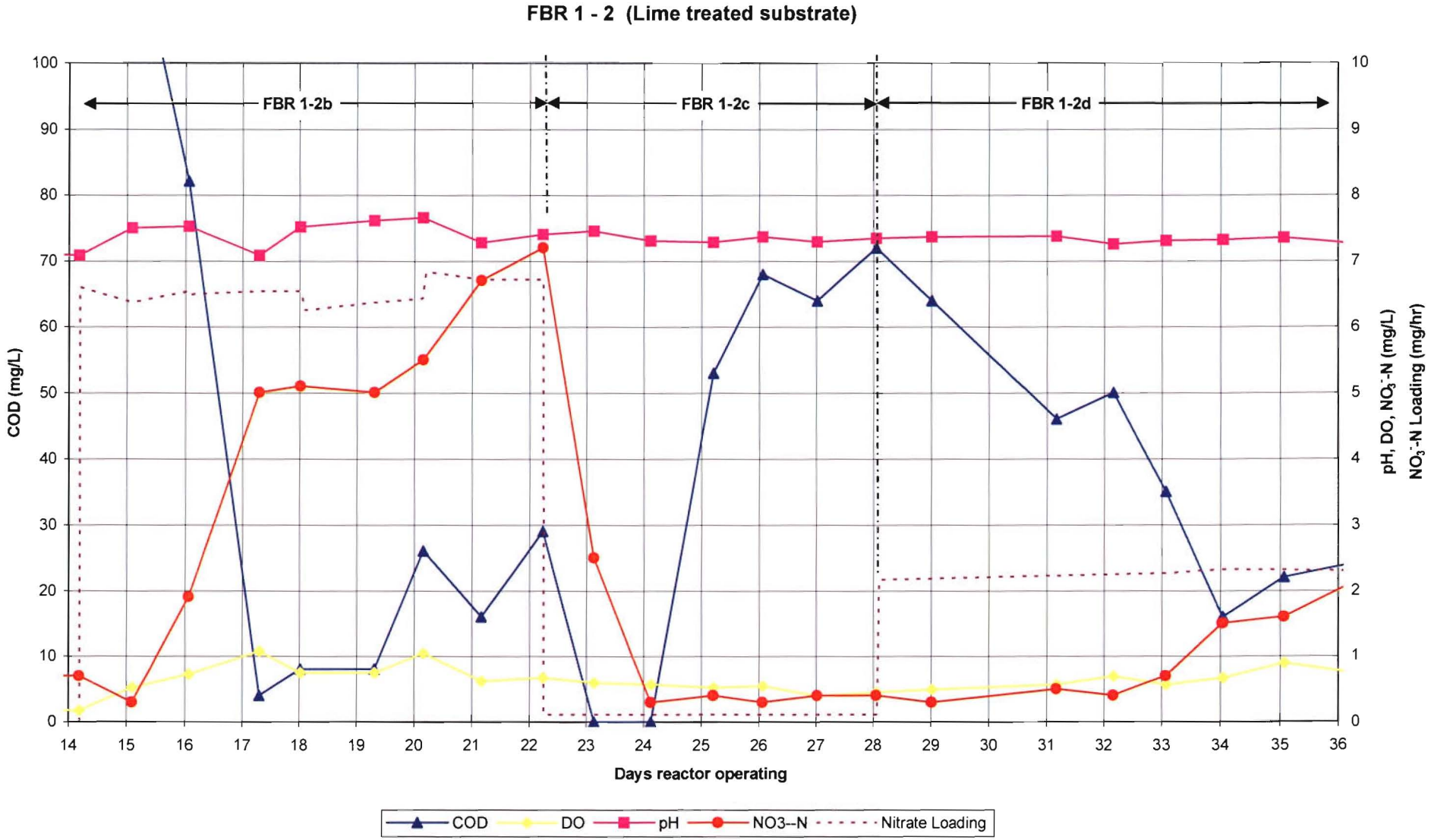

Figure 7-3 Denitrification Trial FBR1-2, the lime treated substrate.

During the first four days of the trial the COD concentration lost 290 mg/L in Reactor 1, and 559 mg/L in Reactor 2, such that the COD in the latter stages of this trial measured in the order of 15mg/L for both Reactor 1 and 2. Therefore, the unavailability of organic carbon in suitable concentrations to sustain bacterial processes in combination with the high nitrate loading, and DO concentration in the reactors during this period would most likely have contributed to the observed increase in nitrate within the reactors. The COD concentrations in both reactors, however, eventually recovered in the later stages of the trial, and organic carbon accumulated at a rate of 5.53 mg/L/day and 4.73 mg/L/day for Reactor's 1 and 2 respectively (as shown in Table 7-1). This corresponded to a reduced rate of nitrate accumulation with the reactors during this period ($17 \leq t \leq 22$) of 0.246 mg/L/day and 0.464 mg/L/day.

Table 7-1 Rate of change of COD and nitrate concentrations for FBR1-X(b)

A +ve rate, indicates accumulation	COD (mg/L/day)		NO_3^--N (mg/L/day)	
	FBR1-1(b)	FBR1-2(b)	FBR1-1(b)	FBR1-2(b)
Phase 1 $(14 \leq t \leq 17)$	-61.9	-159.8	1.97	1.44
Phase 2 $(17 \leq t \leq 22)$	5.53	4.73	0.246	0.464

Figure 7-2 for FBR1-1(b) and Figure 7-3 for FBR1-2(b) both demonstrate the two phases described above (COD loss and nitrate accumulation followed by a recovery in COD concentration within the reactor with a complementary reduction in the rate of nitrate accumulation). Qualitatively it is thought that the first phase reflects a period of bacterial growth of the facultative bacteria in aerobic conditions. Eventually limited by the availability of organic carbon due to COD being flushed from the reactors. However, the rate of heterotrophic growth and nitrate respiration (denitrification) was insufficient to offset the rate of nitrate accumulation due to the nitrate load..

In the second phase, the reduced COD concentration in the liquid medium would stimulate the production of more cellulase enzymes, in turn, resulting in more organic carbon being released from the coconut shell fragments. The rate of hydrolysis of the substrate would then exceed the requirements of the biomass as well as the hydraulic flushing characteristics within the reactors, resulting in the observed recovery of COD within both reactors. During this second phase the rate of nitrate accumulation decreased due to increased biological denitrification within both reactors, stimulated by the recovery in availability of the organic carbon.

A simple numerical CFSTR (continuous flow stirred tank reactor) analysis of the COD in FBR1-1(b) is graphically represented in Figure 7-4. The CFSTR model applied (Appendix M) replicates the three functions thought to be occurring within the reactor: hydraulic flushing ($Qc_1 - Qc$), biological consumption ($Vr_b ct$), and pollutant production/hydraulic solubilisation $\left(\frac{Vc_s}{2k_s}\left(\text{sech}^2\left(\frac{t-r_s}{k_s}\right)\right)\right)$, algebraically these form the following equation (Eqn. 7-1):

$$V\frac{dc}{dt} = Qc_1 - Qc + \frac{Vc_s}{2k_s}\left(\text{sech}^2\left(\frac{t-r_s}{k_s}\right)\right) - Vr_b ct$$

Eqn. 7-1

Where:

V	Reactor volume (11.3L)
c	COD concentration (mg/L)
t	Time (days)
Q	Influent flow rate (L/day)
c_I	COD concentration in the influent (mg/L)
c_s	Maximum soluble COD parameter (mg/L)
r_s	Solubilisation rate parameter (days)
k_s	Solubilisation rate parameter ($days^{-1}$)
r_b	Biological rate of consumption parameter ($days^{-1}$)

The best-fit analysis of the model (Eqn. 7-1) to the COD in FBR1-1(b), as represented in Figure 7-4, determined the following model parameters: Q = *11.16 L/day,* c_I = *0 mg/L,* c_s = *274,200 mg/L,* r_s = *-24.2 days,* k_s = *4.2 days*$^{-1}$ *and* r_b = *1.86 days*$^{-1}$.

The term c_s , maximum soluble COD, when considered with the k_s parameter specified the maximum rate of COD able to be released into solution. This trail (FBR1-2(b)) and subsequent trials indicated that the numerical model, Eqn. 7-1, was not sensitive to changes in c_s , however the term $\frac{c_s}{k_s}$ (mg/L/day) which provides a measure of the rate of COD release into solution was significant. For the purposes of simplifying the anlysis, all numerical evaluations of these series of trials have assumed that c_s equates to 274,200 mg/L. This value was selccted as it provided the best fit across all the numerical evaluations.

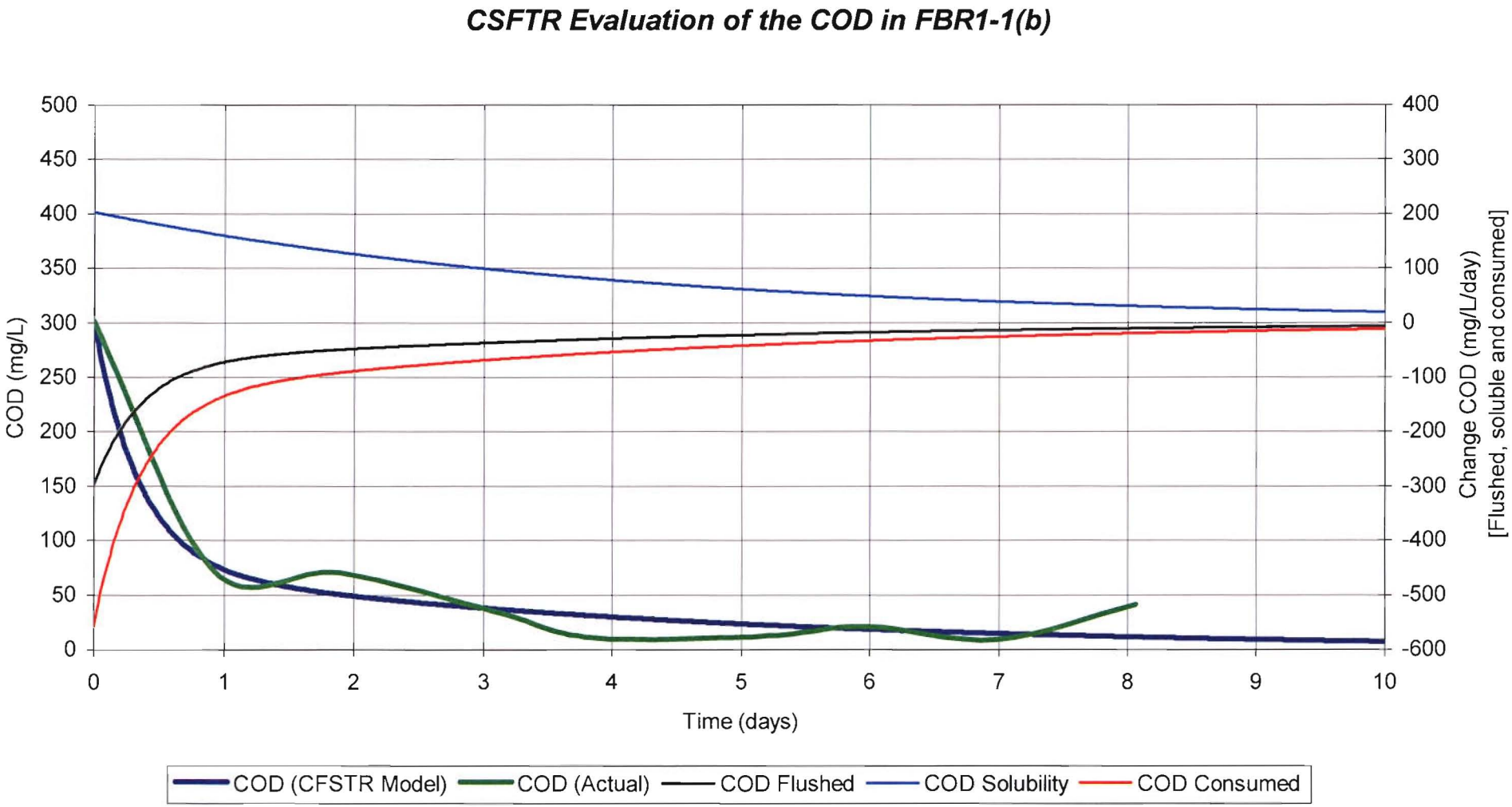

Figure 7-4 Numerical CFSTR model of the COD in FBR1-1(b).

Figure 7-4 indicates that during the initial stages of this trial, the greatest change in COD was the as result of flushing of COD from the reactor. The best-fit analysis determined that the solubilisation of COD was constant at approximately 38.3 mg/L/day. From day three, the rate of solubilisation was unable to match the rate of COD biologically consumed or flushed from the reactor, as apparent by the reducing COD (CFSTR model) profile.

The comparison of the performance of the two reactors FBR1-1(b) and FBR1-2(b), in Figure 7-2 and Figure 7-3 respectively, demonstrates that while the COD from the lime-treated substrate was consistently greater than the untreated substrate, the COD concentrations remained in the untreated substrate reactor for longer (approximately 20 hours longer) before the COD recovery phase. This observation can be explained by the presence of greater biological activity within the lime-treated substrate reactor, [FBR1-2(b)], where relatively greater quantities of COD were consumed once the majority of COD had been flushed from the reactor.

The presence of greater biological processes within the lime-treated reactor could explain the observed disparity between the amounts of nitrate accumulated in the two reactors. During this trial, both reactors were flushed with influent containing 11.3 mg/L of nitrate in solution. CFSTR modelling indicates that the rate of nitrate accumulation would slow as the reactor nitrate concentration tended toward 11.3 mg/L, as observed in the untreated substrate reactor FBR1-1(b). However, the lime-treated reactor, FBR1-2(b), displayed a different profile: where the rate of increase slowed in FBR1-1(b), the lime-treated reactor had a lower rate nitrate concentration suggesting increased denitrification. These observations are supported by the summary presented in Table 7-2, where the biological consumption rates (r_b) in the lime-treated reactor, FBR1-2(b), were approximately 2.5 times greater than the untreated reactor FBR1-1(b).

Inconsistencies in the control of the dosage pumps resulted in the first few trials having variations in the dosage between the two reactors. For the FBR1-X(b) trials, the lime-treated reactor was receiving its nitrate dose at a rate of 1.3 times greater than the untreated reactor (Table 4-9). This differential nitrate loading would have favoured greater nitrate accumulation if in the lime-treated reactor all other variables were equal. Since, the opposite occurred, this supported the premise that the lime-treated substrate had a greater capacity to denitrify.

Table 7-2 Assessment of COD and Nitrate concentrations in FBR1-X(b)

	COD		NO_3^--N	
	FBR1-1(b)	FBR1-2(b)	FBR1-1(b)	FBR1-2(b)
At t = *21 days* (mg/L)	9	16	8.3	6.7
Hydraulic Flushing Scenario at t = *21 days* (mg/L) [#]	0.3	0.1	11.1	11.2
Idealised CFSTR Parameters				
r_b	1.86	4.84	0.46	1.2
k_s	4.18	1.48	-	-
r_s	-24.2	-7.43	-	-
c_s	274,200	274,200	-	-

[#] The assessment conducted in this scenario has excluded the effect of possible formation or biological consumption of COD and nitrate within the reactor.

7.2.1.3 FBR1-X(c)

With the previous set of trials having flushed the readily available COD from the reactors, and accumulated nitrate, it was necessary that the next trial had a lower hydraulic and nitrate loading condition to provide an opportunity for the reactors to recover.

The two FBR1-X(c) trials were operated with a new hydraulic and nitrate load approximately 2% of that of the FBR1-X(b) trials. The average hydraulic load for FBR1-X(c) reactors was 0.009 L/hr (HRT = 59 days), in comparison to the earlier FBR1-X(b) trials with a significantly greater hydraulic load at 0.525 L/hr (HRT = 22 hours). Correspondingly, FBR1-X(c) had a nitrate load of 0.11 mg/hr compared to an average of 5.85 mg/hr for the FBR1-X(b) trials.

Two phases were observed during this trial: in the first phase, from $22 \leq t \leq 25$ days, the high nitrate concentration was denitrified; in the second, $24 \leq t \leq 28$ complete denitrification of the influent nitrate flux occurred, at the same time it accumulated organic carbon (Figure 7-2 and Figure 7-3).

During these two phases, the DO concentration was consistently below 1 mg/L, a favourable condition to promote denitrification. Both of the reactors showed a slight decline in the DO concentration during the course of this trial.

A comparison of the rate of change of the COD and nitrate concentrations within the reactors (Table 7-3) demonstrates that during the first phase, the lime-treated reactor denitrified the initial nitrate concentration at a greater rate, and as a consequence the observed rate of change of nitrate was 3.58 mg/L/day for the lime-treated reactor, while the untreated reactor showed a 2.64 mg/L/day reduction. It is of particular interest that while both reactors started to show evidence of COD accumulation about the same time, the reactor with the untreated substrate, FBR1-1(c), was accumulating the organic carbon prior to the completion of the denitrification of the initial nitrate concentration.

Since the COD accumulation started before the cessation of the initial nitrate consumption, it could indicate that the solubilisation of the organic matter during this phase was primarily extracellular. It is thought that the low COD concentration around *t=22* to *23* days stimulated the production of cellulase enzymes that hydrolysed exposed cellulose sites on the substrate releasing COD.

Table 7-3 Rate of change of COD and nitrate concentrations for FBR1-X(c)

	COD (mg/L/day)		NO_3^--N (mg/L/day)	
	FBR1-1(c)	FBR1-2(c)	FBR1-1(c)	FBR1-2(c)
Phase 1 $(22 \le t \le 25)$	N/A	N/A	-2.64	-3.58
Phase 2 $(25 \le t \le 28)$	7.09	5.0	$\cong 0$	$\cong 0$

Table 7-3 above tabulates the rate of change observed in the two reactors and it is apparent that during the second phase the untreated reactor accumulated COD at a rate greater than that of the lime treated reactor. From earlier trials, it would have been expected that the rate of hydrolysis from the lime-treated substrate was greater, and this can be partly explained by the slightly shorter hydraulic retention time, in addition to the increased nitrate loading of the lime-treated reactor. The lime-treated reactor operated at a 20% shorter HRT as compared to the untreated reactor (as presented in Table 4-9). Not only was the accumulated COD flushed out of the reactor at a faster rate, but also the reactor was being dosed with more nitrate. Since no accumulation of nitrate occurred during this period, this suggests that complete denitrification was occurring with denitrifying bacteria consuming more COD compared to the untreated reactor.

7.2.1.4 FBR1-X(d)

The final set of trials in this series was conducted at an influent flow 20 times greater than the FBR1-X(c) trials. This corresponds to the untreated reactor FBR1-1(d) dosed at 0.16 L/hr (HRT = 3 days) and at 1.8 mg/hr of nitrate, and the lime-pretreated reactor FBR1-2(d) dosed at 0.2 L/hr (HRT = 2.4 days) and at 2.2 mg/hr of nitrate. The duration of the trial was ten days, or approximately three HRT periods.

As described earlier, these fluidised bed reactors behaved hydraulically like a CFSTR. A numerical assessment of the CFSTR model developed earlier (Eqn. 7-1) formed the basis of the two scenarios evaluated in Figure 7-5. The first scenario ("CFSTR Model with Biological Activity") was determined by best fit analysis of the model to the observed dataset, while the second scenario was similar to the first with the exception that the rate of biological consumption parameter (r_b) was equal to zero. The second scenario is entitled "CFSTR Model No Biological Activity".

The disparity between the "CFSTR Model No Biological Activity" and the observed dataset provides evidence of the presence of biological nitrogen consumption in the form of biological denitrification and/or heterotrophic cellular growth during this trial. Had the trial been conducted in the absence of the denitrifying bacteria, it would be expected that the nitrate concentration in reactor FBR1-1(d) at *t=7 days* would be approximately 9 mg/L NO_3^--N greater than observed (Table 7-4).

Table 7-4 Assessment of COD and Nitrate concentrations in FBR1-X(d)

	COD		NO_3^--N	
	FBR1-1(d)	FBR1-2(d)	FBR1-1(d)	FBR1-2(d)
At *t = 35 days* (mg/L)	22	28	1.6	1.3
Hydraulic Flushing Scenario at *t = 35 days* (mg/L) [#]	3.9	8.4	10.9	10.5
Idealised CFSTR Parameters				
r_b	11.66	13.10	2.92	3.28
k_s	6.03	6.00	-	-
r_s	-23.5	-22.7	-	-
c_s	274,200	274,200	-	-

[#] The assessment conducted in this scenario has excluded the effect of possible formation or biological consumption of COD and nitrate within the reactor.

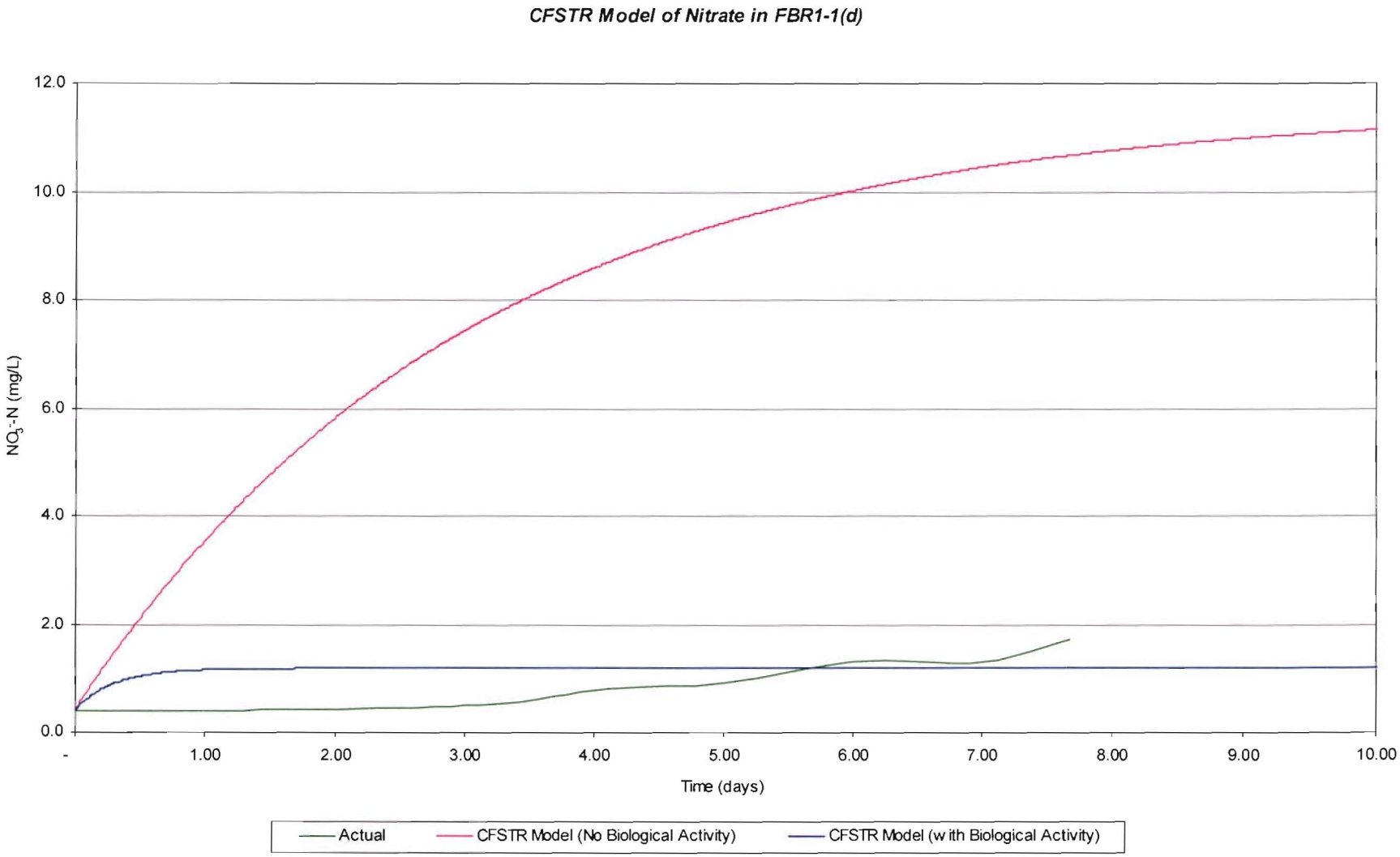

Figure 7-5 CFSTR model of the NO_3^--N concentration with in FBR1-1(d). Similar analysis on the lime-treated substrate reactor FBR1-2(d) showed a comparable result. By the end of this trial both reactors had significantly lower nitrate concentrations than the CFSTR Model No Biological Activity

evaluations would predict, as illustrated in Figure 7-5 and tabulated in Table 7-4.

While the two reactors presented similar denitrification rates (r_b), during the course of this trial the lime-treated reactor accumulated more nitrate within the reactor (Table 7-5), probably due to the slightly shorter HRT and higher nitrate dosage. However the rate of biological consumption of nitrate (r_b or denitrification) summarised in Table 7-4 demonstrates that the lime pretreated reactor (FBR1-2) denitrified at a greater rate.

Table 7-5 Rate of change of COD and nitrate concentrations for FBR1-X(d)

	COD (mg/L/day)		NO_3^--N (mg/L/day)	
	FBR1-1(d)	FBR1-2(d)	FBR1-1(d)	FBR1-2(d)
Period $(28 \le t \le 36)$	-8.62	-6.10	0.17	0.21

Both Figure 7-2 and Figure 7-3 revealed that as the COD concentration progressively declined during the trial, there was a corresponding increase in the rate of nitrate accumulation. It may be possible that as the COD concentration in the reactors became scarce, the biological process may have been stressed – resulting in the observed increase in the rate of nitrate accumulation within the reactors in the later stages of this series of trials.

7.2.2 Fluidised Bed Reactor – Series 2

During the course of the first set of trials, it was observed that the surfaces within the bioreactor and recycle tubing had discoloured and closer inspection revealed that the discolouration was a result of a thin layer of biofilm. The colour of the biofilm was identical to that of the biofilm growing on the substrate, thus it was most likely that the biofilm adhering to the bioreactor and tubing was the same bacteria adhering to the substrate.

The purpose of the second series of fluidised bed reactor trials was to evaluate the influence of biofilm growing within the inside surfaces of the FBR, diffusion and settling chamber, and recycle tubing. Understanding the effect of the bacteria adhering to the bioreactor surfaces would allow corrections to the actual process rates to be undertaken.

This series comprised two trials. In the first ($0 \le t \le 3$ days) the substrate was flushed from the reactor leaving only the biofilm adhering to the internal reactor surface. The reactors were

refilled with tap water and augmented with trace nutrients such that the initial chemical composition was similar to that outlined in Table 4-7. In this set of trials, continuous dosing was ceased and the reactors were operated in a batch mode. In the FBR2-1(x) trials both reactors were injected with sufficient nitrate to increase the reactor nitrate concentration to 100 mg/L (NO_3^--N).

In the second trial ($3 \leq t \leq 6.5$ days), both reactors were pulsed with 4.7 g of glucose. This equated to a reactor COD concentration of 421 mg/L, and 430 mg/L for FBR2-1 and FBR2-2 respectively. The purpose of this pulsing was to obtain an indication of the maximum denitrification rate, with no limitations on the biological process due to COD availability.

7.2.2.1 FBR2-X(a)

The reactors in this trial had an initial DO concentration in the order of 3 mg/L, which was readily consumed in the first 24hours of this trial. Thus, by day one, both reactors were in a DO-limited state (below 1 mg/L), hence in a state conducive to promote the denitrification.

In this trial the COD increase for both reactors was minor, 21 mg/L in three days for FBR2-1(a) and 18 mg/L for FBR2-2(a), as would be expected when no external source of COD was provided within the system. The standard error associated with the COD test was in the order ± 8 mg/L (APHA 1999), and since the observed increase in COD was in excess of this it indicates that the biofilms were releasing COD, which is due to possible degradation of the biofilm (Figure 7-6 and Figure 7-7). Table 7-6 shows that the net release of organic carbon was greater in the previously untreated reactor FBR2-1(a) during the first trial.

Table 7-6 Rate of change of COD and Nitrate+Nitrite Nitrogen concentrations for FBR2-X

Trial	COD (mg/L/day)		Tox-N (mg/L/day)	
	FBR2-1	FBR2-2	FBR2-1	FBR2-2
FBR2-X(a) $(0 \le t \le 3)$	6.98	5.96	-0.66	-2.67
FBR2-X(b) $(3 \le t \le 6.5)$	-61.1	-109	-16.0	-26.4

The previously lime treated reactor FBR2-2(a) consumed a greater concentration of nitrogen from the reactor, suggesting that the biofilm was degrading/releasing a greater quantity of COD than was consumed during the denitrification of the excess nitrate in this reactor. Aesoy et al. (1998) estimated that the COD:NO_3^--N ratio for denitrification was 4.5:1. Using this estimate, the calculations below suggest that the lime-treated reactor (FBR2-2) released approximately 95% more organic carbon from its biofilm than the untreated reactor.

FBR2-1(a)

Change in TN-N during this trial 2 mg/L

COD accumulated during this phase 21 mg/L

$$2\ \text{mg/L} \times 4.5 + 21\ \text{mg/L} = 30\ \text{mg/L}$$

$$30\ \text{mg/L} \times 11.4\ \text{L} = 342\ \text{mg}$$

FBR2-2(a)

Change in TN-N during this phase 9 mg/L

COD accumulated during this phase 18 mg/L

$$9\ \text{mg/L} \times 4.5 + 18\ \text{mg/L} = 58.5\ \text{mg/L}$$

$$58.5\ \text{mg/L} \times 11.4\ \text{L} = 667\ \text{mg}$$

Hence FBR2-2(a) released $\left(\frac{667mg - 342mg}{342}\right) \cdot \frac{100}{1} = 95.0\%$ more COD into solution

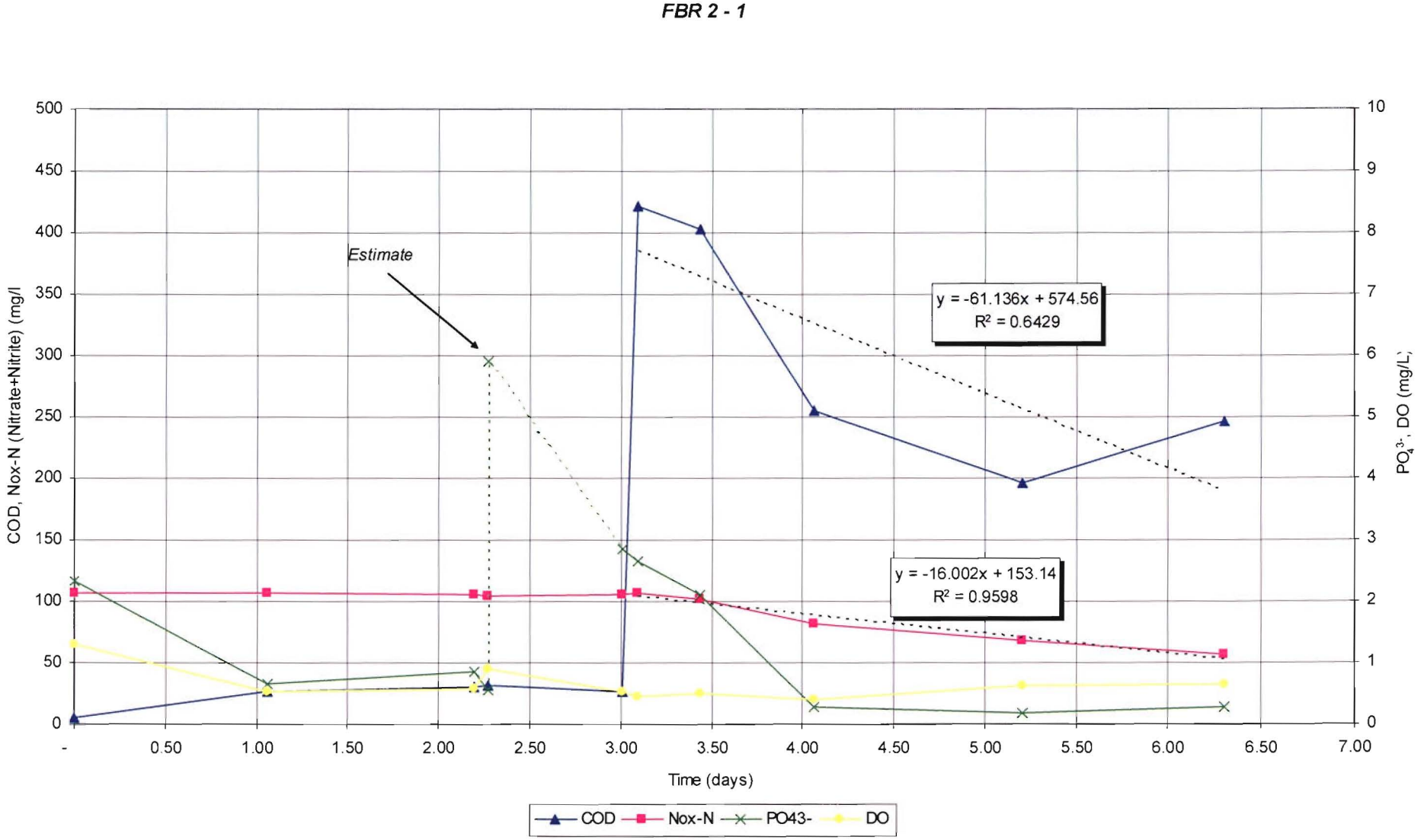

Figure 7-6 Denitrification Trial FBR2-1.

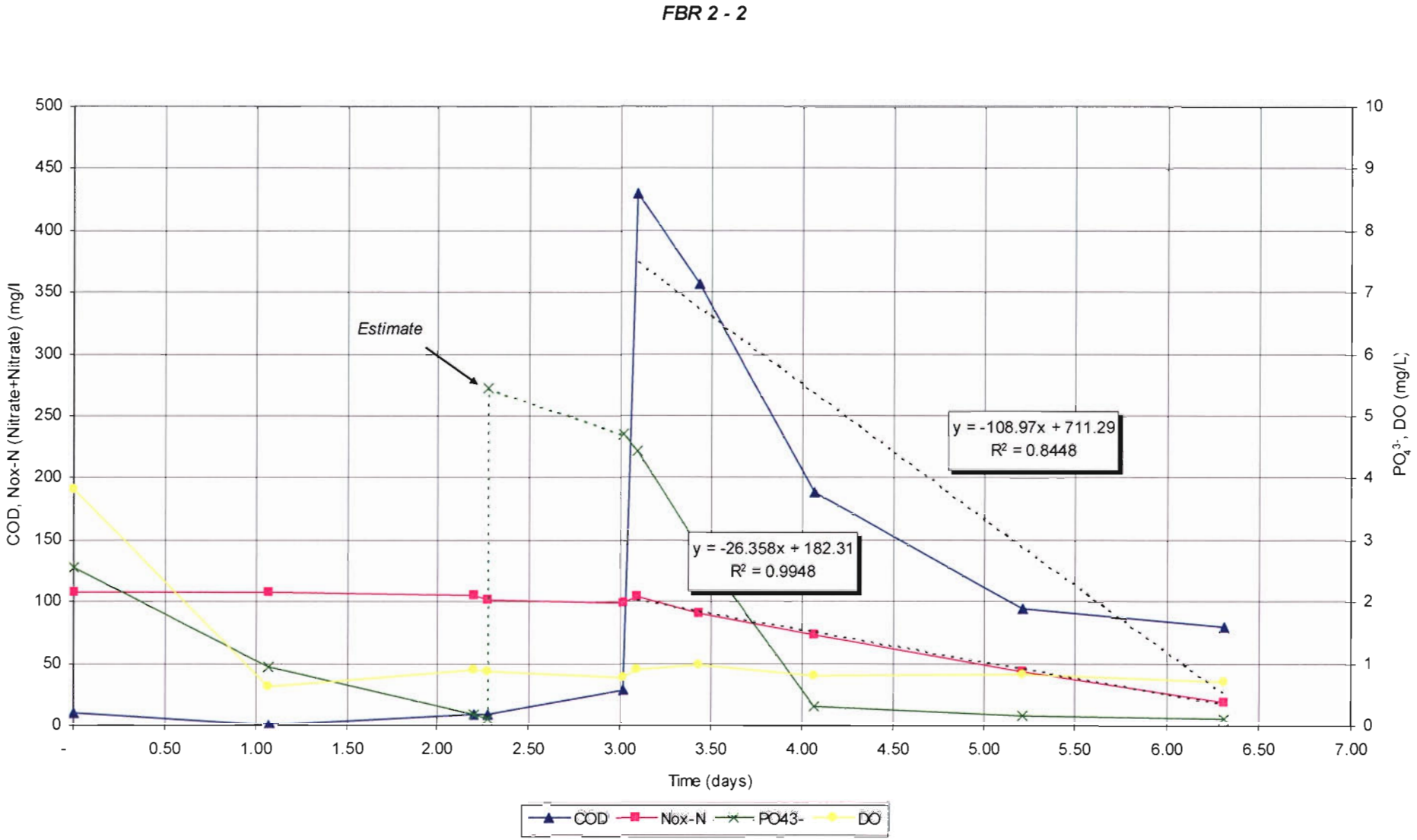

Figure 7-7 Denitrification Trial FBR2-2.

The net reduction in phosphate in Figure 7-6 and Figure 7-7 could suggest that some of the released organic carbon in the first phase was also utilised to build up energy (bio-P) reserves, or possibly some was consumed in the production of the new biofilm.

It should be noted that during day two an extra supplementary source of phosphate in the form of Na_2HPO_4 was injected into both reactors in order to overcome the lack of phosphate occurring within reactor FBR2-2. While these trials suggest that a significant decline in phosphate occurred between the time of injection and day three, no phosphate reading was taken immediately following the injection of the phosphate – rather, the data points (at t = 2.5 days) are calculated estimates of the phosphate concentration expected to be present in the reactors.

7.2.2.2 FBR2-X(b)

As indicated to earlier, 4.9 gms of glucose was injected into each reactor – resulting in the COD in the reactor increasing to approximately 400 mg/L. Immediately following the injection, a significant increase in the rate of denitrification was observed along with a complementary reduction in COD.

Assuming that the bacteria that constituted the biofilm were the same as the denitrifying bacteria that grew on the substrate/substratum in the FBR1-X trials, it follows that in an excess COD and nitrate environment the ratio between the COD and nitrate consumption rates would equate to the COD:NOx-N ratio for this group of bacterium, as calculated:

FBR2-1(b)	COD:NOx-N	3.83:1
FBR2-2(b)	COD:NOx-N	4.12:1
	Average	4.00:1

The calculated COD:NO_3^--N ratio above is very similar to the Christensson et al. (1994) and Æsoy et al. (1998) approximations, at 4.1 g COD/g NO_3^--N and 4.5 g COD/g NO_3^--N respectively. This suggests that glucose is a readily available and utilisable carbon source similar to other commonly utilised simple organic compounds like ethanol or methanol. Christensson et al. (1994) noted that ethanol was a more readily available carbon source for denitrification than methanol and though it was relatively short, this trial demonstrates that glucose appeared as equally readily available.

The fact that the bacteria readily consumed and denitrified immediately after the application of a pure glucose source tends to suggest that the bacteria were already acclimated to glucose. This means that the bacteria were liberating glucose-type molecules from the coconut shell fragments during the earlier series of trials (FBR1-X).

Table 7-6 indicates that the FBR2-2(b) reactor utilised the carbon source at a greater rate than FBR2-1(b). While the rate of nitrate utilisation during this trial was also greater for this reactor. The observed cloudy discolouration in these two reactors (Figure 7-8 and Figure 7-9) observed within the first 24 hours of the start of the FBR2-X(b) trials suggests an increase in biomass within each reactor. In reactor FBR2-1(b) the discolouration was iron-stained, while FBR2-2(b) remained cloudy white until day four, at which time the iron stain became evident. The formation of new bacterial flocs in suspension could to be the source of the observed cloudiness. While the iron discolouration may be due to possible oxidation of the pump mechanism (cast iron impeller and housing) since the remainder of the reactor pumping, tubing and valves were either constructed from stainless steel, glass, or plastic.

A visual increase in biomass within the reactors suggests that the glucose as well as the nitrate was used for the construction of new cells, and to maintain bacterial metabolic processes. The phosphate profiles in Figure 7-6 and Figure 7-7 indicate that all of the reactive phosphate was consumed in the first 48 hours of the trial consistent with the observed increase in biomass (i.e. the degradation of reactor clarity) within the reactors.

Figure 7-8 FBR2-1(b), after the addition of the glucose to the reactor.

The COD increase in FBR2-1(b) from day 5.25 to day 6.25 tends to suggest that the biomass was experiencing a greater rate of cell die-off than cell production and the rise in reactive phosphate during this period supports this hypothesis.

Visual evidence of denitrification occurring within these reactors is shown in Figure 7-9 as minute gas bubbles were observed to form within a few hours of these trials. The accumulation of these bubbles formed a frothy scum on the top of the reactor. A similar occurence was observed in Reactor FBR2-1(b).

Figure 7-9 FBR2-2(b) with foam at the top of the settling chamber.

7.2.3 Fluidised Bed Reactor – Series 3

The biomass from the previous trials FBR2-X was flushed from the reactors and all of the reactor components and tubing were thoroughly cleaned with high-pressure water to dislodge any remaining biomass from the test equipment prior to its reuse. The substrate and inoculum were added to the reactor and augmented with tap water (Table 4-7), then left to acclimate for 24 hours prior to the start of the first series of this next set of trials.

It was intended that each reactor would experience two trials in this series; however, a miscalculation of the remaining influent volume resulted in the reactors running out of influent feed at the end of the first trial (as illustrate in the dosage profile in Figure 7-10 and Figure 7-11). The result was that the reactor was supplied air instead of influent. As a consequence three distinct nitrate loaded regimes exist, FBR3-X(a) and FBR3-X(c) with nitrate dosing, and FBR3-X(b) without.

7.2.3.1 FBR3-X(a)

The FBR3-X profiles shown in Figure 7-10 and Figure 7-11 indicate that while the FBR3-X(a) nitrate dosage (1.6 mg/hr) resulted in a slight (0.25 mg/L NO_3^--N) accumulation of nitrate, the bacteria within the reactor effectively consumed all the dosed nitrate.

The COD profiles show complete consumption of the initial COD within 24 hours of the start of the trial, not unexpected as at the start of the trial the initial COD concentration was only 8 mg/L and 10 mg/L for FBR3-1(a) and FBR3-2(b) respectively. A positive outcome was the sudden increase in COD noted for both reactors during the course of the next two days with the COD concentration in both reactors ultimately peaking at about this time (t=3 days) at 26 mg/L in reactor FBR3-1(a) and 32 mg/L (t=5 days) in reactor FBR3-2(a).

A CFSTR assessment of the COD and nitrate profiles within these reactors is shown in Table 7-7 which demonstrates that while hydraulic flushing processes may be dominant, other processes were present within this reactor that contributed to the observed decline in nitrate within both reactors. The greater than predicted reactor COD concentration at t = *10* days, indicates that biological hydrolysis was present in both reactors.

Table 7-7 Assessment of COD and Nitrate concentrations in FBR3-X(a)

	COD		NO_3^--N	
	FBR3-1(a)	FBR3-2(a)	FBR3-1(a)	FBR3-2(a)
At t = *9 days* (mg/L)	27	24	1.3	2.2
Hydraulic Flushing Scenario at t = *9 days* (mg/L) [#]	2.0	2.0	15.5	16.2
Idealised CFSTR Parameters				
r_b	8.03	5.74	2.01	1.43
k_s	7.56	7.13	-	-
r_s	46.4	47.0	-	-
c_s	274,200	274,200	-	-

[#] The assessment conducted in this scenario has excluded the effect of possible formation or biological consumption of COD and nitrate within the reactor.

Both reactors quickly became DO-limited (within three to four hours), indicating that the biological process had quickly consumed the available initial DO within the reactor. The DO concentration was consistently below the 1 mg/L threshold identified (by Gayle et al., 1989 [1.62 mg/L] and Trivedi and Weir (2004) [1 mg/L]) as a requirement for the occurrence of denitrification processes. While the DO concentration remained constant throughout this period, the reactor with the untreated substrate had a lower average concentration (0.54 mg/L) during this trial compared to FBR3-2(a), which had an average DO concentration 0.85 mg/L. The slightly higher DO in the FBR 3-2(a) trial may have contributed to the slight increase in nitrate (0.1 mg/L NO_3^--N) in the effluent.

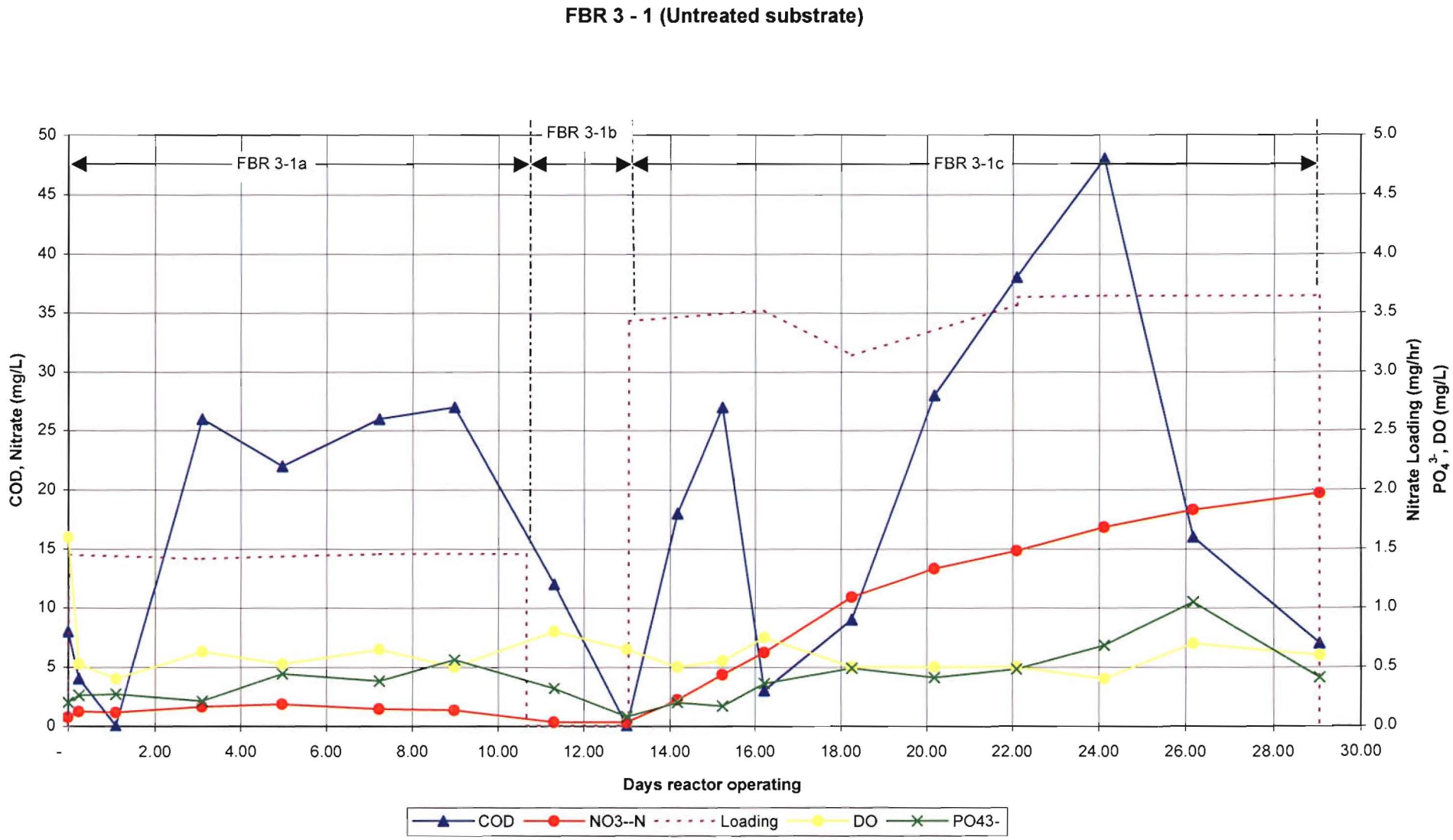

Figure 7-10 Denitrification Trial FBR3-1 for the untreated substrate.

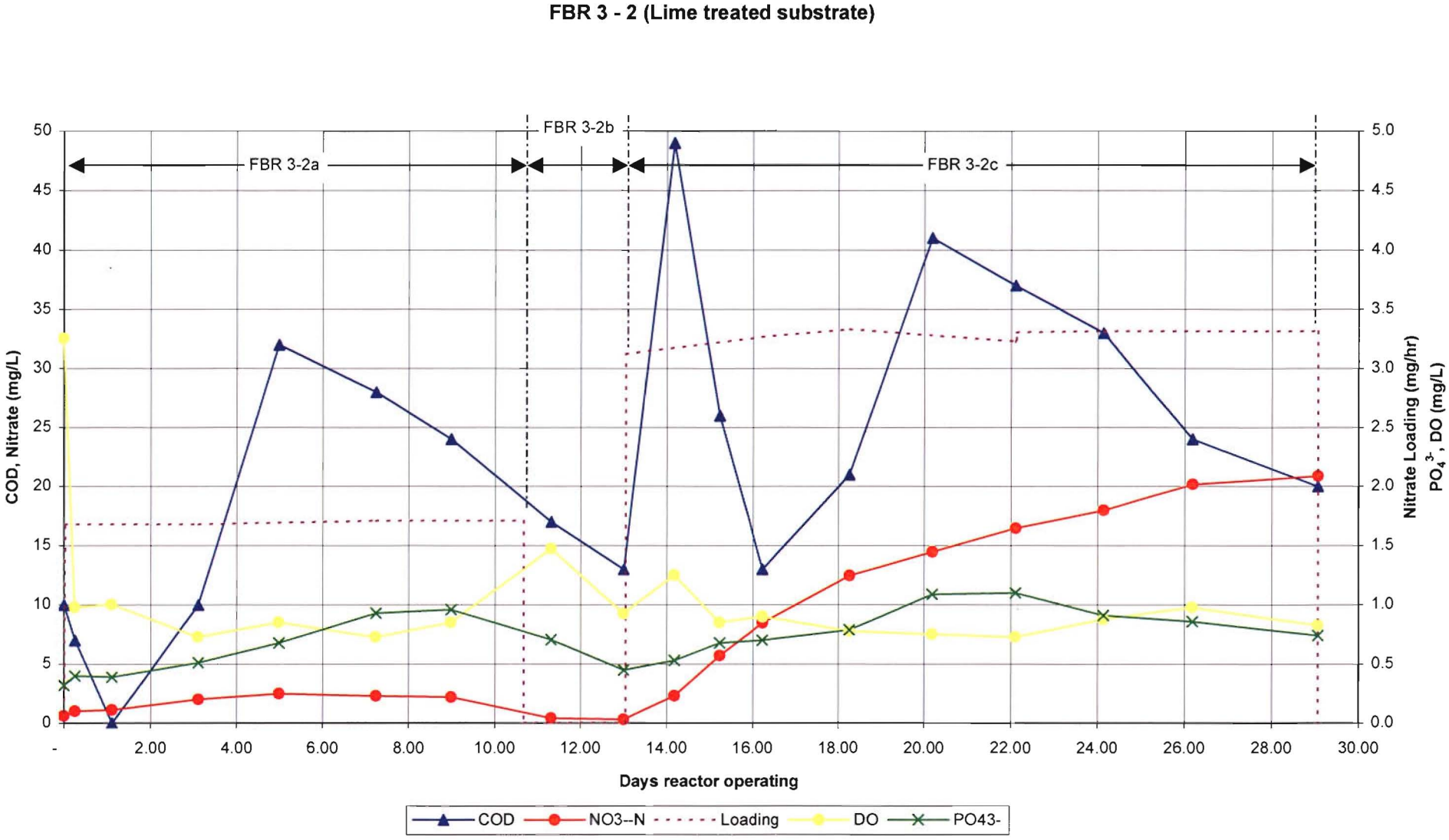

Figure 7-11 Denitrification trial FBR3-2, for the lime treated substrate.

The major difference between the two reactors was that the lime-treated reactor showed a declining COD concentration after the initial peak at day 5, while the untreated reactor's concentration remained static throughout the remainder of this trial. Other parameters such as nitrate showed similar trends between the reactors. This difference in the COD profiles suggests that the biological processes within the lime-treated substrate were unable to produce/release organic carbon in sufficient quantities to meet the requirement of the biomass. This could be due to either limitations in enzyme production or prior hydrolysis of the lime-treated substrate had consumed all the available glucose/cellulose sites.

7.2.3.2 FBR3-X(b)

The miscalculation in the remaining influent volume meant that for a period of 6 hours the dosage pumps were slowly pumping air into the reactors, at a rate of 0.073 and 0.085 L/hour for FBR3-1(b) and FBR3-2(b) respectively. At which time the influent dosage pumps were turned off, and the reactors left for 48 hours.

It is possible that a large proportion of the oxygen in the air would diffuse into the fluid. That is, since the influent gas entered the reactor prior to the recycle pump, the centrifugal pump action effectively distributed the air into minute bubbles within the flow. The minute bubbles in conjunction with the 2200 mm reactor height and the high rate of recycle provides significant opportunity for diffusion.

Normally the molecular dissolved air diffusion from a gas to liquid phase is modelled via Lewis and Whitman's (1924) two-film theory for gas transfer. However, the very low rate of aeration and the presence of facultative denitrifying bacteria resulted in a modest increase in DO within the reactors, from an average of 0.68 mg/L to 1.14 mg/L.

The following calculations provide an estimate of the DO transferred into the liquid phase.

The typical SOTE (standard oxygen transfer efficiency) for fine bubble diffusion is in the order of 3%/ft or 9.9%/m (US EPA, 1989). Since the high internal recycle captures the minute bubbles, the SOTE calculations have to compensate for the oxygen transfer as a result of the multiple passes through the reactor column. Thus:

SOTE for 1st Pass

$$\text{Reactor depth (m)} \times \text{SOTE (\%/m)} = 2.2\text{m} \times 9.9\%/\text{m} = 21.8\%$$

SOTE for 2nd Pass

It was observed and estimated that 70% of the minute air bubbles are recycled, hence:

$$\text{Air flowrate recycled (\%)} \times \text{Relative } O_2 \text{ concentration (\%)} \times \text{Reactor depth (m)} \times \text{SOTE (\%/m)}$$

$$= 70\% \times (100\% - 21.8\%) \times 2.2\text{m} \times 9.9\%/\text{m} = 11.9\%$$

e.t.c. as summarised in Table 7-8.

Table 7-8 FBR3-X(b) Aeration SOTE Evaluation

Pass #	Air flowrate	Relative O_2 []	SOTE (%)
1	100%	100%	21.8%
2	70%	78%	11.9%
3	49%	66%	7.1%
4	34%	59%	4.4%
5	24%	55%	2.9%
6	17%	52%	1.9%
7	12%	50%	1.3%
8	8%	49%	0.9%
9	6%	48%	0.6%
10	4%	47%	0.4%
		Total SOTE %	53.1%

From Table 7-8, 53.1% of the oxygen supplied is estimated the oxygen that would diffuse into the liquid phase. From the partial pressure of oxygen at one atmosphere (Table 7-9) and applying Eqn. 7-2.

Table 7-9 Constituents of Air (Snoeyink & Jenkins, 1980)		
Chemical	% by Volume	Partial pressure (of 1 atm)
N_2	78.1 %	0.781 atm
O_2	20.9 %	0.209 atm
Other gases: $H_2O_{(g)}$, CO_2, Ar etc.	1.0 %	0.010 atm

The ideal gas equation is defined as:

$$PV = nRT \text{ or } n = \frac{PV}{RT}$$

Eqn. 7-2

Where

P Pressure (or partial pressure) (atm)

V Volume (L)

n Number of moles

R Gas constant, 0.082 L.atm.K^{-1}. mol^{-1}

T Temperature (K)

Evaluating the situation outlined above, where: P = 0.209 atm, V = 0.438 L (6hrs @ 0.073L/hr), $T = 35^{\circ}C + 273.15 = 308.2^{\circ}K$ we get:

$$n = \frac{0.209 \times 0.438}{0.082 \times (35 + 273.15)} = 3.62 \times 10^{-3} \text{ moles}$$

or

$$3.62 \times 10^{-3} \times 32 = 0.1158 \text{ gms of oxygen supplied}$$

assuming 53.1% diffusion, this would equate to a raise in the DO concentration within the reactor of:

$$\frac{0.1158}{11.4} \times \frac{53.1}{100} \times 1000 = 5.4 \text{ mg/L}$$

The calculation above indicates that the air dose had the potential to inject 5.4 mg/L of O_2 into the reactor during the 6-hour period. At this rate, denitrification would cease, yet it was observed that during this period at least 0.25 mg/L of nitrate had been consumed in both reactors. The actual DO response in these reactors was a 0.3 mg/L of DO raise in FBR3-1(b) resulting in a 0.8 mg/L DO concentration at day 11. FBR3-2(b) had a 0.625 mg/L DO increase, resulting in a 1.475mg/L DO concentration at day 11.

To explain the discrepancy it must be remembered that the dosage regime, controlled by the PLC, dosed the reactor for 10 minutes every hour.

Each of the 10-minute doses of air equates to a maximum possible increase in the reactor DO concentration of $\frac{5.4\,\text{mg/L}}{6\,\text{hours}} = 0.9\,\text{mg/L}$ every hour. While the reactor DO concentration is less than 1.0 mg/L, some inhibition of the denitrification process would occur until the DO was consumed

With a greater quantity of more readily consumable terminal electron acceptors (O_2) provided, it is thought that a complementary increase in heterotrophic growth would occur. The hypothesis is supported by the observed increase in organic consumption, especially in FBR3-1(b), where a noticeable decline in COD within the reactor was observed. Corresponding to a slight increase in the DO during this period, compared to FBR3-2(b).

Both reactors showed a decline in NO_3^--N and PO_4^{3-} concentrations during this period, supporting the above hypothesis that the increase in oxygen within the reactor promoted heterotrophic growth and resulted in the observed increase in COD, NO_3^--N and PO_4^{3-} utilisation in the formation of new cells. It is thought that the oxygen-induced biomass growth resulted in nitrate becoming the limiting nutrient for heterotrophic growth, hence the observed accumulation of DO within the reactor at day 13.

At day 11 the dosage pumps were switched off and the reactors left operating in a fluidised state for the following two days, which allowed the two reactors to stabilize the nitrate and DO concentrations before the start of the next set of trials FBR3-X(c).

7.2.3.3 FBR3-X(c)

The third loading regime in this series had a higher influent nitrate concentration (32.5 mg/L) and dosage flow rate (0.105 L/hr) than the FBR3-X(a) trials (with 20.1 mg/L and 0.076 L/hr). This corresponded to an average nitrate load for this set of trials of 3.4 mg/hr. The increased nitrate loading resulted in a typical CFSTR response curve for the nitrate profile in both reactors (Figure 7-10 and Figure 7-11).

The DO and PO_4^{3-} concentration during the trials FBR3-1(c) and FBR3-2(c) are in the range conducive to the denitrification process. However, the PO_4^{3-} gradually increased during this trial until day 26, consistent with the CFSTR dosing with a 3 mg/L influent, and assuming no biological consumption.

Both reactors, however, showed a decline in the reactor PO_4^{3-} concentration near the end of these trials. For FBR3-1(c) the decline occurred at t = 26 days, while for FBR3-2(c) it occurred several days earlier at t = 22 days. The transition from accumulating PO_4^{3-} to reducing PO_4^{3-} concentration phase coincides with a similar transition in the COD concentration.

The COD profile in both FBR3-X(c) trials exhibit four separate phases. The first is the sudden increase in the rate of COD accumulation after the start of the dosage. The duration of this phase varied from one day for FBR3-2(c) to two days for reactor FBR3-1(c). The second phase is that of an equally sudden decline in COD within the reactor, thought to be due to the resumption in biological activity and COD consumption outstripping the organic carbon release within this phase. The rate of decline was similar to the rate of accumulation in the first phase. In this phase 24 mg/L/day of COD was consumed in FBR3-1(c), and 17.7 mg/L/day in FBR3-2(c). The third and fourth phases mirrored the response observed in phases one and two of COD accumulation and then decline. However, the duration was greater for these later phases and hence the rate of accumulation and decline was slightly less.

It is not obvious why these reactors repeated the accumulation/decline phases, but the rate of COD accumulation in both reactors during the third phase was similar: 5.68 mg/L/day for FBR3-1(c), and 7.10 mg/L/day for FBR3-2(c). The duration of phase 3 for FBR3-1(c) at 8 days was twice that of FBR3-2(c). Both reactors ceased accumulating COD once the concentration surpassed the 40 mg/L threshold. At this time it is thought the biomass was

consuming the COD at a rate greater than that produced from enzymatic hydrolysis. In the fourth phase FBR3-1(c) had a greater consumption, which, in conjunction with the similar rate of COD accumulation in the earlier phase, would indicate that the rate of biological activity was greater in this reactor.

While the presence of active bacteria within these reactors had been demonstrated during this set of trials, the rate of denitrification exhibited was unable to fully utilise the entire nitrate provided in the influent. As a consequence, nitrate accumulated; surprisingly, the rate of accumulation was identical for both reactors at an average rate of 1.3 mg/L/day. By the end of the trial (at day 29) the eventual reactor concentration in both reactors was 20 mg/L.

A CFSTR assessment of the nitrate concentration in Reactor FBR3-2(c), as graphically represented in Figure 7-12, demonstrated that if no biological activity were present in the reactor, then at the end of the trials (day 29 actual, or day 16 in Figure 7-12) the reactor nitrate concentration would be approximately 31.6 mg/L (cf. actual 20.9 mg/L). Tabular observations of this assessment are included in Table 7-10.

Table 7-10 Assessment of COD and Nitrate concentrations in FBR3-X(c)

	COD		NO_3^--N	
	FBR3-1(c)	FBR3-2(c)	FBR3-1(c)	FBR3-2(c)
At t = *26 days* (mg/L)	16	24	18.3	20.2
Hydraulic Flushing Scenario at t = *26 days* (mg/L) [#]	1.05	3.69	30.2	30.4
Idealised CFSTR Parameters				
r_b	0.816	0.599	0.204	0.150
k_s	5040	6227	-	-
r_s	-3100	1838	-	-
c_s	274,200	274,200	-	-

[#] The assessment conducted in this scenario has excluded the effect of possible formation or biological consumption of COD and nitrate within the reactor.

This discrepancy supports the earlier observation that biological activity was present. The CFSTR model suggests that the rate of the denitrification induced by the bacterial could be described simplistically by the following equation, where the co-efficient r_b defines the rate of biological consumption:

$$V\frac{dc}{dt} = -Vr_b c$$

Eqn. 7-3

As both reactors exhibited similar accumulation profiles, they presented the same value for the biological consumption coefficient, $r_b = 0.15$ day^{-1}.

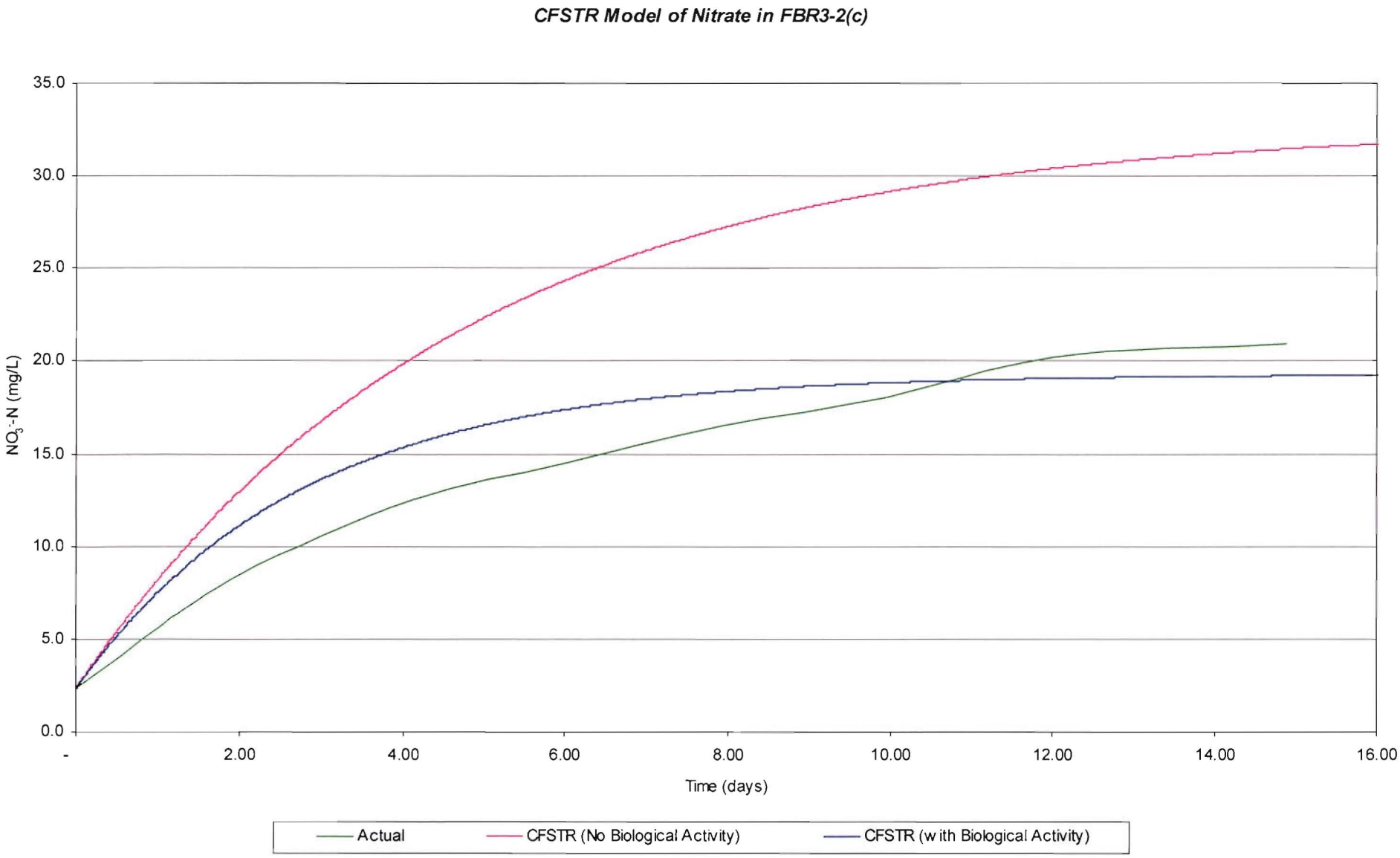

Figure 7-12 CFSTR assessment of the nitrate concentration within FBR 3-2(c).

7.2.4 Fluidised Bed Reactor – Series 4

This series of trials was conducted with new substrate, thus the biomass from the previous trials FBR3-X was flushed from the reactors and all of the reactor components and tubing were thoroughly cleaned with high-pressure water to dislodge any remaining biomass from the test equipment prior to the addition of the new substrate. Like the earlier FBR trials, each reactor contained 2.14 kg (dry weight) of coconut shell fragments and Reactor 2 used lime-pretreated coconut shell fragments.

The substrate was added to both reactors on the 14th July 2000 (t = -10 days), and was left in a fluidised state until the 18th July (t = -6 days) at which time bacteria was injected into the reactors. At the same time, the reactor was pulsed with nitrate (such that the initial concentration within both reactors was 100 mg/L), cycloheximide, phosphate, and nutrients (as per Table 4-6). By the start of the trial (t = 0 days), on the 24th July 2000, the initial nitrate concentration was 47.5 mg/L and 0 mg/L for Reactor 1 and 2 respectively. This indicated that denitrification had occurred during the previous six days, but at a faster rate within FBR4-2.

This series comprised a set of three trials, in which the hydraulic loading was constant during the three trials. However, the nitrate loading varied during the course of the trial from 3.4 mg/hr to 5.6 mg/hr this was because in the earlier series of trials it became apparent that the flushing characteristics of the influent strongly influenced the performance of the reactor, often resulting in the injection of excess nitrate while flushing out organic carbon.

7.2.4.1 FBR4-X(a)

The FBR4-X profiles in Figure 7-13 and Figure 7-14 show that both reactors have a significant initial COD concentration at the start of the trials. It should be noted that five days earlier (Table 7-11), the COD concentration within both reactors was less than that observed at t = 0 days. This increase in COD is thought to be due to biologically induced release of organic carbon. During the course of the trial, the COD concentrations progressively declined such that at day 10 the concentrations were 44 mg/L and 130 mg/L for Reactor 1 and 2 respectively.

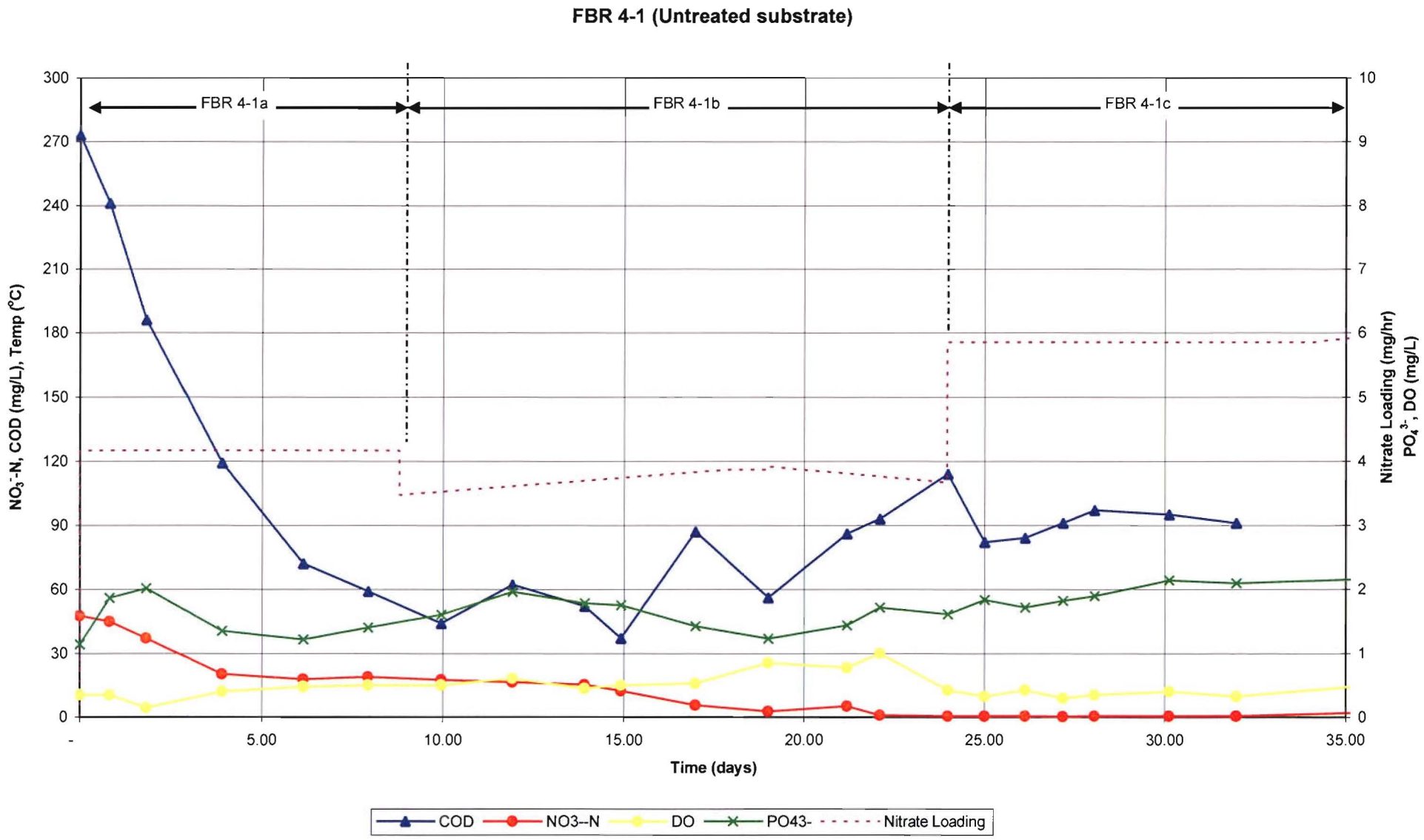

Figure 7-13 Denitrification Trial FBR4-1, for the untreated substrate.

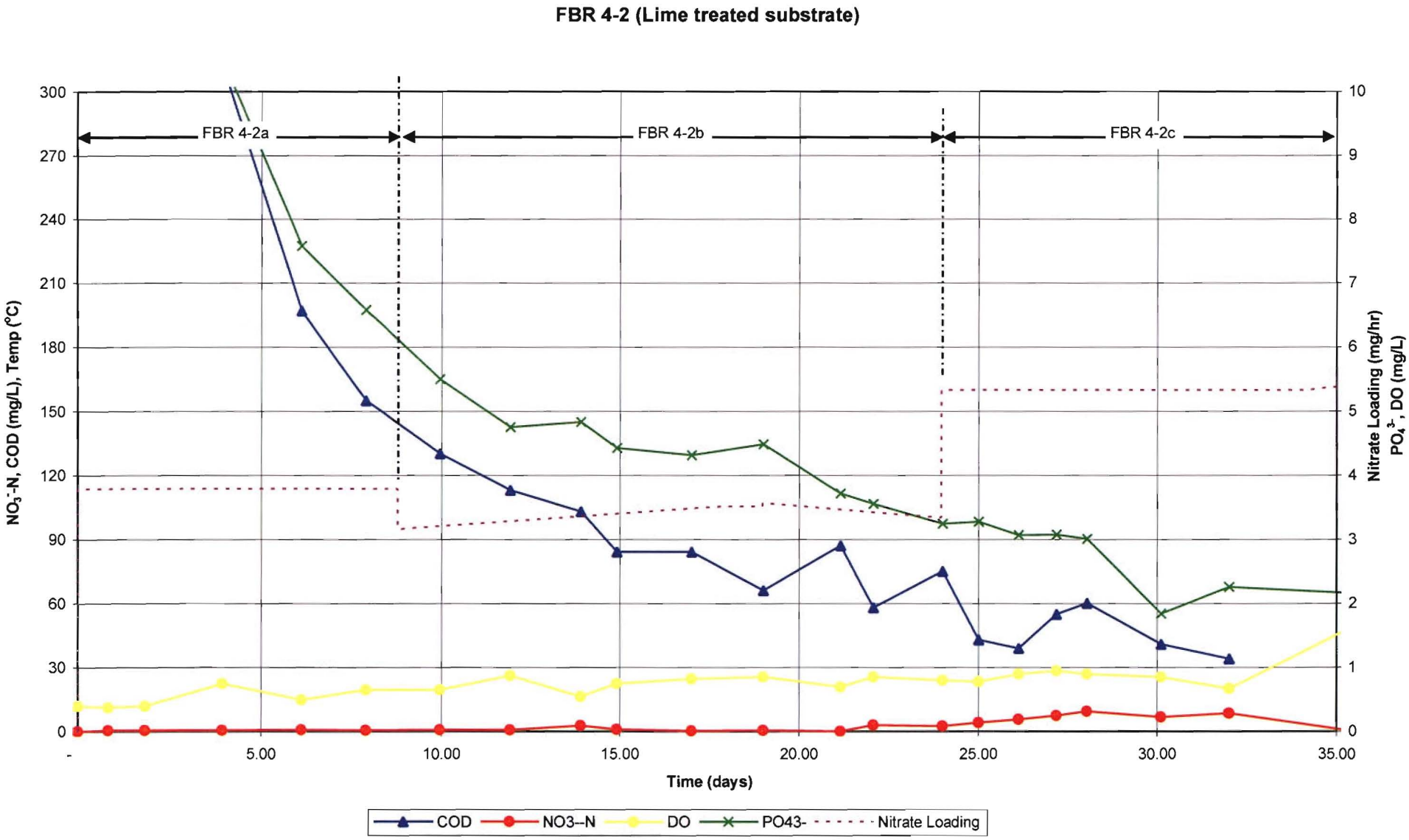

Figure 7-14 Denitrification Trial FBR4-2, for the Lime treated substrate.

Table 7-11 demonstrates that while minimal nitrate was present in FBR4-2 at *t = -5 days*, substantial COD accumulated in this reactor between *t = -5 days* and *t = 0 days* (an increase in 224 mg/L was recorded). Since no nitrate or DO is present, then it follows that the COD gain was due to shedding of the organic carbon from the previously lime-treated substrate.

Table 7-11 Change in COD, NO_3^--N, and PO_4^{3-} Concentrations during FBR4-X trial

	FBR4-1			FBR4-2		
	COD (mg/L)	NO_3^--N (mg/L)	PO_4^{3-} (mg/L)	COD (mg/L)	NO_3^--N (mg/L)	PO_4^{3-} (mg/L)
t = -6 days*	182			512		
t = -5 days	229	95		378	3.5	
t = 0 days	273	47.5	1.14	602	0	18.0 #
t = 6 days	72	17.7	1.21	197	0.6	7.58
t = 10 days	44	17.5	1.6	130	0.7	5.5

* Inoculum added to reactor.

This excessively high initial concentration is thought to be due to a laboratory error during establishment of the reactor in which 10x the required PO_4^{3-} was mistakenly added.

During this trial, nitrate was dosed at a rate of 4.2 mg/hr and 3.8 mg/hr for Reactor 1 and 2 respectively, a dose insufficient to result in an accumulation of nitrate within the reactors. FBR4-1(a) started with an initial NO_3^--N concentration of 47.5 mg/L, and by the end of this trial the NO_3^--N concentration was 17.7 mg/L, whereas FBR4-2(a) remained in the order of 0.5 mg/L throughout the trial.

This trial was operated for over two HRT cycles. In this time if the reactor was operating as an ideal CFSTR reactor where only the hydraulic flushing characteristics were present (i.e. assume that hydrolysis or biological utilisation was not present), then as Table 7-12 summarises, the COD concentration at *t=10 days* would be approximately 88% of the initial COD would be flushed from the reactor, which would equate to approximately 247 mg/L and 531 mg/L from Reactor 1 and 2 respectively (as the calculations below indicate).

FBR4-1(a)

COD at *t=0 days* 273 mg/L

COD at *t=10 days* 26 mg/L

Difference 247 mg/L or 90.4% hydraulically flushed from the reactor

FBR4-2(a)

COD at *t=0 days* 602 mg/L

COD at *t=10 days* 71 mg/L

Difference 531 mg/L or 88.8% hydraulically flushed from the reactor.

As the actual COD concentration in both reactors was greater than the hydraulic flushing model predicts, it follows that both COD hydrolysis and biological consumption of the organic carbon must be present. It also follows that during this trial both reactors released greater quantities of organic carbon (due to hydrolysis) than were consumed due to biological processes.

Since the reactor was consuming nitrate, implicitly it follows that any biological processes would be consuming organic carbon.

Table 7-12 Assessment of COD and Nitrate concentrations in FBR4-X(a)

	COD		NO_3^--N	
	FBR4-1(a)	FBR4-2(a)	FBR4-1(a)	FBR4-2(a)
At t = *8 days* (mg/L)	44	130	17.5	0.7
Hydraulic Flushing Scenario at t = *8 days* (mg/L) [#]	26	70	39	33
Idealised CFSTR Parameters				
r_b	1.16	58.3	0.29	14.7
k_s	4.83	4.29	-	-
r_s	-24.9	-0.77	-	-
c_s	274,200	274,200	-	-

[#] The assessment conducted in this scenario has excluded the effect of possible formation or biological consumption of COD and nitrate within the reactor.

As summarised in Table 7-12, FBR4-2(a) exhibited a greater biological (r_b) consumption rate of both COD and nitrate. For the purposes of this assessment, the rate of biological nitrate consumption was evaluated directly from the actual nitrate profile(s), while the biological COD consumption was assumed to be approximately 1.3 times the nitrate consumption rate (as outlined in Section 7.2.2.1).

Due to the greater COD demand to maintain denitrification in FBR4-2(a), it follows that a higher rate of COD release/hydrolysis was present and hence modelled in the CFSTR analysis. As a consequence, the FBR4-2(a) reactor had a greater r_s value than FBR4-1(a).

The high PO_4^{3-}-P concentration in FBR4-2 was as the result of experimental error in which 10mL of 30 g/L of stock phosphate solution was injected into the reactor during the establishment of the trial, instead of the required 1mL. This is consistent with the initial PO_4^{3-}-P concentration measured at *t=-6 days* of 26.3 mg/L compared to the anticipated 3 mg/L . The decay profile is indicative of hydraulic flushing from the reactor.

7.2.4.2 FBR4-X(b)

This trial can be considered an extension of the FBR4-X(a) as the influent flow rate was identical to the earlier set of trials. The only difference between these trials is that this set was dosed at a slightly lower nitrate concentration rate (34.8 mg/L of NO_3^--N instead of 37.5 mg/L). While this difference in FBR4-1(b) was unintentional, the slightly lower nitrate dose resulted in an interesting phenomenon.

While the hydraulic and nitrate loading for these two reactors was similar, the chemical parameter profiles in Figure 7-13 and Figure 7-14 show different responses to the change in influent nitrate concentration.

The reactor with the untreated substrate, FBR4-1(b), showed a gradual recovery in the COD concentration during this trial. During the 14 days, the COD concentration in the reactor increased from 44 mg/L to 114 mg/L, while the COD in the reactor with lime-treated substrate, FBR4-2(b), continued to decline from 130 mg/L to 43 mg/L at the end of the trial (t= 24 days).

The nitrate concentration in FBR4-1(b) was totally consumed during this trial. While the initial nitrate concentration was not large (17.5 mg/L), by the 10th day (t=19 days) of the trial the reactor concentration was practically zero. This corresponded to the period in which the reactor accumulated COD and suggests that the biological processes present in the reactor were fully using the nitrate. However, the rate of COD hydrolysis must have been in excess of the biological and hydraulic flushing requirements since the COD accumulated.

In the lime-treated reactor FBR4-2(b), the nitrate concentration was effectively zero throughout the trial, indicating that the biological process may have been limited by the lack of nitrate. The CFSTR assessment of the trial indicates that the rate of COD loss was less than would be expected if only hydraulic flushing were present (Table 7-13).

The phosphate profiles for the two reactors show the same characteristics as the FBR4-X(a) trials. That is, FBR4-1(a) remained static around 1.61 mg/L, while FBR4-2(b) gradually declined from 5.50 mg/L to 3.55 mg/L consistent with CFSTR flushing.

The CFSTR model assessment (Table 7-13) of the COD and nitrate profiles for both reactors showed that FBR4-2(b) has the greater denitrification rate since its r_b is greater than FBR4-1(b). Correspondingly FBR4-2(b) required greater quantities of COD biologically; however, the CFSTR assessment determined that even though this substrate was releasing a greater quantity of COD than FBR4-1(b), the biological requirement in conjunction with the hydraulic flushing contributed to the observed COD decline.

Table 7-13 Assessment of COD and Nitrate concentrations in FBR4-X(b)

	COD		NO_3^--N	
	FBR4-1(b)	FBR4-2(b)	FBR4-1(b)	FBR4-2(b)
At t = *24 days* (mg/L)	114	75	0.4	2.4
Hydraulic Flushing Scenario at t = *24 days* (mg/L) [#]	2	6	34	33
Idealised CFSTR Parameters				
r_b	3.48	20	0.87	5
k_s	14.3	22.8	-	-
r_s	69.2	-36.6	-	-
c_s	274,200	274,200	-	-

[#] The assessment conducted in this scenario has excluded the effect of possible formation or biological consumption of COD and nitrate within the reactor.

7.2.4.3 FBR4-X(c)

The two reactors in this set of trials had hydraulic loads identical to the earlier trials; however, the influent nitrate concentration was approximately 50% greater than the earlier set of trials, increasing the nitrate loading to an average of 5.5 mg/hr. However, the nitrate dose was insufficient as a nil increase in nitrate concentration within reactor FBR4-1(c) was observed, while FBR4-2(c) showed a minor increase in nitrate concentration to 6.5 mg/L.

The COD concentrations in both reactors during this trial plateaued. FBR4-1(c) experienced a 32 mg/L drop in COD during the first 24 hours after the new nitrate loading but recovered 10 mg/L before settling on 90 mg/L. The COD concentration in FBR4-2(c) continued to decline, eventually reaching an average concentration within the reactor of 34 mg/L (Table 7-14).

The COD profile in the FBR4-2(c) trial indicates that the biomass within the reactor was capable of denitrifying the nitrate loading; however, the rate of COD released from the substrate would be insufficient to maintain this denitrification rate, as indicated by the declining COD profile throughout this series of trials. This observation matches the CFSTR assessment summarised in Table 7-14.

The phosphate concentrations at the end of these trials were similar at around 2.10 mg/L. FBR4-2 started this series with an extraordinarily high phosphate concentration (18 mg/L). However the high concentration in phosphate was primarily flushed from the reactor, consistent with results that a CFSTR model would predict.

In Table 7-14, the idealised CFSTR parameters indicate that unlike the previous trials the untreated substrate reactor, FBR4-1(c), was denitrifying at a greater rate than that of the lime-treated substrate reactor and consuming a greater quantity of organic carbon. However, this reactor did not demonstrate a major decline in COD, suggesting that the rate of COD hydrolysis matched the biological consumption and hydraulic flushing.

Table 7-14 Assessment of COD and Nitrate concentrations in FBR4-X(c)

	COD		NO_3^--N	
	FBR4-1(c)	FBR4-2(c)	FBR4-1(c)	FBR4-2(c)
At t = *32 days* (mg/L)	91	34	0.4	8.5
Hydraulic Flushing Scenario at t = *32 days* (mg/L) [#]	17	13	45	44
Idealised CFSTR Parameters				
r_b	80.4	5.2	20.1	1.3
k_s	17.8	39.7	-	-
r_s	9.8	-129	-	-
c_s	274,200	274,200	-	-

[#] The assessment conducted in this scenario has excluded the effect of possible formation or biological consumption of COD and nitrate within the reactor.

A comparison of the CFSTR assessments of the trials conducted in this series indicates the untreated substrate reactor, FBR4-1(c), demonstrated the greatest ability to denitrify and also appeared to release the greatest amount of organic carbon in this series. This apparent and sudden increase in COD release and denitrification was inconsistent with the earlier results for that reactor in this series, suggesting that the constant nitrate concentration in the reactor may not be entirely due to denitrification. Given that no other cause has been identified which could have contributed to the increased nitrate consumption, the conclusion drawn from the CRSTR assessment FBR4-1(c) may be unreliable.

7.2.5 Fluidised Bed Reactor – Series 5

This series began on the 9th October 2000, 42 days after the completion of the FBR4-X trials. During this down-time, the substrate was left in the reactor in a submerged yet settled state (i.e. no recycle nor dosage). Prior to re-establishment, the substrate was removed from the reactor to allow for cleaning and minor maintenance. Like the previous reactors, the substrate, nitrate and nutrients, and inoculum were added to the reactors and left to acclimate for four days before the start of the next series of trials.

The nutrient profiles of the two reactors in this trial are presented in Figure 7-15 and Figure 7-16. The results of these trials and figures below are discussed in further detail in the following sections.

7.2.5.1 FBR5-X(a)

A problem occurred with Reactor 2 during cleaning prior to the start of this reactor trial, in which the recycle line mounting on the settling chamber was cracked. However, the mounting did not break until the re-establishment of the reactor. Repairs delayed the start of the FBR5-2(a) trial until the 16th October 2000. Reactor 1 continued to operate in the time proceeding, as the results in Figure 7-15 suggest.

FBR5-1(a) operated for 16 days from $t = 0$ to $t = 16$ days, whilst breakage to Reactor 2 restricted the FBR5-2(a) reactor to operation for only 8 days, from $t = 7$ to $t = 15$. At $t = 15$ days, the excess biological growth in Reactor 2 was sufficient to fully impede the fluidisation state of the reactor, at which time the trial was terminated.

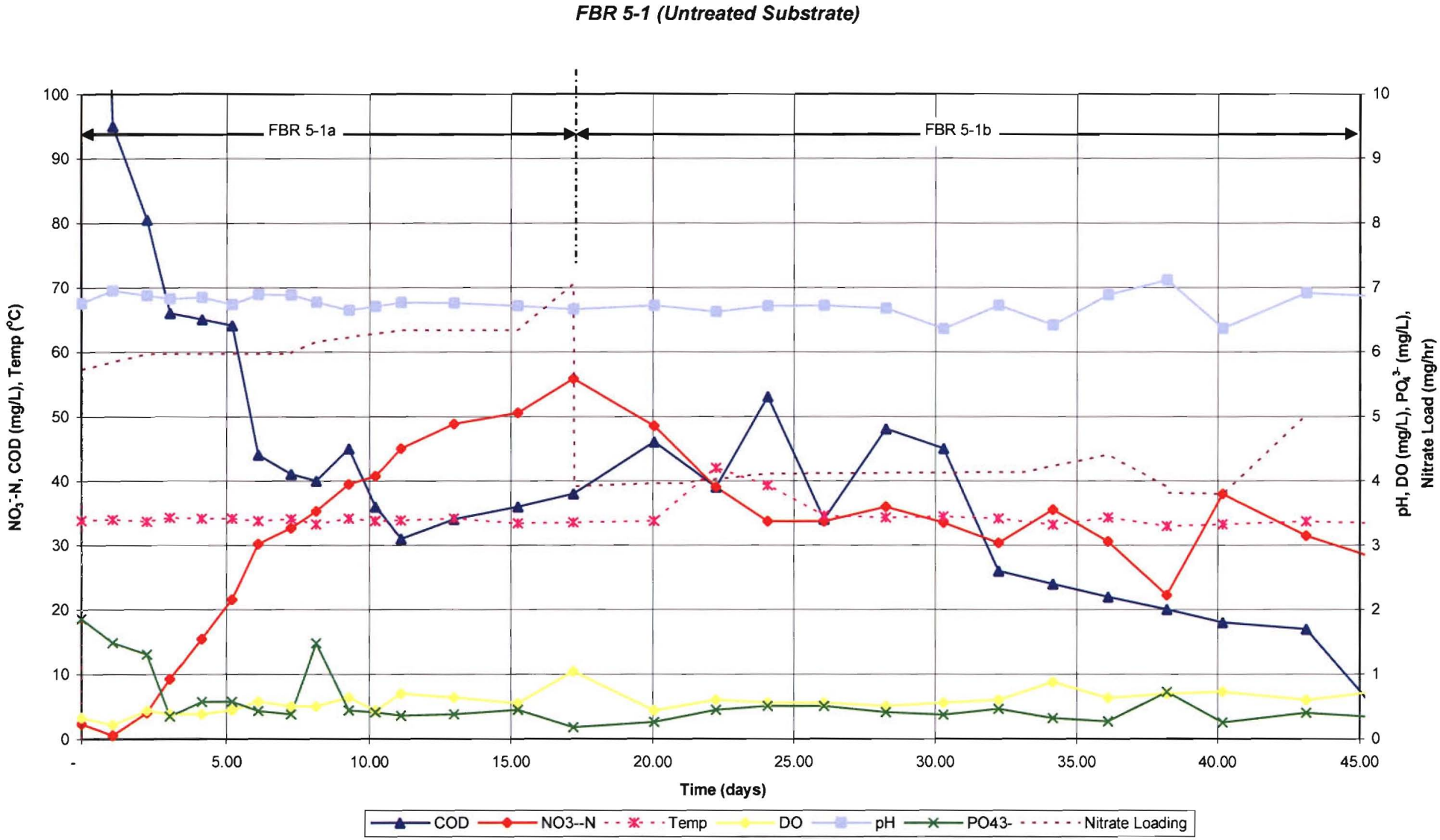

Figure 7-15 Denitrification Trial FBR5-1, for the untreated substrate.

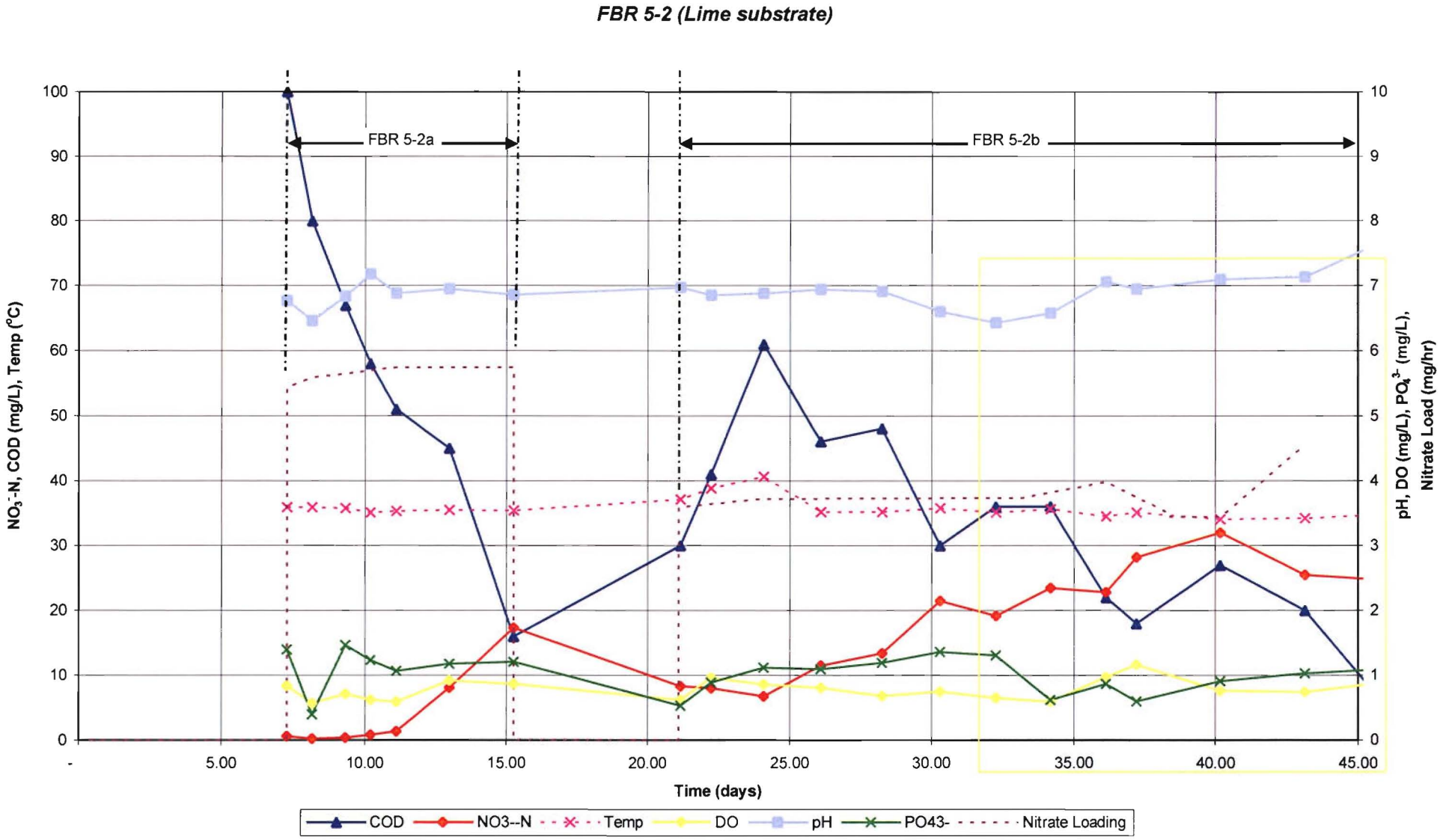

Figure 7-16 Denitrification Trial FBR5-2, for the Lime treated substrate. The reactor was operating as a packed reactor from 32 – 49 days.

The COD and nitrate profiles for the FBR5-1(a) reactor present a bilinear-type relationship[18] (as per Figure 7-15), with each leg of the relationship having an apparent distinct relationship as summarised in Table 7-15.

Table 7-15 Apparent Bilinear Nitrate and COD Concentration Relationships in FBR5-1(a)

Period (days)	COD (mg/L/day)	NO_3^--N (mg/L/day)
$0 \le t \le 6$	-8.611	5.878
$6 \le t \le 17$	-0.669	2.296

The CFSTR assessment determined that both the nitrate and COD profiles followed the CFSTR prediction of the interaction between the hydraulic, solubilisation, and biological consumption processes present in the reactor. As demonstrated in Figure 7-17, the CFSTR model of the COD concentration in FBR5-1(a) reveals a close correlation to the recorded COD profile in the reactor during the trial. Thus, the actual profile exhibits an exponential decay relationship, rather than the bilinear-type suggested earlier.

The initial high rate of COD loss from both reactors, FBR5-1(a) and FBR5-2(a), as the CFSTR analysis demonstrates, can be attributed to the hydraulic flushing characteristic rather than biological consumption, as demonstrated in Figure 7-17. As the trial progressed, the biological consumption and COD hydrolysis processes became move pronounced, however this did not appear to occur in the FBR5-2(a) reactor. Although the duration of the FBR5-2(a) trial was short, contrary to expectations (and earlier observations), neither excess biological consumption nor excess hydrolysis of the substrate was present by the end of the trial

[18] Bilinear is defined as a function of two variables is bilinear if it is linear with respect to each of its variables (Weissten, 2005).

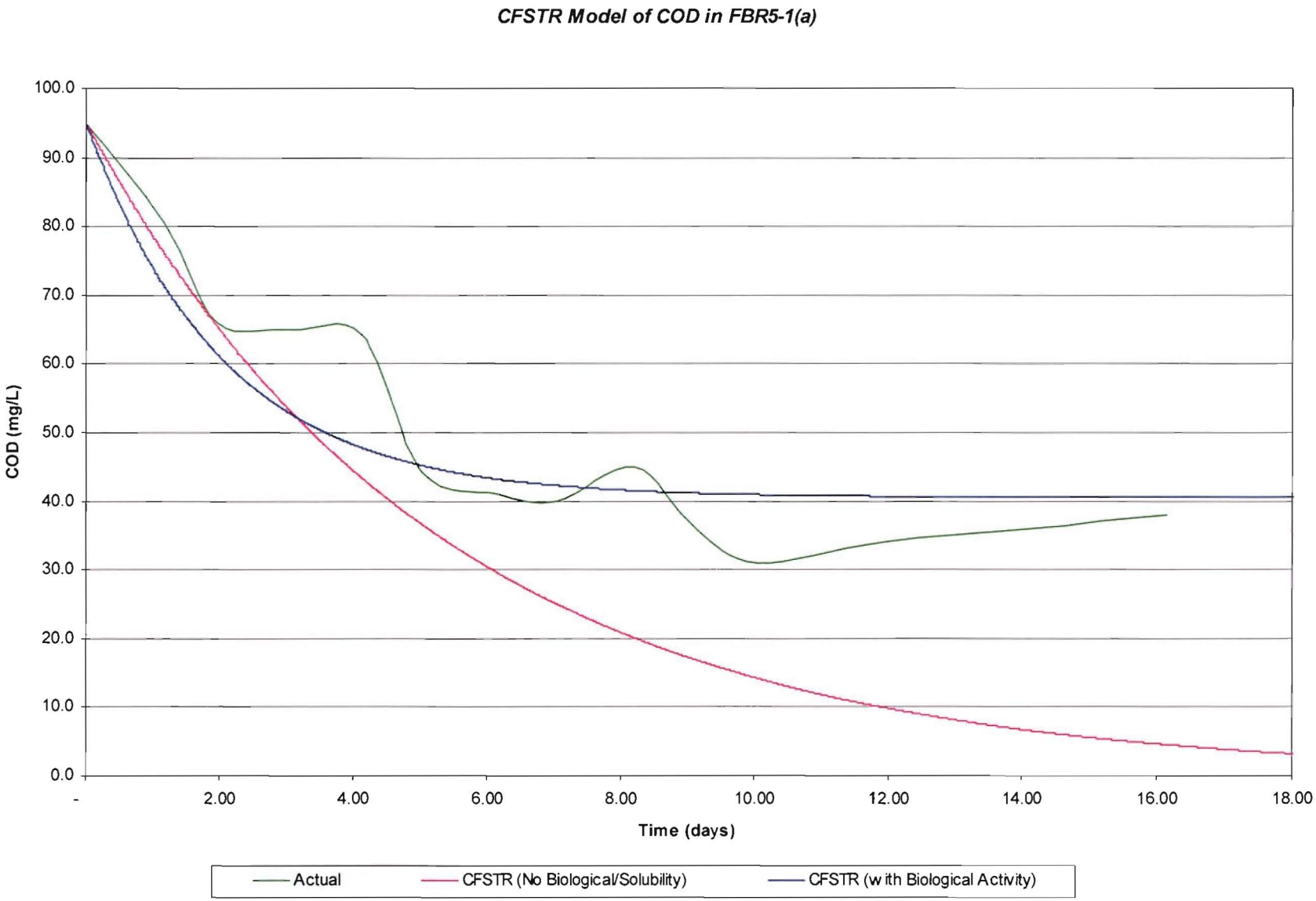

Figure 7-17 CFSTR assessment of the COD concentration of FBR5-1(a).

While the analysis of the results of FBR5-2(a) (in particular the absence of nitrate accumulation in the early stages of the trial) would suggest that complete denitrification was occurring, no apparent accumulation in organic carbon took place. Hence, at this stage of the trial the rate of COD release due to hydrolysis of the coconut shell fragments matched the organic carbon demand.

Visually, it was apparent that during this period the bacterial growth in FBR5-2(a) exceeded the hydraulic wasting capacity of the reactor, resulting in an accumulation of biomass such that the reactor became blocked, in particular at the diffusion filter mechanism at the bottom of the reactor. As a consequence, the rate of internal recycle was significantly impeded such that in later stages of the trial, fluidisation of the substrate was not possible. Hence, the efficiency of the denitrification process was impeded (thought to be due to short-circuiting) resulting in the sudden 16 mg/L increase in nitrate in the last four days of the trial. With the rate of internal recycle declining further, and with no apparent method of correcting the situation without dismantling the reactor and cleaning the diffuser, the trial was terminated.

While a direct comparison of the two reactors is not possible due to the breakage and problems with the excess biological growth in FBR5-2(a), Table 7-16 does demonstrate the rate of biological consumption and organic hydrolysis exhibited by the untreated substrate FBR5-1(a), while the poor denitrification performance of the "blocked" lime-treated substrate reactor demonstrates the effect of short-circuiting within the reactor.

Table 7-16 Assessment of COD and Nitrate concentrations in FBR5-X(a)

	COD		NO_3^--N	
	FBR5-1(a)	FBR5-2(a)	FBR5-1(a)	FBR5-2(a)
At t = *17 days* (mg/L)	38	16 *	55.8	17.3 *
Hydraulic Flushing Scenario at t = *17 days* (mg/L) #	9.6	25.2 *	66.5	51.8 *
Idealised CFSTR Parameters				
r_b	0.354	8.68	0.089	2.17
k_s	7435	6.09	-	-
r_s	2.47	-24.4	-	-
c_s	274,200	274,200	-	-

The assessment conducted in this scenario has excluded the effect of possible formation or biological consumption of COD and nitrate within the reactor.

* At t = *15 days*

7.2.5.2 FBR5-X(b)

During this trial, the two reactors were hydraulically loaded under conditions identical to the earlier set FBR5-X(a) as Table 4-9 demonstrates; however, the nitrate loading in the FBR5-X(b) series of trials was 66% of that in FBR5-X(a) trials.

This series of trials lasted 32 days, and the nitrate concentration in FBR5-1(b) continued to decline for the duration of the trial (Figure 7-16). During the same period, the accumulated COD concentration declined from approximately 50 mg/L to 2 mg/L at the end of the trial. The decline in both COD and nitrate concentrations suggests that if the trial had continued longer the hydrolysis of COD from the substrate may have been insufficient to maintain the denitrification rate. Thus, the nitrate concentration would be expected to recover.

Figure 7-15 shows the nitrate concentration in the untreated substrate reactor (FBR 5-1) declined at a rate of 1.0 mg/L/day indicating that the rate of denitrification within the reactor exceeded the rate of supply (4.0 mg/hr). The rate of nitrate reduction was complemented by a similar decline in the rate of accumulated COD in the order of 1.25 mg/L/day.

During the later period of this trial, FBR5-2(b) exhibited characteristics similar to those observed in the FBR5-2(a) trial with issues arising due to the excessive accumulation of

biomass within the reactor. While trying to dislodge and re-suspend the bed (at t = 32 days), the recycle regulating valve broke. As a result, the internal recycle was unable to be regulated and the reactor continued to operate at maximum possible internal recycle for the remainder of the trial. The fluidised bed expansion following the breakage of the internal recycle regulating valve was in the order of 150 mm, which correlates to a superficial fluid velocity (i.e. the internal recycle) 1.5 times that of the other trials.

While the actual rate of internal recycle was not documented, the declining depth of expansion during the later stage FBR5-2(b) following the valve breakage tends to suggest either the substrate particles were becoming denser, or that additional friction losses were now present in the reactor.

It is highly unlikely that the substrate particle would increase in density, since bacterial adhesion was observed on the particles – as a consequence, the substrate's effective diameter increased. Since the density of a bacterial biofilm is less than that of the substrate, the combined bacteria/substrate density would be less than that of the substrate by itself (Table 7-17).

As Leva (1959) determined, an increase in effective substrate diameter would be expected to increase the minimum fluidisation velocity (u_{mf}) , as derived in Eqn. 3-4:

$$u_{mf} = 1.58 \times 10^{-4} \frac{D_p^{1.82}}{\nu^{0.88}} \left(\frac{\rho_s - \rho_f}{\rho_f} \right)^{0.94}$$

A reduction in particle density reduces the minimum fluidisation velocity. The following evaluation indicates that if 1 mm of bacterial biofilm were to adhere to the substrate, the minimum fluidisation velocity would increase 79.6% of the coconut fragments/substrates by itself.

Table 7-17 Evaluation of Minimum Fluid Velocity FBR5-2(a)						
	Specific Gravity	D_{50} (50%ile, mm)	Volume (mm^3)	$D_p^{1.82}$	$\left(\frac{\rho_s-\rho_f}{\rho_f}\right)^{0.94}$	$u_{mf}=1.58\times10^{-4}\frac{D_p^{1.82}}{\nu^{0.88}}\left(\frac{\rho_s-\rho_f}{\rho_f}\right)^{0.94}$
Coconut Fragments	1.17	5mm	65.4	6.5×10^{-5}	1.92	3.73×10^{-3} m/s
Bacterial Biofilm	1.00	(1mm thick)		n/a	n/a	n/a
Combined Coconut/Bacteria	1.03	7mm	179.6	1.2×10^{-4}	1.87	6.70×10^{-3} m/s

As Figure 7-18 indicates, reducing the minimum fluid velocity subsequent to the regulating valve failure would translate to a reduction in the fluidised bed depth (Δh_s), as observed.

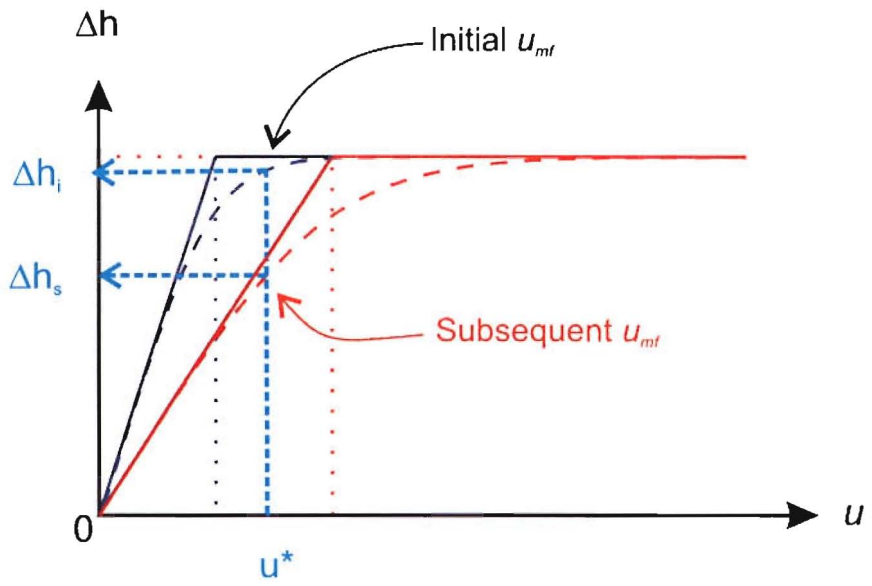

Figure 7-18 Assessment of the change in fluidised bed depth (Δh) subsequent to the regulating valve failure on FBR5-2(b).

Large biological flocs were beginning to accumulate within the reactor and previous experience suggested these preceded the onset of biological blocking of the bed and diffuser filter. This turned out to be the case as by day 38 the fluidised bed expansion was only in the order of 30 mm and continued to decline until the trial was terminated.

The lime-treated substrate reactor trials, FBR5-2(a) and FBR5-2(b), were not continuous and a consequence of the down-time between trials was a slight increase in the accumulated COD

concentrations and, more importantly, an observed drop in the nitrate concentration between the end of FBR5-2(a) and beginning of FBR5-2(b). This drop is explained by the loss of some of the acclimated the reactor fluid/biomass during the unclogging of the reactor diffuser filter.

As mentioned earlier, the FBR5-2(a) trial ceased prematurely and this allowed the reactor to be decommissioned and the internal diffuser/filter to be removed and cleaned. To minimise impact, an effort was made to minimise disturbance to the biomass/substrate and preserve the superficial reactor fluid; hence the FBR5-2(b) trial did not require any additional inoculum, and acclimatisation was expected to occur rapidly. The presupposition was supported by the results of this trial (Figure 7-16), this is, in the first three days of this trial the COD concentration increased from 30 to 61 mg/L, while the reactor nitrate declined slightly. The remainder of the data set showed a general decline in the COD concentration, at a rate of -1.767 mg/L/day, while the nitrate concentration continued to increase at a rate of 0.737 mg/L/day of NO_3^--N.

The actual performance of FBR5-2(a) was unsatisfactory, as by t = 32 days the diffusion chamber had become clogged with biomass again. The recycle flow was sufficiently impeded that the reactor was operating as a packed bed reactor (Figure 7-16). Inefficiencies in the packed bed reactor configuration could explain the observed decline in COD in the fluid phase ($COD_{t=45}$ = 5 mg/L), and thus the denitrification process (being carbon limited) resulted in the accumulation of nitrate.

Table 7-18 Assessment of COD and Nitrate concentrations in FBR5-X(b)

	COD		NO_3^--N	
	FBR5-1(b)	FBR5-2(b)	FBR5-1(b)	FBR5-2(b)
At t = *32 days* (mg/L)	11	17 *	28	25.7 *
Hydraulic Flushing Scenario at t = *32 days* (mg/L) #	1.3	1.0 *	36	44 *
Idealised CFSTR Parameters				
r_b	0.042	0.560	0.01	0.14
k_s	10.2	13.5	-	-
r_s	-75.8	-82.7	-	-
c_s	274,200	274,200	-	-

The assessment conducted in this scenario has excluded the effect of possible formation or biological consumption of COD and nitrate within the reactor.

* At t = *28 days*

As the FBR5-2(b) trial was operating in a packed bed reactor configuration, it is highly likely that the COD hydrolysis process would be detrimentally affected by the preferential flow paths that occur in a packed media. That is, preferential flow paths tend to have elevated fluid velocities and as a consequence, the availability of COD hydrolysis sites is limited and release of COD into solution is impeded.

7.2.6 Fluidised Bed Reactor – Series 6

Two weeks down-time after the termination of the previous series was allotted before re-establishing the reactors on the 13th December 2000. During this period, all the recycling and dosage lines were replaced and/or cleaned.

Reactor 2 was taken apart, cleaned, and the diffusion chamber blockage was determined to be due to biomass escaping the reactor and settling chamber, entering the recycle line, and blocking the diffusion gauze at the bottom of the reactor. This was exacerbated by the lime-treated substrate releasing great quantities (relative to the untreated substrate) of organic carbon over a short time interval, promoting a sudden growth in biomass that exceeded the settling characteristics of the settling chamber. As a consequence, the physical fluidisation process deteriorated and the reactor failed to fully denitrify. To overcome this problem, some

of the biomass was wasted from the reactor. In the previous sets of trials it was noted that the rate of COD release declined with time.

The substrate in both reactors was replaced at the beginning of the FBR4-X trials. Prior to the start of the FBR6-X trials, Reactor 1 had operated for approximately 84 days (35 days for FBR4-X trials and 49 days for FBR5-X), while Reactor 2 had operated for approximately 71 days (36 and 49 days for trial FBR4-X and FBR5-X respectively). Given this length of time, it was reasonable to assume that the rate of COD release would decline; however, this appeared not to be the case for the lime-treated substrate for at day 71 it continued to release COD at a rate in excess of the rate the biomass could consume it.

Series FBR6-X contained five trials, with an HRT varying from 15.6 days to 117 days. Similarly, the nitrate load varied from 0.3 mg/hr to 2.2 mg/hr (Table 4-9).

7.2.6.1 FBR6-X(a)

This set of trials, FBR6-X(a), operated with a low nitrate loading (average 0.55 mg/hr), and Figure 7-19 and Figure 7-20 indicate that the biomass completely consumed the nitrate within 24 hours for FBR6-1(b) and 4 days for FBR6-1(a).

The COD profile of the FBR6-1(a) fluctuated but gradually declined at an average rate of –0.776 mg/L/day. The last two days of the data set indicate that the COD within the reactor was completely consumed.

The initial COD concentration of FBR6-2(a) (23 mg/L) was similar to the initial concentration of FBR6-1(a); however, it dropped suddenly by 11 mg/L in the first 24 hours, corresponding to a similar drop in nitrate concentration within the reactor. Following the initial drop, the COD recovered at a rate of 1.95 mg/L/day, but in the last 24 hours of this trial the COD concentration fell 19 mg/L.

The first half of the nitrate record in FBR6-1(a) shows an initial rise in concentration during the first day and then effectively complete utilisation over the next four days, at a rate of –0.80 mg/L/day. FBR6-2(a) showed a greater capacity to denitrify the initial nitrates within the reactor; since this reactor started with an initial concentration of 8.4 mg/L (8.4 mg/L × 11.26

L = 94.6 mg). In conjunction with the dosed 6.6 mg of nitrate, the entire nitrate was consumed within 25 hours, corresponding to a rate of 97.2 mg/L/day.

The increased ability of FBR6-2(a) to denitrify the influent nitrate could be due to a greater ability of this substrate to release organic carbon. The rate of hydrolysis was apparently sufficient that the release rate exceeded biological demands and resulted in the 1.95 mg/L/day COD accumulation rate.

The numerical assessment of these two trials (Table 7-19) supports the observations made earlier; namely the greater r_b coefficient of Reactor FBR6-2(a) quantifies the improved rate of biological consumption of nitrate ($r_{b,NO3,FBR6\text{-}2(a)}$ = 2.94, compared to $r_{b,NO3,FBR6\text{-}1(a)}$ = 0.95). Similarly FBR6-2(a) has a greater COD consumption directly attributed to biological utilisation ($r_{b,COD,FBR6\text{-}2(a)}$ = 11.7, compared to $r_{b,COD,FBR6\text{-}1(b)}$ = 3.80)

Table 7-19 Assessment of COD and Nitrate concentrations in FBR6-X(a)

	COD		NO_3^--N	
	FBR6-1(a)	FBR6-2(a)	FBR6-1(a)	FBR6-2(a)
At *t = 6 days* (mg/L)	12	29	0.4	0.3
Hydraulic Flushing Scenario at *t = 6 days* (mg/L) [#]	16.2	17.1	12.4	12.1
Idealised CFSTR Parameters				
r_b	3.80	11.7	0.95	2.94
k_s	2649	28.4	-	-
r_s	1.34	109	-	-
c_s	274,200	274,200	-	-

[#] The assessment conducted in this scenario has excluded the effect of possible formation or biological consumption of COD and nitrate within the reactor.

Due to the lower k_s coefficient of the lime-treated substrate [in FBR6-2(a)], it follows that the rate of COD solubilisation was greater than the untreated substrate. Again, this observation is consistent with the observations made in the earlier fluidised bed reactor sets.

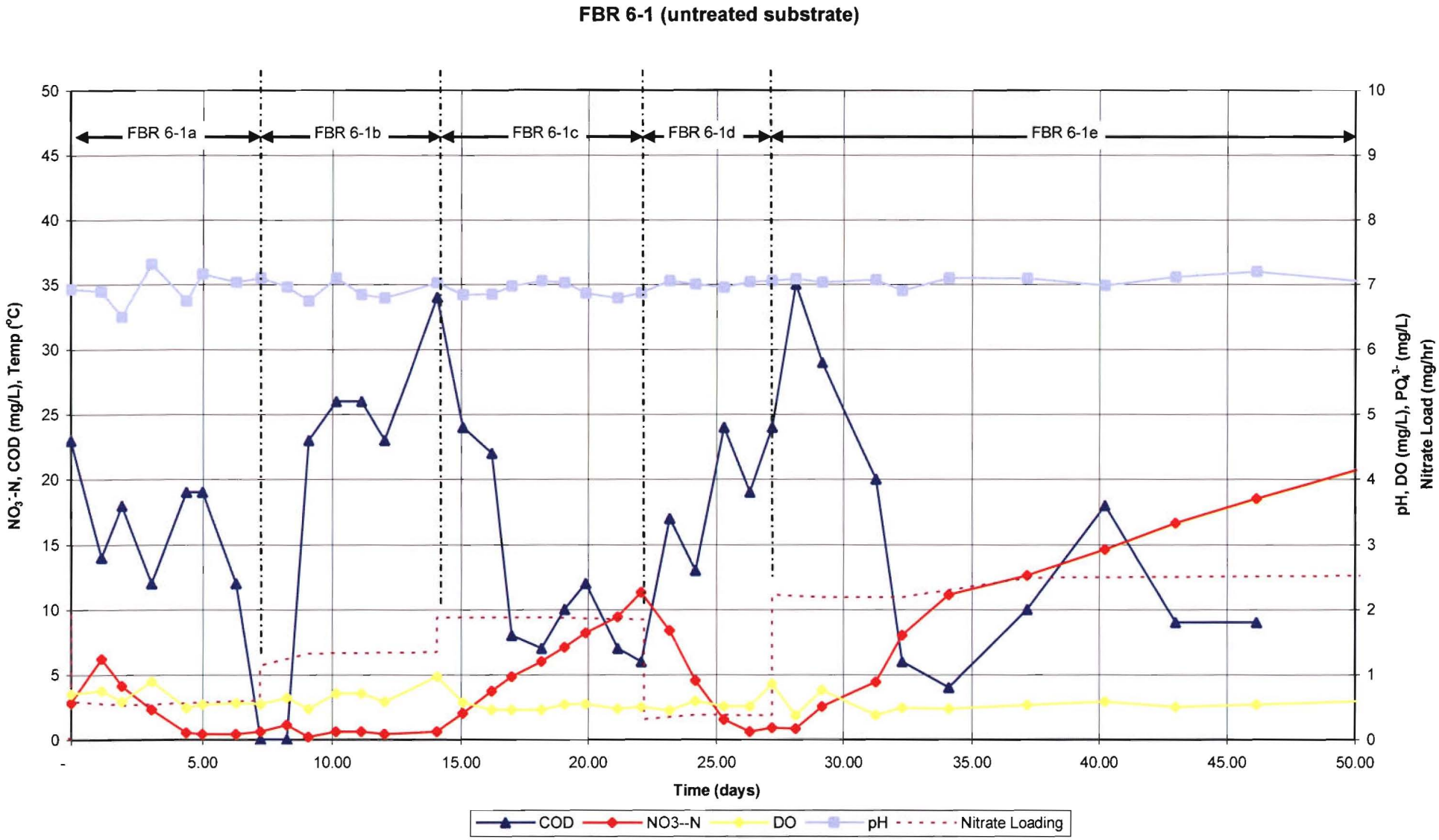

Figure 7-19 Denitrification Trial FBR6-1, for the untreated substrate.

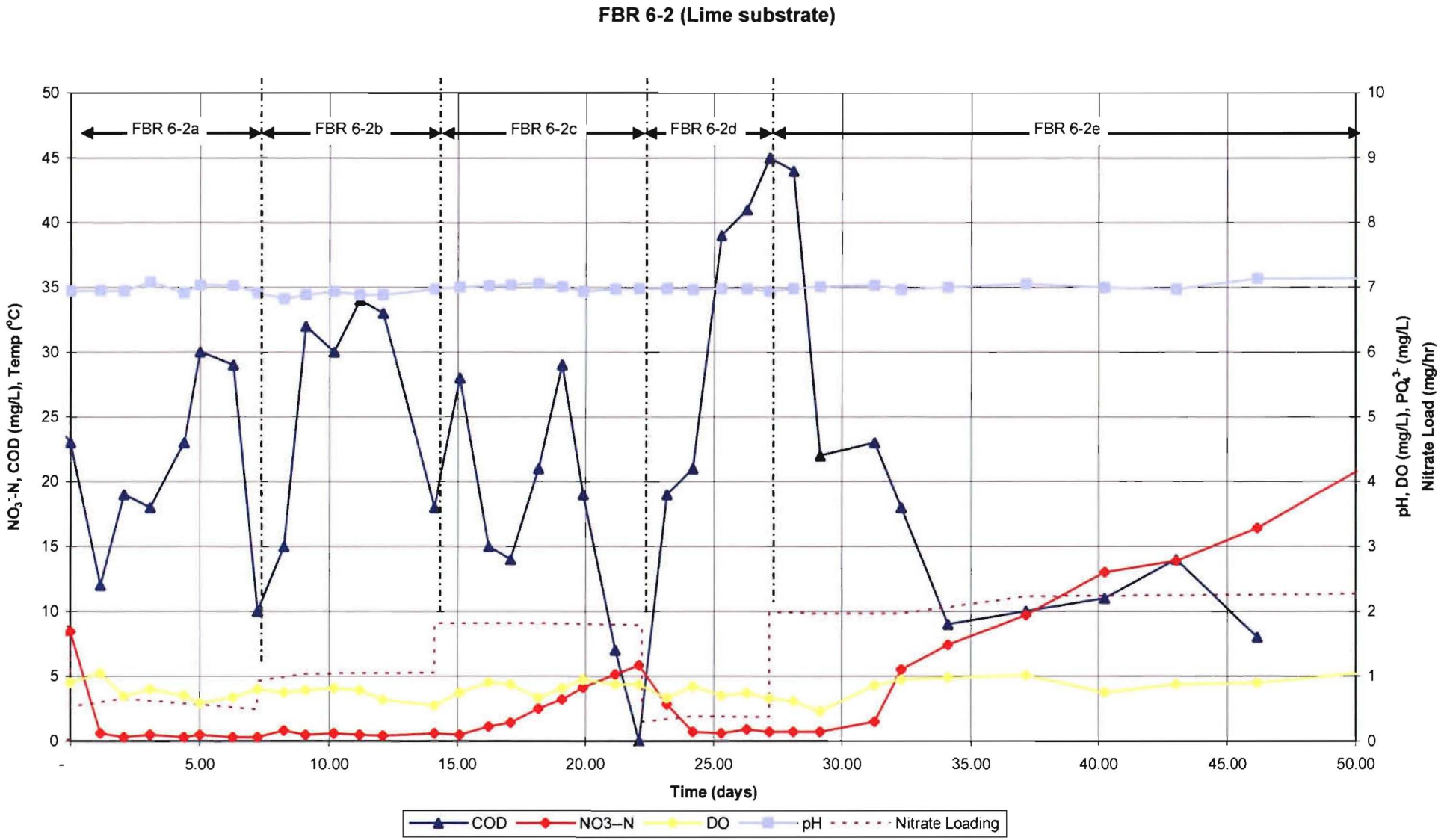

Figure 7-20 Denitrification Trial FBR6-2, for the Lime treated substrate.

7.2.6.2 FBR6-X(b)

In this set of trials, the reactors were operated with influent flow rates similar to the FBR6-X(a) trials; however, the concentration of the influent nitrate was twice the concentration of the earlier trials.

During the first 24 hours of the FBR6-1(b) trial, the COD concentration remained zero. In the following period, the COD concentration in FBR6-1(b) rose 23 mg/L in 20 hours and continued to accumulate COD, eventually peaking at 34 mg/L by the end of the trial. Throughout this period, the nitrate concentration was effectively zero with an average concentration of 0.48 mg/L NO_3^--N.

The reactor with the lime-treated substrate, FBR6-2(b), showed similar nitrate and COD profiles to that of FBR6-1(b), with the exception that the initial COD concentration was 10 mg/L, and increased by 22 mg/L (cf 32 mg/L) during the first two days of the trial. As in the untreated substrate trial, the concentration was maintained until the final two days, in which a 50 % (17 mg/L) drop in COD occurred from t=12 days to t=14 days.

Both demonstrated no accumulation of nitrate even though the reactors were dosed with 1.1 mg/hr of NO_3^--N and 1.0 mg/hr of NO_3^--N for FBR6-1(b) and FBR6-2(b) respectively. The lack of accumulation indicated that denitrification was occurring. Ignoring biological consumption (i.e. denitrification), Table 7-20 indicates that the nitrate consumption at the end of the trial would be expected to be 13.4 and 12.6 mg/L of NO_3^--N respectively, when instead 0.6 mg/L was recorded.

Although both reactors demonstrated similar rates of denitrification, the rate of COD release (hydrolysis induced) appeared to be greater in FBR6-1(b). A comparison of the solubilisation coefficients (k_s, r_s) from Table 7-20 supports this observation (as graphically represented in Figure 7-21). The analysis illustrates that FBR6-1(b) had a greater initial rate of solubilisation, only to plateau at t = 1 day, while FBR6-2(b) initially released COD at a rate approximately half that of the FBR6-1(b). Had the trial extended for a few more days, the numerical model indicates that the rate of COD release from trial FBR6-2(b) would reach and then exceed that of FBR6-1(a).

Table 7-20 Assessment of COD and Nitrate concentrations in FBR6-X(b)

	COD		NO_3^--N	
	FBR6-1(b)	FBR6-2(b)	FBR6-1(b)	FBR6-2(b)
At t = *14 days* (mg/L)	34	18	0.6	0.6
Hydraulic Flushing Scenario at t = *14 days* (mg/L) [#]	0	7.2	13.4	12.6
Idealised CFSTR Parameters				
r_b	17.01	15.68	4.25	3.92
k_s	6.3	322.8	-	-
r_s	33.82	3.50	-	-
c_s	274,200	274,200	-	-

[#] The assessment conducted in this scenario has excluded the effect of possible formation (solubility) or biological consumption within the reactor.

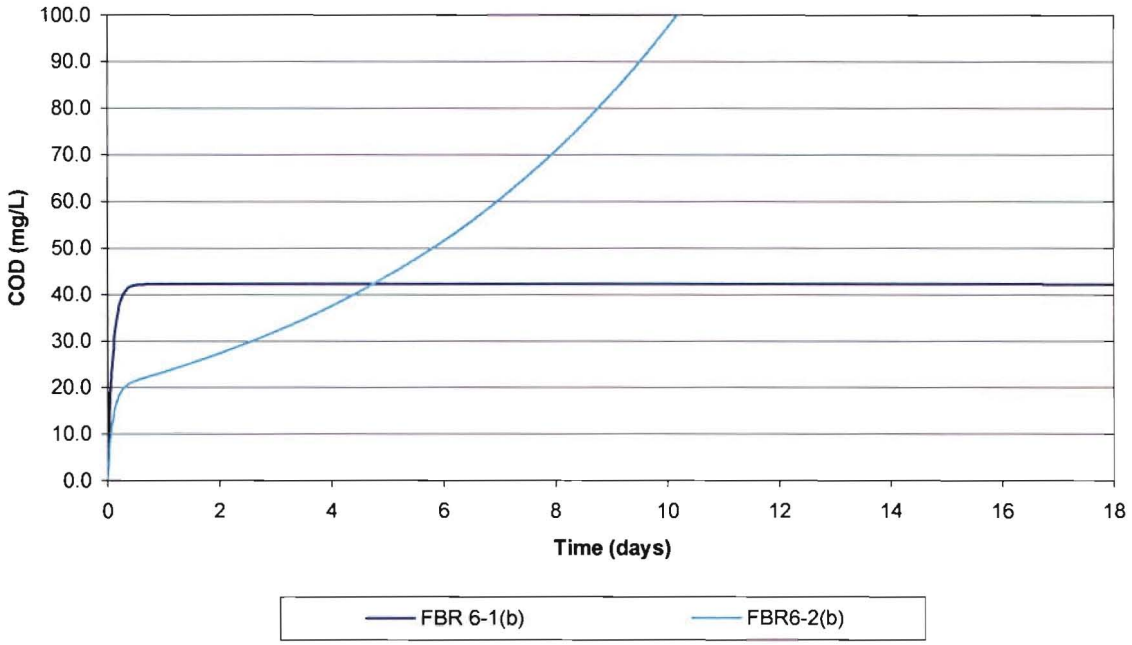

Figure 7-21 Comparative assessment of COD hydrolysis in FBR6-1(b) and FBR6-2(b).

7.2.6.3 FBR6-X(c)

The hydraulic loading of this trial at 0.02 L/hr was approximately a third of the loading in the previous trial, while the nitrate loading increased 76% to 1.9 mg/hr. The duration of this trial was approximately 8 days, which was equivalent to 24 HRT's.

At these loadings the biological denitrification process was unable to fully consume the influent NO_3^-N and as a consequence, both reactors showed of nitrate in the reactors. The rate of nitrate increase was constant in each reactor, and did not appear to fluctuate with the significant changes in COD concentration in the reactors during this trial.

The COD profile of FBR6-1(c) had an initial concentration of 34 mg/L and the COD was consumed at a rate of –7.9 mg/L/day for the first three days (t = 17 days) of the trial and for the remainder of the trial the COD averaged 8.3 mg/L ± 2.1 mg/L. During this trial, the nitrate profile was linear and accumulating within the reactor at a rate of 1.3 mg/L/day (r^2 = 0.995).

While the COD profile of the lime-treated reactor, FBR6-2(c), fluctuated around an average of 20.6 mg/L ± 5.5 mg/L concentration, the last two days of this trial saw the complete utilisation of the accumulated organic matter in the reactor. It is thought that this must have occurred within the few hours of the cessation of this trial, as the nitrate profile showed no observable response.

The observed variation in COD concentration and the apparent independence with the reactor nitrate concentration tends to suggest that some other process was occurring. As all of the earlier trials demonstrated a strong correlation with the rate of nitrate consumption and the availability of organic carbon, it is thought that the residual COD observed during this trial was possibly organic carbon in a non-readily consumable form (e.g.. lignin).

The nitrate profile for FBR6-2(c), showed a linear accumulation within the reactor; however the rate was less than that of FBR6-1(c) being at a rate of 0.792 mg/L/day (r^2 = 0.989). This suggests that the lime-treated substrate was:

1. physically supporting more biomass than the untreated substrate, and
2. hydrolysing more organic carbon

This suggests that the relatively slow rate of nitrate accumulation within reactor FBR6-2(c) was a consequence of greater nitrate respiration.

Table 7-21 Assessment of COD and Nitrate concentrations in FBR6-X(c)

	COD		NO_3^--N	
	FBR6-1(c)	FBR6-2(c)	FBR6-1(c)	FBR6-2(c)
At t = *22 days* (mg/L)	6	0	11.3	5.8
Hydraulic Flushing Scenario at t = *22 days* (mg/L) [#]	24.2	13	27.9	26.6
Idealised CFSTR Parameters				
r_b	1.52	3.56	0.38	0.89
k_s	7854	7.49	-	-
r_s	-1516	-44.09	-	-
c_s	274,200	274,200	-	-

[#] The assessment conducted in this scenario has excluded the effect of possible formation or biological consumption of COD and nitrate within the reactor.

The numerical analysis of these two trials, summarised in Table 7-21, identified that the lime-treated reactor, FBR6-2(c), respired at over twice the rate of nitrate (i.e. $r_{b,NO3}=0.89$ day^{-1} for reactor FBR6-2(c), while FBR6-1(c) consumed $r_{b,NO3}=0.38$ day^{-1}). This is supported by the analysis above, as the lime-treated reactor also released organic carbon at a greater rate, demonstrated by the lime-treated reactor presenting with a greater COD release coefficient (k_s), than FBR6-1(c).

7.2.6.4 FBR6-X(d)

This trial had a comparatively long HRT (117 days) and an associated low nitrate loading (0.35 mg/hr). The COD profiles for both reactors showed significant accumulation of organic carbon within the reactor, while the residual nitrate in the reactors from the previous trials was quickly consumed during the initial 2 – 3 days of this trial.

The rates of COD accumulation for these reactors was 3.8 mg/L/day (r^2 = 0.80) and 8.7 mg/L/day (r^2 = 0.93) for FBR6-1(d) and FBR6-2(d) respectively. During this time, the nitrate was consumed at similar rates, -2.7 mg/L/day (r^2 = 0.97) and –2.4 mg/L/day (r^2 = 0.99 [19]) of NO_3^--N. Figure 7-19 and Figure 7-20 showed similar nitrate consumption rates as calculated

[19] Only three records are involved in this relationship, hence not much confidence can be placed in this measure of correlation.

above. Since this consumption occurred in COD accumulating conditions, this tends to suggest that the rate of denitrification was the rate-limiting condition.

Table 7-22 Assessment of COD and Nitrate concentrations in FBR6-X(d)

	COD		NO_3^--N	
	FBR6-1(d)	FBR6-2(d)	FBR6-1(d)	FBR6-2(d)
At t = *28 days* (mg/L)	5.7	0	0.8	0.7
Hydraulic Flushing Scenario at t = *28 days* (mg/L) [#]	35	44	15.5	10.5
Idealised CFSTR Parameters				
r_b	2.92	4.76	0.729	1.19
k_s	5.89	6.45	-	-
r_s	42.3	39.4	-	-
c_s	274,200	274,200	-	-

[#] The assessment conducted in this scenario has excluded the effect of possible formation or biological consumption of COD and nitrate within the reactor.

While both reactors exhibited similar denitrification rates, the analysis in Table 7-22 demonstrated that the lime-treated substrate in reactor FBR6-2(d) was able to support a greater biological rate of nitrate consumption (r_b). This is complemented by an increased rate of COD release apparent by the greater COD coefficient k_s.

Note the r_b is defers from the nitrate consumption rate estimates calculated above, since r_b as applied in Eqn. 7-1 accounts for the change in nitrate concentration with time, whilst the consumption rate is a measure of the change in nitrate over a specific interval of time.

7.2.6.5 FBR6-X(e)

The hydraulic and nitrate loading in this trial were similar to the FBR6-X(c) trial, the nitrate and hydraulic loads were increased slightly to 2.1 mg/hr and 0.024 L/hr respectively. While these reactors showed the same general nitrate profile response as the FBR6-X(c) reactors, there were some important differences.

The COD concentration of both reactors started from an initial high concentration ($COD_{FBR6\text{-}1(e)}$ = 35 mg/L, $COD_{FBR6\text{-}2(e)}$ = 45 mg/L) which was quickly consumed within the first five days. The rates of COD consumption were –4.10 mg/L/day (r^2 = 0.764) and –5.05 mg/L/day (r^2 = 0.849), for FBR6-1(e) and FBR6-2(e) respectively. The remainder of the COD profiles

for these trials show some fluctuations around average concentrations of COD equal to 9.33 mg/L for FBR6-1(e) and 10.4 mg/L for FBR6-2(e).

The nitrate concentration in both reactors did not show any noticeable response to the increase nitrate loading conditions until the COD concentration fell below 30 mg/L. FBR6-2(e) with its greater initial COD concentration responded to the new nitrate load four days into the trial, while FBR6-1(e) with a lower COD concentration responded in two days.

The rate of nitrate accumulation in both reactors plateaued in the later stages of the trial. By this time, the COD concentration in the respective reactors was either increasing or had reached a static concentration. This is thought to be due to the bacteria acclimating to the new hydraulic conditions, with the rate of COD release due to enzyme hydrolysis equalling or exceeding the quantity of COD either consumed by the bacteria and/or flushed from the reactor.

As Table 7-23 demonstrates, both reactors exhibited similar biological consumption rates (r_b). Similarly the solubilisation rates k_s and r_s were very close as Figure 7-22 illustrates.

Table 7-23 Assessment of COD and Nitrate concentrations in FBR6-X(e)

	COD		NO_3^--N	
	FBR6-1(e)	FBR6-2(e)	FBR6-1(e)	FBR6-2(e)
At t = *46 days* (mg/L)	9	8	18.5	16.4
Hydraulic Flushing Scenario at t = *46 days* (mg/L) [#]	12.8	18.2	53.7	51.4
Idealised CFSTR Parameters				
r_b	0.833	0.865	0.208	0.216
k_s	5374	11896	-	-
r_s	8572	0	-	-
c_s	274,200	274,200	-	-

[#] The assessment conducted in this scenario has excluded the effect of possible formation or biological consumption of COD and nitrate within the reactor.

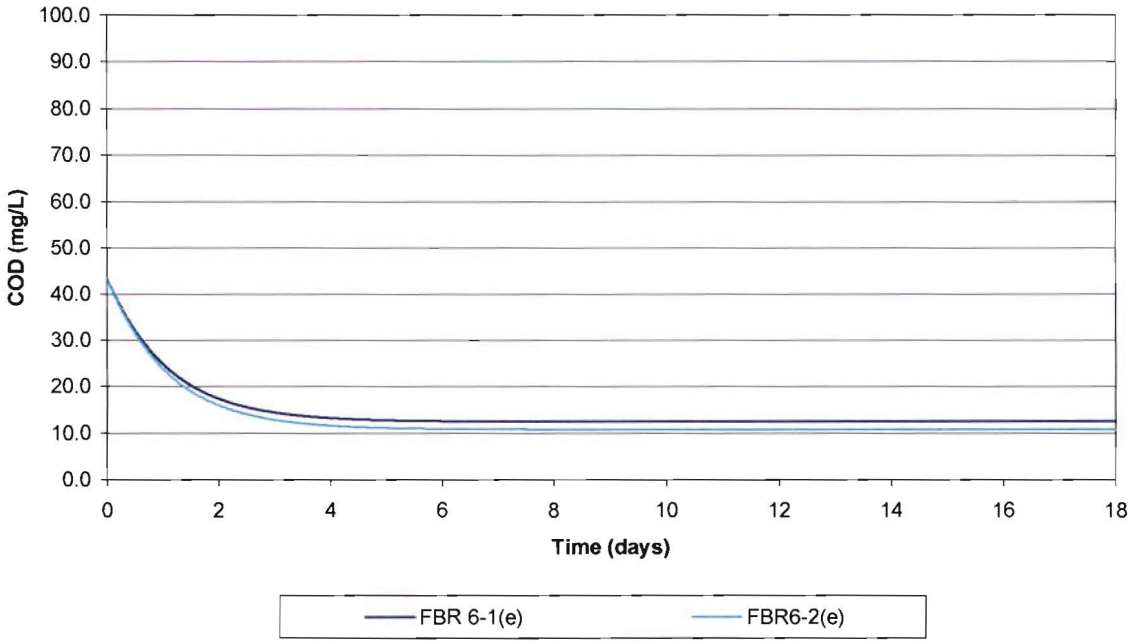

Figure 7-22 Comparative assessment of COD hydrolysis in FBR6-1(e) and FBR6-2(e), based on COD hydrolysis coefficients summaries in Table 7-23.

Since the biological consumption rates (r_b) and more importantly the solubilisation rates (k_s and r_s) are near identical this suggests that the ability of the lime-pretreated coconut fragments to release additional organic carbon was not longer present. Thus the previously lime treated fragments were now releasing COD at a rate consistent with an untreated substrate.

This finding suggests that effect of the pretreatment with lime is limited. In this particular series of the trials the pretreated substrate was able to sustain improved COD solubilisation for approximately 30 days.

7.3 Analysis

As outlined earlier, a numerical CFSTR (continuous flow stirred tank reactor) analysis of the 30 trials in this series of 38 trials has been conducted. The CFSTR model (Appendix M), models the three functions thought to be occurring within the reactor - hydraulic flushing ($Qc_1 - Qc$), biological consumption ($Vr_b ct$), and pollutant production/hydraulic solubilisation $\left(\frac{Vc_s}{2k_s}\left(\text{sech}^2\left(\frac{t-r_s}{k_s}\right)\right)\right)$. Algebraically these form the following equation (reproduced from Eqn. 7-1):

$$V\frac{dc}{dt} = Qc_1 - Qc + \frac{Vc_s}{2k_s}\left(\text{sech}^2\left(\frac{t-r_s}{k_s}\right)\right) - Vr_b ct$$

Both the COD and nitrate profiles were matched to the CFSTR model. A summary of the coefficients has been included in Table 7-24. Since the COD:TN ratio to sustain the biological process was in the order of 4:1, the COD and nitrate CFSTR evaluations were constrained by this relationship. That is, the r_b coefficient for the COD CFSTR model (cr_b) was four times that of the nitrate CFSTR value.

Comparisons between the coefficients are difficult because of the lack of quantitative measurement of the mass of biomass within the reactor. That is, the rate of COD release and denitrification coefficients could not be normalised by the mass of biomass. In addition, other factors influence the biological process, such as the short duration of trials, variations in the superficial fluid velocity, and variations in reactor acidity.

In particular, the short duration of each trial insures that the bacteria were constantly adapting to new hydraulic or nitrate loading and changes in hydraulic or nitrate load may result in a different species dominating. As a consequence the transition from one hydraulic/nitrate environmental condition to another may result in the transition of dominant bacterial species, often at the expense of biological efficiency.

Variations in fluid velocity affect the relative density of the substrate and therefore the denitrification efficiency. Bosman and Hendricks (1981) noted that at higher velocities the

denitrification efficiency of a fluidised bed dropped off as the result of excessive biomass wash off. Observable changes in the thickness of the attached biomass on the substrate were observed during and between trials. As a consequence the density of the biomass/substrate was not constant between trials, thus pressure loss and superficial fluid velocity varied.

Bosman and Hendricks (1981) in their studies noted that for efficient operation of the denitrification process pH values between 6.5-8.5 are required. This was the case for the FBR trials, hence the effect of the minor changes in pH observed during the trials are thought to be negligible.

Some of the above mechanisms may have been present in the fluidised bed reactor, contributing to the variability in FBR performance and the difficulty with relating the process coefficients. A qualitative evaluation of the denitrification performance of the FBRs is presented in Figure 7-23, in which the occurrence of denitrification within the FBR is displayed as a function of the hydraulic and nitrate load.

Figure 7-23 does show that at high nitrate loads (5 to 6 mg/hr) the substrate was on occasion able to support denitrification. However, the majority of the hydraulic loading at the high nitrate loading was predominantly around 0.1 L/hr. Due to the lack of trials at higher hydraulic loads the optimum treatment (nitrate and hydraulic) condition was not able to be determined.

Of the four trials with a hydraulic load in excess of 0.1 L/hr, none showed evidence of denitrification. This suggests a relationship between the hydraulic load and the ability of the substrate to release the organic carbon required to sustain biological denitrification.

Table 7-24 Biological FBR Numerical Coefficients

		(mg/hr)	(L/hr)	(mg/L)	(days)	Nitrate						COD						
Reactor	Treatment	Nitrate Load	Hydraulic Load	Influent []	Duration	C_I	C_o	k_s	r_s	k_b	r_b	C_I	C_o	k_s	r_s	k_b	r_b	c_s
FBR 1-1(b)	None	5.25	0.465	11.29	8	11.14	0.7	1	0	0	0.464	0	301	4.174	-24.152	0	1.858	274200
FBR 1-1(c)	None	0.09	0.008	11.25	6	12.50	8.3	1	0	0	0.711	0	0	2.104	18.712	0	2.842	274200
FBR 1-1(d)	None	1.72	0.155	11.10	8	11.55	0.4	1	0	0	2.916	0	85	6.027	-23.465	0	11.662	274200
FBR 1-2(b)	Lime	6.6	0.584	11.30	8	11.24	0.7	1	0	0	1.209	0	559	1.484	-7.435	0	4.835	274200
FBR 1-2(c)	Lime	0.11	0.01	11.00	6	12.00	7.2	1	0	0	1.326	0	29	3.253	22.703	0	5.305	274200
FBR 1-2(d)	Lime	2.25	0.195	11.54	8	11.49	0.4	1	0	0	3.276	0	72	5.998	-22.719	0	13.102	274200
FBR 3-1(a)	None	1.4	0.073	19.18	10	20.30	0.7	1	0	0	2.007	0	8	7.563	46.450	0	8.028	274200
FBR 3-1(c)	None	3.5	0.111	31.53	16	31.53	0.6	1	0	0	0.204	0	23.8	5039.542	-3100.58	0	0.816	274200
FBR 3-2(a)	Lime	1.7	0.085	20.00	10	20.00	0.6	1	0	0	1.434	0	10	7.125	47.042	0	5.736	274200
FBR 3-2(c)	Lime	3.3	0.101	32.67	16	32.67	2.3	1	0	0	0.150	0	49	6227.450	1837.842	0	0.599	274200
FBR 4-1(a)	None	4.2	0.111	37.84	9	37.7	47.5	1	0	0	0.29	0	273	4.832	-24.861	0	1.160	274200
FBR 4-1(b)	None	3.5	0.111	31.53	15	34.80	17.5	1	0	0	0.870	0	44	14.314	69.220	0	3.480	274200
FBR 4-1(c)	None	5.8	0.111	52.25	11	52.90	0.4	1	0	0	20.100	0	114	17.821	9.758	0	80.400	274200
FBR 4-2(a)	Lime	3.8	0.101	37.62	9	37.70	0	1	0	0	14.710	0	602	4.294	-0.773	0	58.840	274200
FBR 4-2(b)	Lime	3.2	0.101	31.68	15	34.80	0.7	1	0	0	5.000	0	130	22.845	-36.613	0	20.000	274200
FBR 4-2(c)	Lime	5.3	0.101	52.48	11	52.90	2.4	1	0	0	1.300	0	75	39.675	-128.554	0	5.200	274200
FBR 5-1(a)	None	6.2	0.089	69.66	17	69.00	2.3	1	0	0	0.089	0	252	7435.609	2.469	0	0.354	274200
FBR 5-1(b)	None	4.1	0.089	46.07	32	37.70	0.6	1	0	0	0.010	0	38	10.163	-75.818	0	0.042	274200
FBR 5-2(a)	Lime	5.6	0.081	69.14	8	69.00	0.6	1	0	0	2.171	0	100	6.089	-24.416	0	8.686	274200
FBR 5-2(b)	Lime	5.6	0.081	69.14	8	45.20	8.3	1	0	0	0.140	0	30	13.542	-81.746	0	0.560	274200
FBR 6-1(a)	None	0.6	0.026	23.08	7	23.10	8	1	0	0	0.951	0	23	2648.930	1.336	0	3.803	274200
FBR 6-1(b)	None	1.1	0.03	36.67	7	36.70	0.6	1	0	0	4.254	0	0	6.335	33.820	0	17.014	274200
FBR 6-1(c)	None	1.9	0.02	95.00	8	95.00	0.6	1	0	0	0.379	0	34	7854.593	-1516.00	0	1.516	274200
FBR 6-1(d)	None	0.3	0.004	75.00	5	95.00	11.3	1	0	0	0.729	0	6	5.890	42.323	0	2.915	274200
FBR 6-1(e)	None	2.2	0.026	84.62	23	84.60	0.8	1	0	0	0.208	0	35	5373.516	8571.619	0	0.833	274200
FBR 6-2(a)	Lime	0.5	0.022	22.73	7	22.73	8.4	1	0	0	2.935	0	23	28.360	109.252	0	11.740	274200
FBR 6-2(b)	Lime	1	0.023	43.48	7	43.48	0.3	1	0	0	3.920	0	10	322.784	3.499	0	15.680	274200
FBR 6-2(c)	Lime	1.8	0.019	94.74	8	94.74	0.6	1	0	0	0.890	0	18	7.489	-44.091	0	3.560	274200
FBR 6-2(d)	Lime	0.4	0.004	100.00	5	100.00	5.8	1	0	0	1.190	0	0	6.453	39.390	0	4.760	274200
FBR 6-2(e)	Lime	2	0.023	86.96	23	86.96	0.7	1	0	0	0.216	0	44	5762.752	7806.875	0	0.865	274200

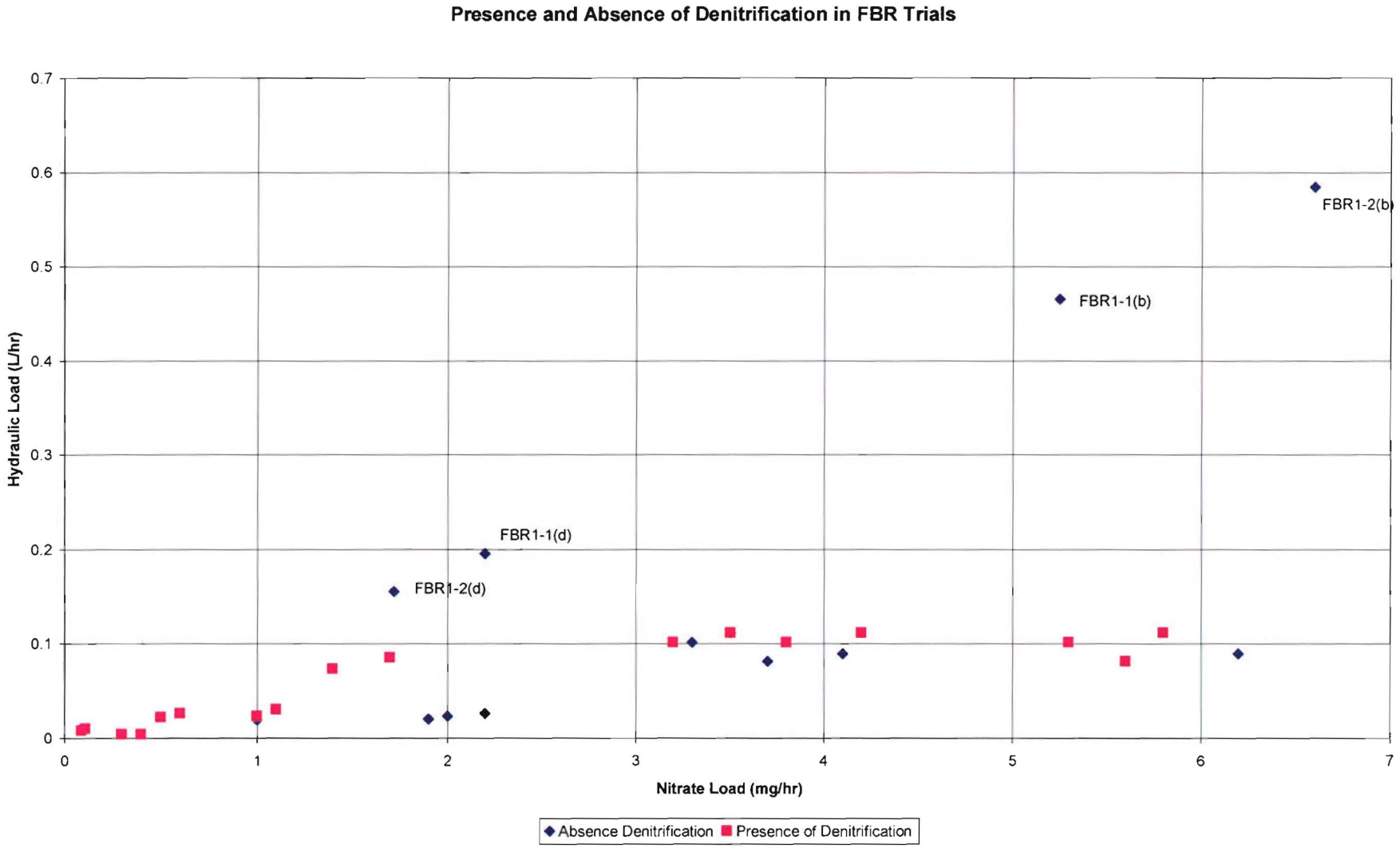

Figure 7-23 The presence and absence of denitrification within all FBR trials, as a function of the nitrate and hydraulic load.

7.3.1 Performance of the Lime and Untreated FBRs

A parallel comparison of the performance of the untreated substrate in reactor FBR Y-1 to that of the lime pretreated substrate in reactor FBR Y-2 is summarised in Table 7-25. The analysis indicates that the lime pretreated provides a noticeable improvement in the ability to coconut shell fragments to denitrify.

Table 7-25 Performance of the Biological Rate of Consumption of Nitrate ($r_{b.NO3}$)

Substrate Age (days)	Untreated Substrate (FBR Y-1)		Lime treated Substrate (FBR Y-2)		$\frac{r_{b\bullet FBRY-2}}{r_{b\bullet FBRY-1}}$	
8	FBR 1-1(b)	0.464	FBR 1-2(b)	1.209	**260%**	**260%**
14	FBR 1-1(c)	0.711	FBR 1-2(c)	1.326	**187%**	**187%**
22	FBR 1-1(d)	2.916	FBR 1-2(d)	3.276	**112%**	**112%**
33	FBR 3-1(a)	2.007	FBR 3-2(a)	1.434	**71%**	**71%**
51	FBR 3-1(c)	0.204	FBR 3-2(c)	0.150	**73%**	**73%**
9	FBR 4-1(a)	0.29	FBR 4-2(a)	14.710	**5072%**	
24	FBR 4-1(b)	0.870	FBR 4-2(b)	5.000	**575%**	**575%**
35	FBR 4-1(c)	20.100	FBR 4-2(c)	1.300	**6%**	
52	FBR 5-1(a)	0.089	FBR 5-2(a)	2.171	**2451%**	
84	FBR 5-1(b)	0.010	FBR 5-2(b)	0.140	**1336%**	
91	FBR 6-1(a)	0.951	FBR 6-2(a)	2.935	**309%**	**309%**
98	FBR 6-1(b)	4.254	FBR 6-2(b)	3.920	**92%**	**92%**
106	FBR 6-1(c)	0.379	FBR 6-2(c)	0.890	**235%**	**235%**
111	FBR 6-1(d)	0.729	FBR 6-2(d)	1.190	**163%**	**163%**
134	FBR 6-1(e)	0.208	FBR 6-2(e)	0.216	**104%**	**104%**
				Average	**737%**	**198%**
				Median	**187%**	**163%**

Ignoring the four outlying results highlighted in blue in Table 7-25, the average relative improvement in the rate of nitrate consumption indicates that the lime pretreatment of coconut shell fragments improves the rate of the nitrate consumption due to denitrification (r_b) in a FBR on average 198%.

The relative improvement in denitrification performance provided by the lime pretreated substrate declined with increase in substrate age, which is to be expected as the readily degradable cellulose sites were hydrolysed.

Two batches of the substrates were utilised in the FBR trials, the first batch was used in the FBR1-X(a) to FBR3-X(c) trials, and the second from FBR4-X(a) to FBR6-(e). The duration of improved denitrification provided by the lime pretreated substrate varied from 22 days in the first batch to 134 days for the second. The cause of the variation is unknown, further investigations via a long term application parallel study is required to explain the variance.

The numerical CFSTR model derived in Appendix M (reproduced below) formed the basis of the numerical assessment of the FBR trials.

$$V\frac{dc}{dt} = Qc_1 - Qc + \frac{Vc_s}{2k_s}\left(\operatorname{sech}^2\left(\frac{t-r_s}{k_s}\right)\right) - Vr_b ct$$

An evaluation of the numerical coefficients from the CFSTR assessment of the FBR trials, on the basis of the substrate pretreatment is summarised in Table 7-26.

Table 7-26 Average Biological FBR Numerical Coefficients

	Nitrate				COD				
	k_s	r_s	k_b	r_b	k_s	r_s	k_b	r_b	c_s
All	1	0	0	2.468	1363.03	451.703	0	9.873	274200
Lime	1	0	0	2.658	830.64	634.684	0	10.631	274200
Untreated	1	0	0	2.279	1895.43	268.723	0	9.115	274200

From Table 7-26, the typical profile of the numerical equations are as follows:

The FBRs with the lime pretreated substrates, presented the following typical profile:

Nitrate:

$$V\frac{dc}{dt} = Qc_1 - Qc - V\cdot(2.468)\cdot ct$$

Eqn. 7-4

COD:

$$V\frac{dc}{dt} = Qc_1 - Qc + \frac{V\cdot(274200)}{2\cdot(830.64)}\left(\operatorname{sech}^2\left(\frac{t-(634.684)}{(830.64)}\right)\right) - V\cdot(10.631)\cdot ct$$

Eqn. 7-5

While the FBRs with the untreated substrates had the following profile:

Nitrate:

$$V\frac{dc}{dt} = Qc_1 - Qc - V\cdot(2.279)\cdot ct$$

Eqn. 7-6

COD:

$$V\frac{dc}{dt} = Qc_1 - Qc + \frac{V\cdot(274200)}{2\cdot(1895.43)}\left(\operatorname{sech}^2\left(\frac{t-(268.723)}{(1895.43)}\right)\right) - V\cdot(9.115)\cdot ct$$

Eqn. 7-7

7.4 Conclusions

1. Glucose is a readily available and utilisable carbon source, similar to other commonly utilised simple hydrocarbons like ethanol or methanol. The rate of utilisation in denitrification bacteria is immediate; no acclimatisation is required unlike some other simple hydrocarbons (Christensson et al. (1994)).

2. Under ideal conditions the COD:TN ratio for the denitrification was observed to be 4:1. This is consistent with observations made by Christensson et al. (1994) and Æsoy et al. (1998) approximations, at 4.1 g COD/g NO_3^--N and 4.5 g COD/g NO_3^--N respectively.

3. In FBR-X(a) trials (presented in Figure 7-1) in which the FBR reactors were operated as a closed system and with nitrate; the lime treated substrate consumed the nitrate (denitrification) at a rate of 11.58 mg/L/day while the untreated substrate consumed the nitrate at a rate of 7.06 mg/L/day. While both reactors were not limited in available COD, the different denitrification rates could be due to variations in biomass between the two reactors.

4. Since the increase in COD was measured in the filtrate of 1.2 μm and 0.45 μm samples from the liquid phase, this suggests that the COD released was extracellular . The variation in COD is indicative of biological interactions, and most likely the result of extracellular cellulase enzymes.

5. The performances of the FBR reactors are analogous to a CFSTR process due to the high internal recycle. To achieve sufficient denitrification whilst maintaining the fluidised bed, a high internal recycle is required.

6. Low COD concentrations in the FBR appeared to stimulate a COD release response. This is thought to be a bacterial response to the lack of available COD, releasing cellulase enzymes, and the extracellular degradation of the organic substrate resulting in the increase in COD in the reactors. This hydrolysis is demonstrated in FBR1-2(d).

7. The improved COD released and hence denitrification as a result of the pretreatment with lime is limited. In this particular series of the trials two batches of pretreated substrate were utilised. The first batch to sustain improved denitrification by the lime pretreated substrate for 22 days, and 134 days for the second.

8. The lime pretreated substrate provided a 198% increase in the rate of the nitrate consumption due to denitrification (r_b).

7.5 References

Æsøy A and Ødegaard H., Bach K., Pujol R., Hamon M. (1998) Denitrification in a packed bed biofilm reactor (BIOFOR) – Experiments with different carbon sources. Water Resources, Vol. 32, No. 5, pp. 1463-1470

APHA (1999) Standard Methods for the examination of water and wastewater. 20th Edition, American Public Health Association, Washington.

Bosman and Christensson M., and Lie E, Welander T (1994) A comparison between Ethanol and Methanol as carbon sources for Denitrification, Wat. Sci. Tech., Vol. 30, No. 6, pp 83-90

Bosman J. and Hendricks F.(1981) The technology and economics of the treatment of a concentrated nitrogenous industrial effluent by biological denitrification using a fluidised-bed reactor. Biological Fluidised Bed Treatment of Water and Wastewater. Editors P F Cooper and B. Atkinson, Ellis Horwood, Chichester England, pp.48-58

Gayle B. P., and Boardman G. D., Sherrard J. H., Benoit R. E. (1989) Biological denitrification of water. ASCE, J. Enviro. Engrg. Vol. 115, No. 5, Oct. pp. 930-943

Lewis W. and Whitman w. (1924) Principle of Gas Absorption, Industrial and Engineering Chemistry, Vol.26, pp.382-385

Trivedi H. and Weir T. (2004) NADH Fluorescence in the SymBio Process Enables Simultaneous Nitrification and Denitrification, Industrial Wastewater Technical Bulletin, WEF Vol.3, No.4 pp. 5-7

United States Environmental Protection Agency (1989) Design Manual Fine Pore Aeration Systems, EPA/625/1-89/023

Weisstein E. W. (2005) "Bilinear Function." From MathWorld--A Wolfram Web Resource. http://mathworld.wolfram.com/BilinearFunction.html

8 Recommendations

It was identified that the denitrification process would be limited by the ability of the coconut shell fragments to release organic carbon (i.e. cellulose) into solution. Since the composition of the shell of the coconut is similar to a hardwood (Nathanel, 1964) an increase in hydrolysis of the shell will need to overcome the lignocellulose structure before additional cellulose can be released.

Of the nine pretreatment techniques considered in this research, the two hydroxide pretreated substrates (sodium hydroxide and lime) exhibited the greatest ability to release COD therefore demonstrating the highest nitrate consumption (denitrification). However, sodium hydroxide was discounted as a feasible pretreatment technique due to the issues associated with a full-scale application of the technique.

The increased COD release into solution as a result of the NaOH and lime pretreatment is thought to be as the result of Alkaline Hydrolysis. Alkaline Hydrolysis is defined as the cleaving of a molecule (in this case it is assumed to be cellulose) into two by the addition of a water molecule in a solution with a pH > 7 (as demonstrated in Figure 5-17).

However Lindgren (2000) noted that for cellulose to be able to react and hydrolyse, the hydrogen bonds in the cellulose need to be ruptured. In the presence of concentrated sodium hydroxide, the hydroxyl hydrogen from the cellulose will form alkali cellulose. The same process is thought to occur in the presence of lime; instead of the formation of the alkoxylate ion ($-O^-Na^+$) a $-O^-CaOH^+$ ion is formed.

$$\text{Cellulose - OH} + \text{NaOH} \rightleftharpoons \text{Cellulose - O}^-\text{Na}^+ + \text{H}_2\text{O}$$

$$\text{Cellulose - OH} + \text{Ca(OH)}_2 \rightleftharpoons \text{Cellulose - O}^-\text{CaOH}^+ + \text{H}_2\text{O}$$

As a consequence the pretreatment of coconut shell fragments will result in the consumption of the hydroxide ions.

As the cellulose fragments containing the $-O^-Na^+$ or $-O^-CaOH^+$ ions are liberated from the cellulose matrix, during the denitrification process, the ability of the cellulose structure to react and hydrolyse will reduce as the remaining intrachain, interchain and intrasheet hydrogen

bonds limit the cellulose from further degradation. It could be possible to then re-treat the substrate to recover its capacity to release further organic carbon, though this hypothesis was not tested in the scope of this research.

The improved COD release and hence denitrification as a result of the pretreatment with lime is limited. In this particular series of the trials two batches of pretreated substrate were utilised. The first batch sustained improved denitrification using the lime pretreated substrate for 22 days, and the second batch sustained 134 days.

Direct comparisons of the performance of the two FBR reactors indicated that while the untreated substrate was able to sustain denitrification, the pretreated substrate improved the ability of coconut shell fragments to denitrify.

This research thesis does demonstrate that coconut shells fragments within a fluidised bed are able to sustain biological denitrification where the coconut shell fragments are the only source of organic carbon. Whilst denitrification was achieved with the untreated substrate, a lime pretreatment provided a 198% increase in the rate of the nitrate consumption due to denitrification (r_b).

8.1 Further Research Opportunities

There has been some useful data and results of coconut shell sustaining biological denitrification in this study. However there is no doubt that there are some issues and topics that need to be studied further in the future, these include:

- The FBR denitrification trials only evaluated the influence of COD:N on the rate of denitrification. Further studies in this topic should evaluate the influence other parameters like temperature, pH, and toxicity of high concentrations of nitrate have on the rate of denitrification.

- The FBR1-X(a) trials appear to indicate that the hydrolysis of COD via the lime treated substrate is more readily biodegradable, than the untreated substrate, hence the greater denitrification rate. Further investigations are required into determining the

composition of the organic carbon released from the coconut shell fragments, and test the assumption that the COD was in the form of glucose.

- Continuous dosage of the denitrification reactor with an aqueous lime solution may the increase hydroxide concentration in the reactor and could promote COD release and hence encourage improved rate of denitrification.

- The duration of additional denitrification from the lime pretreated substrate in the FBR trials varied from 22 to 134 days. Further investigations are required to assess the cause of the variation.

- Unfortunately this research did not assess the mass of biomass within the reactors, thus wasunable to fully quantify the biological processes. Further studies in this area should quantify the biomass produced and wasted, so that mass balances and biological kinetic parameters can be determined, and evaluated.

Appendix A

Evaluation of the Dissolved Oxygen Measurement Technique

Many of the fluid samples require an assessment of the DO concentration even though it was not feasible to monitor DO insitu within the reactor. Hence fluid samples needed to be assessed outside the reactors, whilst preserving the mass of the samples. To minimise reactor disturbance, a 60mL sample was taken, assessed and returned to the reactor. This appendix assesses the validity of the results obtained from the 60mL sample and compares it to that of a standard 300mL and insitu measurements.

The worst-case scenario was to obtain a fluid sample during the batch testing phase, since extraction of the sample via the extraction tube out of the Erlenmyer Flasks had the potential to draw DO out of solution. The sample was then injected into the 60mL DO bottle where the DO measurement was taken with a mechanical stirrer DO probe and digital meter.

Both the standard DO bottle and 500mL Pyrex beaker DO measurement techniques involved pouring the fluid into the appropriate vessel. The 60mL DO bottle measurement requires extracting the sample from a 6L Erlenmeyer flask, via a stainless steel extraction tube into a 60mL plastic syringe. The fluid was drawn into the syringe via a 16 gauge needle; the rate was nominally set at 6mL/sec because rates significantly higher that this resulted in bubbles forming in the syringe as the negative pressures drew gases out of solution.

Since the DO meter was calibrated in a similar method to that used to measure the fluid in a 500mL Pyrex beaker, then the technique of measuring the DO in the small 60mL DO bottle was deemed to be an appropriate technique for measuring small samples of fluid.

Comparative evaluations of the different DO measurement techniques, indicates that withdrawing and then assessing the sample in the 60mL DO Bottle measurement technique is suitable (Table A-1).

Table A-1 Comparison of Different Dissolved Oxygen Measurement Techniques

	Std 300ml DO Bottle	*500ml Pyrex Beaker (stirred manually)*	*60ml DO Bottle (via extraction technique)*
Typical Pretreatment Fluid	5.45 ± 0.1 mg/L	5.75 ± 0.1 mg/L	5.80 ± 0.1 mg/L
Domestic Tap Water	7.2 ± 0.1 mg/L	7.9 ± 0.1 mg/L	8.0 ± 0.1 mg/L

Appendix B

FBR Design Calculations

The two design equations outlined in Chapter 3.1 on Biological Fluidised Beds (Eqn. 3-3 Werther, 1983, and Eqn. 3-4 Leva, 1959) were applied to estimate the likely superficial fluid velocity required to maintain the bed in a fluidised state.

The densities of the coconut shell fragments were determined experimentally, whilst other coefficients like the ε_{mf} (mean void fraction) and S_v (ratio between the surface area of the fragments and the volume of the fragments) were estimated.

For the purposes of this design, it was assumed that the minimum fluidisation velocity of the d_{50} particle size is representative of the particle distribution within the FBR reactors, as presented in Figure B-1.

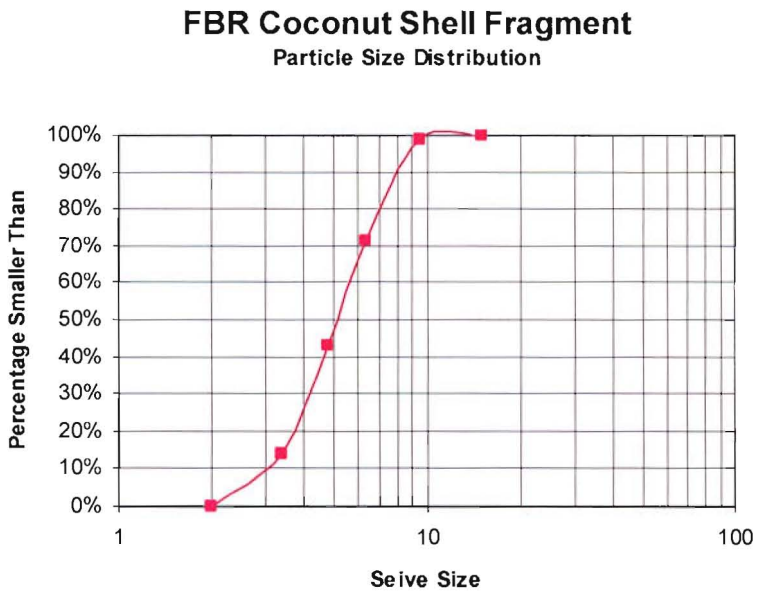

Figure B-1 Particle Size Distribution of Coconut Shell Fragment Utilitised in FBR

As the design calculations following indicate the Werther (1983) estimated a greater superficial fluid velocity is required to sustain fluidisation of the bed, and formed the basis of the design. A value of 0.36m/s became the design superficial fluid velocity. This equated to an internal recycle flowrate of 2.1 L/s.

Fluidised Bed Design Calcs

Variables

Reactor Diameter	rd	0.085 (m)		
Diameter of Coconut Support Medium	ds	5.00E-03 (m)	Note: this is the d_{50} measurement	
Bacteria thickness	tb	1.00E-03 (m)		
Density of Biofilm	pb	1,000 (kg/m^3)		
Density of Support Medium with Biofilm	ppw	1,036 (kg/m^3)		
Density of Substrate @20C	pw	1,100 (kg/m^3)	Range 700-1100 Dry	
Kinematic viscosity of substrate	v	1.01E-06 (m^2/s)		
Void Fraction at min. fluidisation	emf	0.39 (-)		
S.A of all particles/vol.all particle	sv	1.20E+02 (1/m)		
Hydraulic Retention Time	hrt	86400 (sec)	equals	24 (hrs)
Height of the reactor	rh	1.4 (m)		
Fluidisation bed zone height	h	1 (m)		
Factor of Safety	FS	2 (-)		

Calculations

1.0 Design velocity of the superficial fluid in the fluidised bed zone.

Leva (1959) Leva and co-workers developed the following an expression for the superficial fluid velocity:

Superficial fluid velocity	wls	6.70E-03 (m/s)	equals	24.11 (m/hr)

Werther (1983) Developed the following relationship for the pressure drop across the bed at min fluid velocity:

Velocity of fluid at min. fluidisation	Umf	1.80E-01 (m/s)	equals	648.32 (m/hr)
Design Velocity	ud	0.1801 (m/s)	equals	648.32 (m/hr)
Select Design Velocity *	ud* = wd x FS	0.3602 (m/s)	equals	648.32 (m/hr)

2.0 Flow rates

Cross Sectional Area of the Reactor	rxa	5.67E-03 (m^2)		
Upflow flow rate within reactor	qv	2.04E-03 (m^3/s)	equals	122629 (ml/min)
Influent/Effluent flow rate	qie	6.57E-08 (m^3/s)	equals	4 (ml/min)
Recycle Flow rate	qr	2.04E-03 (m^3/s)	equals	122625 (ml/min)

Recycle:Influent flow rate ratio 31118 : 1

Appendix C

Inoculum Selection

Three sources of inoculum were considered:

1. Partial decomposed wood with evidence of bore;
2. Compost from a residential compost pile – degrading domestic green waste;
3. Garden soil, with a high organic content.

Approximately 10gms of each source was placed into a 250mL Erlenmeyer flask. Augmented with 20mL of deionised water containing 2.5mg/L of cycloheximide, 100mg/L nitrate (NO_3^--N), and 3mg/L of phosphate.

The nitrate concentration of each source was assessed 2 days later. The decomposed wood flask was contained 3.3mg/L (NO_3^--N), while the compost flask contained 64.6mg/L, and the garden soil flask 7.9 mg/L. The reduction in nitrate is attributed to biological denitrification.

Both the decomposed wood and garden soil are potential sources of bacteria to biologically denitrify. However decomposed wood was selected as the source inoculum for this research, due to its denitrification ability, and this selection mirrors the approach adopted by Volokita et al. (1996).

Appendix D

Comparative Study on the effect of Filter Paper on COD Measurement

Samples were collected from the FBR 8-X reactors, 22 hours after the addition of the substrate to the reactor, and prior to the addition of the inoculum. Half the volume of each sample was passed through a 0.45μm cellulose filter paper, while the other was passed through 1.2μm GF/C filter paper. The COD from the filtrate is summarised in the table below...

Table D-1 Comparison of the COD of 0.45μm and 1.2μm filtrate from FBR8-X

	Filter Paper		Difference	
Reactor	0.45μm	1.2μm		%
A	106	123	17	13.8
B	233	236	3	1.3
C	216	223	7	3.1
D	361	367	6	1.6
E	1319	1438	119	8.3
F	188	196	8	4.1
			Average	5.4

As expected the COD of the filtrate from the 0.45μm filter paper is less than the 1.2μm filter paper; however the variation is slight, 5.4%, which is within the error associated with the COD test.

The filtrate from the 0.45μm by definition is a measure of the soluble COD. As this COD fraction is preferentially consumed by bacteria, it is the ideal parameter to assess the performance of the biological system and can be taken to be representative of the COD available to the bacteria for these trials. This approach is consistent with the approach adopted by other researchers such as Volokita et al. (1996).

Appendix E

Derivation: Surface Area per gram of Substrate

Formulation of the calculated values for the Surface Area per gram of substrate, for the two distributions considered.

$$Surface\ Area\ per\ gram\ of\ substrate = \%\ substrate\ in\ range\ /\ \rho_c * S.A.\ /\ Vol.$$

Eqn. E-1

Where:

% substrate in range

The mass substrate retained by the sieve / sum of the mass retained by all the sieves. (gms/gms)

ρ_c Density of coconut shell (measured as 1170kg/m^3)

S.A. Surface Area of a sphere:

$$\pi d^2$$

Vol. Volume of a sphere:

$$\frac{4}{3}\frac{\pi d^3}{8}$$

d Nominal diameter of the sieve, which is the average of the upper and lower limits of the particle retained by the sieve.

Example:

Table 4-4 shows that 14.05% of the $2 \le x \le 8mm$ particles are contained within the 4.75mm and 4.00mm sieves. The average diameter of the particles is assumed to be:

$$\frac{(4.75mm + 4.00mm)}{2} = 4.375mm$$

Step 1. 14.05% of the substrate equates to .1405gms per gram of substrate. And the density of the coconut was assessed as 1170kg/m^3.

$$\rho = \frac{m}{v} = \frac{1170 \times 10^{3}\, gms}{10^{9}\, mm^{3}} = 1.17 \times 10^{-3}\, gms / mm^{3}$$

So the volume of substrate in .1405gms is:

$$Vol. = \frac{m}{\rho} = \frac{0.1405 gms}{1.17 \times 10^{-3}\, gms / mm^{3}} = 120.09 mm^{3}$$

Step 2. Assuming the particles are spherical, then the number of 4.375mm particles in .1405gms of substrate is:

$$Vol. = \frac{4}{3}\frac{\pi d^{3}}{8} = \frac{4}{3}\frac{\pi (4.375mm)^{3}}{8} = 43.85 mm^{3}$$

$$\text{Number of particles} = \frac{120.09 mm^{3}}{43.85 mm^{3}} = 2.739$$

Step 3. Therefore the Surface Area of 2.739 particles per gram of substrate is:

$$2.739 \times 4\frac{\pi d^{2}}{4} = 2.739 \times 4\frac{\pi (4.375mm)^{2}}{4} = 164.67 mm^{2} / gm$$

Appendix F

Uncertainty Analysis of the COD Colorimetric Technique

The colourimetric technique utilises a spectrophotometer and requires calibration prior to application. Eighteen synthetic samples containing potassium hydrogen phthalate (KHP)[20] with predetermined COD concentration were utilised resulting in the calibration chart in Figure F-1 below.

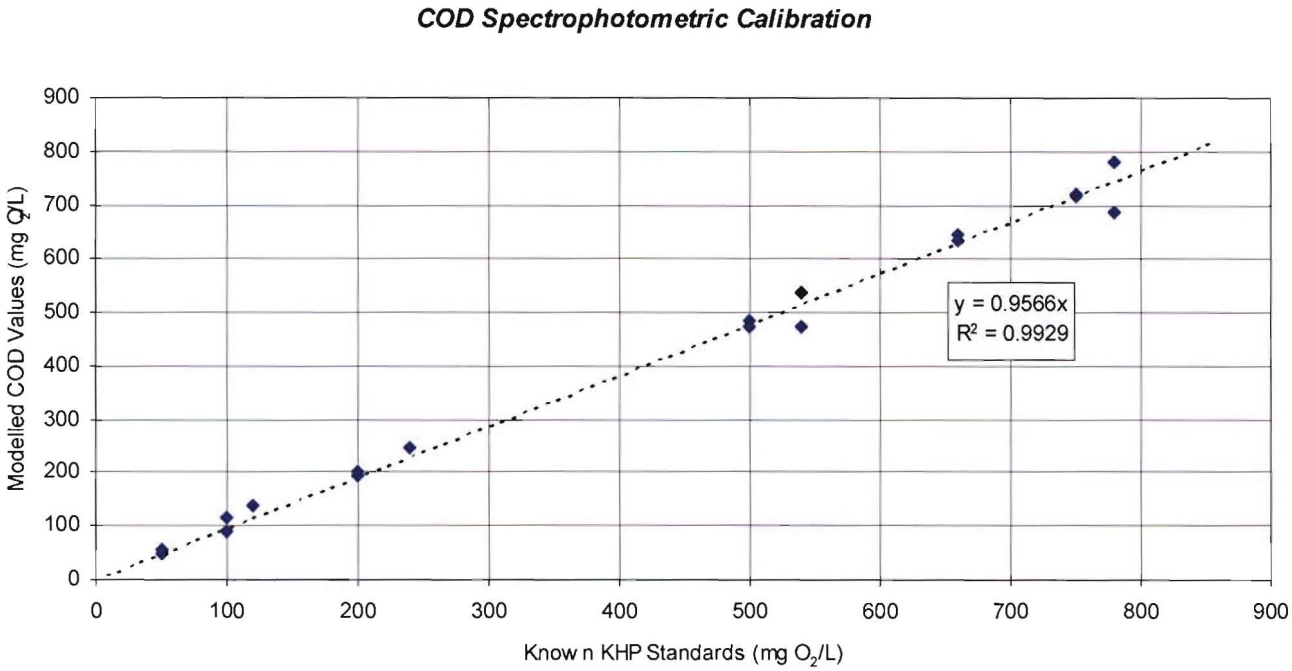

Figure F-1 Verification of the COD Spectrophotometric calibration.

The standard error of this test is due in part to two influences, variability in the sample size, and that of the reagent-spectrophotometer assessment of the chemical oxygen demand. Standard methods (APHA, 1999) indicate that the standard error for the test is 8.7%. However some of the ranges of COD measurements exceed the oxidation ability of the test reagents. In these cases the sample has been dilute resulting in a new source of error.

$$\frac{\sigma_z}{\bar{z}} = \frac{\sigma_x}{\bar{x}} + \frac{\sigma_y}{\bar{y}}$$

[20] KHP is a standard commonly used in COD tests. The dissolution of 425mg of lightly crushed and dry KHP in 1000mL of distilled water has a theoretical COD of 1.176mg O_2 /mg or 500mg/L COD.

Where:

σ_z Standard deviation of the COD spectrophotometric test

σ_x Standard deviation attributed to the volume of the fluid sample

σ_y Standard deviation attributed to the reagents and spectrophotometer

$\bar{z}$ Theoretical mean of a the COD spectrophotometric test

$\bar{x}$ Mean volume of fluid sample

$\bar{y}$ Mean attributable to the reaction of reagents and spectrophotometer measurement

Evaluation of the standard error (S.E.) attributed to the dilution of sample is summarised in Table F-1.

Table F-1 Standard Error of the COD Colorimetric Technique at Various Dilution Rates

Sample size (mL)	COD Range (mg/L)	Dilution	S.E. Test	S.E. Sample	S.E. Reagent/ Spectrophotometer
2.5	0-800	x1	8.7%	1%	7.7%
1.25	0-1600	x2	8.7%	1%	7.7%
1.00	0-2000	x2.5	8.7%	1%	7.7%
0.6	0-3333	x4.17	8.95%	1.25%	7.7%
0.4	0-5000	x6.25	8.95%	1.25%	7.7%
0.2	0-10000	x12.5	8.95%	1.25%	7.7%

Appendix G

Theoretical Oxygen Demand
Pretreatment Acids

The theoretical oxygen demand (ThOD) of the organic pretreatment acids (e.g.: acetic and propionic acid) are influenced by the concentration present, temperature, and the dissociation constant of the particular acid (K_a).

Using the software programme ACID-BASE Equilibrium Calculator, written by the author, it is possible to determine the initial pH of a known concentration of a known multiprotic acid. The programme uses iterative logic test techniques to determine the resulting pH. This programme can also be used to determine the concentration of acid required to have a predetermined pH within the water.

An extract of the ACID-BASE Equilibrium Calculator in Figure G-1 shows the required concentration of conjugate acid and base (CtA) required to dissociate acetic acid to result in an initial pH = 3.00. Other variables of interest include pKa the acid dissociation constant, CtM the concentration of the metal ion associated with the dissociation of the acetic acid.

ACID-BASE Equilibrium Calculator

© Copyright Mark J Ellis (1999)

Input

Initial Conditions		Acetic acid	CH_3COOH	*Variable*		
CtM	1.000E-99	moles/L	pCtM	99.00	Mcharge	0
CtA	5.854E-02	moles/L	pCtA	1.23		
Kw	2.195E-14		pKw	13.66	Temp	35
Ka1	1.738E-05		pKa1	4.76		
Ka2	1.000E-99		pKa2	99		
Ka3	1.000E-99		pKa3	99		

Output

Initial pH 3.0000

COD	H_3A	H_2A-	HA--	A--	Sum
Molar Ratio	2	1.75	0	0	
Moles HxA	5.75E-02	1.00E-03	1.00E-99	1.00E-195	
Moles O_2	1.15E-01	1.75E-03	0.00E+00	0.00E+00	1.17E-01
				COD (mg/L O_2)	3739

Figure G-1 The input and output screen for the programme ACID-BASE Equilibrium Calculator.

Once the concentrations of the acid and its conjugate base have been determined, it is possible to determine the oxygen demand by evaluating the oxidation equations of the acid and base.

e.g.:

$$HA \leftrightarrow A^- + H^+$$
$$CH_3COOH \leftrightarrow CH_3COO^- + H^+$$

the $ThOD_{HA}$ is determined by evaluating the oxidation equation of *HA*,

$$CH_3COOH + 2O_2 \rightarrow 2CO_2 + 2H_2O$$

similarly $ThOD_{A^-}$ from the oxidation of A^-,

$$CH_3COO^- + 1.75O_2 \rightarrow 2CO_2 + 1.5H_2O$$

Hence from these equations and knowing the concentrations of HA and A^- ions present it is possible to determine the oxygen demand.

Where:

HA	Reactant acid
A^-	Conjugate base (product) to the acid HA
H^+	Hydroxide ion produced in the reaction
$ThOD_{HA}$	Theoretical oxygen demand of the acid HA
$ThOD_{A^-}$	Theoretical oxygen demand of the base A^-

The COD section of Figure G-1, determines the associated chemical oxygen demand of a weak acid that is partially dissociated. The actual COD values measured via the Standard Methods (APHA 1999) technique will be different to the chemical oxygen demand calculated above, because the COD test contains concentrated sulphuric acid as one of its reagents. Any weak acid like acetic or propionic acid will remain in the form of *HA*, as indicated by the pC-pH diagram in Figure G-2.

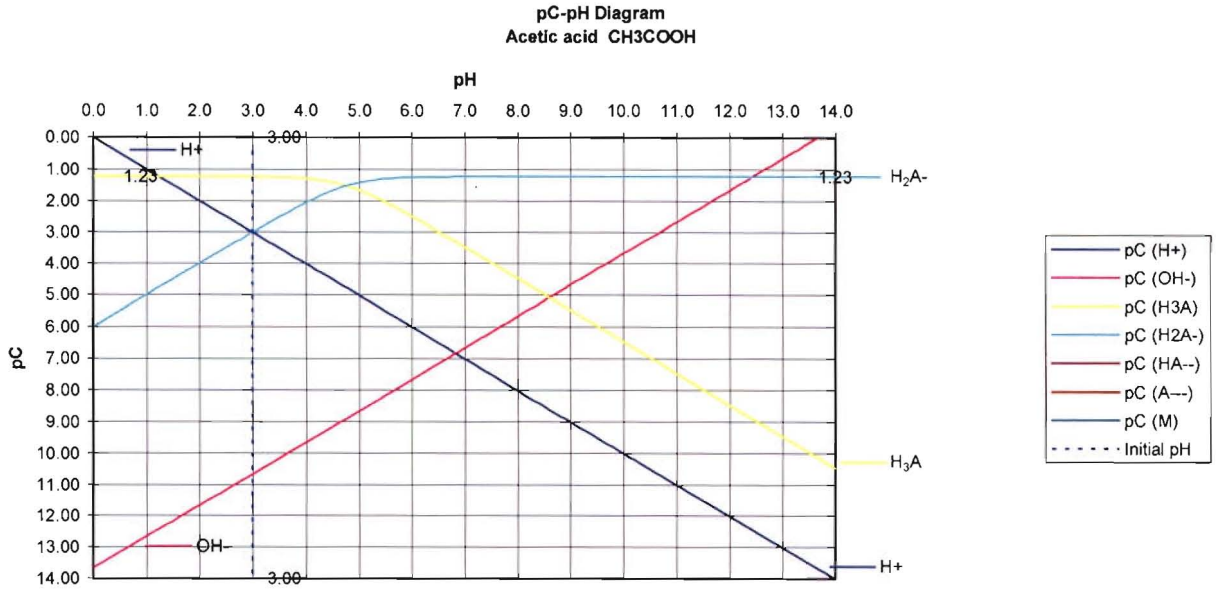

Figure G-2 The pC-pH diagram produced by ACID-BASE Equilibrium Calculator.

Table G-1 Theoretical Oxygen Demand and COD of Applied Acetic and Propionic Acid Utilised as a Chemical Pretreatment

Acid	pH	pKa	Moles acid required	*HA*	O_2 Demand / *HA*	A^-	O_2 Demand / A^-	Theoretical O_2 Demand (mg/L)	COD (mg/L)
Acetic Acid	3	4.76	5.854×10^{-2}	5.75×10^{-2}	2.00	1.00×10^{-3}	1.75	3739	3747
	5		1.575×10^{-5}	5.75×10^{-6}		1.00×10^{-5}		1	1
	5.5		3.730×10^{-6}	5.73×10^{-7}		3.16×10^{-6}		≈ 0	≈ 0
Propionic Acid	3	4.87	7.512×10^{-2}	7.41×10^{-2}	3.50	1.00×10^{-3}	3.25	8405	8413
	5		1.741×10^{-5}	7.41×10^{-6}		1.00×10^{-5}		2	2

Appendix H

Pretreatment Analysis

A summary of the parameters describing the COD hydrolysis and pH consumption profiles.

Reactor	1a	1b	1c	1d	1e	1f	2c
NaN_3	FALSE	FALSE	FALSE	FALSE	FALSE	FALSE	FALSE
Drying Technique	Air	Air	Oven	Oven	Air	Air	Air
Particle Size	2-10mm	2-10mm	2-10mm	2-10mm	2-8mm	2-8mm	2-10mm
Chemical Pretreatment	Deionised	Deionised	Deionised	Deionised	Deionised	Deionised	NaOH
Initial Concentration / Nominal pH	7	7	7	7	7	7	14
Reactor	**1a**	**1b**	**1c**	**1d**	**1e**	**1f**	**2c**
c	76.78	33.17	27911.19	26434.96	84.03	104.08	3164.67
k	24.08	1.03	0.00	0.00	0.80	0.22	1.10
I (pH)	5.63	5.69	4.75	4.75	7.80	5.04	14.17
D (pH)	0.59	0.62	0.24	0.10	2.72	-0.07	0.07
K (pH)	5.45	8.90	11.20	9.26	15.60	1.26	27.64
t COD/2	0.03	0.67	-2824.90	-3097.78	0.87	3.13	0.63
t pH/2	-0.13	-0.08	-0.06	-0.07	-0.04	-0.55	-0.03

Reactor	3c	3d	4c	4d	4e	4f
NaN_3	FALSE	FALSE	FALSE	FALSE	FALSE	FALSE
Drying Technique	Air	Air	Air	Air	Air	Air
Particle Size	2-10mm	2-10mm	2-10mm	2-10mm	2-10mm	2-10mm
Chemical Pretreatment	NaOH	NaOH	HCl	HCl	HCl	HCl
Initial Concentration / Nominal pH	12	9	4	4	2	2
Reactor	**3c**	**3d**	**4c**	**4d**	**4e**	**4f**
c	643.23	159.75	109.08	102.43	113.95	104.93
k	0.67	3.10	0.99	0.72	0.27	0.54
I (pH)	11.99	8.79	3.74	3.89	1.91	1.90
D (pH)	0.65	2.62	-1.45	-1.59	0.10	0.09
K (pH)	2.81	17.86	47.25	13.54	0.78	0.63
t COD/2	1.03	0.22	0.70	0.97	2.56	1.27
t pH/2	-0.25	-0.04	-0.01	-0.05	-0.89	-1.10

Reactor	5a	5b	5c	5d	5e	5f
NaN_3	FALSE	FALSE	FALSE	FALSE	FALSE	FALSE
Drying Technique	Air	Air	Air	Air	Air	Air
Particle Size	2-10mm	2-10mm	2-10mm	2-10mm	2-10mm	2-10mm
Chemical Pretreatment	Lime	Lime	H2SO4	H2SO4	H2SO4	H2SO4
Initial Concentration / Nominal pH	500	500	3	3	2	2
Reactor	**5a**	**5b**	**5c**	**5d**	**5e**	**5f**
c	100.37	91.27	163.23	182.79	119.06	131.88
k	1.69	2.70	0.20	0.15	0.11	0.16
I (pH)	10.19	10.56	3.13	3.05	1.94	1.90
D (pH)	3.10	3.31	-0.82	-0.79	0.10	13.86
K (pH)	0.40	0.43	1.39	1.31	0.84	0.00
t COD/2	0.41	0.26	3.51	4.53	6.35	4.33
t pH/2	-1.73	-1.60	-0.50	-0.53	-0.83	-818.76

Reactor	6a	6b	6c	6d	6e	6f
NaN_3	TRUE	TRUE	TRUE	TRUE	TRUE	TRUE
Drying Technique	Air	Air	Air	Air	Air	Air
Particle Size	2-10mm	2-10mm	2-10mm	2-10mm	2-10mm	2-10mm
Chemical Pretreatment	Deionised	H2SO4	NaOH	NaOH	NaOH	Lime
Initial Concentration / Nominal pH	7	2	14	9	12	500
Reactor	**6a**	**6b**	**6c**	**6d**	**6e**	**6f**
c	187.50	184.05	5841.67	262.98	712.88	464.12
k	0.55	0.18	1.06	0.49	0.48	0.99
I (pH)	6.29	2.62	13.71	10.32	11.43	11.51
D (pH)	0.67	0.86	2.39	4.00	4.11	4.13
K (pH)	0.16	29.55	0.00	1.99	0.15	0.15
t COD/2	1.27	3.87	0.65	1.42	1.44	0.70
t pH/2	-4.47	-0.02	205.83	-0.35	-4.71	-4.56

Reactor	7a	7b	7c	7d	7e	7f
NaN_3	FALSE	TRUE	FALSE	FALSE	TRUE	TRUE
Drying Technique	Air	Air	Air	Air	Air	Air
Particle Size	2-10mm	2-10mm	2-10mm	2-10mm	2-10mm	2-10mm
Chemical Pretreatment	CH3COOH	CH3COOH	CH3COOH	CH2COOH	CH2COOH	CH2COOH
Initial Concentration / Nominal pH	3	3	5	3	3	5
Reactor	**7a**	**7b**	**7c**	**7d**	**7e**	**7f**
c	3636.11	3690.28	193.36	8509.58	8259.72	241.20
k	17.52	23.62	0.43	39.81	30.79	4.66
I (pH)	3.02	3.43	5.45	2.69	3.42	4.18
D (pH)	0.25	-9.95	0.34	-7.72	-1.07	-0.43
K (pH)	0.93	0.00	0.11	0.00	0.02	9.71
t COD/2	0.04	0.03	1.60	0.02	0.02	0.15
t pH/2	-0.75	-730.26	-6.04	-295.23	-38.45	-0.07

Reactor	8a	8b	8c	8d	8e	8f
NaN_3	TRUE	TRUE	TRUE	TRUE	TRUE	TRUE
Drying Technique	Air	Air	Air	Air	Air	Air
Particle Size	2-8mm	2-8mm	2-8mm	2-8mm	2-8mm	2-10mm
Chemical Pretreatment	Lime	Lime	Lime	Lime	Lime	Lime
Initial Concentration / Nominal pH	50	100	500	500	50	50
Reactor	**8a**	**8b**	**8c**	**8d**	**8e**	**8f**
c	82.41	105.97	429.82	466.36	77.80	126.07
k	0.27	0.96	1.15	1.39	0.32	0.30
I (pH)	10.06	11.73	11.68	11.75	10.37	10.47
D (pH)	3.16	4.88	4.21	3.76	3.30	3.49
K (pH)	0.99	0.30	0.28	0.33	0.49	0.68
t COD/2	2.55	0.72	0.60	0.50	2.15	2.28
t pH/2	-0.70	-2.31	-2.46	-2.11	-1.42	-1.02

Appendix I

Solubility of Dissolved Oxygen and Corresponding DO Concentration

Table I-1 Solubility of Dissolved Oxygen		
Temperature	*[H+]*	*DO (mg/L)*
25 °C	4.38 x 10^4	9.13
30 °C	4.75 x 10^4	8.30
35 °C	5.07 x 10^4	7.89

(Source: Perry, 1997)

Henry's Law:

$$\rho = \frac{H}{x}$$

Where:

ρ Partial pressure in the gas phase *(atm)*

H Proportionality constant ($atm / moles\ O_2 / moles\ H_2O$)

x Fraction of solute in the liquid phase

Example:

$$x = \frac{0.20 atm}{4.28 \times 10^4\ atm / moles\ O_2 / moles\ H_2O} \times \frac{32}{16} \times 1000^2 \frac{mg}{L} = 7.89\ mg / L$$

Appendix J

Denitrification Batch Reactor Trials - Rate of Reaction Parameters and Normalisation Factors

Table J-1 Evaluation of the reaction rates for the denitrification batch reactors

Reactor	Substrate Pretreatment	*COD*	*pH*	NO_3^--*N*	*DO*	PO_4^{3-}
Anoxic Pretreated						
1DRa	Untreated	$COD = 0.28t + 28.7$ $r^2 = 0.015$	$pH = -0.027t + 6.53$ $r^2 = 0.588$	$NO_3^-N = -0.034t + 191$ $r^2 = 0.004$	$DO = -0.109t + 2.87$ $r^2 = 0.244$	$PO_4^{3-} = -.006t + 3.14$ $r^2 = 0.192$
1DRb	Lime 500 mg/L	$COD = 2.18t + 16.7$ $r^2 = 0.682$	$pH = -0.021t + 7.26$ $r^2 = 0.817$	$NO_3^-N = -0.857t + 196$ $r^2 = 0.344$	$DO = -0.006t + 0.97$ $R^2 = 0.227$	$PO_4^{3-} = -0.006t + 3.14$ $r^2 = 0.192$
1DRc	Lime 500 mg/L + NaN_3	$COD = 2.13t + 34.3$ $r^2 = 0.692$	$pH = -0.028t + 7.42$ $r^2 = 0.88$	$NO_3^-N = -0.683t + 198$ $r^2 = 0.509$	$DO = 0.002t + 0.913$ $r^2 = 0.037$	$PO_4^{3-} = -.003t + 3.12$ $r^2 = 0.074$
1DRd	NaOH pH=14	$COD = 8.49t + 92.4$ $r^2 = 0.897$	$pH = -0.055t + 8.62$ $r^2 = 0.802$	$NO_3^-N = -2.166t + 210$ $r^2 = 0.927$	$DO = -0.025t + 1.39$ $r^2 = 0.555$	$PO_4^{3-} = -0.0381t + 3.24$ $r^2 = 0.892$
1DRe	NaOH pH=14 + NaN_3	$COD = 9.69t + 321$ $r^2 = 0.901$	$pH = -0.035t + 9.95$ $r^2 = 0.834$	$NO_3^-N = -0.259t + 204$ $r^2 = 0.228$	$DO = 0.059t + 1.54$ $r^2 = 0.538$	$PO_4^{3-} = 0.00347t + 3.36$ $r^2 = 0.262$
1DRf	HCl pH=2	$COD = 1.60t + 36.4$ $r^2 = 0.489$	$pH = 0.006t + 4.62$ $r^2 = 0.211$	$NO_3^-N = -0.240t + 203$ $r^2 = 0.141$	$DO = -0.021t + 1.61$ $r^2 = 0.126$	$PO_4^{3-} = -0.023t + 3.09$ $r^2 = 0.646$
2DRa $7<t<12$	NaOH pH=9	$COD = -0.086t + 1.65$ $r^2 = 0.326$	$pH = 0.098t + 5.24$ $r^2 = 0.433$	$NO_3^-N = -0.256t + 110$ $r^2 = 0.015$	$DO = 0.80t + 17.7$ $r^2 = 0.059$	$PO_4^{3-} = -0.009t + 1.82$ $r^2 = 0.045$
2DRb $6<t<11$	HCl pH=2	$COD = -0.003t + 42.6$ $r^2 = 3x10^{-7}$	$pH = 0.099t + 4.73$ $r^2 = 0.670$	$NO_3^-N = 0.348t + 183$ $r^2 = 0.060$	$DO = 0.005t + 0.529$ $r^2 = 0.030$	$PO_4^{3-} = -0.053t + 2.44$ $r^2 = 0.008$
2DRc $7<t<12$	HCl pH=4	$COD = 1.145t + 10.07$ $r^2 = 0.115$	$pH = -0.021t + 5.83$ $r^2 = 0.238$	$NO_3^-N = 0.597t + 185$ $r^2 = 0.191$	$DO = 0.526t - 2.794$ $r^2 = 0.978$	$PO_4^{3-} = 0.055t + 1.66$ $r^2 = 0.590$
2DRd $8<t<13$	NaOH pH=12	$COD = 4.384t - 17.08$ $r^2 = 0.482$	$pH = 0.027t + 6.43$ $r^2 = 0.304$	$NO_3^-N = 0.027t + 182$ $r^2 = 0.0003$	$DO = 0.0827t + 0.347$ $r^2 = 0.389$	$PO_4^{3-} = 0.013t + 2.347$ $r^2 = 0.012$
2DRe $9<t<13$	Lime 500 mg/L	$COD = 2.435t - 9.052$ $r^2 = 0.409$	$pH = 0.0253t + 6.042$ $r^2 = 0.097$	$NO_3^-N = -0.284t + 188.5$ $r^2 = 0.076$	$DO = 0.188t - 1.10$ $r^2 = 0.958$	$PO_4^{3-} = 0.052t + 1.752$ $r^2 = 0.546$
2DRf $8<t<12$	Acetic Acid pH=5	$COD = -0.261t + 18.8$	$pH = 0.187t + 4.00$	$NO_3^-N = 0.074t + 188.8$	$DO = -0.170t + 2.68$	$PO_4^{3-} = -0.062t + 3.19$

Table J-1 Evaluation of the reaction rates for the denitrification batch reactors

Reactor		Substrate Pretreatment	*COD*	*pH*	NO_3^--*N*	*DO*	PO_4^{3-}
			$r^2 = 0.001$	$r^2 = 0.790$	$r^2 = 0.001$	$r^2 = 0.334$	$r^2 = 0.701$
Initial Aerobic Cond.							
2DRa	*0<t<7*	NaOH pH=9	*COD* = 2.021*t* + 10.5 $r^2 = 0.233$	*pH* =-0.112*t* + 6.53 $r^2 = 0.746$	NO_3^--*N* =-1.338*t* + 198.9 $r^2 = 0.629$	*DO* = 0.179*t* + 2.528 $r^2 = 0.174$	PO_4^{3-} =-0.158*t* + 2.21 $r^2 = 0.320$
2DRb	*0<t<6*	HCl pH=2	*COD* = 5.649*t* + 13.82 $r^2 = 0.772$	*pH* =-0.095*t* + 5.607 $r^2 = 0.562$	NO_3^--*N* =-0.602*t* + 189.3 $r^2 = 0.161$	*DO* = 0.353*t* + 0.549 $r^2 = 0.873$	PO_4^{3-} =-0.029*t* + 2.03 $r^2 = 0.076$
2DRc	*0<t<7*	HCl pH=4	*COD* = 0.409*t* + 17.05 $r^2 = 0.020$	*pH* =-0.079*t* + 6.17 $r^2 = 0.732$	NO_3^--*N* =-0.849*t* + 188 $r^2 = 0.200$	*DO* = 0.086*t* + 2.419 $r^2 = 0.158$	PO_4^{3-} = 0.007*t* + 1.853 $r^2 = 0.419$
2DRd	*0<t<8*	NaOH pH=12	*COD* = 1.829*t* + 11.83 $r^2 = 0.338$	*pH* =-0.115*t* + 7.378 $r^2 = 0.890$	NO_3^--*N* =-2.597*t* + 198 $r^2 = 0.915$	*DO* =-0.343*t* + 5.188 $r^2 = 0.435$	PO_4^{3-} =-0.072*t* + 3.039 $r^2 = 0.534$
2DRe	*0<t<9*	Lime 500 mg/L	*COD* =0.927*t* + 10.41 $r^2 = 0.238$	*pH* =-0.125*t* + 7.084 $r^2 = 0.748$	NO_3^--*N* =-1.824*t* + 197 $r^2 = 0.712$	*DO* =-0.411*t* + 5.510 $r^2 = 0.653$	PO_4^{3-} =-0.089*t* + 2.892 $r^2 = 0.421$
2DRf	*0<t<8*	Acetic Acid pH=5	*COD* =-0.829*t* + 22.04 $r^2 = 0.035$	*pH* =-0.174*t* + 6.652 $r^2 = 0.919$	NO_3^--*N* =-2.545*t* + 203.6 $r^2 = 0.292$	*DO* = 0.237*t* + 3.48 $r^2 = 0.922$	PO_4^{3-} = 0.029*t* + 2.43 $r^2 = 0.107$

Table J-2 Evaluation Denitrification Batch Reactor Normalisation Factors				
Denitrification Reactor	Corresponding Pretreatment Reactor	Dry Weight of Substrate (Coconuts Fragments) (g)	Volume of fluid added (@ 20°C) (L)	Normalisation Factor (mg/L)
1 DR a	NIL	101.51	4.0	25,377
1 DR b	5a/5b	104.56	4.0	26,140
1 DR c	6f	103.31	4.0	25,827
1 DR d	6c	85.13	4.0	21,282
1 DR e	2c	93.44	4.0	23,360
1 DR f	4e/4f	102.70	4.0	25.675
2 DR a	3d	101.51	4.0	25.377
2 DR b	4e/4f	104.56	4.0	26,140
2 DR c	4c/4d	103.31	4.0	25,827
2 DR d	3c	85.13	4.0	21,282
2 DR e	5a/5b	93.44	4.0	23,360
2 DR f	7c	102.70	4.0	25,675

Appendix K

Average (time-weight) DO concentration in 1DRb

Calculations of the time weighted average DO concentration of anoxic regime in reactor 1DRb.

Table K-1 Batch Reactor 1DRb - Average DO Concentration					
Date	***Time***	***Days***	***DO***	***t***	***DO x t***
15-Feb	15:30	(2.91)			
15-Feb	16:30	(2.87)	8.7		
17-Feb	09:28	(1.16)	6.9		
18-Feb	13:20	-	7.15		
18-Feb	14:41	0.06	5.75		
19-Feb	11:04	0.91	1.125		
20-Feb	11:03	1.90	1.05		
22-Feb	10:56	3.90	0.85	1.99	1.69
24-Feb	10:45	5.89	0.85	2.01	1.71
26-Feb	11:20	7.92	0.775	1.97	1.52
28-Feb	09:05	9.82	0.85	3.01	2.56
03-Mar	11:45	13.93	0.875	3.46	3.03
06-Mar	07:20	16.75	0.95	3.44	3.27
10-Mar	09:05	20.82	0.95	3.53	3.36
13-Mar	09:00	23.82	0.9	3.50	3.15
17-Mar	09:10	27.83	0.7	2.00	1.40
			Sum	24.92	21.70
				Weighted Average	0.8705

Where:

t is the period of time that is half of the time between the previous and successive record.

Note: That the anoxic regime occurs when the DO concentration falls below the 1 mg/L threshold.

Appendix L

Time-Weighted Average Methodology

The interval between samples was not consistent. Typically more frequent samples were conducted at the earlier stages of the trial. As a consequence the best fit analyses will provide closer fit to the earlier stage of the trial at the expense to the later data from the trial.

To overcome the potential error the bias to the earlier stages of the trials, a time-weighted methodology was developed (Eqn. L-1) and applied. Whilst the evaluation utilises DO, the same approach was adopted for the other chemical parameters numerically evaluated.

Eqn. L-1 essentially evaluated the difference between the numerical model approximation and recorded data divided by the representative time interval, as demonstrated in Figure L-1. An optimum numerical model is when the evaluated value from Eqn. L-1 is closest to zero.

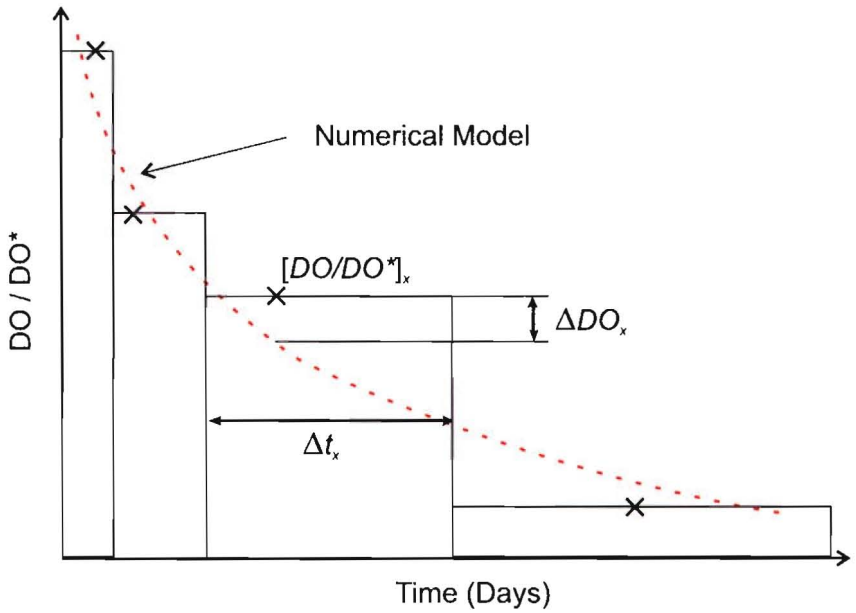

Figure L-1 Time-weighted approach to evaluating a numerical model

$$\sum_{x=1}^{n} \frac{|\Delta DO_x|}{\Delta t_x} \rightarrow 0$$

Eqn. L-1

Where:

Δt_x is the change in time between $\frac{T_{x-1} + T_x}{2}$ and $\frac{T_x + T_{x+1}}{2}$

ΔDO_x is the difference between the model value for $\left[\frac{DO}{DO*}\right]_m$ and the observed $\frac{DO}{DO*}$ value

$DO/DO*$ the DO normalised against the maximum DO value in the data set (DO*)

$[DO/DO*]_x$ is the observed normalised DO value at record x

$\left[\frac{DO}{DO*}\right]_m$ is the modeled value of $\frac{DO}{DO*}$

Appendix M

Fluidised Bed Reactor Trial Explanation of CFSTR Analysis Model

Simple continuous flow stirred tank reactor (CSFTR) models have the following form:

$$\frac{d(cV)}{dt} = Qc_I - Qc + f_s(c,t) - f_b(c,t)$$

Eqn. M-1

Or in words, the rate of change of the mass inside the control volume is equal to the mass flux in less the mass flux out plus the mass produced less the mass consumed.

Where:

c	Reactor concentration (mg/L)
V	volume of the CFSTR (L)
Q	flow rate of the fluid into and out of the reactor (L/day)
c_I	Influent concentration (mg/L)
$f_s(c,t)$	Reactant production function (mg/day)
$f_b(c,t)$	Reactant consumption function (mg/day)

Since the volume of the FBR remains constant $\left(\frac{dV}{dt} = 0\right)$ then:

$$\frac{d(cV)}{dt} = V\frac{dc}{dt} + c\frac{dV}{dt} = V\frac{dc}{dt}$$

Eqn. M-2

Several versions of the CFSTR model expressed in Eqn. M-1 were considered and evaluated. Examples are shown in Eqn. M-3 to Eqn. M-6.

$$V\frac{dc}{dt} = Qc_I - Qc + Vr_s c - Vr_b c$$

Eqn. M-3

$$V\frac{dc}{dt} = Qc_I - Qc + Vr_s e^{-k_s t} - Vr_b e^{-k_b t}$$

Eqn. M-4

$$V\frac{dc}{dt} = Qc_I - Qc + Vr_s e^{-k_s t} - Vcr_b e^{-k_b t}$$

Eqn. M-5

$$V\frac{dc}{dt} = Qc_I - Qc + \frac{Vc_s}{2k_s}\left(\operatorname{sech}^2\left(\frac{t-r_s}{k_s}\right)\right) - Vr_b c$$

Eqn. M-6

Expression Eqn. M-6 provided the best correlation with experimental data. The $Qc_I - Qc$ term quantifies the hydraulics flushing characteristics, the $-Vr_b c$ term quantifies the rate of reactant production, while the $\frac{Vc_s}{2k_s}\left(\operatorname{sech}^2\left(\frac{t-r_s}{k_s}\right)\right)$ term describes the reactant consumption. The hyperbolic secant function, is consistent with experimental observations of the COD profiles as they tended to have a hyperbolic tangent form.

For example the numerical assessment of FBR1-2(b), where:

Q 14.02 L/day

V 11.3 L

r_s -7.43

k_s 1.484

r_b 4.84

c_s 274,200 mg/L

As demonstrates in Figure M-1, the numerical model provided close correlation with the observed data set. This was typical of most of the FBR trials.

During the analysis of the FBR data, most of the trails resolved that best fit occurred when c_s was $\approx$274,200 mg/L, hence to reduce the complexity of this model all the analyses were re-evaluated with c_s = 274,200mg/L. Since the numerical model is insensitive to minor changes in c_s, minimal changes to the other parameters were noted.

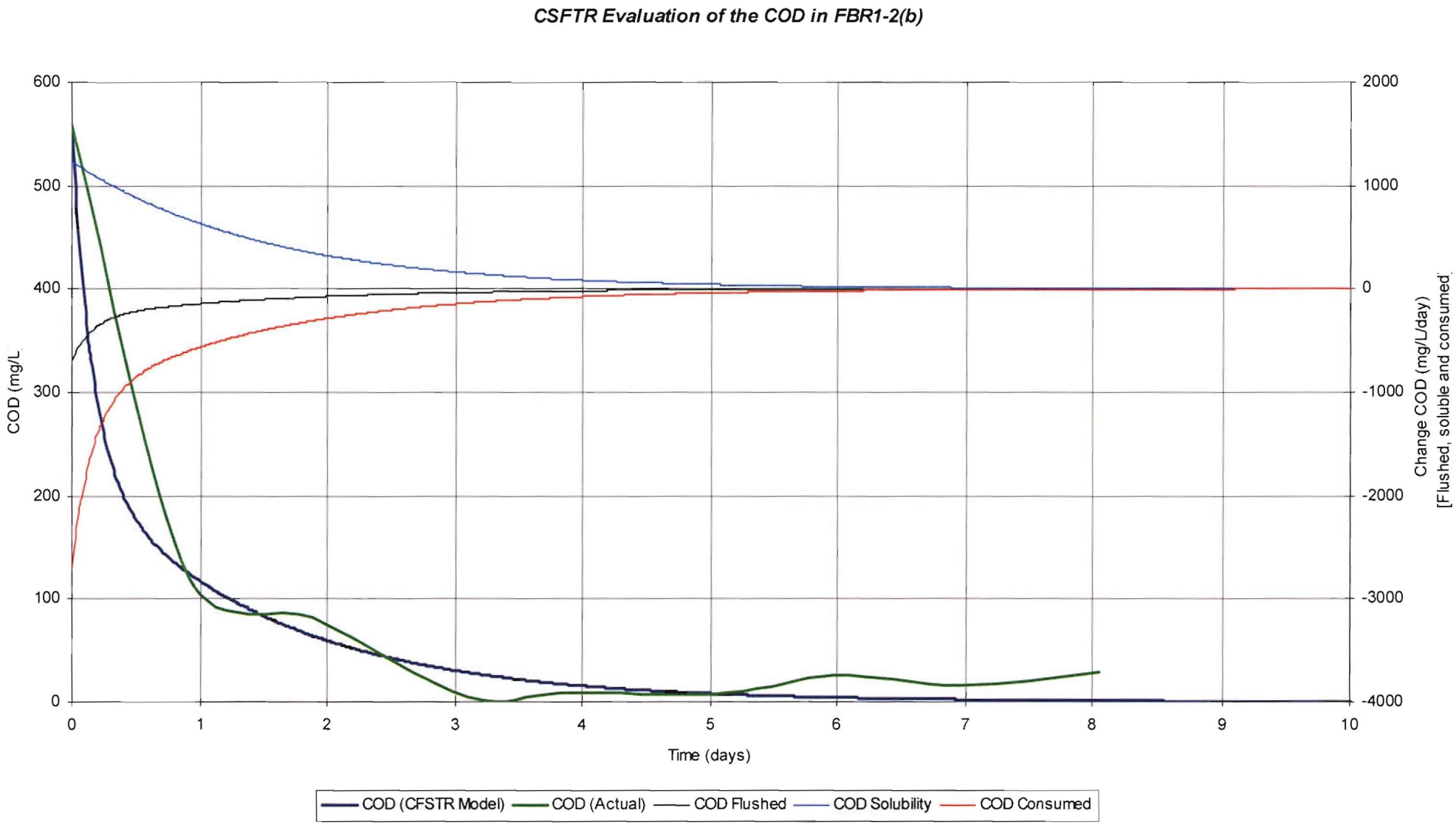

Figure M-1 Numerical analysis of COD within FBR1-2(b)

END